European Journal of Taxonomy 1071: 1–138
https://doi.org/10.5852/ejt.2026.1071.3296

europeanjournaloftaxonomy.eu
ISSN 2118-9773
2026 · Frick H. *et al.*

Received: 7 July 2025 • *Accepted: 22 December 2025* • *Published: 25 June 2026*

Topic editor: Magalie Castelin • *Section editor: Arnaud Henrard* • *Desk editor: Pepe Fernández*

Monograph

urn:lsid:zoobank.org:pub:CFCE23F0-2120-4178-B02D-5C5871E202EA

Systematic revision of the *Savignia* genus group (Araneae: Linyphiidae: Erigoninae) with notes on their cephalic lobe evolution

Holger FRICK [1,*], Annui M. SANZ-LAPARRA [2,*] & Christian KROPF [3]

[1] Museum.BL, Department of Collections, Zeughausplatz 28, 4410 Liestal, Switzerland.
[2] University Museum of Bergen, Department of Natural History, Allégaten 41, 5007 Bergen, Norway.
[3] Natural History Museum Basel, Biosciences, Augustinergasse 2, CH-4001 Basel, Switzerland.
[3] Natural History Museum of Bern, Department of Invertebrates, Bernastrasse 12, 3005 Bern, Switzerland.
[3] University of Bern, Institute of Ecology and Evolution, Baltzerstrasse 6, CH-3012 Bern, Switzerland.

[*] Corresponding authors: holger.frick@bl.ch; anuimalla@gmail.com
[3] Email: christian.kropf@bs.ch

Abstract. The *Savignia* genus group includes nine morphologically complex yet similar genera where species were assigned based mainly on the cephalic lobes. Among these genera, males of *Diplocephalus* Bertkau, 1883, *Savignia* Blackwall, 1833 and *Araeoncus* Simon, 1884 show some of the most extraordinary cephalic lobes among dwarf spiders (Linyphiidae, Erigoninae). In this study we undertake the first phylogenetic analysis of the *Savignia* genus group. We use 269 morphological characters (175 newly defined) and 70 taxa (59 ingroup taxa) to reconstruct the relationships and evolutionary trends of cephalic lobes in this lineage. Our findings show that cephalic lobes with varying shapes and sizes appear in several *Savignia* genus group lineages, highlighting that it is not a good diagnostic character. The high support in several clades allows the redefinition of the genera *Savignia*, *Diplocephalus*, *Araeoncus*, *Erigonella* Dahl, 1901, *Dicymbium* Menge, 1868 and *Glyphesis* Simon, 1926 based on synapomorphies and leads to new species assignments. Our results also show that while genera are well supported, their interrelationships are not, suggesting that genera closely related with the *Savignia* genus group may need further revision. Simplified, the generic relationships of the *Savignia* genus group are *Glyphesis* (*Dicymbium* ((*Erigonella* (*Hemistajus* **resurrected rank**, *Savignia*)) (*Diastanillus* (*Diplocephalus*, *Araeoncus*))).

Keywords. Dwarf spiders, male cephalic lobes, morphology, phylogeny.

Frick H., Sanz-LaParra A.M. & Kropf C. 2026. Systematic revision of the *Savignia* genus group (Araneae: Linyphiidae: Erigoninae) with notes on their cephalic lobe evolution. *European Journal of Taxonomy* 1071: 1–138. https://doi.org/10.5852/ejt.2026.1071.3296

Introduction

Early attempts to classify genera of Erigoninae Emerton, 1882 were mainly based on single character systems, i.e., spination of leg tibia and position of metatarsal trichobothrium (e.g., in Wiehle 1960). The aim of Wiehle (1960) and of most other works before Merrett (1963) was to develop tools to delimit species and genera rather than to reconstruct evolutionary trends. Merrett (1963) noted that it is important to gather information from all available character systems for the reconstruction of generic relationships. He focused on the morphology of the expanded male copulatory organ, the palp, and similarities among its different sclerites. Millidge (1977) used the conformation of unexpanded male palps to discuss relationships of Erigoninae genera and draw the first phylogenetic tree of the group (albeit not based on quantitative analyses). Based on general similarities, he defined different genus groups and discussed their relations. Hormiga (1994a, 2000) carried out the first efforts to resolve the phylogeny of linyphiids and especially erigonines. His work was expanded by Miller & Hormiga (2004) and later by Arnedo *et al.* (2009) and Wang *et al.* (2015), the latter two also adding molecular evidence.

While trying to define suprageneric groups, Merrett (1963) noted that a group of "six genera *Glyphesis* Simon, 1926, *Dicymbium* Menge, 1868, *Erigonella* Dahl, 1901, *Araeoncus* Simon, 1884, *Diplocephalus* Bertkau, 1883 and *Savignia* Blackwall, 1833, all show several distinct similarities". In the terminology of Hormiga (2000) and the current work, these are the mesally curved, circular suprategulum (as "median apophysis" in Merrett 1963) with a distal and an inner suprategular apophysis (as "two dorsal processes" in Merrett 1963), and the bisected epigyne (as "central fissure" or "median fissure" of the epigyne in Merrett 1963 and Holm 1977, respectively). Holm (1977) explicitly mentions the inner suprategular apophysis (as "median tooth") as present in all members of this group. Soon after, Millidge (1977) added several similar genera to that list and defined it as the "*Savignia* genus group" including: *Alioranus* Simon, 1926, *Araeoncus*, *Diastanillus* Simon, 1926, *Dicymbium*, *Diplocephalus*, *Delorrhipis* Simon, 1884, *Erigonella*, *Glyphesis*, *Saloca* Simon, 1926 and *Savignia*. *Delorrhipis* is a junior synonym of *Savignia* (Wunderlich 1995) so in total 9 genera conform to the "*Savignia* genus group". However, Millidge (1977) mentions several other genera as close relatives: *Dactylopisthes* Simon, 1884, *Janetschekia* Schenkel, 1939, *Thaumatoncus* Simon, 1884 and *Aulacocyba* Simon, 1926 (the latter is a junior synonym of *Microctenonyx* Dahl, 1886; Prószyński & Staręga 1971). For all these genera together Millidge (1977) suggested the name "*Savignia*-group" which he defines based on the following characters: the nearly circular suprategulum that forms "a kind of hook above which lies the embolic division" and the tibial spine formula of 2211 (Millidge 1977). Additionally, the column emerges from the suprategulum either ventrally or dorsally and is relatively distant to the base of the suprategulum (Millidge 1977). Representatives of all genera but *Dicymbium* lack a trichobothrium on metatarsus four.

However, most discussions referring to the *Savignia*-group only focus on the *Savignia* genus group, i.e., excluding *Dactylopisthes* and other miscellaneous genera. The bisected epigyne was also considered as specific for the *Savignia*-group (e.g., Millidge 1984; Bosmans 1996), but it is only present in the *Savignia* genus group. The definition of the latter subgroup is well founded (also by the current analysis) but the broader *Savignia*-group including the taxa with simple palpal conformations is problematic as it is harder to define.

In the meantime, more genera were assigned to the *Savignia*-group. Since there are over 630 genera known to belong to Linyphiidae Blackwall, 1859 (World Spider Catalog 2025) it is difficult to find all genera that were explicitly assigned to the *Savignia*-group at some point. Known to the authors are the following: *Savigniorrhipis* Wunderlich, 1992, *Archaraeoncus* Tanasevitch, 1987, *Caucasopisthes* Tanasevitch, 1990, *Dactylopisthoides* Eskov, 1990 and *Paraglyphesis* Eskov, 1991. Altogether, the *Savignia*-group currently includes 179 species in 17 genera and the *Savignia* genus group in the sense of Millidge (1977): 147 species in nine genera. The focus of our study are the relationships and limits of the core members of the *Savignia* genus group, as delimited by Merrett (1963): *Savignia*, *Diplocephalus*, *Araeoncus*, *Erigonella*, *Dicymbium* and *Glyphesis*.

In Hormiga (2000), the *Savignia*-group was one of only two genus groups that emerged as monophyletic out of the 15 groups proposed by Millidge (1977). However, this group was paraphyletic in Miller & Hormiga (2004) which included one species from each *Araeoncus*, *Savignia* and *Diplocephalus* (as did Hormiga 2000). The latest major expansion of that phylogeny was made by Frick *et al.* (2010) who improved the taxon sampling of the *Savignia*-group. Frick *et al.* (2010) added representatives of another five genera from the *Savignia*-group (plus representatives of another five potentially closely related genera) to the matrix of Miller & Hormiga (2004). This analysis revealed that the *Savignia*-group (only taxa from the *Savignia* genus group were considered) is not monophyletic with respect to *Alioranus* and *Saloca*. The genera *Diplocephalus* and *Erigonella* were also not monophyletic (Frick *et al.* 2010). Based on that analysis, here, we chose outgroup taxa from Linyphiinae and Erigoninae (mainly from Millidge's *Pelecopsis*- and *Entelecara*-group) for the current analysis.

Several authors (e.g., Millidge 1977; Bosmans 1996; Breitling 2021) suggested synonymizing all genera that Millidge assigned to the *Savignia*-group. Formally, this has never been proposed or not followed by the World Spider Catalog (2025). Eskov (1988) for example pointed out that *Savignia* has an isolated position in this group based on some very derived characters (see Systematics section of *Savignia*). The need for a systematic revision of the *Savignia*-group (probably mainly referring to the *Savignia* genus group) was mentioned by several authors (e.g., Bosmans 1996) but has never been carried out. Holm (1977) wrote: "A more extensive analysis of the taxonomical relations of the genera and species within the *Savignia*-group is under preparation" but never published anything in that regard. The aim of the current paper is to fulfil this need, at least on the level of the *Savignia* genus group and to propose a new classification based on phylogenetic evidence and morphological synapomorphies.

Material and methods

Taxon sampling

The *Savignia* genus group includes 147 species. Of these, we scored a sample that was considered representative for the observed morphological heterogeneity of each genus.

For an overview, we compared literature data (mainly figures) of all 147 species belonging to the *Savignia* genus group with a focus on *Diplocephalus*, *Araeoncus*, *Erigonella*, *Dicymbium* and *Glyphesis*. *Diplocephalus* was the most heterogeneous genus and therefore we included 22 out of 52 species (42%). *Araeoncus* and *Savignia* were both morphologically homogenous, and only a small number of species were scored (7 out of 38 species or 18% in *Araeoncus*; 6 out of 24 or 25% in *Savignia*). From the less species-rich genera of the *Savignia* genus group, we scored approximately 50% of the known species: *Alioranus* (3 out of 4 species), *Erigonella* (3 out of 5 species), *Dicymbium* (3 out of 10 species), *Glyphesis* (4 out of 7 species), *Diastanillus* (monotypic) and *Saloca* (4 out of 6 species). Additionally, we scored representatives of each of the following genera, which Millidge (1977) included in his more inclusive Savignia-group: *Archaraeoncus* (1 out of 4 species), *Caucasopisthes* (monotypic), and *Dactylopisthes* (2 out of 11 species). Of the genera that were later assigned to the *Savignia*-group, we only included *Paraglyphesis* (1 out of 3 species) as they seemed very close to *Glyphesis*.

The final matrix included a total of 70 taxa, 59 representing the ingroup (the *Savignia* genus group) and 11 outgroup taxa.

Ingroup (*Savignia* genus group, 59 taxa):
Alioranus chiardolae (Caporiacco, 1935)
UZBEKISTAN • 2 ♀♀, 2 ♂♂; Pamir-Alai Mountains, Surkhandarya area, Kuhitang-Tau mountain ridge, Bagly-Dara valley; 25–27 May 1985; Tanasevitch leg. and det.; SMF 34846.

Alioranus pastoralis (O. Pickard-Cambridge, 1872)
ISRAEL • 1 ♀; Wadi Grar; 20 Feb. 2007; E. Gavish-Regev leg. and det.; priv. coll. E. Gavish-Regev 4266-4267 • 1 ♂; Tal Or.; 19 Feb. 2007; E. Gavish-Regev leg. and det.; priv. coll. E. Gavish-Regev 3934-3936 • 1 ♀; Sede Teiman; 11–18 Feb. 2007; T. Plüss leg. and det.; priv. coll. E. Gavish-Regev (3232) • 2 ♂♂; Eshkol; 12–19 Feb. 2007; T. Plüss leg. and det.; priv. coll. E. Gavish-Regev (3695 to 3702).

Alioranus pauper (Simon, 1882)
ALGERIA • 1 ♀, 1 ♂; Wil. El Tarf, Lac Oubeira; 1 May 1990; R. Bosmans leg., det. and coll.

Araeoncus anguineus (L. Koch, 1869)
AUSTRIA – 1 ♀; Styria, Seckauer Alpen, Ringkogel; 11–21 Jun.1993; H. Brunner leg.; C. Kropf det.; NMBE Ar3652 • 1 ♂; Salzburg, Gastein, Weissenbachtal; 29 May–19 Jun. 1993, V. Relys leg. and det.; NMBE Ar3203.

Araeoncus caucasicus Tanasevitch, 1987
AZERBAIDJAN • 1 ♂ (paratype); Shemaka district, Pirkuli State Reserve; 19 Nov. 1984; D. Logunov leg.; Tanasevitch det.; SMF 33781. Females were coded according to Tanasevitch (1987).

Araeoncus crassiceps (Westring, 1861)
SWITZERLAND • 2 ♀♀, 2 ♂♂; Bern, Bremgarten, Riederenwaldmoos; 2–6 Jun. 1980; A. Hänggi leg. and det.; NMBE Ar1428.

Araeoncus galeriformis (Tanasevitch, 1987)
AZERBAIDJAN • 2 ♀♀, 1 ♂ (paratypes); Caucasus, Shemakha District, Pirkuli State Reserve; 3 Jun.1984; D. Logunov leg.; Tanasevitch det.; SMF 33822.

Araeoncus humilis (Blackwall, 1841)
AUSTRIA – 1 ♀; Styria, Bad Gleichenberg, Rudorfkogel; 8 Jul. 1991; C. Kropf leg. and det.; NMBE Ar3836 • 2 ♀♀, 3 ♂♂; Salzburg, Gastein, Kötschachtal; 19 Apr.–10 May 1994; V. Relys leg. and det.; NMBE Ar3186.

Araeoncus vaporariorum (O. Pickard-Cambridge, 1875)
FRANCE • 1 ♀, 1 ♂; Col du Galibier; 23 Sep. 1983; H.G. Müller leg.; J. Wunderlich det.; SMF 33257.

Araeoncus victorianyanzae Berland, 1936
TANZANIA • 1 ♀, 1 ♂; Uzungwe mountains, Kigogo forest, Mufindi; 10 Oct. 1984; N. Scharff leg. and det.; ZMUC 00006708.

Archaraeoncus prospiciens (Thorell, 1875)
IRAN • 1 ♀, 1 ♂; Lorestan, Dizgaran; 25 Jun. 1974; A. Senglet leg.; A. Tanasevitch det.; MHNG 7444.

Caucasopisthes procurvus (Tanasevitch, 1987)
RUSSIA • 1 ♂ (paratype); Krasnodar province, Caucasian State Reserve, mount Chugush; 22–28 Jun. 1975; V. Ovcharenko leg.; A. Tanasevitch det.; SMF 33788.

Dactylopisthes locketi (Tanasevitch, 1983)
UZBEKISTAN • 1 ♀, 1 ♂; W-Tien-Shang mountains, Tashkent area, Ugamsky mountain ridge close to Sidjak, Kainar-Sai valley; 22–25 Apr. 1983; Zonstein leg.; A. Tanasevitch det.; SMF 34850.

Dactylopisthes mirabilis (Tanasevitch, 1985)
KYRGYZSTAN • 1 ♀, 1 ♂; Kirghizia, N-Tien-Shang mountains, Issyk-Kul area, close to Dolinka; 31 Aug. 1979; Zonstein leg.; A. Tanasevitch det.; SMF 34851.

Diastanillus pecuarius (Simon, 1884)
AUSTRIA • 1 ♂; Obergurgl; 3 Sep. 1965; K. Thaler leg. and det.; NMBE Ar51359 • 1 ♀; same data as for preceding; 17 Sep. 1968; NMBE Ar51358.

Dicymbium libidinosum (Kulczyński, 1926)
RUSSIA • 2 ♀♀, 2 ♂♂; Evenkia, Taimura river mouth of Chambe river; 1982; Eskov leg.; Y. Marusik det.; SMF 39587.

Dicymbium nigrum (Blackwall, 1834)
AUSTRIA • 2 ♂♂; Styria, Graz; 10 Jul. 1995; W. Paill and O. Winder leg.; C. Kropf det.; NMBE Ar6602.

DENMARK • 1 ♀; Jægersborg Dyrehave; 9 Apr. 2003; J. Pedersen leg.; O. Gudik-Sørensen det.; ZMUC 9996.

GERMANY • 2 ♀♀; Thuringia, Südharz, Ilfeld, Brandesbachtal; 12–19 May 1996; Taeger leg.; B. von Broen det.; NMBE Ar1189 • 1 ♂; Berlin, Berlin-Friedrichsfelde, Tierpark; 28 Apr. 1985; B. von Broen leg. and det.; NMBE Ar637.

Dicymbium tibiale (Blackwall, 1836)
AUSTRIA • 1 ♀; Styria, Graz; 10 Jul. 1995; W. Paill and O. Winder leg.; C. Kropf det.; NMBE Ar6610.

DENMARK • 1 ♂; Rise Skov; 22 Apr. 2003; H. Liljehult and J. Pedersen leg.; J.-B. Schmidt det.; ZMUC 11430 • 1 ♀; Hestehaven, Rønde; 1 Oct. 1994; P. de P. Bjørn *et al*. leg.; P. de P. Bjørn det.; ZMUC 11213.

GERMANY • 1 ♂; Lower Saxony, Fischbeker Heide; 21 Apr. 1993; A. Lisken-Kleinmans leg.; NMB 1507e.

Diplocephalus alpinus (O. Pickard-Cambridge, 1873)
AUSTRIA • 1 ♀, 1 ♂; Salzburg, Gastein; 28 Jul.–17 Aug. 1993; V. Relys leg. and det.; NMBE Ar3234.

Diplocephalus arnoi Isaia, 2005
ITALIA • 1 ♂, 1 ♀; Abruzzo, L'Aquila, La Camosciara; 24 Sep. 2000; G. Osella leg.; M. Isaia det. and coll.

Diplocephalus caucasicus Tanasevitch, 1987
GEORGIA • 2 ♀♀, 2 ♂♂; Caucasus, Abkhazia, Myussera state reserve; 8–10 Jun. 1983; Golovatch leg.; Tanasevitch det.; SMF 33790.

Diplocephalus connatus Bertkau, 1889
LITHUANIA • 1 ♀, 2 ♂♂; Vilnius; 18 Apr.–13 May 1998; V. Relys leg. and det.; NMBE Ar2281.

Diplocephalus connatus jacksoni O. Pickard-Cambridge, 1904
LITHUANIA • 1 ♀; Vilnius, Botanical garden; 18 Apr.–13 May 1998; V. Relys leg. and det.; NMBE Ar2281. Subspecies included in the analysis to account for morphological differences to *D. connatus*. We agree that it is a synonym of *D. connatus* as proposed by Sherwood (2024).

SWITZERLAND • 1 ♂; location unknown; Tr. 180; De Lessert leg.; MHNG.

Diplocephalus crassilobus (Simon, 1884)
AUSTRIA • 1 ♀; Styria, Laufnitzdorf; May 1995; W. Paill and O. Winder leg.; C. Kropf det.; NMBE Ar67172 • 2 ♂♂; same data as for preceding; NMBE Ar6668.

Diplocephalus cristatus (Blackwall, 1833)
GERMANY • 2 ♀♀, 1 ♂; Berlin, Köpenick; 1 Oct. 1983; B. von Broen leg. and det.; NMBE Ar1187.

SWITZERLAND • 1 ♂; Bern, Köniz, Wabern; 5 May 1996; C. Kropf leg. and det.; NMBE Ar138.

Diplocephalus dentatus Tullgren, 1955
SWITZERLAND • 1 ♀, 2 ♂♂; Vaud, Domaine de Changins; 15–22 May 1996; G. Blandenier leg.; NMB 2598a.

Diplocephalus helleri (L. Koch, 1869)
AUSTRIA • 1 ♀; Styria, Oppenberg; 12 Jul. 1995; C. Kropf leg. and det.; NMBE Ar1264 • 1 ♀, 2 ♂♂; Salzburg, Gastein, Hinteres Weissenbachtal, 3–16 Oct. 1993; V. Relys leg. and det.; NMBE Ar3235.

Diplocephalus latifrons (O. Pickard-Cambridge, 1863)
AUSTRIA – 1 ♂; Styria, Laufnitzdorf; Jun. 1995; W. Paill and O. Winder leg.; C. Kropf det.; NMBE Ar6699 • 2 ♂♂; Styria, Unterzeiring; 13 Oct.1994; C. Kropf leg. and det.; NMBE Ar3662 • 1 ♀; Styria, Oppenberg; 10 May 1995; C. Kropf leg. and det.; NMBE Ar48 • 1 ♂; Styria, Oppenberg. Gulling bank, SW Rottenmann; 12 Jul. 1995; C. Kropf leg. and det.; NMBE Ar1262 • 1 ♀; same data as for preceding; 17 Jul. 1995; NMBE Ar1261.

Diplocephalus lusiscus (Simon, 1872)
GERMANY • 2 ♀♀, 1 ♂; Westfalen, Bismarck-cave; Wunderlich det.; SMF 37577.

Diplocephalus marusiki Eskov, 1988
RUSSIA • 2 ♀♀, 1 ♂ (paratypes); Siberia, Magadan area, Sibit-Tyellakh, Bolshoy Annachag mountain; Aug. 1985; Y. Marusik leg.; Eskov det.; SMF 36878.

Diplocephalus mirabilis Eskov, 1988
RUSSIA • 1 ♀, 1 ♂ (paratypes); Siberia, Sibit-Tyellakh, Kolyma river; 10 Sep. 1987; Y. Marusik leg.; Eskov det.; SMF 36881.

Diplocephalus montanus Eskov, 1988
RUSSIA • 1 ♀, 1 ♂ (paratypes); Siberia, Magadan area, Sibit-Tyellakh, Bolshoy Annachag mountain; 6 Sep. 1985; Y. Marusik leg.; Eskov det.; SMF 36879.

Diplocephalus pavesii Pesarini, 1996
ITALY • 1 ♂; Piemont, Cuneo, Gindo; 10 Oct. 2004; A. Maisi leg.; M. Isaia det. and coll.

SWITZERLAND • 1 ♀; Ticino, Genestrerio close to Mendrisio; 6–11 Oct. 1994; N. Patocchi leg.; A. Hänggi det.; NMB 2577b.

Diplocephalus permixtus (O. Pickard-Cambridge, 1871)
GERMANY • 2 ♀♀, 1 ♂; close to Wuppertal; 1984; Wunderlich det.; SMF 33430.

Diplocephalus picinus (Blackwall, 1841)
AUSTRIA • 1 ♂; Styria, Rothleiten; 3 May–4 Jun. 1995; C. Kropf leg. and det.; NMBE Ar95 • 2 ♀♀; Styria Laufnitzdorf; Jun. 1995; W. Paill and O. Winder leg.; C. Kropf det.; NMBE Ar6694 • 1 ♂; Styria Graz; 3 Jun. 1995; W. Paill and O. Winder leg.; C. Kropf det.; NMBE Ar6645.

SWITZERLAND • 1 ♂; Bern, Wohlen; 4–7 Jul. 1925; Bartels leg.; A. Hänggi det.; NMBE Ar2629.

Diplocephalus protuberans (O. Pickard-Cambridge, 1875)
ITALY • 1 ♂; Piemont, Cuneo, Alpi Maritimi, Valdieri; M. Isaia and Berelutta leg.; M. Isaia det. and coll.

Diplocephalus rostratus Schenkel, 1934
AUSTRIA • 1 ♂ (holotype); Tyrol, Ötztaler Alps; Aug. 1930; Schenkel leg. and det.; NMB 1509a • 1 ♀ (paratype); Tyrol, south side of the Amthorspitze at the Brenner; Aug. 1949; Schmötzer leg.; Schenkel det.; NMB 1509a.

Diplocephalus subrostratus (O. Pickard-Cambridge, 1873)
RUSSIA • 2 ♀♀, 2 ♂♂; river Norilsk Kharealath; 29 Aug. 1983; Eskov leg. and det.; SMF 36882.

Diplocephalus turcicus Brignoli, 1972
TURKEY • 1 ♀, 1 ♂ (paratypes); Burdur, Insuyu magarasi, grotta; 13 Aug. 1967; P. Brignoli and V. Sbordoni leg.; P. Brignoli det.; MHNG, MHNG-ARTO-0027059.

Diplocephalus uliginosus Eskov, 1988
RUSSIA • 1 ♀, 1 ♂ (paratypes); Siberia, Magadan area, Sibit-Tyellakh; 23 Aug. 1984; Y. Marusik leg.; Eskov det.; SMF 36887.

Erigonella hiemalis (Blackwall, 1841)
DENMARK • 1 ♂, 1 ♀; Zealand, Enemaerket, v. Naesbyholm; 19 Feb. 1997; J. Pedersen leg.; N. Scharff det.; ZMUC, NHMD1785383.

GERMANY • 1 ♀, 2 ♂♂; Berlin, Berlin-Friedrichshain; 20 Mar. 1977; B. von Broen leg. and det.; NMBE Ar1164.

Erigonella ignobilis (O. Pickard-Cambridge, 1871)
GERMANY – 2 ♂♂; Brandenburg, Uckermark, Lychen; 18 May 1998; B. von Broen leg. and det.; NMBE Ar2881 • 1 ♀; Dresden, Moritzburger Teiche; May 1979; S. Heimer leg. and det.; MHNG, MHNG-ARTO-0030876.

SWITZERLAND • 1 ♀; Aargau, Siggenthal; 1974; R. Maurer leg. and det.; NMB 792f (misidentified as *Glyphesis servulus*).

Erigonella subelevata (L. Koch, 1869)
SWITZERLAND • 3 ♀♀, 2 ♂♂; Grisons, Alp Flix, Salategnas. 28 Oct. 2003–24 May 2004; H. Frick leg. and det.; NMBE Ar5604 • 1 ♀; Grisons, Alp Flix, Salategnas; 24 Jul. 2005–21 Aug. 2005; P. Muff leg. and det.; NMBE Ar7656.

Glyphesis cottonae (La Touche, 1946)
GERMANY • 1 ♀, 1 ♂; Wesel; 18 Mar. 1956; Casemir leg.; H. Wiehle det.; SMF 18756. Male prosoma according to Wiehle (1960).

Glyphesis nemoralis Esyunin & Efimik, 1994
UKRAINE • 2 ♀♀, 1 ♂ (paratypes); Cherkassy area, Kanev state reserve; 25–29 May 1988; Golovatch and Penev leg.; Esjunin and Efimik det.; *Carpinus* forest; SMF 38882.

Glyphesis servulus (Simon, 1882)
SWITZERLAND • 2 ♀♀, 2 ♂♂; Basel; E. Schenkel leg. and det.; NMB 792a • 2 ♂♂, 1 ♀; Aargau, Siggenthal; 1974: R. Maurer leg. and det.; NMB 792f.

Glyphesis taoplesius Wunderlich, 1969
AUSTRIA • 1 ♂ (paratype); Gamig/Ötscher; Oct.; Ressel leg.; Wunderlich det.; SMF 23978. Females scored according to Wunderlich (1969), Loksa (1981) and Blick & Szinetar (1996).

Janetschekia monodon (O. Pickard-Cambridge, 1873)
AUSTRIA • 1 ♀, 1 ♂; Tyrol; 1937; Reimoser det.; ex coll. L. Koch; SMF RII 7033.

Paraglyphesis polaris Eskov, 1991
RUSSIA • 2 ♀♀, 2 ♂♂ (paratypes); Siberia, Taimyr autonomous Okrug (Area), Putorana Plateau, Lake Ayan; 16 Aug. 1983; K. Eskov leg. and det.; coll. A. Tanasevitch.

Saloca diceros (O. Pickard-Cambridge, 1871)
AUSTRIA • 1 ♀; Gastein, Kötschachtal; 13 Jun.–5 Jul. 1994; V. Relys leg. and det.; NMBE Ar3290 • 1 ♂; Steiermark, Grimming; 22. Sept. 1985; C. Kropf leg.; A. Rohner det.; NMBE Ar2188 • 1 ♂; Gastein, Kötschachtal, Salzburg, Prossau; 25 May– 17 Jun. 1993; V. Relys leg. and det.; NMBE Ar3289.

Saloca gorapaniensis Wunderlich, 1983
NEPAL • 1 ♂; southern Annapurna massive; 10–14 Dec. 1969; Martens leg.; Wunderlich det.; SMF 31715 • 1 ♀; Thakkola, Chadziou Khola; Oct. 1969; Martens leg.; Wunderlich det.; SMF 31714.

Saloca khumbuensis Wunderlich, 1983
NEPAL • 1 ♀, 1 ♂ (paratypes); Khumbu, Lughla; 22–23 Oct. 1970; Martens leg.; Wunderlich det.; SMF 31712.

Saloca kulczynskii Miller & Kratochvíl, 1939
POLAND • 2 ♀♀, 1 ♂; Gorce region, valley of Jaszcze; 2 Sep. 1986; Jedryczkowski and Starega leg.; Starega det.; SMF 36804.

Savignia birostra (Chamberlin & Ivie, 1947)
USA • 5 ♀♀, 5 ♂♂; Alaska, Alaska, Kodjak Island; NMBE Ar6744.

Savignia frontata Blackwall, 1833
GERMANY • 1 ♀, 2 ♂♂; Mecklenburg, Göldenitzer moor; Rabeler leg.; NMB 1611c.

Savignia harmsi Wunderlich, 1980
SPAIN • 1 ♂ (holotype); Málaga, 7 Oct. 1972; Harms leg.; J. Wunderlich det.; SMF 29187 • 2 ♀♀ (paratypes); same data as for preceding; SMF 29188.

Savignia producta Holm, 1977
RUSSIA • 1 ♀, 1 ♂; Komi Aut. Republic, Vorgashor; Jul. 1984; Tanasevitch leg.; Eskov det.; SMF 36885.

Savignia saitoi Eskov, 1988
RUSSIA • 1 ♂ (paratype); Sakhalin, Kunashir Island, Otrandnoye; 19 Sep. 1987; A.M. Basarukin leg.; coll. Y.M. Marusik • 1 ♀; Southeast port, Mereya river; 28 Jul. 2001; Y.M. Marusik leg. and coll.

Savignia zero Eskov, 1988
RUSSIA • 2 ♀♀, 2 ♂♂; NE Sibiria, 25 km E of Magadan; 18 Sep. 1990; Marusik leg. and det.; SMF 39671.

Outgroup (11 taxa)

Linyphiinae
Bolyphantes luteolus (Blackwall, 1833)
SWITZERLAND • 1 ♀, 1 ♂; Grisons, Sur, Alp Flix, Salategnas; 28 Oct. 2003–24 May 2004; H. Frick leg. and det.; NMBE Ar4630.

Linyphia triangularis (Clerck, 1757)
AUSTRIA • 1 ♀; Styria, Northeast Frohnleiten; 4 Aug. 1995; NMBE Ar271 • 1 ♂; same data as for preceding; NMBE Ar272.

Tenuiphantes tenuis (Blackwall, 1852)
AUSTRIA • 1 ♀; Styria, Graz; 10 Jul. 1995; Paill and Winder leg.; NMBE Ar6654 • 1 ♂; same data as for preceding; NMBE Ar6661.

Erigoninae
Dismodicus bifrons (Blackwall, 1841)
GERMANY • 3 ♀♀, 2 ♂♂; Thuringia, Südharz, Brandesbachtal; 12–27 May 1996; Taeger leg.; B. von Broen det.; NMBE Ar1192.

Dismodicus elevatus (C.L. Koch, 1838)
SWITZERLAND • 4 ♀♀, 4 ♂♂; Bern, Bremgartenwald; H. Frick. leg., det. and coll.

Entelecara acuminata (Wider, 1834)
AUSTRIA • 1 ♂; Styria, Gleichenberg; 1 Jun. 1991; C. Kropf leg. and det.; NMBE Ar 3771 • 2 ♀♀; Lower Austria, Eckhardsau; 7 Jun.1985; C. Kropf leg. and det.; NMBE Ar3990.

Entelecara erythropus (Westring, 1851)
AUSTRIA • 3 ♂♂; Styria, Rothleiten; 4 Jun. 1995; C. Kropf leg. and det.; NMBE Ar172 • 3 ♀♀; same data as for preceding; NMBE Ar173.

Hilaira excisa (O. Pickard-Cambridge, 1871)
AUSTRIA • 1 ♀; Styria, Oppenberg; 12 Jul. 1995; NMBE Ar1265.

GERMANY • 1 ♂; Mecklenburg, Poppendorf/Rostock; 16 Jun. 1984; NMBE Ar1097.

Hypomma bituberculatum (Wider, 1834)
GERMANY • 2 ♀♀, 3 ♂♂; Brandenburg, Criewen, Uckermark; 5–25 May 1995; M. Sommer leg.; B. von Broen det.; NMBE Ar553.

Pelecopsis elongata (Wider, 1834)
SWITZERLAND • 1 ♂; Grisons, Sur, Alp Flix, Salategnas; 16 May–14 Jun. 2003; H. Frick leg. and det.; NMBE Ar4869 • 1 ♀; same data as for preceding; NMBE Ar4860.

Walckenaeria acuminata Blackwall, 1833
GERMANY • 1 ♂; Berlin, Friedrichsfelde; 8 Dec. 1993; B. von Broen leg. and det.; NMBE Ar620 • 1 ♀; Brandenburg, Eberswalde; 13 May 1996; B. von Broen leg. and det.; NMBE Ar1130.

Specimen examination

Specimens were examined in 80% ethanol under a Leica MZ16 stereo microscope. Male palps were dissected at the femur-patella joint. Photographs were taken using Light Microscopy (LM) and Scanning Electron Microscopy (SEM). LM photos were taken with a Leica DMC5400 digital camera connected to LAS ver. 4.13 software for habitus photos, and a Keyence Digital Microscope VHX-X1 for images of genital features. Stacks of photos were combined using Zerene Stacker ver. 1.04 software. Some samples were illustrated with a Leica MZ16 stereo microscope and or an Axioplan 2 compound microscope each connected to a camera lucida. Drawings were performed by hand. Scanned drawings were edited in Adobe Photoshop 7.

For the SEM specimens were prepared as follows: first they were dehydrated in a dilution series from 80% to 100% ethanol using 5% steps for 10 minutes each. They remained in absolute ethanol for 2–4 hours and were subsequently cleaned with ultrasound for approximately 1 minute before drying in a BAL-TEC CPD 030 critical point dryer. Later, specimens and their dissected parts were mounted on aluminium rivets with transparent nail polish and subsequently coated with a 20 nm thick layer of platinum/palladium using a JEOL JFC-2300HR high resolution fine coater. Specimens were photographed with a JEOL JSM 840 scanning electron microscope with digital image processing equipment (JEOL SemAfore).

Character scoring

Specimen preparation and character scoring follows the methodology described in Frick & Muff (2009) and Frick *et al.* (2010). In total, we scored 269 morphological characters for the 70 taxa included, almost four times more characters than species representing a total of 18 830 homology statements. 175 characters are first described here. Another 94 characters from former analyses (Hormiga 2000; Arnedo *et al.* 2004; Miller & Hormiga 2004) on linyphiid relationships and especially erigonine spiders turned out to be informative for the current study and were also included. To account for differences at the species level, a few scorings mentioned in Frick *et al.* (2010) had to be adjusted. They are discussed in the character descriptions. All new characters are defined and discussed below in the characters description section. The character descriptions of Hormiga (2000), Miller & Hormiga (2004) and Arnedo *et al*. (2009) were omitted. The data matrix (Supp. file 1) was compiled and managed in Mesquite ver. 2.74 (Maddison & Maddison 2010).

Analysis

Maximum parsimony (MP) analyses were performed in TNT ver. 1.1 (Goloboff *et al.* 2008a), using heuristic methods ("traditional search") for both equal and implied weighting. We applied the same procedures and batches as in Frick & Scharff (2014).

Equal weighting

Traditional tree searches used tree bisection-reconnection (TBR) based on the standard settings for starting trees (commands: *mult = tbr replic 1000 hold 1000*). Branches with no possible support were collapsed ("rule 3", min. length = 0) during searches and condensed after the tree search (commands: *collapse 1; collapse [;*). All characters were unordered. To check for missing most parsimonious trees, we broadened the search by changing the number of replicates and the number of trees kept per replicate (100 000:10, 10 000:500, 10 000:100, 1000:1000, 100:10 000, 10:100 000). We also repeated the analysis using a TBR-ratchet (commands: *ratchet: iter 1000; mult = ratchet replic 1000 tbr hold 1000;*). The resulting trees were checked for zero-length branches (Coddington & Scharff 1994).

Implied weighting

We reran the analysis with 1000 replications holding 1000 trees each for the implied weights analysis (commands: *piwe = 1; mult = tbr replic 1000 hold 1000;*). The constant of concavity (*k*) which modulates the weights against homoplasies varied from relatively high (homoplastic characters are mildly penalized) to low (homoplastic characters are highly penalized) *k*-values, i.e., 1–50, 100, 250, 500 and 1000 (Goloboff 1993; Goloboff *et al.* 2008b). Above $k = 27$, trees were effectively identical to results from equal weights analyses (tree length = 1025).

Optimisation, support values, synapomorphies and editing

TNT was also used to calculate support values for the preferred tree. To calculate Bremer support (BS; Bremer 1994) a rough precedent search setting suboptimal to 50 was made to find the upper limit of supports. The more thorough search was based on the original equal weight trees. Subsequently, the suboptimal was increased stepwise by 1 up to 16 and so was the tree buffer by 5000 for 16 cycles

(commands: *mult 50; sub 1; hold 5000; bbreak = fillonly; sub 2; hold 10000; bbreak = fillonly; sub 3; hold 15000; bbreak = fillonly; ...; sub 16; hold 80000; bbreak = fillonly; bsupport;*).

For the jackknife support (JK; Farris *et al.* 1996), we performed 1000 jackknife pseudoreplicates of 100 random sequence additions, keeping 10 trees, each using TBR as swapping algorithm (commands: *mult: noratchet repl 100 tbr hold 10; resample jak repl 1000 freq from 0 [mult];*). Values above 50% threshold are given for the equal weights tree.

We used WinClada ver. 1.00.08 (Nixon, 2002) to study character optimisations on the preferred tree. Ambiguous character optimisations were resolved to favour reversal or secondary loss over convergence (ACCTRAN or Fast Optimisation in WinClada).

Mesquite ver. 2.73 (Maddison & Maddison 2010) was used to build and edit the character matrix, to reconstruct character evolution, to calculate tree length, the ensemble consistency index (CI) and the ensemble retention index (RI). The consensus tree was exported from TNT including Bremer support values. All figures were finished with Adobe Illustrator 9.0.

Maximum likelihood

Maximum likelihood (ML) analyses were performed with IQ-TREE ver. 1.6.12 (Trifinopoulos *et al.* 2016). We used the MK unordered model of evolution and nodal support was assessed using ultrafast bootstrap (Hoang *et al.* 2018) with 10 000 replicates and SH-aLRT branch test using 1000 iterations.

Tracing character history

We traced the character history using the "Parsimony Ancestral States" method in Mesquite ver. 3.70 of the cephalic modifications that show a great variation among the *Savignia* genus group taxa.

Nomenclatural changes

We redefine genera based on synapomorphies of the corresponding well-supported clades from the phylogenetic analysis. We also use inferred synapomorphies to define species groups within the three most species-rich genera, i.e., *Diplocephalus*, *Savignia* and *Araeoncus*, to simplify future revisions of these genera. Nearly one hundred taxa from the *Savignia*-group were not scored for the current analysis. Most of these taxa are well described and illustrated and it is possible to assign them to species groups within the respective genera based on shared synapomorphies. Some species could not be assigned to species groups and affinities of those were tentatively discussed. We prefer to keep nomenclatural changes at a low number, since linyphiid systematics already suffers from too many described genera of uncertain phylogenetic placement. Therefore, nomenclatural consequences resulted only in taxa that could unambiguously be assigned to a genus within the *Savignia*-group (see Table 9). Taxa with ambiguous phylogenetic positions are provisionally kept in their current genera. The only exception is *Saloca ryvkini* Eskov & Marusik, 1994 that could be transferred to *Walckenaeria* Blackwall, 1833 based on phenotypic evidence from the literature.

Abbreviations for morphological terms

ALE = anterior lateral eyes
AME = anterior median eyes
bRP = basal radical process (ch159)
CO = column (ch96)
CPA = cymbium prolateral basal glabrous apophysis (ch60)
CRA = cymbial retrobasal thin apophysis (ch54)
cRP = central radical process (ch152)
CRP = cymbial retrobasal process (ch53)

DP = dorsal plate
dRP = dorsal radical process (ch139)
dSTA = distal suprategular apophysis (ch90)
dTP = dorsal tibial protuberance (ch43)
E = embolus (ch105)
EM = embolic membrane (ch99)
ETO = embolic transparent outgrowth (ch116)
iSTA = inner suprategular apophysis (ch84)
mSTA = marginal suprategular apophysis (ch78)
oSTA = outer suprategular apophysis (ch82)
PC = paracymbium (ch61)
PCrP = paracymbium retrolateral process (ch62)
PCvP = paracymbium ventral process (ch63)
PLE = posterior lateral eyes
PME = posterior median eyes
pRP = prolateral radical process (ch157)
PT = protegulum (ch72)
pTA = prolateral tibial apophysis (ch7)
R = radix
rdL = retrolateral distal lobe (ch38)
rpTA = retrolateral proximal tibial appendix (ch44)
rRP = retrolateral radical process (ch155)
rTA = retrolateral tibial apophysis (ch28)
RTdT = radical tailpiece, distal tooth (ch170)
RTP = radical tailpiece (ch160)
RTpT = radical tailpiece, ventral to prolateral tooth (ch168)
RTrP = radical tailpiece, dorsal to retrolateral process (ch169)
S = spermathecae (ch193)
SB = sclerotised band
SPT = suprategulum (ch77)
ST = subtegulum
SU = sulcus (ch212)
T = tegulum
TS = tegular sac (ch75)
VP = ventral plate
vRP = ventral radical process (ch130)
vTP = ventral tibial process (ch47)

Institutional abbreviations

MHNG = Natural History Museum of Geneva, Switzerland
MRAC = Royal Museum for Central Africa, Tervuren, Belgium
NMB = Natural History Museum Basel, Switzerland
NMBE = Natural History Museum Bern, Switzerland
SMF = Senckenberg Museum Frankfurt, Germany
ZMUC = Natural History Museum of Denmark, Copenhagen, Denmark

Private collections abbreviations

E.G. = E. Gavish-Regev
M.I. = M. Isaia
A.T. = A. Tanasevitch

Characters and character state descriptions

The phylogenetic analyses are based on 269 characters of which 175 are described here for the first time and marked with brackets. The other characters were described and discussed in detail in other papers and referred to in abbreviation as follows: A09 (Arnedo *et al.* 2009), MH04 (Miller & Hormiga 2004), H00 (Hormiga 2000), FS14 (Frick & Scharff 2014) followed by the character number, e.g., H00-28 refers to character 28 in the matrix of Hormiga (2000). Character where a state has been deleted, added, or modified is indicated with an asterisk (*). To keep the manuscript short, illustrations are only given for characters that cannot be described based on published illustrations (Figs 1–24). Most can be found elsewhere (Wiehle 1960; Merrett 1963; Thaler 1972; Millidge 1977; Tanasevitch 1985a, 1987; Roberts 1987; Eskov 1988; Hormiga 2000). Directions are used as defined in Frick & Scharff (2014: fig. 8a). Node numbers mentioned in this section refer to the preferred tree (Fig. 25).

Male genital morphology

Palpal patella

1. Palpal patella, distal dorsal macroseta

0: absent (Wiehle 1960: fig. 429, *Araeoncus humilis*).
1: present (Wiehle 1960: fig. 932, *Diplocephalus cristatus*). MH04-77*.

Weak setae are scored as present (e.g., *Diplocephalus dentatus*, *Savignia frontata*), if their position and the typical right-angled direction suggested homology with macroseta. Vestigial macrosetae are also observed on the male leg tibia (e.g., see Roberts 1987: fig. 37c, *Diplocephalus picinus* with leg formula 2211 or 0011).

2. Palpal patella, distal dorsal macroseta, strength

0: weak to moderate (Wiehle 1960: figs 914–915, *Gongylidiellum vivum* (O. Pickard-Cambridge, 1875)).
1: very strong (Wiehle 1956: fig. 266, *Bolyphantes luteolus*). MH04-78, A09-64.

Moderate macrosetae resemble body setae in size and length, while very strong macrosetae are much thicker.

3. Palpal patella dorsal length

0: less than twice as long as wide (Roberts 1987: fig. 36c, *Savignia frontata*).
1: between 2.1 and 3.4 times as long as wide (Roberts 1987: fig. 40b, *Araeoncus crassiceps*).
2: more than 3.5 times as long as wide (Roberts 1987: fig. 10f, *Dicymbium tibiale*). MH04-76*, A09-63*.

State 2 was added to account for the considerably elongated patella found in *Dicymbium* and two species of *Diplocephalus*.

Palpal tibia

4. Palpal tibia, prolateral trichobothria

0: two (H00: fig. 19b, *Leptorhoptrum robustum* (Westring, 1851)).
1: one (Fig. 1A, *Alioranus pastoralis*; Eskov 1988: fig. 85, *Savignia zero*).
2: zero (H00: fig. 26e, *Sisicus apertus* (Holm, 1939)). MH04-73, H00-30, A09-61*.

The loss of prolateral trichobothria is an ambiguous synapomorphy of *Glyphesis* (node 22), also lost in *Savignia harmsi*.

5. Palpal tibia, retrolateral trichobothria

0: four.
1: three (H00: fig. 19a, *Leptorhoptrum robustum*).

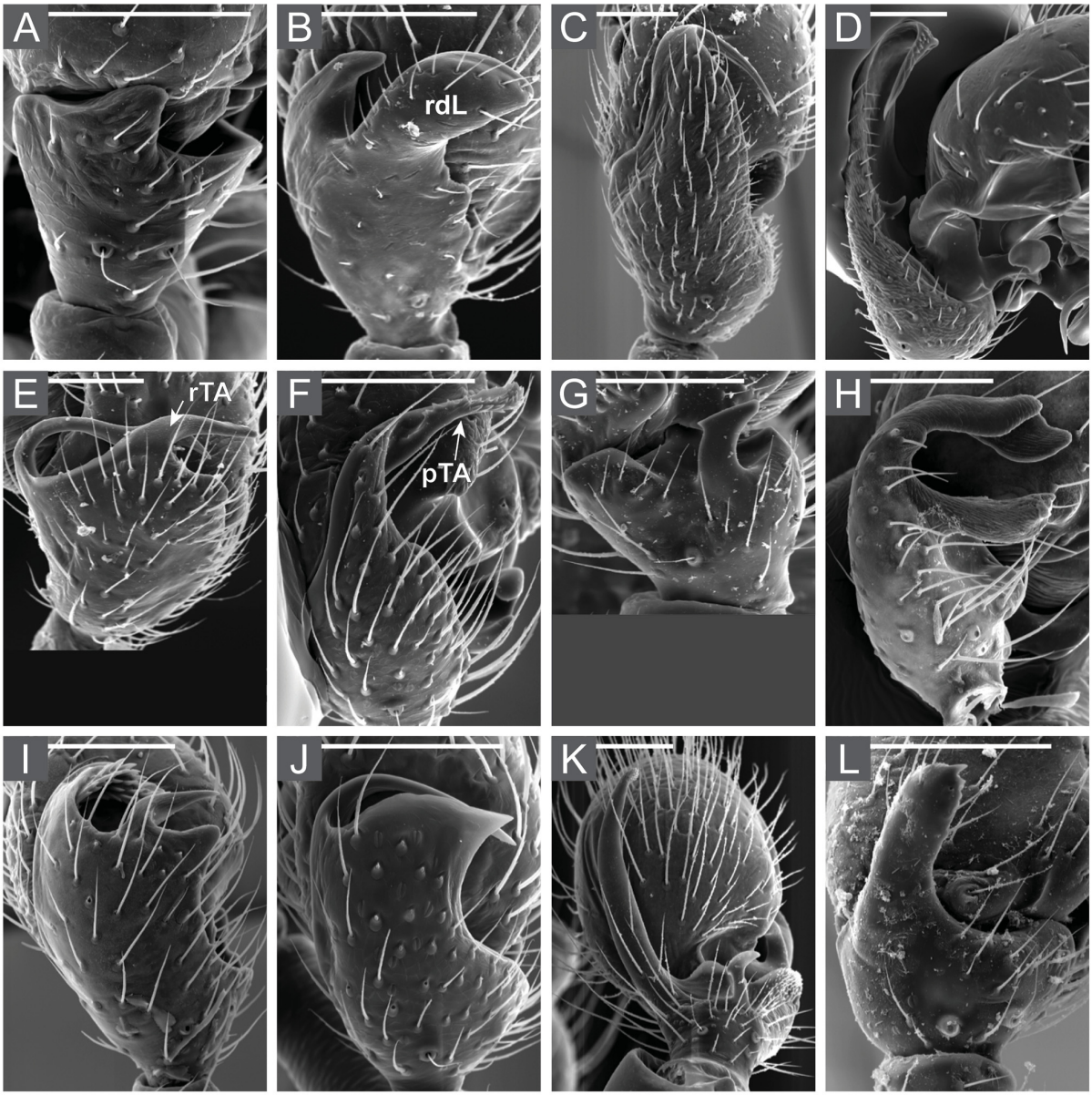

Fig. 1. Scanning Electron Microscope pictures of different male palpal tibial apophyses in dorsal view. **A**. *Alioranus pastoralis* (O. Pickard-Cambridge, 1872) (2695-3702; coll E.G.). **B**. *Araeoncus humilis* (Blackwall, 1841) (Ar3186; NMBE). **C**. *Dicymbium nigrum* (Blackwall, 1834) (Ar637; NMBE). **D**. *Dicymbium tibiale* (Blackwall, 1836), retrolateral view (11430; ZMUC). **E**. *Diplocephalus latifrons* (O. Pickard-Cambridge, 1863), (Ar1262; NMBE). **F**. *Diplocephalus picinus* (Blackwall, 1841) (Ar6645; NMBE). **G**. *Dismodicus bifrons* (Blackwall, 1841) (Ar1192; NMBE). **H**. *Entelecara erythropus* (Westring, 1851) (Ar172; NMBE). **I**. *Erigonella hiemalis* (Blackwall, 1841) (ZMUC). **J**. *Erigonella ignobilis* (O. Pickard-Cambridge, 1871) (Ar2880; NMBE). **K**. *Hypomma bituberculatum* (Wider, 1834) (Ar553; NMBE). **L**. *Saloca diceros* (O. Pickard-Cambridge, 1871) (Ar3289; NMBE). Abbreviations: see Material and methods. Scale bars = 100 µm.

2: two (Eskov 1988: fig. 21, *Diplocephalus mirabilis*; Fig. 1H, *Entelecara erythropus*).
3: one (Fig. 1A, *Alioranus pastoralis*; Eskov 1988: fig. 85, *Savignia zero*). MH04-74, H00-31, A09-62.

(6). Palpal tibia, general conformation

0: two long fingers (Thaler 1971: fig. 3, *Erigonella subelevata*; Fig. 1H, *Entelecara erythropus*).
1: two short fingers on broad base (Fig. 1I; Wiehle 1960: fig. 1030, *Erigonella hiemalis*; Fig. 1E, *Diplocephalus latifrons*).
2: one short finger on broad base (Roberts 1987: fig. 36d, *Diplocephalus cristatus*; Fig. 1B, *Araeoncus humilis*).
3: one long finger (Roberts 1987: fig. 36c, *Savignia frontata*; Fig. 1C, *Dicymbium nigrum*).
4: one short finger (Fig. 1A, *Alioranus pastoralis*).

Only the prolateral and the retrolateral tibial apophyses are considered for the general conformation, lobes and smaller appendices are not. Species with other conformations were coded as inapplicable for this character. Based on the comparison of very closely related taxa, several types of tibial apophyses were found and defined as separate statements of homology. In most of the scored ingroup taxa, the tibia is distally enlarged and bears one or more sclerotised (and or lobe-like) structures on its retrolateral, prolateral or distal section.

Palpal tibia prolateral apophysis

7. Prolateral tibial apophysis (pTA)

0: absent (H00: plates 7A and C, *Linyphia triangularis*).
1: present (Fig. 1F, *Diplocephalus picinus*).

MH04-67, H00-28, A09-57. H00 discusses tibial apophyses in detail. If the tibia has a single apophysis, it is a prolateral tibial apophysis unambiguously supporting Erigoninae in MH04.

Several apophyses arise from the male tibia in erigonines, making homology assessments difficult. Every projection arising from a *Linyphia* Latreille, 1804 type of tibia (e.g., H00: pl. 7a, c) is a tibial apophysis. Only highly sclerotised structures arising from the prolateral side of the tibia (or a non-sclerotised enlargement of the tibia) were scored as a prolateral tibial apophysis. *Hilaira excisa* and *Dismodicus* Simon, 1884 lack a prolateral apophysis but instead have other tibial apophyses (see discussion of the pseudo prolateral tibial apophysis character 11 and the retrolateral sac character 41). This character is a synapomorphy of node 4 with one reduction in node 15.

(8). Palpal tibia, prolateral sclerotised band

0: absent.
1: present (Fig. 19B–C; Roberts 1987: fig. 36c–d, *Savignia frontata*, *Diplocephalus cristatus*).

This is a highly sclerotised band with honey-like colour (differing from the pale surface of the remaining tibia) that runs along the prolateral margin of the prolateral tibial apophysis. It is at least broader than the diameter of the cuticle but can cover nearly half the tibia. Also, taxa without a tibial apophysis can have sclerotised bands at the distal dorsal margin of the tibia (e.g., *Linyphia triangularis*). They are considered to have both a prolateral and a retrolateral sclerotised band.

(9). Palpal tibia, prolateral sclerotised band, proximal width

0: about as broad proximally as distally (Fig. 18C; Roberts 1987: fig. 40b, *Araeoncus crassiceps*).
1: proximally broader than distally (Fig. 19B; Roberts 1987: fig. 36d, *Diplocephalus cristatus*).

In some taxa, the sclerotised band is considerably broadened proximally, exceeding nearly half the tibia. In dorsal view a circular sclerotised structure often shines through the area of the proximally broadened

band of the tibial apophysis. This is the junction of the tibia and the subtegulum (Roberts 1987: fig. 36d, *Diplocephalus cristatus*). This character is an ambiguous synapomorphy of node 21 with four reductions and one secondary gain.

(10). Palpal tibia, prolateral sclerotised band, distal expansion

0: restricted to prolateral margin (Fig. 19C; Roberts 1987: fig. 36c, *Savignia frontata*).
1: tip distally free standing from the margin (Fig. 19D; Wunderlich 1980a: fig. 47, *Savignia harmsi*).

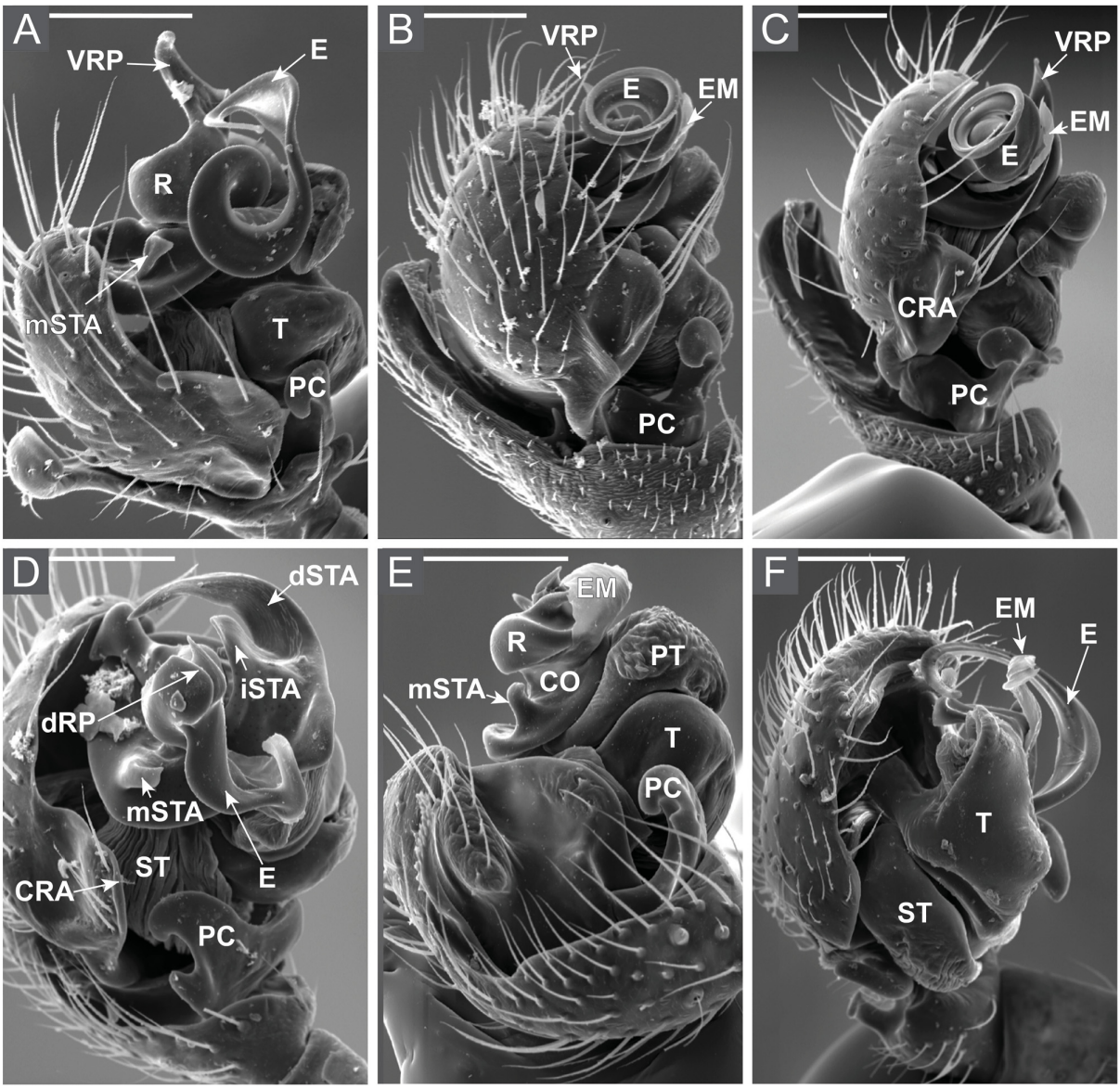

Fig. 2. Scanning Electron Microscope pictures of the male palp in retrolateral view. **A**. *Araeoncus humilis* (Blackwall, 1841) (Ar3186; NMBE). **B**. *Dicymbium nigrum* (Blackwall, 1834) (Ar637; NMBE). **C**. *Dicymbium tibiale* (Blackwall, 1836) (11430; ZMUC). **D**. *Diplocephalus latifrons* (O. Pickard-Cambridge, 1863) (Ar1262; NMBE). **E**. *Diplocephalus picinus* (Blackwall, 1841) (Ar6645; NMBE). **F**. *Dismodicus bifrons* (Blackwall, 1841) (Ar1192; NMBE). Abbreviations: see Material and methods. Scale bars = 100 μm.

The free standing tips can either form a small tip emerging from the prolateral side of the tibial apophysis (e.g., Wunderlich 1980a: fig. 47, *Savignia harmsi*) or else are much larger than the prolateral apophysis, exceeding the distal end of the tibial apophysis (e.g., Tanasevitch 1987: fig. 72, *Archaraeoncus proscipiens*). This sclerotised and glabrous structure is an appendix of the prolateral sclerotised band and/or the prolateral tibial apophysis, emerging from the prolateral side of the tibial apophysis. It is usually smaller, less sclerotised and thinner than the prolateral tibial apophysis and hidden behind the prolateral tibial apophysis as in, e.g., *Araeoncus victorianyanzae* and *Diplocephalus lusiscus* (i.e., it is not illustrated in Wiehle 1963: figs 31a, 33, *Diplocephalus lusiscus*). It emerges from the inner (ventral) rather than from the outer (dorsal) side of the tibial apophysis (e.g., Tanasevitch 1987: fig. 72, *Archaraeoncus proscipiens*). The inner side (proximal and or distal part) of the prolateral apophysis is often covered with papillae. These inner papillae are also present on the inside of the freestanding tip of the sclerotised band in *Araeoncus victorianyanzae* and some other species. State 1 emerges six times independently in the current analysis suggesting that it includes several non-homologous structures.

(11). Palpal tibia, pseudo prolateral tibial apophysis

0: absent (Roberts 1987: fig. 36c, *Savignia frontata*; Fig. 1B, *Araeoncus humilis*).
1: present (H00: fig. 7g, *Dismodicus decemoculatus* (Emerton, 1882); Fig. 1G, K, *Dismodicus bifrons*, *Hypomma bituberculatum*).

Sclerotised tibial apophyses arise from the margin of the tibia or else from the non-sclerotised tibial apophysis (e.g., Roberts 1987: fig. 36d, *Diplocephalus cristatus*). However, in *Dismodicus* (e.g., H00: fig. 7g, *Dismodicus decemoculatus*; Fig. 1G, *Dismodicus bifrons*) the single tibial apophysis emerges from the tibia, well separated from the margin around the joint to the cymbium. It is highly sclerotised and distally directed. This apophysis has so far been considered as homologous to the prolateral tibial apophysis (e.g., MH04). However, *Hypomma bituberculatum* has an apophysis that is very similar to what is seen in *Dismodicus bifrons* (compare Fig. 1G, K) but additionally, it has an apophysis at the prolateral side of the tibia, looking similar to what is found in *Hilaira excisa* (e.g., H00: pl. 33b).

Other authors considered this highly sclerotised apophysis as prolateral and retrolateral tibial apophysis in *Dismodicus* and *Hypomma*, respectively (*Dismodicus* in MH04; both genera in Frick *et al.* 2010). We considered the similar form to be a more important indicator of homology than the relative position and recoded these two species correspondingly. This is a synapomorphy of node 14.

(12). Prolateral tibial apophysis, retrobasal process

0: absent (Fig. 19C; Roberts 1987: fig. 36c, *Savignia frontata*).
1: present, blunt (Fig. 19E; Wiehle 1960: "c" in fig. 1147, *Diplocephalus dentatus*).
2: present, pointed (Fig. 19F; Wiehle 1967: fig. 29, above the pTA, *Diplocephalus helleri*).

A blunt process emerges from the base of the prolateral apophysis in *Diplocephalus dentatus*. It is bifurcate with one very large arm (with a papillate tip) and a second, short arm. Both are as pale and glabrous as the prolateral tibial apophysis and share a common origin with the prolateral tibial apophysis on the tibia (Fig. 19E). The presence of papillae at the tip of this structure argues for it being derived from the prolateral tibial apophysis that also bears such papillae.

A smaller sclerotised process is also present in *Entelecara acuminata* (see, e.g., Wiehle 1960: fig. 651). The retrolateral origin of this apophysis is sometimes difficult to see: the prolateral tibial apophysis of *Diplocephalus helleri* (Fig. 19F; Wiehle 1967: fig. 29) is twisted towards the ventral side of the tibia so that the basal process seems to be prolateral even though it emerges from the retrolateral side of the prolateral tibial apophysis. This process is slightly shifted inwards and prolaterally in *Diplocephalus turcicus*.

(13). Prolateral tibial apophysis, prolateral sickle

0: absent (Fig. 19C; Roberts 1987: fig. 36c, *Savignia frontata*).
1: present (Fig. 19P; Wiehle 1960: fig. 1121, pictured with dots, *Glyphesis servulus*).

This is a sickle-shaped outgrowth of the prolateral band. It is a synapomorphy of the distal *Glyphesis* species within node 24.

(14). Prolateral tibial apophysis, distal part dorsal texture

0: setose, like the cymbium (Fig. 1L; Roberts 1987: fig. 33f, *Saloca diceros*).
1: glabrous, no setae (Fig. 1B, *Araeoncus humilis*; Roberts 1987: fig. 36d, *Diplocephalus cristatus*).
2: papillate (Fig. 1I; Wiehle 1960: fig. 1030, *Erigonella hiemalis*).
3: ridged (Fig. 19N, *Glyphesis cottonae*).
4: scaled (Figs 3D, 19P, *Glyphesis servulus*).

In some taxa the prolateral tibial apophysis is twisted so that the inside (ventral side) is turned dorsally and vice versa. Also, in these cases the dorsal side should be scored and not the ventral side. One example is *Diplocephalus picinus* with papillae at the inside that seem to be outside due to the twisted conformation (Fig. 1F).

There are different types of papillae present on different parts of the prolateral tibial apophysis. It is not clear if they are homologous. Therefore, separate characters were defined for the minute ventral inside-papillae (character 24) and for the marginal papillae (character 15). *Erigonella subelevata* and *Erigonella hiemalis*, have very large papillae arising from both the ventral and the dorsal side of the prolateral tibial apophysis. Only one more species, *Diastanillus pecuarius*, has small dorsal papillae (Thaler 1969: fig. 31). These are like the ventral inside-papillae (character 24) that are also present in this species.
The texture can vary also among closely related taxa: in *Glyphesis* the tip of the prolateral apophysis shows ridges (*Glyphesis cottonae*) or scales (*G. taoplesius*, *G. servulus*) or even scales together with small papillae at the tip (*G. nemoralis*).

(15). Prolateral tibial apophysis, papillate distal tip margin

0: absent (Fig. 1L, *Saloca diceros*).
1: present (Fig. 19G; Thaler 1970: fig. 3, *Diplocephalus rostratus*).

The dorsal (character 14) and the ventral (character 24) papillae are restricted to one or the other side, with some exceptions where the whole prolateral tibial apophysis is covered with papillae. The current character accounts for very small papillae arising from the distal margin of the prolateral tibial apophysis (altogether in four species).

The taxa in node 43 plus *Diplocephalus uliginosus* are very similar concerning this character: first, the tip of their prolateral tibial apophysis is broad rather than pointed and directed ventrally, which is extraordinary in the context of the current analysis (state 2 in character 19; e.g., Eskov 1988: fig. 15, *Diplocephalus marusiki*). Second, the remaining dorsal side of the tibial apophysis is glabrous in these species. Third, these species also have minute papillae at the ventral side of the prolateral tibial apophysis. These minute marginal papillae are very similar to those found at the inside of the prolateral tibial apophysis (character 24; e.g., Millidge 1977: fig. 125, *Araeoncus anguineus*) and might be homologous with them or derived from them. However, they are clearly different from the much more distinct papillae found on the dorsal side of the prolateral tibial apophysis and also from the papillae found in taxa with entirely papillate prolateral tibial apophysis (e.g., Fig. 1I; Wiehle 1960: fig. 1030, *Erigonella hiemalis*).

(16). Prolateral tibial apophysis, tip folded inwards with elongation

0: absent, tip unmodified.
1: present (Fig. 1H, *Entelecara erythropus*).

In distal view, the tip of the prolateral apophysis of *Entelecara erythropus* and *Walckenaeria acuminata* is folded inwards and bears an elongated inner tip.

(17). Prolateral tibial apophysis, tip folded outwards

0: absent, tip unmodified.
1: present (Fig. 19H; Thaler 1971: fig. 7, *Erigonella subelevata*).

The tip of the prolateral tibial apophysis of *Erigonella subelevata* and *Diplocephalus latifrons* is clearly folded outwards.

(18). Prolateral tibial apophysis, double folded

0: absent, not double folded.
1: present (Fig. 19I; Isaia 2005: fig. 4, *Diplocephalus arnoi*).

The entire prolateral tibial apophysis is folded. The margin protrudes inwards (Isaia 2005: fig. 4, *Diplocephalus arnoi*) and a thinner outwards folded outgrowth (with papillae at its tip) emerges from a ridge in the middle of the ventral proximal side of the prolateral tibial apophysis. This is a synapomorphy of node 55, uniting *Diplocephalus arnoi* and *D. pavesii.*

(19). Prolateral tibial apophysis, distal part, orientation

0: distal (Fig. 1L; Locket & Millidge 1953: 168c, *Saloca diceros*).
1: retrolateral (Fig. 1E, *Diplocephalus latifrons*; Roberts 1987: fig. 36c, *Savignia frontata*).
2: ventral (Fig. 19G, *Diplocephalus rostratus*; Eskov 1988: fig. 15, *Diplocephalus marusiki*).

The retrolateral direction is most widespread. The distal direction is limited to three nodes (12, 19 and 28) plus five single taxa while the ventrally-directed one is an ambiguous synapomorphy present in *Diplocephalus uliginosus* and node 43. State 2 describes a conformation where the prolateral tibia is bent (Thaler 1970: fig. 3, *Diplocephalus rostratus*) or even curled ventrally (e.g., Eskov 1988: fig. 28, *Diplocephalus montanus*).

(20). Prolateral tibial apophysis, distal part, form

0: plane (Fig. 1B, *Araeoncus humilis*; Roberts 1987: fig. 36c, *Savignia frontata*).
1: twisted (Fig. 19I, *Diplocephalus arnoi*; Fig. 1F; Roberts 1987: fig. 37c, *Diplocephalus picinus*).

Usually, the apophysis is bent on one or the other side but still in one plane. In some species the apophysis is twisted 180° so that the inner (ventral) side of the apophysis is visible in dorsal view.

(21). Prolateral tibial apophysis, ventral inside-tooth

0: absent.
1: present (Fig. 1D, *Dicymbium tibiale*; Fig. 17F; Wiehle 1960: fig. 337, *Dicymbium nigrum*).

The ventral inside-tooth is much smaller and emerges from the inside of the prolateral apophysis rather than from the membranous tissue, as does the larger distal tibial apophysis of MH04-71. It is also very similar to the distal tooth (MH04-69) but emerges from the inside of the prolateral tibial apophysis rather than from its margin as seen in, e.g., *Psylocymbium* (Miller 2007: fig. 172b). This is a synapomorphy of node 30 including *Dicymbium nigrum* and *Di. tibiale*.

(22). Prolateral tibial apophysis, distinct longitudinal ventral inside-ridge

0: absent or reduced to a very minor elevation or ridge.
1: distinct ridge present (Fig. 20A, *Diplocephalus cristatus*).

In most species, the inside of the prolateral tibial apophysis is not plane but has small elevations or small vertical or longitudinal ridges. In node 58 (*Diplocephalus cristatus* and *D. alpinus*) and in *Dicymbium libidinosum* a very distinct longitudinal ridge is visible.

(23). Prolateral tibial apophysis, proximal inner ridge

0: absent.
1: present (Fig. 19J; Tanasevitch 1987: fig. 91, small line right above the trichobothrium, *Caucasopisthes procurvus*).

This margin/ridge separates the tibia from the tibial apophysis (Tanasevitch 1987: fig. 91, small line right above the trichobothrium). It differs from the frequently found, less pronounced ridge connecting the prolateral tibial apophysis with the ventral margin of the tibia (Tanasevitch 1987: fig. 91, distinct line on the right side). This is an autapomorphy of *Caucasopisthes procurvus* and therefore phylogenetically uninformative.

(24). Prolateral tibial apophysis, ventral inside-papillae

0: absent.
1: present (Millidge 1977: fig. 125, *Araeoncus anguineus*; Fig. 20I; Wiehle 1960: figs 412, 414, *Saloca diceros*).

The ventral side of the prolateral apophysis sometimes bears a field of minute papillae. They can be well distinguished from the much larger ones found in, e.g., *Erigonella hiemalis* (Fig. 1I; Wiehle 1960: fig. 1030).

This papillate field differs in its position and range. Usually, it is a small area at the prolateral side of the tibial apophysis but it might be extended over the prolateral margin (Millidge 1977: fig. 125, *Araeoncus anguineus*) or the distal margin (Thaler 1969: fig. 31, *Diastanillus pecuarius*) to the dorsal side of the tibial apophysis. In *Araeoncus vaporariorum* the papillate area on the inside covers the entire area between the prolateral and the retrolateral side. The form of this area is also variable, e.g., it ranges from a longitudinal line (e.g., in *Diplocephalus picinus*) to a round area at the prolateral side (e.g., *Araeoncus anguineus*) or they occur on a protuberance at the prolateral margin (*D. lusiscus*). Despite their larger size, the dorsal and ventral papillae of *Erigonella subelevata* and *Erigonella hiemalis* were coded as ventral inside-papillae.

Palpal tibia appendices between prolateral- and retrolateral tibial apophysis

(25). Palpal tibia, inter pTA-rTA, long, strong macrosetae

0: absent (Fig. 1H; *Entelecara erythropus*).
1: present (Figs 3D, 19P; Wiehle 1960: fig. 1121, *Glyphesis servulus*).

These very long and thick macrosetae arise between the prolateral and the retrolateral tibial apophysis and are a synapomorphy of *Glyphesis taoplesius* and *Glyphesis servulus* (node 25). They are also present in *Glyphesis idahoanus* and *G. scopulifer* (Paquin & Dupérré 2003: figs 1051 and 1054, respectively) two North American species not included in the current analysis. *Paraglyphesis polaris* lacks these macrosetae but instead has long slightly sigmoidal setae at the same position.

(26). Palpal tibia, inter-pTA-rTA, tooth

0: absent (Fig. 1E; Wiehle 1960: fig. 950, *Diplocephalus latifrons*).
1: present (Fig. 19F; Wiehle 1967: fig. 29, *Diplocephalus helleri*; Eskov 1991b: fig. 2: *Paraglyphesis polaris*).

This tooth is situated at the base of the retrolateral tibial apophysis.

(27). Palpal tibia, distal spines

0: absent (Roberts 1987: fig. 36c, *Savignia frontata*).
1: present (Fig. 19L; Roberts 1987: 36e; Wiehle 1960: fig. 939b, *Diplocephalus permixtus*).

These are three considerably thickened but short setae with sclerotised bases on the retrolateral distal thickening (character 37). This is an autapomorphy of *Diplocephalus permixtus*.

Palpal tibia retrolateral apophysis

28. Retrolateral tibial apophysis (rTA)

0: absent (Fig. 1C, *Dicymbium nigrum*).
1: present (Figs 1E, H, *Diplocephalus latifrons*, *Entelecara erythropus*).

MH04-70, A09-59. The retrolateral tibial apophysis is a sclerotised apophysis arising from the margin of the tibia or the non-sclerotised tibial apophysis. The retrolateral tibial apophysis was only present if also a prolateral tibial apophysis was present. This apophysis is an ambiguous synapomorphy for three clades, *Entelecara* Simon, 1884, *Glyphesis* and *Erigonella* (nodes 9, 22 and 33 respectively) with only one reversal in *Erigonella ignobilis* (Fig. 1J).

(29). Palpal tibia, retrolateral socket

0: absent (Fig. 1I, *Erigonella hiemalis*).
1: present (Fig. 1H, *Entelecara erythropus*).

This socket is situated right below the retrolateral tibial apophysis and is a synapomorphy of *Entelecara* (node 9).

(30). Palpal tibia, retrolateral sclerotised band

0: absent.
1: present (Fig. 19A, *Diplocephalus cristatus*; Roberts 1987: fig. 40b, *Araeoncus crassiceps*).

This band is usually very narrow and considerably narrower than the prolateral band (character 8). To be scored as present the sclerotised part must be well visible and the glabrous margin has to be broader than the thickness of the cuticle. In some species the band does not run along the entire margin i.e., is restricted to its lower half (e.g., in *Diplocephalus helleri*).

(31). Retrolateral tibial apophysis, distal part texture

0: setose, like the cymbium (Fig. 19M, *Dicymbium libidinosum*).
1: glabrous, no setae (Fig. 1I, *Erigonella hiemalis*).
2: scaled (Fig. 1H, *Entelecara erythropus;* Fig. 3D, *Glyphesis servulus*).

The setose apophysis is autapomorphic for *Dicymbium libidinosum*, the glabrous one is synapomorphic for node 26 but is only present in *Erigonella* (node 33) (as an artifact of inapplicables considering fast character optimisation) and the scaled type is found in *Entelecara* (node 9) and in *Glyphesis* (node 22).

(32). Retrolateral tibial apophysis, initial orientation

0: distal (Fig. 1E; Roberts 1987: fig. 37a, *Diplocephalus latifrons*).
1: retrolateral (Fig. 1H; Roberts 1987: fig. 11d, *Entelecara erythropus*).
2: towards the inside (Fig. 19N; Roberts 1987: fig. 35d, *Glyphesis cottonae*).

The distally facing type is synapomorphic for node 31 although it is only present in *Erigonella* (node 33) (as an artifact of inapplicables considering fast character optimisation), the retrolateral state is found in *Entelecara* (node 9), in *Dicymbium libidinosum* and in *Glyphesis* without *Glyphesis cottonae* (node 22) which has an autapomorphous inside facing retrolateral tibial apophysis (also present in *Glyphesis asiaticus* (Eskov 1989: figs 1–2) which is not included in the current analysis) and the towards the inside state is an autapomorphy of *Glyphesis cottonae* in this analysis.

(33). Retrolateral tibial apophysis, distal part direction

0: distal (Fig. 19M, *Dicymbium libidinosum*).
1: retrolateral (Fig. 1H; Roberts 1987: fig. 11d, *Entelecara erythropus*).
2: prolateral (Fig. 19N; Roberts 1987: fig. 35d, *Glyphesis cottonae*).

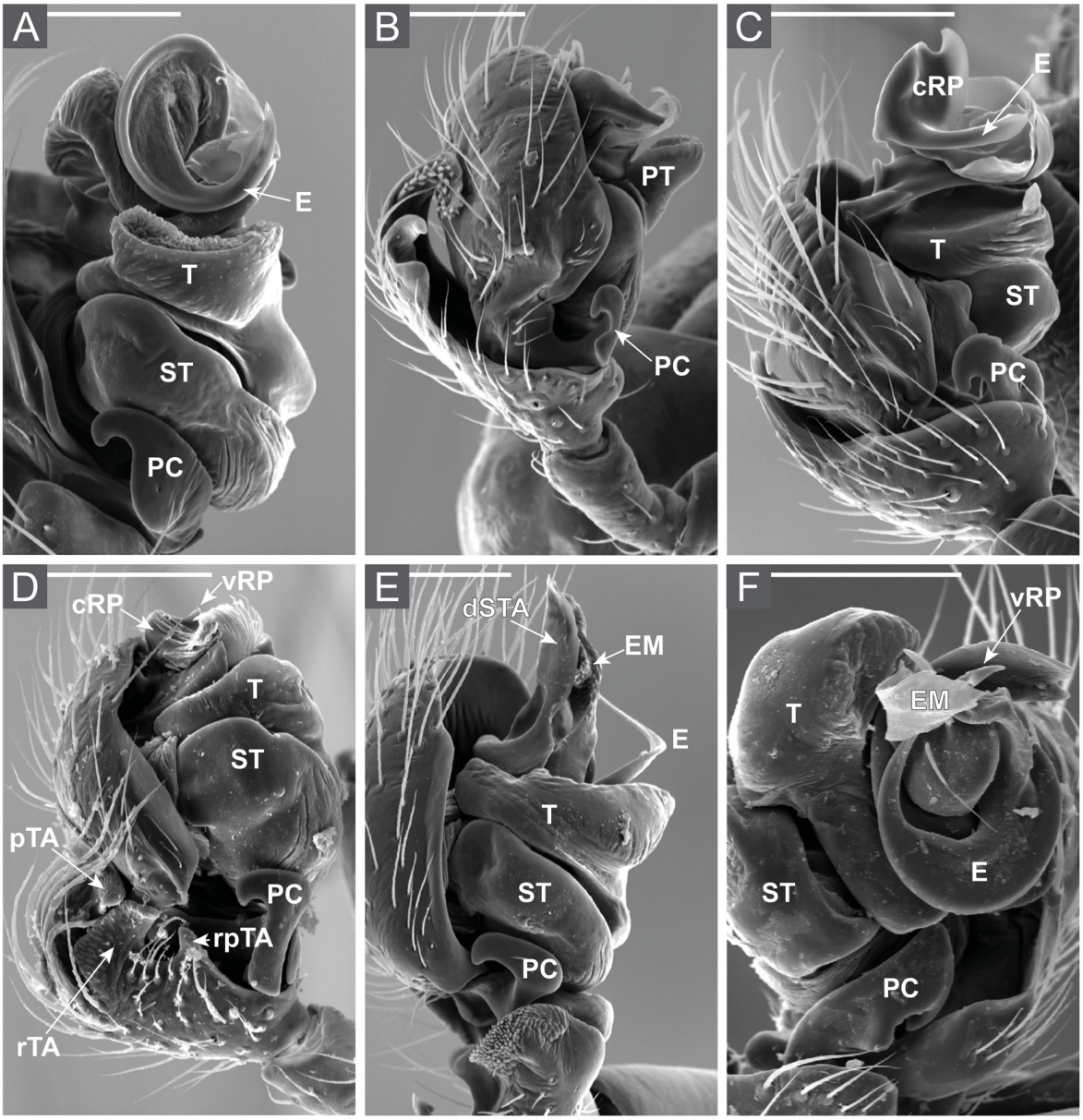

Fig. 3. Scanning Electron Microscope pictures of the male palp in retrolateral view. **A**. *Entelecara erythropus* (Westring, 1851) (Ar172; NMBE). **B**. *Erigonella hiemalis* (Blackwall, 1841) (ZMUC). **C**. *Erigonella ignobilis* (O. Pickard-Cambridge, 1871) (Ar2880; NMBE). **D**. *Glyphesis servulus* (Simon, 1882) (792f; NMB). **E**. *Hypomma bituberculatum* (Wider, 1834) (Ar553; NMBE). **F**. *Saloca diceros* (O. Pickard-Cambridge, 1871) (Ar3289; NMBE). Abbreviations: see Material and methods. Scale bars = 100 μm.

The retrolateral tibial apophysis of most scored taxa was directed retrolaterally (nodes 9, 21 and 33). The only exceptions are *Dicymbium libidinosum* and *Glyphesis cottonae* with a distally or prolaterally facing retrolateral tibial apophysis, respectively. However, the prolaterally facing type is also found in *Glyphesis asiaticus* (Eskov 1989: figs 1–2), which was not scored in the current analysis.

Palpal tibia retrolateral appendices

(34). Palpal tibia, retrolateral marginal seta bases

0: nearly flush with margin (Fig. 1C, *Dicymbium nigrum*).
1: distinct bumps arising from the margin (Fig. 19O; Wiehle 1960: fig. 925, *Diplocephalus connatus*).

The distinct bumps are present at the retrolateral margin of the retrolateral tibial apophysis of *Diplocephalus connatus* and *D. connatus jacksoni* (node 38). However, they could also be present if a species is lacking a retrolateral tibial apophysis.

(35). Palpal tibia, retrolateral glabrous edge

0: absent (Fig. 1C, *Dicymbium nigrum*).
1: present (Fig. 1I; Wiehle 1960: fig. 1030, *Erigonella hiemalis*).

This is a small, usually glabrous edge at the distal to retrolateral side of the tibial apophysis. *Erigonella hiemalis* (Wiehle 1960: fig. 1030) has a distal glabrous edge, plus a prolateral and a retrolateral tibial apophysis and is therefore presumably not homologous with the latter two. However, in taxa with only one retrolateral apophysis (e.g., Fig. 1J; Wiehle 1960: fig. 1038, *Erigonella ignobilis*), it is difficult to judge whether this glabrous area is a vestigial retrolateral apophysis or a retrolateral glabrous edge. The comparison of *E. ignobilis* with *E. hiemalis* showed more similarities with the glabrous edge than with the retrolateral tibial apophysis. The glabrous distal structure seems to be formed like the prolateral and retrolateral tibial apophysis (see description of character 7) as outgrowth of a margin.

(36). Palpal tibia, retrolateral thickenings, lobes or sacs

0: absent, unmodified surface (Fig. 1I; Wiehle 1960: fig. 1030, *Erigonella hiemalis*).
1: present (Fig. 1B; Bosmans 1996: fig. 5, *Araeoncus humilis*).

While all other apophyses are supposed to arise from a margin along the tibia or the non-sclerotised tibial apophysis, these thickenings, lobes and sacs arise directly from the non-sclerotised tibial apophysis. Common to these retrolateral structures is the lack of a discrete, sclerotised margin at any side. Instead, they are carnous and coloured like the non-sclerotised part of the tibia.

Some of them are relatively simple (Pesarini 1996: fig. 15, *Diplocephalus crassilobus*) while others are complex, forming a broad short spoon-like lobe (Wiehle 1967: figs 27, 29, *Diplocephalus helleri*), or even bear some distal thickened setae (Wiehle 1960: fig. 939a, *Diplocephalus permixtus*). The spoon-like lobe is elongated in many species of *Araeoncus* (Bosmans 1996: fig. 5, *Araeoncus humilis*). In others a dorsal distinct lobe (Tanasevitch 1987: fig. 127, *Araeoncus galeriformis*) emerges from the tibia while some species of *Diplocephalus* have a small, long sac (Wunderlich 1980a: figs 47–48, *Savignia harmsi*). It is assumed that all these structures have a common origin. The different types are defined as the subsequent characters. This character is present in a large monophyletic group (nodes 49) with only one reduction in node 58 (see discussion of character 37) and five independent gains in other, more basal taxa.

(37). Palpal tibia, retrolateral distal thickening

0: absent (Fig. 1I; Wiehle 1960: fig. 130, *Erigonella hiemalis*).
1: present (Fig. 19I, *Diplocephalus arnoi*).

This structure is presumably related to the retrolateral distal lobe found in *Araeoncus humilis* or *Araeoncus crassiceps*. It is a thickened margin at the distal to retrolateral side of the tibia and has in most cases a more or less pronounced edge at the inner (ventral) side of the lobe that separates from the remaining tibia. The distal thickening is synapomorphic for node 53 (inapplicable in node 58). However, the members of node 58 and *Diplocephalus picinus* are the only taxa among node 49 that lack any thickening, lobe or sac (character 36) and were therefore considered as inapplicable for the distal thickening. Instead, the members of node 58, i.e., *Diplocephalus cristatus* (see, e.g., Roberts 1987: fig. 36d) and *D. alpinus* have a setose outgrowth, which might be a vestigial, homologous version of this distal thickening.

This thickening is also found in taxa not included in the current analysis like the potential sister-taxon of *Diplocephalus crassilobus*, *D. pseudocrassilobus* Gnelitsa, 2006 (Gnelitsa 2006: fig. 1a). This thickening is quite derived in *Diplocephalus permixtus* where it slightly exceeds the distal tibial margin and bears three distal spines on top of it (character 27).

(38). Palpal tibia, retrolateral distal lobe (rdL)

0: absent (Bosmans 1996: fig. 63, *Diplocephalus algericus*).
1: present (Fig. 1B; Bosmans 1996: fig. 5, *Araeoncus humilis*).

This lobe is a setose extension arising from the retrolateral side of the non-sclerotised tibial apophysis (Fig. 1B, *Araeoncus humilis*). This lobe is not an extension of the sclerotised, honey coloured margin of the tibia but a carnous extension of the palp itself (like the non-sclerotised tibial apophysis that emerges from the tibia; see discussion of character 7). It has a slightly sclerotised surrounding and seen from the ventral side (inside) it is somewhat formed like a glabrous spoon. Due to its carnous structure, it lacks sharp margins which makes it easy to distinguish it from any other tibial apophysis apart from the sacs. It is more sclerotised and less thick than the retrolateral sac (character 41) or the cone-like lobe (character 42).

This character is a synapomorphy of node 59 with only one reduction in *Araeoncus galeriformis* and inapplicable in *D. picinus*. *Araeoncus galeriformis* also has a lobe-like projection that was coded as cone-like lobe (character 42). However, the current analysis shows that the cone-like lobe is homologous with the distal lobe, despite its derived shape.

(39). Palpal tibia, retrolateral distal lobe, direction

0: distally facing (Wiehle 1960: fig. 445a, *Araeoncus anguineus*).
1: retrolaterally facing (Fig. 1B; Bosmans 1996: fig. 5, *Araeoncus humilis*).

The distally facing lobe is a synapomorphy of *Araeoncus vaporariorum* plus *A. anguineus* (node 68).

(40). Palpal tibia, retrolateral distal lobe, size

0: longer than broad (Fig. 1B; Bosmans 1996: fig. 5, *Araeoncus humilis*).
1: broader than long (Fig. 19F; Wiehle 1967: figs 27, 29, *Diplocephalus helleri*).

A new character was defined to account for the massively broadened and still very short distal lobe that is found in *Diplocephalus helleri*. It is setose outside and glabrous spoon-like inside. The broad type is synapomorphic for node 60 (which includes the taxa that are newly assigned to *Araeoncus* except *D. picinus* where it is inapplicable) while the taxa with a more derived male genital morphology of *Araeoncus* (node 64) have a longer lobe.

(41). Palpal tibia, retrolateral sac

0: absent (Fig. 1B; Bosmans 1996: fig. 5, *Araeoncus humilis*).
1: present (Fig. 19D; Wunderlich 1980a: figs 47–48, *Savignia harmsi*).

This sac is a carnous non-sclerotised and presumably soft, white sac without a visible sclerotised margin. Instead, a margin runs from the prolateral apophysis to the retrolateral side of the tibia behind the sac, i.e., ventral (inside) to it. In *Hilaria excisa* it also has setae at its dorsal and ventral side (H00: pl. 33b). This structure was recoded from Frick *et al.* (2010) as being a retrolateral sac instead of a prolateral tibial apophysis.

(42). Palpal tibia, dorsal cone-like lobe

0: absent (Fig. 19L, *Diplocephalus permixtus*; Bosmans 1996: fig. 63, *Diplocephalus algericus*).
1: present (Fig. 20D; Tanasevitch 1987: fig. 127, *Araeoncus galeriformis*).

This is an autapomorphy of *Araeoncus galeriformis*. This type of sac is also present in *A. mitriformis* Tanasevitch, 2008 (Tanasevitch 2008: figs 3–4) that was not scored here. The phylogenetic analysis showed that the cone-like lobe is homologous with the retrolateral distal lobe (character 38), despite its derived shape. See also discussion in the Systematics section of *Araeoncus*.

(43). Palpal tibia, inter pTA-rTA dorsal protuberance (dTP)

0: absent (Figs 3D, 19P; Wunderlich 1969: fig. 26, *Glyphesis servulus*).
1: present (Fig. 19K; Wunderlich 1969: figs 25, 27: *Glyphesis taoplesius*).

This is a dorsal protuberance situated between the prolateral and the retrolateral tibial apophysis and bears the long strong macrosetae found in *Glyphesis* (character 25; Wunderlich 1969: figs 25, 27). This lobe differs in shape, size and direction from the retrolateral lobe present in *Araeoncus* (character 38). It mostly resembles the cone-like lobe of *Araeoncus galeriformis* (character 42) but is not homologous with it. It is not well pronounced in *Glyphesis taoplesius* and bears the same type of macrosetae (character 25) as the type species of *Glyphesis*, *G. servulus*. In the current analysis as an artifact of inapplicables and considering the fast optimisation this character is a synapomorphy of *Glyphesis* (node 22). However, for all taxa with the pTA-rTA structures it is only present in *Glyphesis taoplesius*.

(44). Palpal tibia, retrolateral proximal appendix (rpTA)

0: absent (Fig. 1I; Wiehle 1960: fig. 1030, *Erigonella hiemalis*).
1: present (Fig. 3D; Wunderlich 1969: fig. 26, *Glyphesis servulus*).

This is a glabrous blunt apophysis emerging from the central part of the retrolateral margin of the tibial apophysis. It is very similar to the retrolateral glabrous edge (character 35) in *Erigonella hiemalis* but shifted proximally. The presence of both appendices in *Erigonella subelevata* (Thaler 1971: fig. 3) argues against the homology of both these structures. It is questionable if the structure coded as proximal appendix in *Erigonella subelevata* is homologous with what is seen in *Glyphesis servulus*. This is an ambiguous synapomorphy, occurring in node 23, that includes most species of *Glyphesis* except for *Glyphesis cottonae*, and in *E. subelevata*.

(45). Palpal tibia, retrolateral proximal blunt sclerotised structure

0: absent (Fig. 19C; Roberts 1987: fig. 36c, *Savignia frontata*).
1: present (Fig. 19A; Roberts 1987: fig. 36d, H00: pl. 19a, *Diplocephalus cristatus*).

The margin can either run smoothly from the retrolateral border to the ventral side of the tibia (state 0) or form a kind of distinct edge/bump (state 1). This bump is clearly visible in *Diplocephalus cristatus* and *D. alpinus* but is absent in *D. crassilobus*. Instead, the latter species has a ventral thin protuberance (character 49). It is not homologous with either the ventral thin protuberance or the ventral tibial apophysis since both structures are present side by side in *Diastanillus pecuarius* and in *Diplocephalus cristatus*. This character is an ambiguous synapomorphy of node 58 with one convergent occurrence in *Diastanillus pecuarius*.

(46). Palpal tibia, retrolateral proximal big broad setose bump

0: absent.
1: present (Figs 1L, 20I, *Saloca diceros*; Wiehle 1960: fig. 45, *Pelecopsis elongata*).

This setose bump is situated proximally at the retrolateral side of the tibia and has a broad sclerotised lateral band at its margin. This structure is an ambiguous synapomorphy of nodes 20 and 28 with one other, likely convergent, occurrence in *Pelecopsis elongata*.

Palpal tibia, different distal and ventral appendices

47. Palpal tibia, ventral tibial process (vTP)

0: absent (Miller 2007: fig. 96b, *Mermessus rapidulus* (Bishop & Crosby, 1938)).
1: present (Fig. 19A; H00: pl. 19a, *Diplocephalus cristatus*).

MH04-72, A09-60. This carnous apophysis emerges from the ventral side of the tibia and has the same colour and surface as the tibia. It is a synapomorphy of nodes 57 and 62 and also emerges in two more taxa (*Walckenaeria acuminata* and *Archaraeoncus proscipiens*).

(48). Palpal tibia, ventral process, form

0: simple (H00: pl. 54a, *Parapelecopsis nemoralis* (Blackwall, 1841)).
1: with indentation (Fig. 19A; H00: fig. 6a–b, *Diplocephalus cristatus*).
2: curved retrolaterally (Fig. 19F; Wiehle 1967: fig. 27, *Diplocephalus helleri*).

This is a more or less squarish ventral tibial apophysis with a slight central indentation occurring in *Diplocephalus cristatus* and *D. alpinus*. State 1 is a synapomorphy of node 58 and state 2 is an autapomorphy of *Diplocephalus helleri.*

(49). Palpal tibia, ventral thin protuberance

0: absent (Fig. 6D; Locket *et al*. 1974: fig. 59e, *Glyphesis servulus*).
1: present (Fig. 6C, *Erigonella hiemalis*; Wiehle 1960: fig. 947, *Diplocephalus latifrons*; Eskov 1988: fig. 68, *Savignia saitoi*).

The margin or where present the sclerotised bands (characters 8 and 30) of the tibia usually run smoothly from one side of the apophyses along the ventral side to the other side of the apophyses. In some taxa the margin is broadened at the ventral side of the tibia forming a sclerotised bump, the ventral thin protuberance. It can be narrow or broad (character 50) but should at least form a slight sclerotised bump emerging from the tibia to be coded as present.

(50). Palpal tibia, ventral thin protuberance, dimension

0: narrow (Fig. 5B, *Araeoncus humilis*; Eskov 1988: fig. 68, *Savignia saitoi*).
1: broad (Fig. 6C, *Erigonella hiemalis*; Wiehle 1960: fig. 947, *Diplocephalus latifrons*).

The ventral thin protuberance can either emerge from the distal margin of the tibia along nearly the whole ventral side of the tibia (state 1) or else only at a narrow section (state 0). The position of this protuberance is usually in the centre of the distal margin but in some cases it is shifted retrolaterally and emerges from the proximal margin of the retrolateral tibial apophysis (e.g., in *Dactylopisthes locketi*, *Da. mirabilis* and *Janetschekia monodon*).

(51). Palpal tibia, ventral sclerotised band

0: absent.
1: present (Fig. 20B, *Diplocephalus helleri*; Wiehle 1960: fig. 947, *Diplocephalus latifrons*).

A sclerotised band runs along the distal margin of the ventral side of the tibia in most scored taxa. This band is of the same origin as the lateral bands (characters 8 and 30) and one is often the continuation of the other.

Cymbium

52. Cymbium size

0: longer and wider than palpal tibia and patella (H00: fig. 8b–c, *Drepanotylus uncatus* (O. Pickard-Cambridge, 1873)).
1: smaller relative to the size of the pedipalpal tibia and patella (H00: fig. 19a–b, *Leptorhoptrum robustum*; Tanasevitch 1989: fig. 110, *Alioranus chiardolae* as *Al. avanturus* Andreeva & Tystshenko, 1970).

MH04-05. This is an autapomorphy of *Alioranus chiardolae*.

53. Cymbial retrobasal process (CRP)

0: absent.
1: present (Fig. 20I, *Saloca diceros*; MH04: fig. 15c, *Labicymbium sturmi* Millidge, 1991).

MH04-04, A09-08*. MH04 described this apophysis as emerging from the proximal region of the cymbium, directing retrolaterally or dorsally. Contrary to the retrobasal thin apophysis (character 54) this process is supposed to be a carnous outgrowth of the cymbium (e.g., Miller 2007: fig. 119b and Roberts 1987: fig. 75a) rather than a thin sclerotised apophysis. However, it is not clear whether the cymbial retrobasal thin apophysis (character 54) is homologous with this character. Within the Erigoninae, we only coded *Saloca diceros* and *Saloca kulczynskii* as having this apophysis (Fig. 1L). They have a longitudinally thickened apophysis arising from the proximal part of the cymbium, which is separated from the cymbium by a retrolateral groove (character 59).

(54). Cymbial retrobasal thin apophysis (CRA)

0: absent (Fig. 3E; Roberts 1987: 13d, *Hypomma bituberculatum*).
1: present, round (Fig. 2D; Roberts 1987: fig. 37a, *Diplocephalus latifrons*).

This is a sclerotised outgrowth of the cymbial margin similar to the lateral bands on the tibial apophysis. It is honey-coloured and thin and covered with a few setae along its margin. It is separated from the cymbium by a ridge and usually also a retrolateral groove (character 59). It is coded as present if at least a small ridge was present, separating the sclerotised part from the remaining cymbium. Usually, this apophysis is clearly separated from the cymbium (e.g., Roberts 1987: fig. 36c, *Savignia frontata*). However, in a few taxa the ridge is very close to the retrolateral margin of the cymbium lacking a lobe (e.g., in *Diplocephalus cristatus*). In these taxa the setae emerge from this narrow area (*D. cristatus*). It is synapomorphic for node 1 and is only lacking in *Bolyphantes luteolus*, *Alioranus* (node 5) and node 11.

Dismodicus bifrons, *Dis. elevatus* and *Hypomma bituberculatum* might show an ancestral state towards such an apophysis. It is completely covered with setae but has the typical honey-like coloration and lacks the ridge that separates it from the remaining cymbium.

(55). Cymbial retrobasal thin apophysis, macroseta

0: absent (Fig. 2D; Roberts 1987: fig. 37a, *Diplocephalus latifrons*).
1: present (Fig. 2C, Wiehle 1960: fig. 343, *Dicymbium tibiale*).

Dicymbium (node 29) and *Araeoncus galeriformis* have macrosetae emerging from the retrobasal thin apophysis.

(56). Cymbial retrobasal thin apophysis, form

0: more or less round (Fig. 2D; Roberts 1987: fig. 37a, *Diplocephalus latifrons*).
1: projecting distally (Fig. 20C; Wunderlich 1980a: fig. 48, *Savignia harmsi*).
2: narrow (Fig. 3A, *Entelecara erythropus*; H00: pl. 19a, *Diplocephalus cristatus*).

In *Savignia harmsi*, the retrobasal thin apophysis is distally directed with a small projection. State 2 describes narrow apophyses that are reduced to not much more than a margin with a few setae (H00: pl. 19a, *Diplocephalus cristatus*).

(57). Cymbial retrobasal vertical ridge

0: absent (Fig. 2D; Roberts 1987: fig. 37a, *Diplocephalus latifrons*).
1: present (Fig. 16D; Roberts 1987: fig. 40b, *Araeoncus crassiceps*; Pesarini 1996: fig. 3, *Araeoncus anguineus*).

This distinct ridge borders the cymbial retrobasal thin apophysis and/or the retrolateral groove. It is not just a slightly sclerotised ridge as seen in, e.g., *Savignia frontata* but a distinct vertical ridge on the retrolateral side of the cymbium, sloping at its retro- and prolateral side. On its prolateral side it seems to form a sclerotised area proximally which is especially well visible in *Araeoncus anguineus*. It is very distinct in all coded species of *Araeoncus* except for *Araeoncus humilis* that has a small ridge as seen in, e.g., *Savignia frontata* and others.

This character is an ambiguous synapomorphy of node 64 (*Araeoncus* excluding *A. humilis*), *Dicymbium* (node 29), node 37 and is also present in *Diplocephalus protuberans* and *Diplocephalus turcicus*.

(58). Cymbial retrobasal striated glabrous bump

0: absent (Fig. 2D; Wiehle 1960: fig. 947, *Diplocephalus latifrons*).
1: present (Fig. 20G, *Diplocephalus arnoi*; Thaler 1972: fig. 24, *Diplocephalus procer*).

This bump emerges from the dorsal proximal side of the cymbium. It is glabrous and bears distinct, well visible longitudinal striations. This bump is a synapomorphy of *Diplocephalus arnoi* plus *D. pavesii* (node 55), but it is also present and even enlarged in *Diplocephalus procer* (Thaler 1972: fig. 24).

59. Cymbium retrolateral groove

0: absent (Fig. 2F, *Dismodicus bifrons*; Roberts 1987: fig. 75a, *Bolyphantes luteolus*).
1: present (Fig. 2D; Roberts 1987: fig. 37a, *Diplocephalus latifrons*; MH04: fig. 15b, *Neocautinella neoterica* (Keyserling, 1886)).

MH04-07, A09-09. This groove defines the attachment of a lobe at the retrolateral side of the cymbium. It is independent of the retrobasal thin apophysis, i.e., in *Alioranus* (node 5) and "*Saloca*" (node 12) a groove is present without the apophysis and *Diplocephalus crassilobus* and *Tenuiphantes tenuis* lack a groove but have a retrobasal thin apophysis.

(60). Cymbium prolateral basal glabrous apophysis (CPA)

0: absent (Fig. 6E, *Hypomma bituberculatum*; Roberts 1987: fig. 37a, *Diplocephalus latifrons*).
1: present (Fig. 6D, *Glyphesis servulus*).

This apophysis emerges proximally from the prolateral side of the cymbium and extends to the paracymbium with its bulb-like tip. It is sclerotised, slightly twisted and not fused to the tibia but flush with it. Some species (e.g., H00: pl. 39b, *Islandiana cristata* Eskov, 1987) have similar but less pronounced tips and are less sclerotised. This apophysis is a synapomorphy of *Glyphesis* (node 22).

Paracymbium

61. Paracymbium (PC), apophyses

0: absent (MH04: fig. 15d, *Valdiviella trisetosa* Millidge, 1985).
1: present (Hormiga 1994a: fig. 13a, *Tenuiphantes tenuis*).

MH04-13, A09-13. This character describes the large distal apophysis present in some Linyphiinae. We found additional less distinct processes (scored as separate characters) that are presumably not homologous with the massive apophyses seen in Linyphiinae (e.g., Roberts 1987: figs 72a–b, 75a–b).

(62). Paracymbium, retrolateral process (PCrP)

0: absent to a small bump (Fig. 4F; Roberts 1987: fig. 13b, *Dismodicus bifrons*).
1: distinct lobe present (Fig. 4C; Roberts 1987: fig. 10f, *Dicymbium tibiale*).

The conformation seen in *Silometopus elegans* (O. Pickard-Cambridge, 1873) (Frick *et al*. 2010: pl. 18d) is supposed to be the basic shape, lacking any processes. However, most scored species have processes of different shape and size (e.g., small bumps in *Diplocephalus latifrons*, Fig. 4D and very large ones in *Erigonella hiemalis*, Fig. 4H), which emerge retrolaterally from the paracymbium. State 1 accounts for the distinct lobe seen in *Dicymbium* and state 0 for all taxa with smaller appendices. This character is not possible to code in taxa with paracymbium apophyses (character 61) since homologies are not clear yet. The distinct lobe is an ambiguous synapomorphy of *Dicymbium* (node 29) and *Glyphesis* without *G. cottonae* (node 23).

(63). Paracymbium, ventral process (PCvP)

0: absent (Fig. 4F; Roberts 1987: fig. 13b, *Dismodicus bifrons*).
1: present (Fig. 4C; Roberts 1987: fig. 10f, *Dicymbium tibiale*).

Like the retrolateral process (character 62), the ventral process emerges from the center of the ventral margin of the paracymbium. It can either be just a small bump or a distinct lobe (character 64).

(64). Paracymbium, ventral process, form

0: small lobe (Fig. 5E, *Diplocephalus latifrons*; Roberts 1987: fig. 37d, *Diplocephalus protuberans*).
1: distinct lobe (Fig. 4C; Roberts 1987: fig. 10f, *Dicymbium tibiale*).

Small lobes are at most as long as broad, while distinct lobes as seen in *Dicymbium* are longer than broad. A distinct lobe is present in *Dicymbium* (node 29) and in node 37.

(65). Paracymbium distal end, form

0: continuous with basal part of paracymbium (Fig. 4F, Roberts 1987: fig. 13b; *Dismodicus bifrons*).
1: narrow hook-like curved and broadened ectally (Fig. 4B; Roberts 1987: fig. 40a, *Araeoncus humilis*).

State 1 is an ambiguous synapomorphy of the *Savignia*-group (node 16) and is only also present in three more taxa: *Entelecara acuminata* and in *Alioranus* (node 6, Fig. 4A, *Alioranus pastoralis*).

(66). Paracymbium distal end, with mesal elongation

0: not elongated (Fig. 4F, Roberts 1987: fig. 13b; *Dismodicus bifrons*).
1: mesally elongated (Fig. 20E; Thaler 1969: fig. 27, *Diastanillus pecuarius*).

The mesally elongated tip is an autapomorphy of *Diastanillus pecuarius*.

67. Paracymbium base

0: glabrous (Fig. 4E, *Diplocephalus picinus*).
1: with cluster of setae (Fig. 4H, *Erigonella hiemalis*; H00: pl. 62a, *Tapinocyba praecox* (O. Pickard-Cambridge, 1873)).

MH04-14, A09-14. Most species have a cluster of setae. Glabrous bases are found in nodes 10, 60 and *Savignia saitoi*.

(68). Paracymbium base, number of setae

0: glabrous, no setae (Fig. 4E, *Diplocephalus picinus*).
1: one seta (Fig. 4G, *Entelecara erythropus*).
2: two setae (Fig. 20I, *Saloca diceros*; Fig. 4I, *Glyphesis servulus*).
3: three setae (Fig. 4H, *Erigonella hiemalis*).
4: four setae (*Diplocephalus rostratus*).
5: five or more setae (H00: pl. 7a, *Linyphia triangularis*).

The number of setae can be typical for certain taxa; e.g., one seta in many species of *Savignia* and five setae in all but one species of *Caracladus* (Frick & Muff 2009). The intraspecific variation was not

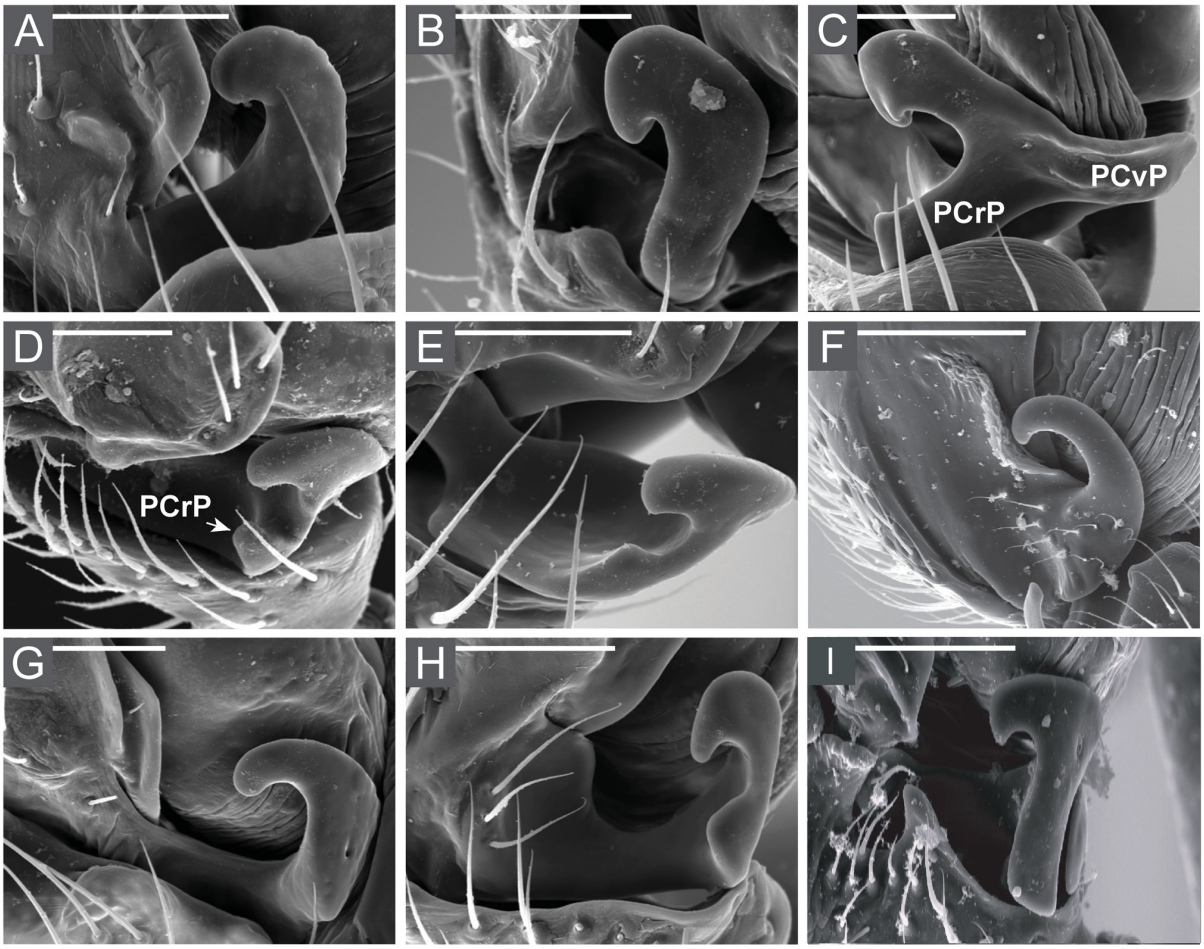

Fig. 4. Scanning Electron Microscope pictures of the male palp paracymbium in retrolateral view. **A**. *Alioranus pastoralis* (O. Pickard-Cambridge, 1872) (3695-3702; coll. E.G.). **B**. *Araeoncus humilis* (Blackwall, 1841) (Ar3186; NMBE). **C**. *Dicymbium tibiale* (Blackwall, 1836) (11430; ZMUC). **D**. *Diplocephalus latifrons* (O. Pickard-Cambridge, 1863) (Ar1262; NMBE). **E**. *Diplocephalus picinus* (Blackwall, 1841) (Ar6645; NMBE). **F**. *Dismodicus bifrons* (Blackwall, 1841) (Ar1192; NMBE). **G**. *Entelecara erythropus* (Westring, 1851) (Ar172; NMBE). **H**. *Erigonella hiemalis* (Blackwall, 1841), (ZMUC). **I**. *Glyphesis servulus* (Simon, 1882) (792f; NMB). Abbreviations: see Material and methods. Scale bars = 50 μm.

explored in the current or any other analysis known to the authors, besides Frick & Muff (2009), who scored several specimens per species without observable intraspecific variation.

(69). Paracymbium, pubescence excluding the paracymbium base

0: glabrous (Fig. 4E; Roberts 1987: fig. 37c, *Diplocephalus picinus*).
1: central setose area (Fig. 4F, *Dismodicus bifrons*; Roberts 1987: fig. 13e, *Dismodicus elevatus*).

This character describes the setae presence of the entire paracymbium excluding the paracymbium base. State 1 is an ambiguous synapomorphy of *Dismodicus* (node 15) also present in all taxa basal to node 4.

Subtegulum and tegulum

70. Sperm duct switchback in first loop

0: absent (H00: fig. 4a, *Ceratinops inflatus* (Emerton, 1923)).
1: present (Hormiga 1994b: fig. 9, *Pimoa altioculata* (Keyserling, 1886); H00: fig. 13b, *Grammonota pictilis* (O. Pickard-Cambridge, 1875)). MH04-22.

71. Papillae on tegulum

0: absent (Fig. 5D, *Dicymbium tibiale*; H00: pl. 25a, *Erigone psychrophila* Thorell, 1871).
1: present (Fig. 5E, *Diplocephalus latifrons*; H00: pl. 22a, *Dismodicus decemoculatus*).

MH04-20, A09-20. This accounts for papillate areas on the protegulum that extend over the tegulum.

72. Protegulum (PT)

0: absent (H00: pl. 33d, *Hilaira excisa*).
1: present (Fig. 5D, *Dicymbium tibiale*; H00: pl. 15e, *Ceratinops inflatus*).

MH04-16, H00-08, A09-16. The definition and especially the limits of the protegulum are ambiguous. MH04 defined it as "a membranous sac, usually located on the distoventral part of the tegulum". *Linyphia triangularis* was recoded as having a protegulum (see H00: pl. 7a, right of "TA"). All taxa were scored as having a protegulum if at least a slight protuberance from the tegulum was present. In unexpanded palps, it fits well together with neighbouring structures like the suprategulum as seen in, e.g., *Diplocephalus latifrons* (Fig. 5E).

(73). Protegulum, form

0: thick (Fig. 3B, *Erigonella hiemalis*; Fig. 5D; Roberts 1987: fig. 10f, *Dicymbium tibiale*).
1: thin (Fig. 5E; Roberts 1987: fig. 37a, *Diplocephalus latifrons*).

A thick protegulum looks like a protruding part of the tegulum (with volume) that is as sclerotised as the rest of the tegulum. The thin protegulum looks like an apophysis emerging distally from the tegulum. It appears more sclerotised due to its thin conformation (nearly no volume). *Dismodicus bifrons* and *Dis. elevatus* have an elongated, sac-like protegulum (e.g., Fig. 6A, *Dismodicus bifrons*). A thin protegulum is only found in *Diplocephalus mirabilis*, *D. latifrons* and *Erigonella ignobilis*.

74. Protegular papillae

0: absent (*Erigone psychrophila*, Hormiga 2000: pl. 25d).
1: present (Fig. 5E, *Diplocephalus latifrons*; H00: pl. 15e, *Ceratinops inflatus*).

MH04-17, H00-09, A09-17.

75. Tegular sac (TS)

0: absent (Fig. 5E, *Diplocephalus latifrons*; H00: pl. 18c, *Diplocentria bidentata* (Emerton, 1882)).
1: present (Fig. 5B, *Araeoncus humilis*; Fig. 16A, *Araeoncus anguineus*; H00: pl. 30d, *Gongylidium rufipes* (Linnaeus, 1758)).

MH04-19, H00-10, A09-19. The structure coded as tegular sac in *Gongylidium rufipes* is also found in the same position and with the same shape in *Araeoncus anguineus* (Fig. 16A; Pesarini 1996: fig. 3). The other scored species of *Araeoncus* show less distinct (e.g., Tanasevitch 1987: figs 126–127: *Araeoncus galeriformis*) or very small tegular sacs (Fig. 5B, *Araeoncus humilis*). The tegular sac is a synapomorphy of *Araeoncus* (node 63) in the current analysis.

(76). Tegular sac, length

0: about as long as broad (Fig. 5B, *Araeoncus humilis*; H00: pl. 49b, d, *Oedothorax gibbosus* (Blackwall, 1841)).
1: much longer than broad (Figs 16A, 20F, Pesarini 1996: fig. 3, *Araeoncus anguineus*; H00: pl. 30d, *Gongylidium rufipes*).

The long tegular sac is a synapomorphy of node 67.

Suprategulum

(77). Suprategulum (SPT), form in distal view

0: straight (*Alioranus chiardolae*).
1: circular (Fig. 23A, *Diplocephalus cristatus*; H00: fig. 1e, *Araeoncus crassiceps*).

In some taxa the suprategulum defines a full circle forming a kind of "hook" fitting together with the distally positioned embolic division. Millidge (1977) based his definition of the *Savignia*-group on this type of suprategulum. The circular suprategulum is a synapomorphy of node 4 and is present in the *Savignia*-group (node 16), in *Entelecara* (node 9) and in *Alioranus pauper* and *Al. pastoralis* (node 6).

78. Marginal suprategular apophysis (mSTA)

0: absent (H00: fig. 3e; *Asthenargus paganus* (Simon, 1884)).
1: present (Fig. 23D–E, *Erigonella hiemalis*; H00: fig. 1e, *Araeoncus crassiceps*).

MH04-34, H00-14, A09-28. This is a tooth like structure next to the column. H00 proposed the term "marginal suprategular apophysis" for this structure. It is synonymous with the "basal tooth" in Bosmans (1996). The marginal suprategular apophysis is an ambiguous synapomorphy of node 4 with three reductions in *Alioranus pauper* and *Al. pastoralis* (node 6), *Saloca diceros* and *Sa. kulczynskii* (node 28) and node 10 with one secondary gain in *Dismodicus* (node 15).

(79). Marginal suprategular apophysis (mSTA), position

0: arising from the suprategulum or the sclerotised base of the column (Fig. 23A, *Diplocephalus cristatus*; H00: fig. 2b, *Araeoncus humilis*).
1: arising from the column (Fig. 7E, *Dismodicus bifrons*; H00: fig. 7c, *Dismodicus decemoculatus*).

In most scored taxa the marginal suprategular apophysis emerges from the suprategulum in a right angle or from the sclerotised base of the column in an angle of ca 45°. There is a second type of marginal apophysis arising from the proximal part of the column directing distally flush with the column. This type is a synapomorphy of node 10 (as an artifact of inapplicables considering fast character optimisation) but only present in *Dismodicus* (node 15) in the current analysis.

(80). Marginal suprategular apophysis (mSTA), form

0: straight tooth (Fig. 23D–E, *Erigonella hiemalis*; Fig. 23C, *Diplocephalus crassilobus*; Fig. 9B; H00: fig. 2b, *Araeoncus humilis*).
1: distinctly curved forward (Fig. 18A; Thaler 1972: fig. 17, *Diplocephalus pavesii*).

The forms of the marginal suprategular apophysis are very diverse and difficult to define as discrete characters. The most distinct form is the forward curved one (state 1), which is a synapomorphy of *Diplocephalus caucasicus*, *D. arnoi* and *D. pavesii* (node 54).

(81). Suprategular apophysis, diameter around column

0: suprategulum equally broad (Fig. 23A; H00: fig. 6g, *Diplocephalus cristatus*).
1: clearly broader around/after the column (Fig. 7E, *Dismodicus bifrons*; H00: fig. 7c, *Dismodicus decemoculatus*).

In most taxa the diameter of the suprategulum is more or less equal basal and distal to the marginal suprategular apophysis (state 0). In a few taxa with membranous distal suprategular apophyses the suprategulum is much broader around and distal to the marginal suprategular apophysis than it is basal to it. This is a synapomorphy of node 13.

(82). Outer suprategular apophysis (oSTA)

0: absent (Fig. 23F–G, *Erigonella subelevata*; H00: fig. 1e, *Araeoncus crassiceps*).
1: present (Figs 5E, 23J–K, *Diplocephalus latifrons*; H00: pl. 56a–b, *Savignia frontata*).

This apophysis emerges ectally from the proximal part of the distal suprategular apophysis. Usually, it is a broad, hill-like lobe that may be nearly as thick as the suprategular apophysis (e.g., Figs 5E, 23J–K, *Diplocephalus latifrons*) or thin like a lamella (e.g., Fig. 23D–E, *Erigonella hiemalis*). The form and direction seems to depend on the form and direction of the protegulum on which it is flush fitting in unexpanded palps. It keeps the suprategulum in position in unexpanded erigonine palps (see fit in Fig. 5E, *Diplocephalus latifrons*). The presence of this apophysis supports several nodes and a few single taxa. Larger nodes are *Erigonella* (node 33), *Dicymbium* (node 29) and *Savignia* (node 45).

(83). Outer suprategular apophysis, tip shape

0: blunt (Figs 5E, 23J–K, *Diplocephalus latifrons*; H00: pl. 56a–b, *Savignia frontata*).
1: pointed (Fig. 5C; Merrett 1963: fig. 63b, *Dicymbium nigrum*).

The pointed apophysis is an ambiguous synapomorphy present in two nodes each including two very similar sister taxa: *Dicymbium nigrum* plus *Di. tibiale* (node 30) and *Diplocephalus connatus* plus *D. connatus jacksoni* (node 38).

Male palpal inner suprategular apophysis

(84). Inner suprategular apophysis (iSTA)

0: absent (H00: fig. 2b, *Araeoncus humilis*).
1: present (Fig. 23D–E, *Erigonella hiemalis*; H00: fig. 1e, *Araeoncus crassiceps*).

This apophysis emerges mesally from the proximal part of the distal suprategular apophysis close to the column.

(85). Inner suprategular apophysis (iSTA), form

0: short, lamelliform and blunt (Merrett 1963: fig. 29a, e, *Linyphia triangularis*).
1: short, robust, blunt and twisted triangle (Fig. 17B; Tanasevitch 1983: fig. 3, *Dactylopisthes locketi*).
2: short, robust blunt with rounded tip (Figs 9E, 23J, *Diplocephalus latifrons*).

3: short, blunt triangle (Figs 6D, 9J, 17C; Merrett 1963: fig. 62c, *Glyphesis servulus*).
4: thin, long with blunt tip (Figs 9H, 23D; Merrett 1963: fig. 64c, *Erigonella hiemalis*).
5: broad, long with blunt tip (Tanasevitch 2008: fig. 16, *Archaraeoncus proscipiens*).
6: pointed, flush with distal suprategular apophysis (Fig. 17E, *Savignia producta*; Roberts 1987: fig. 37b, Lockett & Millidge 1953: fig. 177c, *Diplocephalus connatus*).

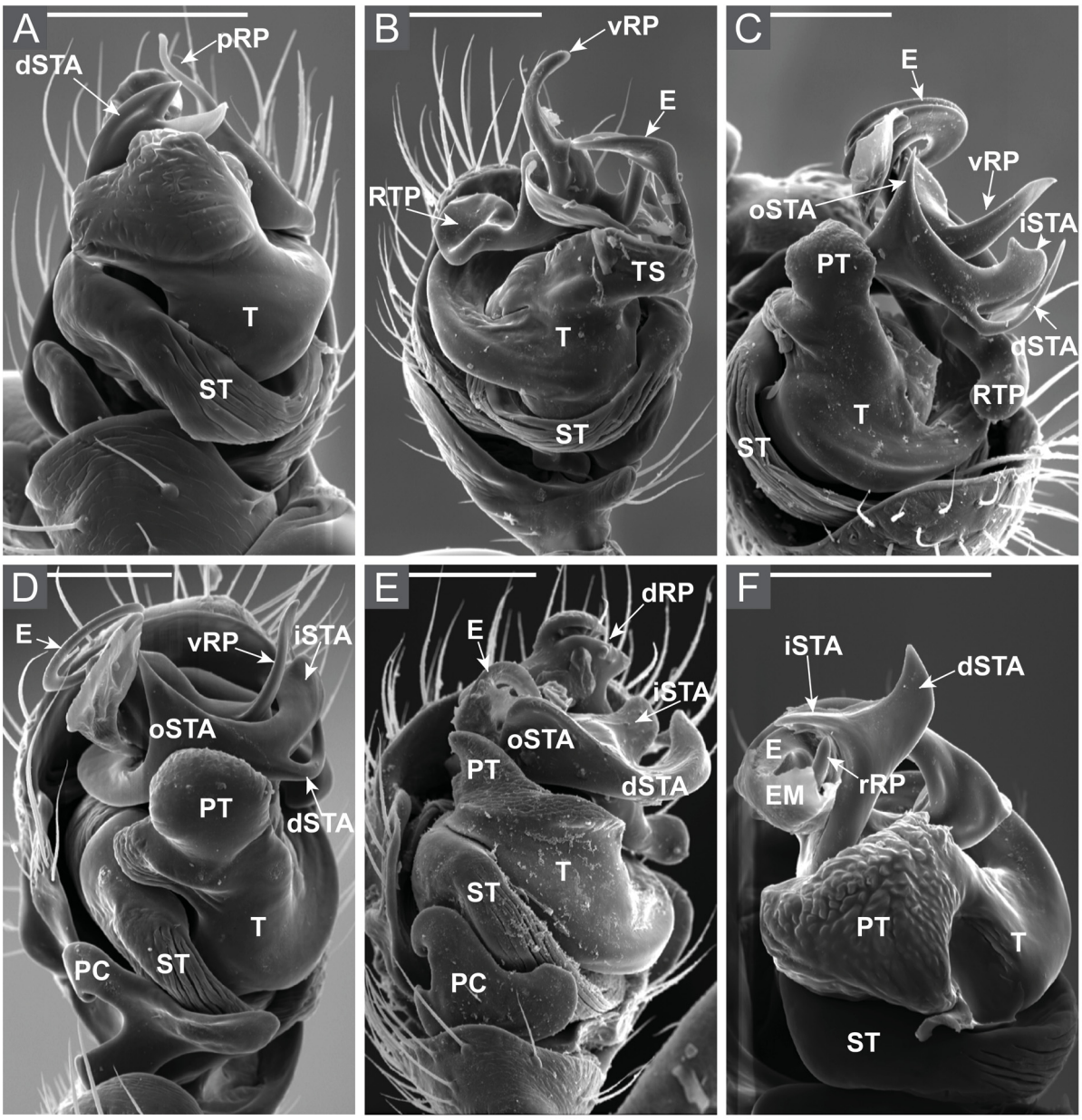

Fig. 5. Scanning Electron Microscope pictures of the male palp in ventral view. **A**. *Alioranus pastoralis* (O. Pickard-Cambridge, 1872) (3695-3702; coll. E.G.). **B**. *Araeoncus humilis* (Blackwall, 1841) (Ar3186; NMBE). **C**. *Dicymbium nigrum* (Blackwall, 1834) (Ar637; NMBE). **D**. *Dicymbium tibiale* (Blackwall, 1836) (11430; ZMUC). **E**. *Diplocephalus latifrons* (O. Pickard-Cambridge, 1863) (Ar1262; NMBE). **F**. *Diplocephalus picinus* (Blackwall, 1841) (Ar6645; NMBE). Abbreviations: see Material and methods. Scale bars = 100 μm.

7: massive, thin to leaf-like with longitudinal backing (Figs 5C, 7B, 9C, 17F; Merrett 1963: fig. 63a, *Dicymbium nigrum*).
8: massive, highly sclerotised distal facing (Fig. 17G; Merrett 1963: fig. 68a; Tanasevitch 1985a: fig. 21, *Savignia frontata*).
9: short and pointed, tooth-like (Fig. 23A; H00: pl. 19b, *Diplocephalus cristatus*).
10: robust, backwards facing and pointed (Fig. 9F; Merrett 1963: fig. 67c, *Diplocephalus picinus*).
11: very large, flat equilateral triangle (Fig. 17D; Thaler 1970: fig. 6, *Diplocephalus rostratus*).
12: big, twisted and triangular with distinct outer ridge (Fig. 18A; Thaler 1972: fig. 17, *Diplocephalus pavesii*).

The form of the inner suprategular apophysis is highly variable and often species specific. Some types were identifiable and defined here as different states. There are many more different types of inner suprategular apophyses and therefore this apophysis is a large source of potentially phylogenetically useful information between and especially within genera. The state 0 apophysis is rather thin, membranous and is much less sclerotised than the distal suprategular apophysis (Merrett 1963: fig. 29e). It is folded in *Linyphia triangularis* (Merrett 1963: fig. 29a) and somewhat spoon-like in *Bolyphantes luteolus* (Merrett 1963: fig. 16d).

State 1 describes a highly sclerotised short and robust bump. It is an ambiguous synapomorphy (as an artifact of inapplicables considering fast character optimisation) but only present in *Dactylopisthes locketi* and *Da. mirabilis* (Tanasevitch 1985b: fig. 3) in the current analysis (node 20). Due to the perspective, the tip of this apophysis appears pointed rather than blunt in Tanasevitch (1989: fig. 126). The apophysis in state 2 is also highly sclerotised and has a roundish tip. This type is present only in *Diplocephalus latifrons* and *Erigonella ignobilis* (Figs 9I, 23H).

State 2 is a synapomorphy of node 35.

The apophysis in state 3 is covered with stria at its inner side between the inner and the distal suprategular apophysis (Fig. 9J). It was only coded as present if well visible as in *Glyphesis servulus* and *G. taoplesius*. However, all *Glyphesis* have at least a small blunt and triangular apophysis. This is a synapomorphy of node 25 and of *Alioranus* (node 6).

State 4 is a finger-like and blunt apophysis. It is much thinner than the diameter of the suprategular apophysis and much longer than thick. It is an ambiguous synapomorphy (as an artifact of inapplicables considering fast character optimisation) but only present in *Erigonella subelevata* (Fig. 23F) and *Erigonella hiemalis* (node 34).

State 5 describes apophyses that are at least as broad as long (also the shortest margin). The apophysis of *Archaraeoncus prospiciens* is longer than broad and positioned in a right angle to the distal suprategular apophysis (Tanasevitch 2008: fig. 16). It is an autapomorphy of *Archaraeoncus proscipiens*. The apophysis of *Archaraeoncus alticola* Tanasevitch, 2008, which was not scored here, is about as broad as long (Tanasevitch 2008: fig. 11). It is similar to what is seen in *Diplocephalus latifrons* (Figs 9E, 23J) but its inner margin is much longer.

Apophyses of state 6 are highly sclerotised and flush with the distal suprategular apophysis. Only a close look reveals that these are indeed two structures. This is an ambiguous synapomorphy (as an artifact of inapplicables considering fast character optimisation) but only present in node 37, including *Savignia producta*, *Diplocephalus connatus* and *D. connatus jacksoni*.

The massive but thin apophysis of state 7 is synapomorphy of *Dicymbium* (node 29). It is about as long as its basal breadth and is about as broad as the suprategulum (Eskov 1988: fig. 70).

The massive apophysis of state 8 is highly sclerotised. It is split into one, usually not pointed, tip facing distally (this character) and a second one facing proximally (character 87). It is an ambiguous synapomorphy of node 45 including *Savignia* and also found in *Diplocephalus subrostratus*.

The type described as state 9 is found among members of *Araeoncus* (in node 59 all three species with an inner suprategular apophysis: *Araeoncus crassiceps*, *A. anguineus* and *Diplocephalus protuberans*) and in other members of node 51 (*Diplocephalus turcicus* and node 57).

State 9 is a synapomorphy of node 51. The one of *Diplocephalus protuberans* looks exactly as the one in *Araeoncus crassiceps*.

State 10 is typical for some species of *Tenuiphantes* (Merrett 1963: fig. 10d, *T. zimmermanni* (Bertkau, 1890)) but also found in *Diplocephalus picinus*. However, the homology of these distant relatives is questionable (compare Merrett 1963: figs 10d, 67c for *T. zimmermanni* and *D. picinus*, respectively).

State 11 is found in three species of *Diplocephalus* with a dagger-like distal suprategular apophysis (character 90, state 1), i.e., node 43. It is also present in their close common ancestors *Diplocephalus uliginosus* and *D. lusiscus* and one far distant relative *Diplocephalus caucasicus*. It is very large in distal view (i.e., larger than seen in ventral view, Eskov 1988: fig. 27). The same form and conformation but smaller is found in *D. caucasicus*. The phylogenetic analysis showed that this smaller type is not homologous with what is found in the members of node 39. The basal species of node 39 differ from the presumably more derived and homogenous forms in node 43: the inner suprategular apophysis of *Diplocephalus lusiscus* is bent distally rather than totally flat and a small ridge runs from the suprategular apophysis to the tip of the outer suprategular apophysis. The same form is also found in *Diplocephalus uliginosus* but it is membranous and smaller than in members of node 39.

State 12 is an unshaped apophysis with membranous parts besides sclerotised ones. It has either a blunt or pointed tip, depending on the perspective. The outer ridge is very distinct. It is highly sclerotised and adapts the dSTA longitudinally while the inner part is less sclerotised and triangular in diameter. This type is only present in *Diplocephalus arnoi* and *D. pavesii* (node 55) but might also occur in some closely related taxa as, e.g., *D. longicarpus* and *D. procer* (which were not scored in this analysis).

(86). Inner suprategular apophysis, mesal second pointy tip

0: absent (H00: fig. 2b, *Araeoncus humilis*).
1: present (Figs 7B, 17F; Merrett 1963: fig. 63a, *Dicymbium nigrum*).

This is a synapomorphy of *Dicymbium nigrum* and *Di. tibiale* (node 30). It is a small pointed mesally facing tip emerging from the massive but thin to leaf-like inner suprategular apophysis (character 85). This tip is much smaller than the actual inner suprategular apophysis (character 84).

(87). Inner suprategular apophysis, massive, highly sclerotised proximal facing

0: absent (H00: fig. 2b, *Araeoncus humilis*).
1: present (Tanasevitch 1985a: fig. 17, *Savignia nenilini* Marusik, 1988; Lasut *et al.* 2009: fig. 16, *Savignia zero*).

In the most distally placed Far East species of *Savignia* (node 47) the tip of the inner suprategular apophysis is split into two. One tip faces distally (character 85, state 8), the second one proximally, together resembling a ship's screw with two more or less equally sized lobes. The tip of this apophysis is usually blunt. This form is supposedly a derived form of the simple distal facing tip found in more basal species of *Savignia*, i.e., *Diplocephalus mirabilis* and *S. frontata* (see small hook in, e.g., Merrett 1963: fig. 68a). *Savignia zero* has even a third small proximally facing tip that has not been coded here as extra character.

Distal suprategular apophysis

88. Distal suprategular apophysis (dSTA), initial orientation

0: extends distally beyond suprategulum (H00: fig. 19c, *Leptorhoptrum robustum*).
1: extends ventrally from suprategulum (Fig. 18C; H00: fig. 1e, *Araeoncus crassiceps*).

MH04-31, A09-27. In all erigonines the distal suprategular apophysis extends ventrally from the suprategulum while it extends distally beyond the suprategulum in all Linyphiinae in the current dataset. The definition and general discussion of the dSTA is given in MH04-29 and H00-13. As the dSTA is present in all scored taxa in the current analysis, it is phylogenetically uninformative and therefore not discussed again here.

89. Distal suprategular apophysis, texture

0: smooth (MH04: fig. 15b, *Neocautinella neoterica*).
1: with distal grooves or papillae (H00: pl. 38c–d, *Hylyphantes nigritus* (Simon, 1882)).

MH04-32. In the current analysis the distal suprategular apophysis is smooth in all scored taxa. However, there are yet excluded but presumably closely related taxa like *Dactylopisthoides hyperboreus* Eskov, 1990 with papillate suprategular apophyses (Tanasevitch & Marusik 2023: fig. 1e).

(90). Distal suprategular apophysis, form

0: protruding and covering the tegulum (Fig. 17B, *Dactylopisthes locketi*; Tanasevitch 1989: figs 126, 129, *Dactylopisthes locketi*, *Da. mirabilis*).
1: dirk- to dagger-like (Fig. 18B; Eskov 1988: fig. 14, *Diplocephalus marusiki*).
2: delicate, sigmoid (Fig. 23A–B; H00: fig. 6a, c, *Diplocephalus cristatus*).
3: right angled (Fig. 18C; H00: fig. 1e, *Araeoncus crassiceps*).
4: simple straight to slightly curved (Fig. 23D–E, *Erigonella hiemalis*; Holm 1977: fig. 7, *Savignia producta*).
5: massive, short sigmoid (Fig. 18F, *Dicymbium libidinosum*).
6: flattened with round tip (Figs 6B, 7F, *Entelecara erythropus*; Fig. 18G, Thaler 1969: fig. 43, *Janetschekia monodon*).
7: pointed, short hook (Fig. 17A; Merrett 1963: fig. 29a, e, *Linyphia triangularis*).
8: simple, pointed (Fig. 5F: Merrett 1963: fig. 67c, *Diplocephalus picinus*).
9: simple, broad with incised tip (Fig. 18I; Merrett 1963: fig. 91c, *Saloca diceros*).
10: highly sclerotised, massive blunt (Figs 17G, 21G, *Savignia frontata*; Tanasevitch 1985a: figs 17, 21, *Savignia nenilini*, *Savignia frontata*, respectively).
11: small with blunt or pointed tip (Figs 6D, 9J, 17C; Merrett 1963: fig. 62c, *Glyphesis servulus*).
12: whip-like with pointed tip (Fig. 5C–D; *Dicymbium nigrum*, *Dicymbium tibiale*; Merrett 1963: fig. 63a–b, *Di. nigrum*).
13: membranous (Figs 3E, 9K, *Hypomma bituberculatum*; Figs 7E, 9G; Merrett 1963: fig. 96b–c, *Dismodicus bifrons*).

The forms of the distal suprategular apophysis is often species specific. It varies from thin thread-like types in *Diplocephalus crassilobus* (Millidge 1979: fig. 56) to massive ones in *Dactylopisthes mirabilis* (Tanasevitch 1989: fig. 56; Gnelitsa 2006: fig. 3b). Due to the lack of phylogenetic information autapomorphic types have not been defined as separate states.

State 0 is distinctly curved and shifted ventrally, protruding/covering the tegulum at the retrolateral side and exceeding the cymbium. It is an ambiguous synapomorphy (considering fast character optimisation) but only present in *Dactylopisthes* (node 20).

State 1 is dagger-like and very robust compared to other dSTAs and looks triangular in cross-section. Its proximal part is twisted right where the outer suprategular apophysis ends. Due to the general similarity, *Diplocephalus mirabilis* was coded as having this type, despite it being much shorter and blunt (Eskov 1988: fig. 20). It is an ambiguous synapomorphy of node 39, but it is only present in *Hemistajus* Schenkel, 1934 (genus name is restored in the Systematics section) (node 43) and *Diplocephalus mirabilis*.

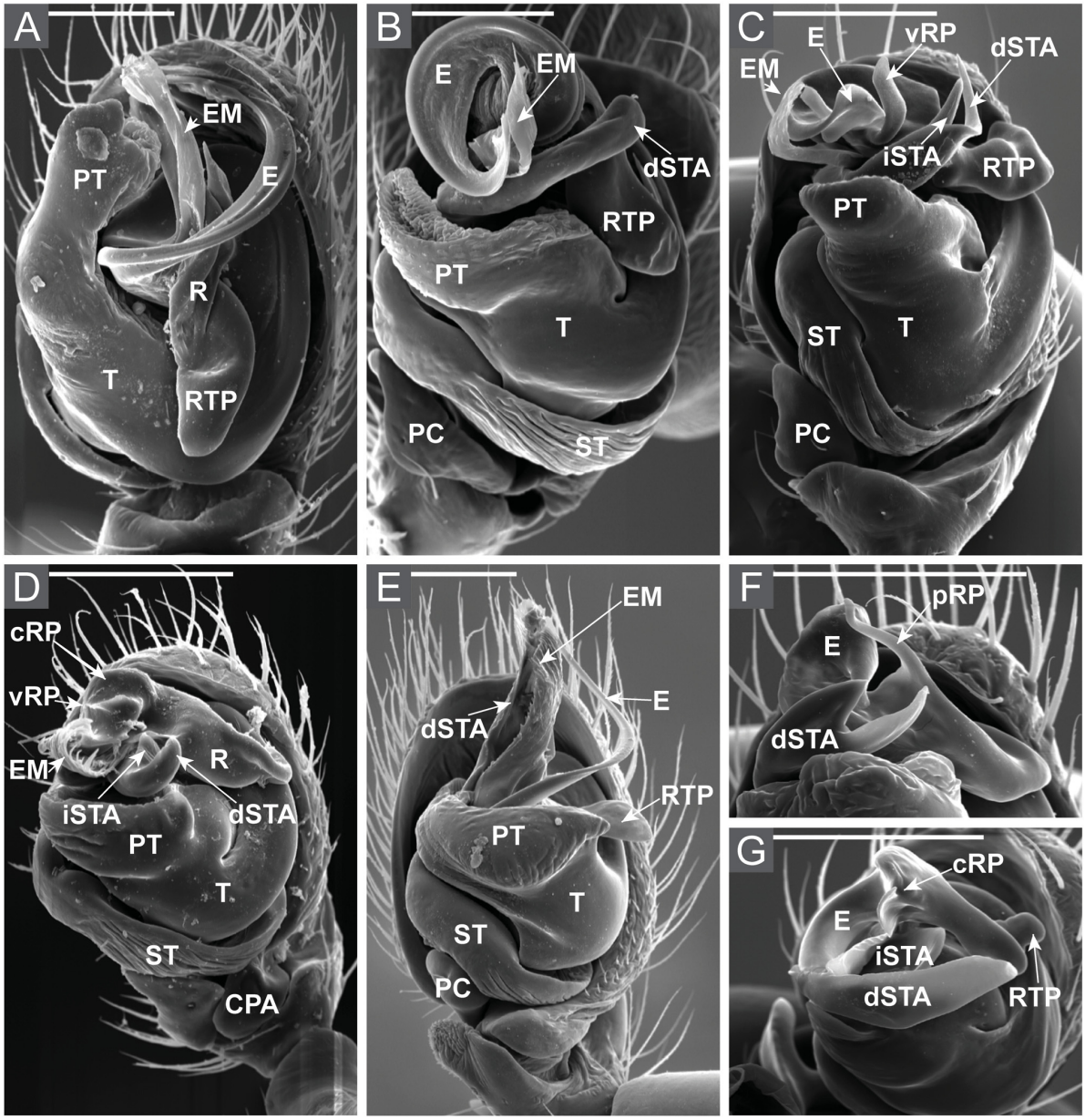

Fig. 6. Scanning Electron Microscope pictures of the male palp in ventral view. **A**. *Dismodicus bifrons* (Blackwall, 1841) (Ar1192; NMBE). **B**. *Entelecara erythropus* (Westring, 1851) (Ar172; NMBE). **C**. *Erigonella hiemalis* (Blackwall, 1841) (ZMUC). **D**. *Glyphesis servulus* (Simon, 1882) (792f; NMB). **E**. *Hypomma bituberculatum* (Wider, 1834) (Ar553; NMBE). **F**. *Alioranus pastoralis* (O. Pickard-Cambridge, 1872), embolic division (3695-3702; coll. E.G.). **G**. *Erigonella ignobilis* (O. Pickard-Cambridge, 1871) (Ar2880; NMBE). Abbreviations: see Material and methods. Scale bars = 100 μm.

State 2 is a delicate pointed apophysis, which is relatively narrow at its base and narrows even more towards the tip. It is a synapomorphy of node 57.

State 3 is kinked, relatively robust compared to state 2 and sometimes slightly twisted. More delicate differences are scored in character 91. It is an ambiguous synapomorphy of *Araeoncus* (node 59) with one reversal in node 61 (*Diplocephalus dentatus* and *Diplocephalus picinus*). *Diplocephalus dentatus* shows simple shapes in most of the male genital characters compared to the remaining members of *Araeoncus* (node 59).

State 4 is a synapomorphy of *Erigonella* (node 33). The different types of tips are scored in character 93. The dSTA of *Diplocephalus latifrons* is slightly different. It is highly sclerotised, massive, and blunt and has a unique additional fold arising at its distal end (Fig. 23J–K).

State 5 is very similar to state 2 but is highly enlarged and more robust and massive. It is present in *Dicymbium libidinosum* and *Diplocephalus turcicus*.

State 6 is homoplastic, i.e., defines different paraphyletic groups (e.g., node 53 with reduction in node 57 or node 3 with reduction in node 11) but is also one of only a few structures that appear on the three earliest branching *Savignia*-group taxa together: *Janetschekia*, *Caucasopisthes* and *Archaraeoncus*. Some of these taxa have inner ridges which is scored as a separate character 92.

State 7 is a highly sclerotised short hook with a pointed tip common only to *Linyphia triangularis* and *Bolyphantes luteolus* (Merrett 1963: 16a, d).

State 8 is sclerotised and constantly narrows towards its pointed tip. It is found in three distantly related species. This state potentially includes non-homologous structures: e.g., *D. dentatus* has the simplest bulbus of *Araeoncus* and the bulbus of *D. picinus* has very few to no derived characters and consequently ambiguous positions in the cladograms.

State 9 constantly broadens towards the tip. The tip is either only slightly incised as in *Saloca diceros* (Merrett 1963: fig. 91c) or about as much as the width of the dSTA and forms two pointed tips (e.g., *Saloca kulczynskii*, shaped like *Alioranus pastoralis*, Fig. 5A, but much less sclerotised, see discussion of state 11). The lower half is highly sclerotised while the upper half is very thin and membranous (Merrett 1963: fig. 91c). This is a synapomorphy of *Saloca* (node 28).

State 10 is an ambiguous synapomorphy present in node 46 within *Savignia* and *D. subrostratus.* This dSTA is usually pointed (Tanasevitch 1985a: fig. 21, *Savignia frontata*).

State 11 includes small dSTAs, which are not much longer than the inner suprategular apophysis. It forms a twist together with the inner suprategular apophysis (where present) and bears striae between the two (Fig. 9J) in all species of *Glyphesis*. This type is an ambiguous synapomorphy present in node 22 (*Glyphesis*) and in node 6 (*Al. pauper* and *Al. pastoralis*). All species coded as present have a blunt tip except for *Alioranus pastoralis*. The shape in *Alioranus pastoralis* (Figs 5A, 9A) is equal to what is seen in *Saloca kulczynskii*.

State 12 is a whip-like shape that is presumably round in cross section and not flattened as in most other types. It slightly narrows towards the tip. It is a synapomorphy of node 30 only being present in *Dicymbium nigrum* and *Di. tibiale*.

State 13: the dSTA of *Hypomma bituberculatum* is elongated by a distal facing membranous appendix. It is usually broadened and has a blunt to round tip. In *Dismodicus bifrons* and *Dis. elevatus* it is unclear if this truly is an elongation of the distal suprategular apophysis or if it emerges from the column. This state is a synapomorphy of node 11.

(91). Distal suprategular apophysis, right angle type, kinks

0: simple roundish right angle (Figs 7A, 18D, *Araeoncus humilis*).
1: simple edgy right angle (Fig. 18C; H00: fig. 1e, *Araeoncus crassiceps*).
2: robust with second kink (Fig. 18E, *Araeoncus victorianyanzae*).

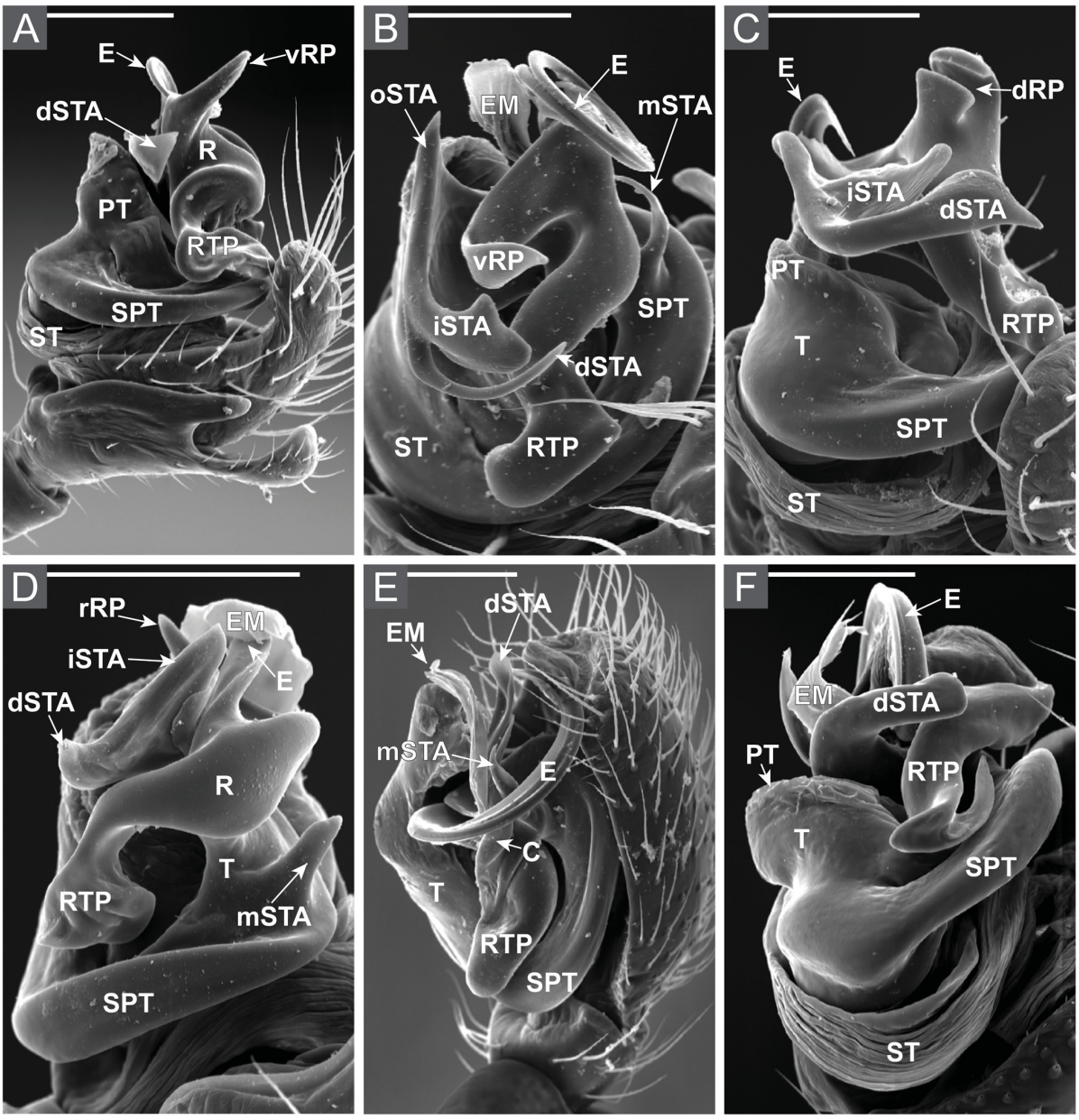

Fig. 7. Scanning Electron Microscope pictures of the male palp in prolateral view. **A**. *Araeoncus humilis* (Blackwall, 1841) (Ar3186; NMBE). **B**. *Dicymbium nigrum* (Blackwall, 1834) (Ar637; NMBE). **C**. *Diplocephalus latifrons* (O. Pickard-Cambridge, 1863) (Ar1262; NMBE). **D**. *Diplocephalus picinus* (Blackwall, 1841) (Ar6645; NMBE). **E**. *Dismodicus bifrons* (Blackwall, 1841) (Ar1192; NMBE). **F**. *Entelecara erythropus* (Westring, 1851) (Ar172; NMBE). Abbreviations: see Material and methods. Scale bars = 100 µm.

This character accounts for the different types of right-angled dSTAs. State 0 is found in *Diplocephalus helleri* and *Araeoncus humilis*. State 1 is a synapomorphy of node 64 with a reversal in node 66, and state 2 is an ambiguous synapomorphy of node 66 seen in *Diplocephalus protuberans* also.

(92). Distal suprategular apophysis, flattened with round tip, inner ridge

0: without inner ridge (Fig. 18H; Tanasevitch 1987: fig. 104, *Diplocephalus caucasicus*)
1: with inner ridge (Fig. 18A; Thaler 1972: fig. 17, *Diplocephalus pavesii*).

An inner ridge is found on the flattened with round tip type of the distal suprategular apophysis in *Diplocephalus pavesii* and *D. arnoi* (node 55) and also in *Savignia harmsi*. This character is only applicable for taxa having a flattened dSTA with a round tip (character 90, state 6) and therefore not independent.

(93). Distal suprategular apophysis, simple straight to slightly curved type, tip

0: blunt to slightly pointed (Figs 6C, 9H, 23D, *Erigonella hiemalis*; Thaler 1971: fig. 4, *Erigonella subelevata*).
1: sharply pointed (Fig. 17E; Holm 1977: fig. 7, *Savignia producta*).

The taxa of node 37 (*Savignia producta* and *Diplocephalus connatus* plus *D. connatus jacksoni*) have additionally to the simple straight to slightly curved type also a sharply pointed flat and sclerotised tip. This character is only applicable for taxa with simple straight to slightly curved dSTAs (character 90, state 4) and therefore not independent.

(94). Distal suprategular apophysis, tip

0: blunt to round (Fig. 7F, *Entelecara erythropus*; Fig. 18G, Thaler 1969: fig. 43, *Janetschekia monodon*).
1: pointed (Fig. 23A; H00: pl. 19b, *Diplocephalus cristatus*).

This character accounts for clearly blunt to round tips in contrast to pointed tips.

(95). Distal suprategular apophysis, direction

0: mesal (Fig. 23H–I, *Erigonella ignobilis*; H00: fig. 9c, *Entelecara acuminata*).
1: distal (Fig. 23J–K, *Diplocephalus latifrons*; H00: fig. 1e, *Araeoncus crassiceps*).

The definition of directions is sometimes difficult to define since a sclerite often lies somehow skewed in the bulbus. State 1 accounts for distal suprategular apophyses clearly arising from the transverse plane, directing distally. Apophyses that do not, or only slightly raise from this plane are coded as mesally directed (state 0).

Male palpal structures and column

(96). Column (CO), orientation

0: straight, facing distally to slightly ventrally (Fig. 2E, *Diplocephalus picinus*; H00: fig. 6a–b, d, g, *Diplocephalus cristatus*).
1: twisted, facing proximally to slightly ventrally (Fig. 7E, *Dismodicus bifrons*; H00: fig. 7c–f, *Dismodicus decemoculatus*).

The column emerges either ventrally from the suprategulum and enters the radix at its prolateral to ventral side or else emerges distally from the suprategulum and enters the radix proximally. State 1 is an ambiguous synapomorphy present in node 10 (and typical for the *Pelecopsis*-group) with a convergent occurrence in *Hilaira excisa*.

(97). Column, sclerotisation

0: absent, whole column transparent (H00: 2c, *Araeoncus humilis*).
1: basally sclerotised with mesal knob (Fig. 21D, *Savignia birostra*; Lasut *et al.* 2009: figs 4, 8, 12, *Savignia birostra*, *S. saitoi*, *S. zero*).

The proximal part of the column is sometimes sclerotised. This is not a marginal apophysis that fused with the column, since both are present side aside in, e.g., *Savignia* (Fig. 21D, *Savignia birostra*). This is an ambiguous synapomorphy of *Savignia* and *Hemistajus* (node 42) with a reversal in *D. montanus* and with additional occurrences in *Pelecopsis elongata*, *Hypomma bituberculatum* and in *Saloca* (node 28).

(98). Column, apophysis

0: absent (H00: 2c, *Araeoncus humilis*).
1: present (Fig. 21D, *Savignia birostra*; Lasut *et al.* 2009: figs 4, 8, 12, *Savignia birostra*, *S. saitoi*, *S. zero*).

This is a slightly sclerotised knob arising from the dorso-prolateral side of the column and is synapomorphic for *Savignia* (node 45).

99. Embolic membrane (EM), papillae

0: absent (Figs 2E, 7D, *Diplocephalus picinus*; H00: pl. 18b, *Diplocentria bidentata*).
1: present (Fig. 9J, *Glyphesis servulus*; H00: pl. 27b, *Gonatium rubens* (Blackwall, 1833)).

MH04-41, A09-35. Papillae are present in nodes 20, 23, 34, *Alioranus pastoralis* and *Dicymbium libidinosum*.

(100). Embolic membrane, sclerotisation

0: absent (Fig. 2E, *Diplocephalus picinus*; H00: pl. 18b, *Diplocentria bidentata*).
1: present (Fig. 21E; Thaler 1969: fig. 44; Millidge 1977: fig. 142, *Janetschekia monodon*).

The distinct pointed hook of *Janetschekia monodon* (Thaler 1969: fig. 44; Millidge 1977: fig. 142) emerges from below the radix and is supposed to be a sclerotised embolic membrane. It is an ambiguous synapomorphy of *Saloca* (node 28) and *Janetschekia monodon*.

Male palpal radix

101. Fickert's gland

0: absent.
1: present (Hormiga 1994a: fig. 14a–b, *Tenuiphantes tenuis*).

MH04-64, H00-25, A09-45. The presence of this structure supports node 2.

102. Terminal apophysis

0: absent.
1: present (Hormiga 1994a: fig. 12b, *Bolyphantes luteolus*).

MH04-65, H00-26, A09-46. The absence of this apophysis supports Erigoninae (node 3).

103. Lamella characteristica

0: absent (MH04: fig. 17b, *Spanioplanus mitis* Millidge, 1991).
1: present (H00: pl. 5a–c, *Tenuiphantes tenebricola* (Wider, 1834)).

MH04-66, H00-27, A09-51. The absence of this sclerite supports Erigoninae (node 3).

104. Radix-embolus connection

0: continuous (MH04: fig. 17h, *Rhabdogyna patagonica* (Tullgren, 1901)).
1: membranous (H00: fig. 9d, f–g, *Entelecara acuminata*).

MH04-51, A09-51. The membranous radix-embolus connection is an ambiguous synapomorphy of *Entelecara* (node 9) and also present in *Hilaira excisa*.

Embolus and its shapes

105. Embolus (E), length

0: long (MH04: fig. 18b, *Notiomaso exonychus* Miller, 2007).
1: short (MH04: fig. 18c, *Microplanus odin* Miller, 2007).

MH04-43, H00-17. The long embolus is at least a third the length of the cymbium. The short embolus is usually tooth-like or slightly longer.

(106). Contact embolus

0: absent, short to long.
1: present, tiny (Fig. 9F, *Diplocephalus picinus*; Fig. 21E, *Janetschekia monodon*; Merrett 1963: figs 16a, 67b, *Bolyphantes luteolus*, *Diplocephalus picinus*).

Contact emboli are tiny, pointed, highly sclerotised emboli (Burger & Nentwig 2002 and references to Wiehle therein). They are often a hardly visible structure on the radix with an opening for the sperm duct. They contrast with other types of emboli that are introduced into the vulva (like lamelliform or whip-like emboli, see following characters) rather than only contacting it. A very short contact embolus "Anschlussembolus" (Wiehle 1960) is found in many erigonines but also in *Bolyphantes luteolus*. Even though their function might be the same, their conformation seems different. The embolus of, e.g., *Caucasopisthes procurvus* is a very short contact embolus with a high degree of sclerotisation. A contact

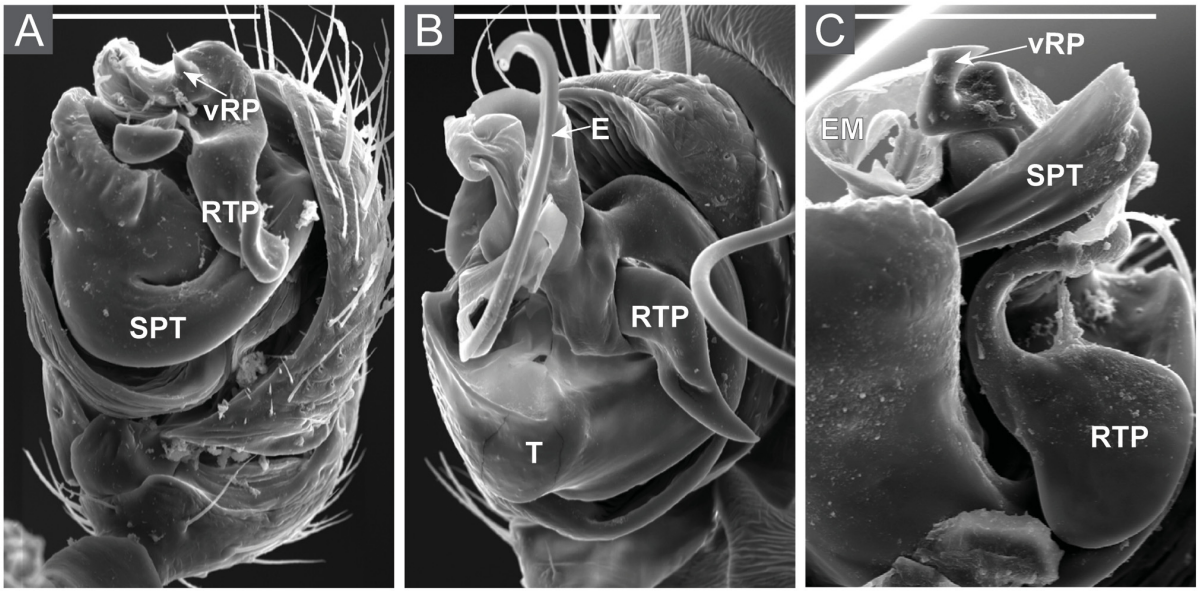

Fig. 8. Scanning Electron Microscope pictures of the male palp in prolateral view. **A**. *Glyphesis servulus* (Simon, 1882) (792f; NMB). **B**. *Panamomops tauricornis* (Simon, 1882) (NMBE). **C**. *Saloca diceros* (O. Pickard-Cambridge, 1871) (Ar3289; NMBE). Abbreviations: see Material and methods. Scale bars = 100 μm.

embolus is found in taxa basal to node 26 (exceptions are *Linyphia triangularis*, nodes 8 and 20 with injection emboli) and in *Diplocephalus picinus*.

107. Embolic shape

0: straight to curved (MH04: fig. 17g, *Rhabdogyna patagonica*).
1: spiral (Fig. 2F, *Dismodicus bifrons*; H00: fig. 7d, *Dismodicus decemoculatus*).

MH04-44, A09-37. Most scored linyphiids have a somewhat spiral embolus. The only exceptions are node 45 plus *Diplocephalus lusiscus*, *D. subrostratus* and *D. turcicus*. Straight to only slightly curved emboli were scored as state 0, more strongly curved taxa as spiral (state 1). This character is applicable to long emboli only (character 105, state 0).

(108). Embolus, spiral-dimension

0: spiral in sagittal plane, divides palp into pro- and retrolateral side (Fig. 5D; Roberts 1987: fig. 10f, *Dicymbium tibiale*).
1: spiral in transverse plane, divides palp into proximal and distal side (Figs 9H, 24K–L; Merrett 1963: fig. 64b, *Erigonella hiemalis*).
2: spiral in coronal plane, divides palp into dorsal and ventral side (Figs 3A, 6B, *Entelecara erythropus*; H00: fig. 1a, *Araeoncus crassiceps*).

The coding of the embolus of *Diplocephalus latifrons* is very difficult. In its general appearance it is very close to *Erigonella hiemalis* and was therefore coded accordingly. However, its embolus is not only spiral in a transverse plane but also curved (not spiralled) in a sagittal and additionally curved in a coronal plane (ventral/dorsal).

(109). Embolus, long, robust, widely curved

0: absent, of another shape.
1: present (Fig. 21A; Millidge 1977: fig. 131, *Diplocephalus helleri*; H00: fig. 1a–b, *Araeoncus crassiceps*).

This type of embolus is present in taxa with a relatively small radix compared to the enlarged radical appendices. It emerges distally from the radix, has an outstanding base, formed like a squarish socket (Thaler 1978: fig. 14) and is widely curved. There are different forms ranging from a simple curve (*A. crassiceps*, *A. anguineus* and *A. vaporariorum*) to a U-shape (*A. caucasicus*, *A. victorianyanzae*) or to more complex shapes (*Diplocephalus helleri*), scored as separate character 110. The proximal part of the embolus continues proximally over the dorsal side of the column. This character is a synapomorphy of *Araeoncus* (node 59) with a reversal in *Diplocephalus picinus*.

(110). Embolus, long, robust, widely curved, form

0: present, simple curve (Fig. 16A; Wiehle 1960: fig. 444, *Araeoncus anguineus*).
1: present, U-form (Fig. 21C; Tanasevitch 1987: fig. 63, *Araeoncus caucasicus*).
2: present, complex curves (Fig. 21A; Millidge 1977: fig. 131, *Diplocephalus helleri*).

This character accounts for the different forms of long, robust, widely curved emboli. The simple curve initially directs retrolaterally and then curves distally. The U-form also initially directs retrolaterally but then turns proximally before it curves distally. The complex type emerges distally from the radix, then curves retrolateral, then dorsal and proximal and the tip directs ventrally. However, apart from its initial turns it is very similar to the U-curved conformation. The embolus of *Araeoncus anguineus* is intermediate between *A. crassiceps* (U-form) and *A. vaporariorum* (curve). State 1 is a synapomorphy of node 63 with a reversal to state 2 in *A. humilis* and to state 0 in *A. galeriformis* and in node 68 (*A. vaporariorum* and *A. anguineus*).

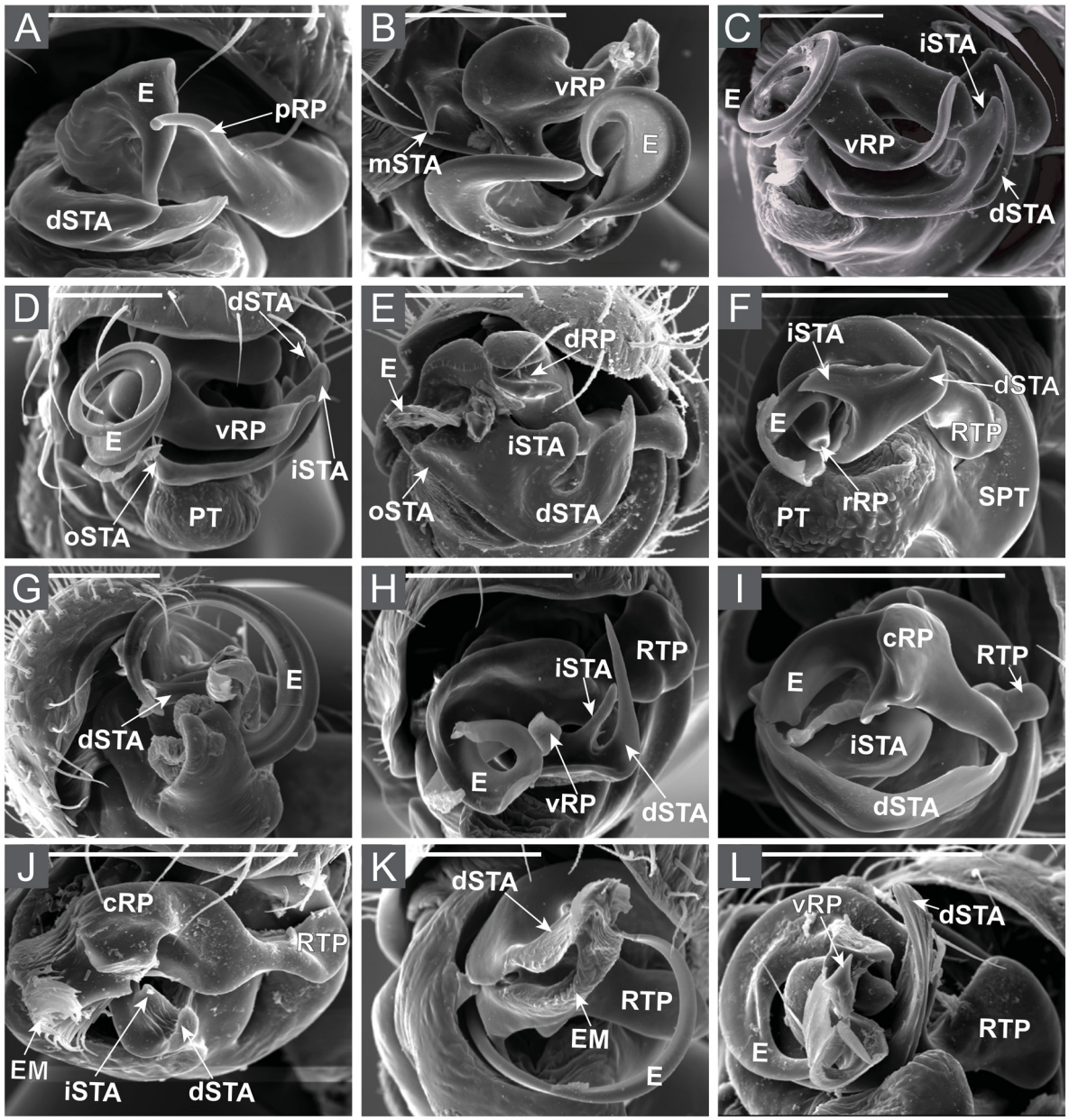

Fig. 9. Scanning Electron Microscope pictures of the male palp distal view. **A**. *Alioranus pastoralis* (O. Pickard-Cambridge, 1872) (3695-3702; coll. E.G.). **B**. *Araeoncus humilis* (Blackwall, 1841) (Ar3186; NMBE). **C**. *Dicymbium nigrum* (Blackwall, 1834) (Ar637; NMBE). **D**. *Dicymbium tibiale* (Blackwall, 1836) (11430; ZMUC). **E**. *Diplocephalus latifrons* (O. Pickard-Cambridge, 1863) (Ar1262; NMBE). **F**. *Diplocephalus picinus* (Blackwall, 1841) (Ar6645; NMBE). **G**. *Dismodicus bifrons* (Blackwall, 1841) (Ar1192; NMBE). **H**. *Erigonella hiemalis* (Blackwall, 1841) (ZMUC). **I**. *Erigonella ignobilis* (O. Pickard-Cambridge, 1871) (Ar2880; NMBE). **J**. *Glyphesis servulus* (Simon, 1882) (792f; NMB). **K**. *Hypomma bituberculatum* (Wider, 1834) (Ar553; NMBE). **L**. *Saloca diceros* (O. Pickard-Cambridge, 1871) (Ar3289; NMBE). Abbreviations: see Material and methods. Scale bars = 100 μm.

(111). Embolus, elongated lamella-like

0: absent, of another shape.
1: present (Fig. 24H–J, *Erigonella subelevata*; Figs 9H, 24K–L, *Erigonella hiemalis*; H00: pl. 19b, *Diplocephalus cristatus*).

This is a relatively thin, flattened embolus. In a few species (e.g., Figs 2D, 9E, 24E–G, *Diplocephalus latifrons*) the whole embolus is highly sclerotised, but still flattened. A similar situation is found in *Diplocephalus arnoi* and *D. pavesii* where the embolus has a velum about as broad as the embolus and the sperm duct is visible. This is very similar to the type of embolus with a transparent outgrowth (character 116) but much narrower. Most of these emboli have a lamellar extension of some kind. A distal extension at the retrolateral side is found in, e.g., *Erigonella hiemalis*, while other taxa have a velum at the inner side.

This type of embolus is longest in *Diplocephalus caucasicus*, *D. permixtus*, *D. arnoi* and *D. pavesii* and is homologous with what is seen in the *cristatus*-group (node 57) where it is considerably shortened so that its tip is fused to the radix (character 114; H00: pl. 19b, *Diplocephalus cristatus*). This character is a synapomorphy of node 31 with one reversal in node 59.

(112). Embolus, elongated lamella, flattened orientation

0: distal to proximally flattened (Fig. 24H–J, *Erigonella subelevata*; Fig. 9H, *Erigonella hiemalis*; H00: pl. 19b, *Diplocephalus cristatus*).
1: laterally flattened (Fig. 21D, *Savignia birostra*; Lasut *et al.* 2009: figs 4, 8, 12, *Savignia birostra*, *S. saitoi*, *S. zero*).

This character is applicable only in taxa with an elongated lamella-like embolus (character 111). The direction separates node 31 into two groups: node 33 and nodes 49-58 have a distal to proximal flattened elongated lamella-like embolus, while the laterally flattened elongated lamella-like embolus is a synapomorphy of node 39.

(113). Embolus, elongated, flattened form

0: simple flattened.
1: with right angled distal protuberance (Fig. 24H–J, *Erigonella subelevata*; Figs 9H, 24K–L, *Erigonella hiemalis*; Thaler 1969: fig. 25, *Diastanillus pecuarius*).

This is only accessible for distal to proximally flattened types (character 112, state 0). A thin protuberance emerges distally from the distal to proximally flattened elongated lamella-like embolus in nodes 34, 54 and in *Diastanillus pecuarius* and *Diplocephalus turcicus*.

(114). Embolus, elongated lamella, shortened with tip fused to the radix

0: absent.
1: present (Fig. 24A–B; H00: pl. 19d, *Diplocephalus cristatus*).

This lamelliform embolus looks like a folded lamella that contains the sperm duct, which ends on the edge of that lamella (see also Comstock 1910 “lamelliform embolus”). This type seems to be a secondarily shortened elongated lamella-like embolus and is therefore only applicable for taxa with an elongated lamella-like embolus (character 111). This is a synapomorphy of node 57, the *cristatus*-group.

(115). Embolus, whip-like spiralled distally with velum

0: absent.
1: present (Figs 6A, E, 9G, K, *Dismodicus bifrons*, *Hypomma bituberculatum*; Millidge 1977: figs 94, 97, *Hypomma bituberculatum*, *Dismodicus elevatus*).

This is a more delicate version of the long, robust, widely curved type of embolus (character 109) found in *Araeoncus*. Here, the sclerotised part is very thin and whip-like and accompanied by a velum at the inner side, which is about as broad as the sclerotised part. Different to the *Araeoncus* type, this is a rather thin embolus and spirals distally rather than proximally. In the current analysis, it is an ambiguous synapomorphy present in nodes 10 and 27. *Dicymbium* has a very similar type as seen in *Dismodicus* but it is much broader and the spiral is sagittal instead of transverse.

(116). Embolus, transparent outgrowth (ETO)

0: absent.
1: present (Fig. 21G, *Savignia frontata*; Lasut *et al.* 2009: figs 4, 8, 12, *Savignia birostra*, *S. saitoi*, *S. zero*).

In *Savignia* the embolus is a composite of a sclerotised backing (as seen in most taxa with a long embolus) plus an additional lamellar/transparent outgrowth connecting the radix with the tip of the sclerotised section of the embolus.

In most erigonine species, the spermduct runs from the column into the sclerotised radix and subsequently into the embolus. In *Savignia*, the spermduct runs from the column along the lamellar/transparent outgrowth of the radix to the tip of the sclerotised part of the embolus. This lamellar outgrowth seems to be stretched between the sclerotised section of the embolus, the column and the radix to which it is fused. It is much broader than the sclerotised part of the embolus. We coded this whole structure as an embolus in *Savignia*. This character is a synapomorphy of *Savignia* (node 45).

(117). Embolus, transparent outgrowth, length

0: embolus ends with transparent outgrowth (Fig. 21D, *Savignia birostra*; Lasut *et al.* 2009: figs 4, 8, 12, *Savignia birostra*, *S. saitoi*, *S. zero*; Tanasevitch 1985a: fig. 18, *Savignia nenilini*).
1: embolus protrudes the transparent outgrowth (Fig. 21G; Tanasevitch 1985a: fig. 22, *Savignia frontata*).

Within the genus *Savignia* we find a transparent outgrowth (character 116) of the radix that is connected to a sclerotised needle-like margin. In most species this margin is only slightly longer than the outgrowth while it is elongated in others. This character is only applicable for taxa with a transparent outgrowth. State 0 is a synapomorphy of node 47.

(118). Embolus, inner structure

0: straight.
1: twisted (Fig. 2A, *Araeoncus humilis*; Figs 9H, 24K–L, *Erigonella hiemalis*; H00: fig. 56b, *Savignia frontata*).

The embolus can be formed like a rod (state 0) or else is twisted like a screw (state 1). The twist can be unidirectional (screw-like) or go back and forth.

(119). Embolus, initial orientation

0: distal (Fig. 21A; Millidge 1977: fig. 131, *Diplocephalus helleri*).
1: ventral (Fig. 2F, *Dismodicus bifrons*; H00: pl. 19b, *Diplocephalus cristatus*).
2: proximal (Wiehle 1960: fig. 40, *Pelecopsis elongata*).
3: retrolateral (Figs 2A, 9B; H00: pl. 13a, *Araeoncus humilis*).

(120). Embolus, distal part orientation

0: in line with embolus (Fig. 21A; Millidge 1977: fig. 131, *Diplocephalus helleri*).
1: bent proximally to dorsally (Fig. 21D, *Savignia birostra*; Lasut *et al.* 2009: figs 12–13, *Savignia zero*).

The tip of the embolus of a few species initially orientates retrolaterally but then curves proximally to dorsally. This is a synapomorphy of node 42 with a reversal in node 44.

(121). Embolus, velum

0: absent (Fig. 9I, *Erigonella ignobilis*; H00: fig. 10f, *Gonatium rubens*).
1: present (Figs 6A, 9G, *Dismodicus bifrons*; H00: fig. 7d, *Dismodicus decemoculatus*; Fig. 6B, *Entelecara erythropus*).

The velum is a transparent thin band alongside the embolus. It ranges from very thin in, e.g., *Dismodicus bifrons* to relatively broad as in, e.g., *Entelecara erythropus*. The transparent outgrowth (character 116) of *Savignia* is presumably a very distinct velum with a connection to the column. This is an ambiguous synapomorphy of *Savignia* (node 45) and *Diplocephalus* (node 53).

(122). Embolus velum, extension

0: alongside the embolus (Figs 6A, 9G, *Dismodicus bifrons*; H00: fig. 7d, *Dismodicus decemoculatus*).
1: restricted to a narrowly curved section (Figs 2A, 19B; H00: pl. 13a, *Araeoncus humilis*).

The restricted velum is an autapomorphy of *Araeoncus humilis* in the current analysis. However, it is also present in *Araeoncus hanno* Simon, 1884 (Bosmans 1996: fig. 14), a species that was not scored in this analysis. This character is only applicable for taxa with a velum (character 121).

123. Embolus, tip

0: terminating in embolic opening (Fig. 9B; H00: pl. 13d, *Araeoncus humilis*).
1: with projection beyond embolic opening (Fig. 21D, *Savignia birostra*; H00: pl. 56d, *Savignia frontata*).

MH04-45. This character is an ambiguous synapomorphy of *Savignia* (node 45) and *Saloca* (node 28) with independent occurrences in another five taxa.

(124). Embolus tip shape

0: blunt/cut (Figs 9I, 24C, *Erigonella ignobilis*; H00: fig. 6e: *Diplocephalus cristatus*).
1: pointed (Fig. 9B, *Araeoncus humilis*; H00: fig. 1a: *Araeoncus crassiceps*).

A pointed embolus tip should be narrower than three times the diameter of the sperm duct. Emboli of this kind usually get narrower towards the tip. In, e.g., *E. ignobilis* it is not easily seen whether the tip is narrower than three times the diameter of the sperm duct or not, but the tip looks broken off rather than getting narrower towards the end.

(125). Embolus tip, narrowly curved

0: absent (Fig. 21D, *Savignia birostra*; H00: pl. 56d, *Savignia frontata*).
1: present (Fig. 9B, *Araeoncus humilis*; Thaler 1972: fig. 18, *Diplocephalus pavesii*).

The whole embolus is narrowly curved at its tip. In the *cristatus*-group (node 57) the embolus is reduced to a short lamella; however, the sperm duct is narrowly curved in this lamella and therefore coded as present. This character is an ambiguous synapomorphy present in nodes 34, 53, and 67 but also present in *Linyphia triangularis*, *Araeoncus humilis* and *Diplocephalus lusiscus*.

(126). Embolus, inner tip flag

0: absent (Fig. 9G, *Dismodicus bifrons*; H00: fig. 7d, *Dismodicus decemoculatus*).
1: present (Fig. 3A, *Entelecara erythropus*; H00: fig. 1a).

A small, flag-like, lamelliform protuberance is present in some taxa. It emerges near the tip of the embolus and faces towards the inside. This character is an ambiguous synapomorphy of *Entelecara* (node 9) but also present in *Araeoncus galeriformis*.

A similar but even smaller structure facing outwards is present in some species of *Araeoncus* (e.g., H00: fig. 1a, *Araeoncus crassiceps*). Since it is difficult to see without a SEM we did not score it.

127. Embolic papillae

0: absent (H00: pl. 13a, *Araeoncus humilis*).
1: present (H00: pl. 6a, *Tenuiphantes tenebricola*). MH04-46. Embolic papillae are only present in node 2 of the current analysis.

128. Embolic basal process

0: absent (MH04: fig. 19a, *Ceratinopsis interpres* (O. Pickard-Cambridge, 1874)).
1: present (MH04: fig. 18e, *Sphecozone spadicaria* (Simon, 1894)).

MH04-48. This is a process arising from the proximal part of the embolus, where the sperm duct passes from the radix to the embolus. The embolic basal process is absent in all scored taxa and therefore phylogenetically uninformative. As homologies of the different appendices arising from the radix are very difficult, we kept this character in the matrix.

Anterior radical process

129. Anterior radical process

0: absent (H00: pl. 52d, *Ostearius melanopygius* (O. Pickard-Cambridge, 1880)).
1: present (H00: fig. 18c *Laminacauda plagiata* (Tullgren, 1901)).

MH04-55, H00-23, A09-43. Hormiga (2000) defined the anterior radical process, based on the "rpp" of Merrett (1963), and described it in Miller & Hormiga (2004) as "an apophysis originating near and usually ventral to the origin of the embolus". This character was highly homoplastic in Miller & Hormiga (2004) suggesting that several non-homologous structures were included in that character. Most of the ingroup taxa scored here (node 16) had at least one more radical process besides the embolus and the radical tailpiece (character 160). This third process was coded as an anterior radical process independent of its position apart from clearly different structures like the thread-like prolateral radical process (character 158) and others. In a second step, we defined extra characters to account for the many different radical process forms (characters 130–159). Also we established four characters to account for the position, as we consider the position from which a process emerges is an equally valuable homology criterion as its shape (characters 130, 139, 155 and 157, the ventral, dorsal, retrolateral and prolateral radical process, respectively). In the current analysis, the anterior radical process is a synapomorphy of the *Savignia*-group (node 16) with two reductions in *Diplocephalus dentatus* and *D. subrostratus* and additional occurrences in *Hilaira excisa* and *Alioranus pauper*.

Ventral radical process

(130). Ventral radical process (vRP)

0: absent (Fig. 16C; Millidge 1977: fig. 129, *Diplocephalus dentatus*).
1: present (Fig. 2C, *Dicymbium tibiale*; H00: fig. 1c–d, *Araeoncus crassiceps*).

This character accounts for all processes emerging from the ventral part of the radix. The different types of ventral processes are scored in separate characters (135–138). Most members of the *Savignia*-group have a vRP. Exceptions are *Janetschekia monodon*, *Dactylopisthes* (node 20), *Diplocephalus picinus*, *D. dentatus*, *D. subrostratus* and all members of node 35. It additionally occurs in *Hilaira excisa* and in *Alioranus pauper*. The interference with the anterior radical process (character 129) is relatively high.

(131). Ventral radical process, general shape

0: straight (Fig. 2B, *Dicymbium nigrum*; H00: fig. 1a–d, *Araeoncus crassiceps*).
1: twisted (Fig. 9L; Merrett 1963: fig. 91b, *Saloca diceros*).

The twisted conformation is a synapomorphy of node 28.

(132). Ventral radical process, tip shape

0: blunt (Figs 6C, 9H, 24K, L; Merrett 1963: fig. 64b, *Erigonella hiemalis*).
1: pointed (Fig. 24H–I; Thaler 1971: fig. 4, *Erigonella subelevata*).

Blunt vRPs are only found in nodes 55 and 57, in *Paraglyphesis polaris*, *Glyphesis nemoralis* and in *Erigonella hiemalis*. The presence of a blunt and a pointed ventral apophysis in the sister taxa *Erigonella hiemalis* and *E. subelevata*, respectively, indicates a fast evolution of the tip shape.

(133). Ventral radical process, size

0: smaller to slightly bigger than the radix (Figs 6C, 24L; Merrett 1963: fig. 64b, *Erigonella hiemalis*).
1: much larger than the radix (Figs 5B, 7A, *Araeoncus humilis*; H00: fig. 1d, *Araeoncus crassiceps*).

All species of *Araeoncus* (but the most basal and simple *Diplocephalus dentatus*; Fig. 16C and *D. picinus*) have a considerably enlarged vRP and is therefore an ambiguous synapomorphy of node 59. However, *Hilaira excisa* also has a highly enlarged vRP (H00: "LC" in pl. 33a–c).

(134). Ventral radical process, initial orientation

0: distal (Figs 24H–J; Thaler 1971: fig. 4, *Erigonella subelevata*).
1: ventral (Fig. 16D; H00: fig. 1d, *Araeoncus crassiceps*).

In most taxa the vRP is more or less curved and therefore slightly facing ventral. The vRP has to emerge from the ventral rather than the distal side of the radix to be scored as state 1. Since state delimitations are sometimes difficult to see (e.g., Fig. 2C, *Dicymbium tibiale*) also the overall similarity of the vRP with *Araeoncus crassiceps* was considered.

(135). Ventral radical process, shape

0: radical hook (Fig. 8C; Merrett 1963: "rpp" in fig. 91a, *Saloca diceros*).
1: embolus supporter (Fig. 24A; H00: pl. 19b, d, labelled as "R", *Diplocephalus cristatus*).
2: ridged sail (Fig. 16B; Thaler 1978: fig. 14, *Diplocephalus protuberans*).
3: massively kinked (Fig. 16D; H00: fig. 1d, *Araeoncus crassiceps*).
4: robust, sclerotised with longitudinal striations (H00: pl. 33a–c, *Hilaira excisa*).
5: laterally flattened with dorsal facing sclerotised tip (Fig. 16F; Tanasevitch 1987: figs 126–127, *Araeoncus galeriformis*).
6: bifurcate thin sclerotised distal tip (Fig. 16G; Tanasevitch 1987: figs 101–102, 105, *Diplocephalus caucasicus*).
7: thin dorso-ventrally flattened (Figs 6C, 24L; Merrett 1963: fig. 64b, *Erigonella hiemalis* or Fig. 24H–I; Millidge 1977: fig. 137, *Erigonella subelevata*).
8: blunt, small, thin, short (Fig. 16H; Eskov 1991b: fig. 1, *Paraglyphesis polaris*).
9: pointed small tooth (Figs 3D, 8A, 17C; Merrett 1963: fig. 62a–b, *Glyphesis servulus*).
10: sclerotised radical tooth (Fig. 16I, Eskov 1988: fig. 27, *Diplocephalus montanus*).
11: embolic protuberance (Fig. 21D, *Savignia birostra*; Lasut *et al.* 2009: figs 4, 8, 12, *Savignia birostra*, *S. saitoi*, *S. zero*; H00: fig. 24a, *Savignia frontata*).

This character accounts for the different types of vRPs. Autapomorphic types were only coded as extra states if another species that was not included in the current analysis showed the same structure. State 0

describes a highly sclerotised dorsal facing edged hook, on top of a distal facing process. This is an ambiguous synapomorphy (as an artifact of inapplicables considering fast character optimisation) but only present in *Saloca* (node 28).

State 1 is situated below the lamelliform embolus and seems to support or protect the embolus. It emerges ventrally from the basal to ventral part of the radix. It is very small in some species (e.g., *Diplocephalus cristatus*) but very distinct and even sclerotised in others (e.g., *Diplocephalus arnoi*). In *D. arnoi* it even has a part protruding distally from the main part. This is an ambiguous synapomorphy of nodes 55 and 57 with one additional occurrence in *Diplocephalus lusiscus*.

State 2 emerges ventrally from the radix and is flattened dorso-ventrally. From it emerges a ridge dorsally that continues to the base of the embolus and becomes its dorsal margin (Thaler 1978: fig. 14). In *Diplocephalus helleri* there is also a distal tooth on top of the ridge. A prolateral facing pointed tip emerges right below this ridge (Thaler 1978: fig. 14). In *Diplocephalus protuberans* a second tip with another dorsal ridge is formed at the retrolateral side of this apophysis. This is lacking in *D. helleri* where the margin runs in a continuous curve back to the radix. This type is common only to *D. helleri* and *D. protuberans* (node 62) and might be an ancestral form of state 3. This state is a synapomorphy of node 60.

State 3 is a synapomorphy of node 52 although only present in *Araeoncus* (node 63) with a reversal in *Araeoncus galeriformis*. It emerges ventrally from the ventral side of the radix and kinks dorsally (H00: fig. 1d). The basal (ventral facing) part is usually constricted (character 136) while the distal part is enlarged and triangular in cross-section (H00: fig. 1d). Along its retrolateral side runs a ridge (character 137) and in certain taxa there are also additional processes arising from the retrolateral side (character 138).

State 4 is highly sclerotised, emerging ventrally from the radix but then facing distally (Merrett 1963: fig. 47a). It differs from state 3 by the lack of lateral ridges or appendices but instead has several longitudinal striations on its ventral side. This is an autapomorphy of *Hilaira excisa*.

State 5 is very similar to the dorsal radical process of *Diplocephalus arnoi* (character 143) but mirrored to the ventral side of the radix. Its margins are not folded inside but instead the process is flattened laterally and has a rather thin base and a sclerotised tip that faces dorsally. It is very simple in *Alioranus pauper* without any ridges or second appendices but bears a ridge (third margin) in *Araeoncus galeriformis* that is also found in many other species of *Araeoncus* (character 137). This type emerges independently in *Alioranus pauper*, *Caucasopisthes procurvus* and *Araeoncus galeriformis*.

State 6 is a distinct type occurring in *Diplocephalus permixtus* with moderate tips and in *D. caucasicus* with more distinct, longer tips. It emerges from the ventral side of the radix and directs distally. In *D. caucasicus* it is connected to the prolateral margin of the dorsal radical apophysis but separated from it in *D. permixtus*. *Diplocephalus turcicus* also has this apophysis, but it is much smaller and the tips are less sclerotised and thinner. The two long, thin, sclerotised appendices have been coded as such an apophysis since they are very similar to what is figured in Tanasevitch (1987: fig. 105, *D. caucasicus*). However, true homologies are questionable but the phylogenetic study at least suggests a close relation of the four taxa that have this type of process.

State 7 emerges from the ventral side of the radix and directs distally. It is usually free standing from other radical appendices and is dorso-ventrally flattened. It is either equally broad from the base to the blunt tip (*Erigonella hiemalis*, *Dicymbium libidinosum*) or narrowing towards its pointed tip (Fig. 2B, *Dicymbium nigrum*; Millidge 1977: fig. 137, *Erigonella subelevata*). Its size ranges from what is seen in, e.g., *Erigonella hiemalis* (Figs 6C, 24L; Merrett 1963: fig. 64b) to very large as in *Dicymbium nigrum* (Fig. 2B) or *Erigonella subelevata* (Fig. 24H–I; Millidge 1977: fig. 137, *Erigonella subelevata*). An exception is *D. lusiscus* that has a small very pointy tooth right next to the embolic basal protuberance (state 11). It might not be homologous with what is seen in *Diastanillus pecuarius* (Millidge 1977:

fig. 138) and others. This state is a synapomorphy of node 18 and emerges four times independently and presumably contains non-homologous structures.

State 8 is a dorso-ventrally flattened lamella-like process that is broader than long. It is present in *Paraglyphesis polaris* and *Glyphesis nemoralis*. This state is a synapomorphy of node 22.

State 9 is a small tooth that is not flattened (as is state 8). *Glyphesis cottonae* (Merrett 1963: fig. 61a–b) has a similar but more sclerotised and more ventrally directed apophysis. It is somewhat twisted with two edges that in lateral view look like a square (e.g., Wiehle 1960: fig. 1131). This character is present in *Glyphesis* (node 22, apart from the taxa scored as state 8).

State 10 is a highly sclerotised tooth-like appendix emerging from the ventral side of the radix. It is dorso-ventrally flattened and about as long as broad. In *Diplocephalus montanus* it is found ventral to the basis of the embolus, which would argue to be homologous with the embolic protuberance (state 11). *Diplocephalus montanus* and *D. uliginosus* are the only two species that have the sclerotised tooth in node 39.

State 11, in *Savignia* the delimitations of the embolus are sometimes difficult (see character 116). However, where the backing of the embolus emerges from the radix, it is slightly extended in the opposite direction to the 'embolus'. This definition is equal to character 128 (embolic basal process of MH04) with the exception that in *Savignia*, the sperm duct does not pass by this structure (47 in MH04). Since MH04 did not code *Savignia frontata* as having such an embolic basal process, we assume that the embolic protuberance is not homologous with the embolic basal process (character 128). It is triangular like a tooth in *D. marusiki*. *Savignia frontata* was recoded from Frick *et al.* 2010 as lacking the distinct angle of the embolic axis (47 in MH04) but instead having an embolic protuberance (state 11). There seems to be a transition series in the Far East *Diplocephalus* towards *Savignia*. This state occurs in node 42 with the exception of *D. montanus* that is coded as having the sclerotised radical tooth instead (state 10). The current analysis suggests that these two structures are homologous despite their differences in form.

(136). Ventral radical process, basal constriction

0: unconstricted.
1: basally constricted (Fig. 16D; H00: fig. 1d, *Araeoncus crassiceps*).

The basal part of the ventral radical process is constricted in some species within *Araeoncus*. This character is a synapomorphy of node 65.

(137). Ventral radical process, longitudinal ridge

0: absent.
1: present (Fig. 16D; H00: fig. 1d, *Araeoncus crassiceps*).

This ridge is found at the retrolateral side of the ventral radical process in all scored species of *Araeoncus*. It runs from the proximal part of the ventral radical process up to the central (H00: fig. 1b, *A. crassiceps*) part or even up to the tip. Due to this ridge the ventral radical process seems to have a triangular cross-section seen in distal view. The longitudinal ridge on the ventral radical process is a synapomorphy of *Araeoncus* (node 63).

(138). Ventral radical process, retrolateral side process

0: absent.
1: tiny denticle (Fig. 5B; H00: fig. 2c, pl. 13d, *Araeoncus humilis*).
2: pointed distal tip on horizontal protuberance (Fig. 16E; Holm 1962: fig. 25a–b, *A. victorianyanzae*).

The tiny denticle is a synapomorphy of node 63 (considering fast character optimisation) although it is only present in *Araeoncus humilis*. State 2 is a very distinct form that is found in all derived species

of *Araeoncus* (node 65) and is a synapomorphy of node 65: the distal part of this apophysis is white at its dorsal side. The basal part of the dorsal side is highly sclerotised. At its retrolateral side is a horizontal protuberance with a pointed distal tip. It is very distinct in *A. victorianyanzae* and very small in *A. crassiceps*.

Dorsal radical process

(139). Dorsal radical process (dRP)

0: absent (Fig. 16C; Millidge 1977: fig. 129, *Diplocephalus dentatus*).
1: present (Figs 7C, 9E, 24E-G, *Diplocephalus latifrons*; H00: fig. 6b, pl. 19a, c, *Diplocephalus cristatus*).

This accounts for all different types of dorsal radical apophyses. Some autapomorphic characters were excluded, i.e., the dorsal small sclerotised tooth (Tanasevitch 1987: figs 91–92, *Caucasopisthes procurvus*).

Another one is the very large and laterally flattened dorsal apophysis that initially faces distally while its tip directs retrolaterally. It is present in *Araeoncus galeriformis* (Fig. 16F; Tanasevitch 1987: figs 126–127) and also in *Araeoncus mitriformis* (Tanasevitch 2008: figs 3–4), which was not scored in this analysis. Dorsal radical processes are found mainly in node 31.

(140). Dorsal radical process, tip shape

0: blunt (Figs 7C, 9E, 24E–G; Wiehle 1960: "z.A." in fig. 949, *Diplocephalus latifrons*).
1: pointed (Fig. 24A; H00: fig. 6b, pl. 19a, c, *Diplocephalus cristatus*).

Most taxa in node 32 have blunt tips (pointed in node 44) and most taxa in node 49 have pointed tips (blunt in *Diplocephalus permixtus*).

(141). Dorsal radical process, radical fold

0: absent.
1: present (Fig. 21D, *Savignia birostra*; Lasut *et al.* 2009: figs 4, 8, 12, *Savignia birostra*, *S. saitoi*, *S. zero*; H00: fig. 24a, d, as "ARP": *Savignia frontata*).

This is a distally facing fold-like structure originating at the dorsal side of the radix. In some cases it continues into the tooth-like basal radical process (character 159). In *Diplocephalus mirabilis* this fold is present and continues into the proximal embolic tooth (Eskov 1988: fig. 21). The radical fold is a synapomorphy of *Savignia* (node 45).

(142). Dorsal radical process, size

0: smaller to slightly bigger than the radix (Figs 7C, 9E, 24E–G; Wiehle 1960: "z.A." in fig. 949, *Diplocephalus latifrons*).
1: much larger than the radix (Fig. 21B; H00: fig. 6b, pl. 19b–c, *Diplocephalus cristatus*).

This character contains several potentially homologous large dorsal radical apophyses (node 53) of which the different forms are coded as separate characters (143–146). The large radical process is a synapomorphy of node 52 but with only one occurrence in node 59, in *Araeoncus galeriformis*.

(143). Dorsal radical process, large, flat, ventrally folded

0: absent, dRP of another shape.
1: present (Fig. 18A; Thaler 1972: fig. 18: *Diplocephalus pavesii*).

This apophysis emerges from the dorsal side of the radix and directs distally. Its tip is pointed and curves ventrally (Thaler 1972: fig. 18) in *Diplocephalus arnoi* and *D. pavesii* but dorsally in *D. caucasicus*. It looks like a flat (dorso-ventrally flattened) apophysis that narrows towards the tip while its two margins

are folded ventrally and are fused ventrally in the distal half of its length. The retrolateral side of the apophysis is sclerotised and has latitudinal striations. The prolateral side is membranous and seems to lack these striations. It is a synapomorphy of node 54.

The curved dorsal radical process with a broad round tip, found in *Diplocephalus permixtus* (Millidge 1977: fig. 133; Roberts 1987: fig. 36e) is presumably a simple version of what is found in *D. arnoi* and others. Its base is sclerotised and thicker than the lamelliform distal half of this apophysis. The whole apophysis is curved ventrally, and its tip is rather broad and round.

(144). Dorsal radical process, flat, simple with pointed tip

0: absent, dRP of another shape.
1: present (Fig. 21B; H00: fig. 6b, d, pl. 19a, c, *Diplocephalus cristatus*).

This apophysis is a synapomorphy of the *cristatus*-group (node 57). It is very similar to what is seen in *Diplocephalus permixtus* but its tip is pointed and evenly sclerotised. *Diplocephalus turcicus* also has this type of apophysis but it is very small and less sclerotised than in the others. The overall similarity of the radical apophyses indicates that this is a simple, ancestral form of the larger ones.

(145). Dorsal radical process, tip orientation

0: ventral (Fig. 18A; Thaler 1972: fig. 18: *Diplocephalus pavesii*).
1: dorsal (Fig. 21B; H00: fig. 6b, d, pl. 19a, c, *Diplocephalus cristatus*).

The tip of the large dorsal process is either curved ventrally or dorsally. The dorsal type is found in node 58 and *Diplocephalus caucasicus*, the ventral type in *D. turcicus*, *D. crassilobus* and node 55.

(146). Dorsal radical process, distinct retrolateral tooth

0: absent (Fig. 21B; H00: figs 6b, d, pl. 19a, c, *Diplocephalus cristatus*).
1: present (Fig. 21F; Millidge 1979: fig. 55, *Diplocephalus crassilobus*).

Diplocephalus crassilobus has a distinct, pointed apophysis emerging at the retrolateral side of the dorsal apophysis. This character is phylogenetically uninformative but also present in *D. pseudocrassilobus* (Gnelitsa 2006: fig. 1a, labelled as "i"), which was not scored in this analysis.

(147). Dorsal radical process, triangular type

0: absent (Fig. 21B; H00: fig. 6b, d, pl. 19a, c, *Diplocephalus cristatus*).
1: present (Fig. 18B; Eskov 1988: fig. 14, *Diplocephalus marusiki*; Thaler 1970: figs 1–2, *Diplocephalus rostratus*).

The radical process in *Diplocephalus rostratus* and some Far East species of *Diplocephalus* is very special in its form. It resembles forms found in *Araeoncus* but it is very short, with a tip or small appendix that directs retrolaterally. Its origin is at the distal-dorsal side of the radix.

The one in *D. uliginosus* is very similar to the one of *D. marusiki* (and its relatives) but lacking a ventral ridge (character 148). This character is a synapomorphy of node 39 with a reversal at node 45, and it is present in *Hemistajus* (node 43) and in *D. uliginosus*.

(148). Dorsal radical process, triangular type, ventral ridge

0: absent (Fig. 21B; H00: fig. 6b, d, pl. 19a, c, *Diplocephalus cristatus*).
1: present (Fig. 18B; Eskov 1988: fig. 14, *Diplocephalus marusiki*).

Seen in distal view there are two ridges, one starting at the dorsal side of the radical tailpiece (character 160) continuing to the retrolateral side of the radix and a second one emerging from that ridge rectangular

to the ventral sclerotised radical tooth or the ventral embolic protuberance, respectively (character 135, states 10, 11). This second ridge, i.e., the ventral ridge, is very similar to the longitudinal ridge on the ventral radical process in *Araeoncus* (character 137). The ventral ridge is a synapomorphy of *Hemistajus* (node 43).

(149). Dorsal radical process, triangular type, retrolateral protuberance

0: absent (Fig. 21B; H00: fig. 6b, d, pl. 19a, c, *Diplocephalus cristatus*).
1: present (Fig. 18B; Eskov 1988: fig. 14, *Diplocephalus marusiki*).

On top of the triangular apophysis (character 147) is a protuberance facing retrolaterally. This is a synapomorphy of *Diplocephalus montanus* and *D. marusiki* (node 44).

(150). Dorsal radical process, cramp-like

0: absent (Fig. 21B; H00: fig. 6b, d, pl. 19a, c, *Diplocephalus cristatus*).
1: present (Figs 7C, 9E, 24E–G; Wiehle 1960: "z.A." in fig. 949, *Diplocephalus latifrons*).

The dorsal radical process of some taxa is two-fold. Either it is a second process of similar size and shape aside the actual dorsal process. The more probable explanation in the context of the different shapes of radical appendices found in the *Savignia* genus group and the overall similarity of both these structures is that the dorsal process has a central depression. Wiehle (1960) termed this process "zangenförmige Apophyse", pincer-like apophysis. The cramp-like dorsal radical process is a synapomorphy of *Erigonella* (node 33) and within this node is found in all species with a dorsal process, i.e., *Diplocephalus latifrons*, *Savignia producta*, *Diplocephalus connatus* and *D. connatus jacksoni*.

(151). Dorsal radical process, cramp-like, form

0: carnous with blunt tips (Figs 7C, 9E, 24E–G; Roberts 1987: fig. 37a, *Diplocephalus latifrons*).
1: flat with pointed central tip (Fig. 21H; Wiehle 1960: fig. 923; Roberts 1987: fig. 37b, *Diplocephalus connatus*; Holm 1977: fig. 6, *Savignia producta*).

This character accounts for the two different types of cramp-like dorsal processes; the carnous type found in *Diplocephalus latifrons* and the flat and the pointed one synapomorphic for node 36 and present in *S. producta*, *D. connatus* and *D. connatus jacksoni*. This character is inapplicable in all taxa without a cramp-like dorsal radical process (character 150).

Different radical processes

(152). Central radical process (cRP)

0: absent.
1: present (Figs 3C, 9I, 24B–D; Wiehle 1960: figs 1035–1036, *Erigonella ignobilis*; Figs 3D, 6D, 9J; Millidge 1977: fig. 123, *Glyphesis servulus*).

This accounts for all different types of radical apophyses that emerge in the centre of the radix. In the case of *Erigonella ignobilis* this apophysis covers the dorsal and the ventral part altogether. It is dorsal to ventral orientated in *Erigonella ignobilis* (Figs 3C, 9I) and retro- to prolateral in *Glyphesis servulus* (Figs 3D, 6D, 9J). This character is only present in *Erigonella ignobilis* and in *Glyphesis* (node 22).

(153). Central radical process, retro- to prolateral bulb-like

0: absent.
1: present (Figs 3D, 6D, 9J; Millidge 1977: fig. 123, *Glyphesis servulus*).

This dorsal bulb-like distal extension is a synapomorphy of *Glyphesis* (node 22). Due to its close resemblance to the central bulb found in *Erigonella* and since the bulb covers the central and dorsal side of the radix it is assumed to be closer to a central than to a dorsal radical process.

(154). Central radical process, dorso-ventral bulb-like

0: absent.
1: present (Figs 3C, 9I, 24B–D; Wiehle 1960: figs 1035–1036, *Erigonella ignobilis*).

This bulb emerges in the centre of the radix covering the range from dorsal to ventral and has a sickle like prolongation at its ventral side with a distally directing tip. This type is found in *Erigonella ignobilis*, *Paraglyphesis polaris* and *Glyphesis nemoralis*.

(155). Retrolateral radical process (rRP)

0: absent.
1: present (Fig. 21H; Roberts 1987: fig. 37b; Wiehle 1960: fig. 923, *Diplocephalus connatus*).

This accounts for all different types of retrolateral radical apophyses. Some autapomorphic characters that were excluded are the retrolateral round process (Thaler 1969: fig. 44, *Janetschekia monodon*) and the retrolateral radical tooth-like ventral facing process (Merrett 1963: fig. 67b, *Diplocephalus picinus*). Apart from these two species, only *Diplocephalus connatus* and *D. connatus jacksoni* have a retrolateral radical process.

(156). Retrolateral radical process, hook-like

0: absent.
1: present (Fig. 21H; Roberts 1987: fig. 37b; Wiehle 1960: fig. 923, *Diplocephalus connatus*).

This apophysis is a long hook that emerges next to the embolus and exceeds it clearly by its length. It emerges from the retrolateral side of the radix and faces retrolaterally to basally. In our analysis, it is only present in *Diplocephalus connatus* and *Diplocephalus connatus jacksoni* (node 38).

(157). Prolateral radical process (pRP)

0: absent.
1: present (Figs 5A, 9A; Wunderlich 1980b: figs 11–13, *Alioranus pastoralis*).

The prolateral radical apophysis emerges from the prolateral side of the radix, right above the radical tailpiece (character 160), facing distally. It is present in *Savignia harmsi*, *Dactylopisthes* (node 20) as well as *Alioranus pauper* and *Al. pastoralis* (node 6) in different forms. It is not homologous with the anterior radical process, e.g. *Alioranus pauper* has both an anterior radical process (coded as ventral radical process) and a prolateral thread-like appendix.

(158). Prolateral radical process, form

0: thread-like (Figs 5A, 6F, 9A; Wunderlich 1980b: figs 11–13, *Alioranus pastoralis*).
1: tooth-like (Fig. 20C; Wunderlich 1980a: figs 48–49, *Savignia harmsi*).

The relatively long thread-like form is only present in *Alioranus pauper* and *Al. pastoralis* (node 6), two closely related Mediterranean species. Frick *et al.* (2010) coded this process as anterior radical process in *Alioranus*.

The tooth-like form with a pointed tip appears as a synapomorphy at node 7 (as an artifact of inapplicables considering fast character optimisation) but is only present in *Savignia harmsi* (Wunderlich 1980a: figs 48–49) and in *Dactylophistes* (node 20) where it is very thin and delicate. This form is found only in

these two distantly related taxa. The different overall conformation of the bulb argues against a homology of this form in both taxa.

(159). Basal radical process (bRP)

0: absent (H00: pl. 19a, *Diplocephalus cristatus*).
1: present, tooth-like (Fig. 21D, *Savignia birostra*; Lasut *et al.* 2009: figs 4, 8, 12, *Savignia birostra*, *S. saitoi*, *S. zero*; H00: pl. 56b, *Savignia frontata*).

It emerges from the dorsal side of the radix, right above the embolus and is directed proximally. It seems to lack a sclerotised connection to the radix and is above the transparent outgrowth and not attached to it (see character 116). The presence of this tooth is a synapomorphy of *Savignia* (node 45) and not known to occur in any other erigonine spider. It differs from an anterior radical process and also the ventral radical process by its proximal instead of distal direction, its origin between the column and the embolus as well as its tooth-like shape. *Diplocephalus mirabilis* shows a presumably ancestral shape, which is an elongation of the dorsal radical fold (character 141; Eskov 1988: fig. 21). The proximal tooth is separated from the dorsal radical fold in all other species (Fig. 21D, *Savignia birostra*).

Radical tailpiece

160. Radical tailpiece (RTP)

0: absent (Hormiga 1994a: fig. 9d, *Linyphia triangularis*).
1: present (Fig. 7D, *Diplocephalus picinus*; H00: pl. 19b–c, *Diplocephalus cristatus*).

MH04-52, H00-21, A09-42. The presence of a radical tailpiece is a synapomorphy of the Erigoninae (node 3).

161. Radical tailpiece, shape

0: straight (MH04: fig. 15f, *Spanioplanus mitis*).
1: spiralled (H00: fig. 13f, *Grammonota pictilis*).
2: recurved ventrally (MH04: fig. 18f, *Mermessus dentiger* O. Pickard-Cambridge, 1899).
3: projecting mesally (MH04: fig. 19c, *Scolecura propinqua* Millidge, 1991).
4: projecting anteriorly (MH04: fig. 18b, *Notiomaso exonychus*).

MH04-53, H00-22. Most scored species have a straight radical tailpiece. A spiralled radical tailpiece is present in *Dicymbium* (node 29), *Walckenaeria acuminata* and in "*Saloca*" (node 12).

(162). Radical tailpiece, conformation

0: not twisted (Figs 7C, 24E–G, *Diplocephalus latifrons*; H00: fig. 24b, *Savignia frontata*).
1: twisted (Fig. 8A; *Glyphesis servulus*; H00: fig. 6f, *Diplocephalus cristatus*).

The twisted conformation is found in *Glyphesis* (node 22), *Dicymbium* (node 29) and in node 51 with reversals in node 55, *Diplocephalus permixtus* and *Diplocephalus dentatus.*

(163). Radical tailpiece, diameter

0: uniform (Fig. 8A; Millidge 1977: fig. 123, *Glyphesis servulus*).
1: narrowing towards the tip (Fig. 8B; Wiehle 1960: fig. 395, *Panamomops tauricornis* (Simon, 1882)).

Some radical tailpieces constantly narrow towards the tip, rather than having an abruptly pointed triangular tip (e.g., not like the distal tooth, character 170). In certain cases as in, e.g., *Saloca khumbuensis* the radical tailpiece is slightly narrowing towards the tip, but is not pointed (Wunderlich 1983: fig. 68). The narrowing form is a synapomorphy of node 10 and is found in *Walckenaeria acuminata* and in "*Saloca"* (node 12).

(164). Radical tailpiece, tip strongly broadened

0: absent (Fig. 8A; Millidge 1977: fig. 123, *Glyphesis servulus*).
1: present (Fig. 8C; Millidge 1977: fig. 132, *Saloca diceros*).

This form summarises RTPs with strongly broadened tips and constricted basal sections, e.g., *Saloca diceros* (Fig. 8C). In *Janetschekia monodon*, the tip is also massively broadened but not constricted at its base and has therefore not been coded as present (see Millidge 1977: fig. 142). This character occurs in *Saloca* (node 28) and in *Diastanillus pecuarius*.

(165). Radical tailpiece, tip strongly broadened, with inner thickening

0: absent (Fig. 8C; Millidge 1977: fig. 123, *Glyphesis servulus*).
1: present (Fig. 18A; Thaler 1972: fig. 18, *Diplocephalus pavesii*).

In *Diplocephalus arnoi* and *D. pavesii* (synapomorphy of node 55) the tip forms nearly a circle. Its distal half is very flat while the basal half is thickened towards the inner side. Together forming a kind of clamp around the suprategulum.

(166). Radical tailpiece, basal tiny denticle

0: absent (Figs 6G, 9I, *Erigonella ignobilis*; H00: fig. 7d, *Dismodicus decemoculatus*).
1: present (Fig. 20D, *Araeoncus galeriformis*; Fig. 20F, *Araeoncus anguineus*).

This denticle is directed mesaly at the base of the radical tailpiece, where it emerges from the radix. This denticle is very tiny in size. It is the tip of a margin at the inside of the radical tailpiece. This is not homologous with the basal tooth (character 167) that is indeed a process arising from the radical tailpiece. This character is a synapomorphy of node 64 within *Araeoncus* with a reversal at node 66.

(167). Radical tailpiece, basal tooth

0: absent (Figs 6G, 9I, *Erigonella ignobilis*; H00: fig. 7d, *Dismodicus decemoculatus*).
1: present (Fig. 16G, *Diplocephalus caucasicus*).

This tooth is directed mesally at the base of the radical tailpiece, where it emerges the radix. This tooth is well visible in ventral view and a synapomorphy of node 54.

(168). Radical tailpiece, ventral to prolateral tooth (RTpT)

0: absent (Fig. 6A, *Dismodicus bifrons*; H00: fig. 7d, *Dismodicus decemoculatus*).
1: present (Fig. 20H; H00: fig. 24b, behind the DSA, *Savignia frontata*).

Arising from the ventral (to prolateral) side of the radical tailpiece, this triangular protuberance directs to the column and is separated from the column (e.g., H00: fig. 24d, *Savignia frontata*). Similar (maybe ancestral) structures occur in *Dismodicus elevatus* where it defines the base of the column.

(169). Radical tailpiece, dorsal to retrolateral process (RTrP)

0: absent (Fig. 6A, *Dismodicus bifrons*; H00: fig. 7d, *Dismodicus decemoculatus*).
1: knob- to tooth-like (Fig. 20H; H00: fig. 24b, *Savignia frontata*).
2: lobe-like (Fig. 20D, *Araeoncus galeriformis*; Millidge 1977: fig. 125, *Araeoncus anguineus*).
3: proximally directed and pointed (Fig. 21I; Holm 1977: fig. 6, *Savignia producta*).

The retrolateral process comes in different forms but they always emerge from the end of the radical tailpiece at its dorsal (to retrolateral) side. If prolateral and retrolateral processes are present, the retrolateral process is situated more distal on the radical tailpiece than the prolateral one. The process is either knob-like as in *Erigonella ignobilis* (Fig. 24B–D) (present in different taxa within

the *Savignia*-group) or can be a distinct flat, lobe-like ectal elongation from the radical tailpiece as in *Araeoncus* (synapomorphy of *Araeoncus*; node 63). A slightly dorsally broadened end as seen in, e.g., *Caucasopisthes procurvus* (Tanasevitch 1987: fig. 92) is not coded as such a lobe. The proximally directed and pointed process is a synapomorphy of node 37.

(170). Radical tailpiece, distal tooth (RTdT)

0: absent (Fig. 6A, *Dismodicus bifrons*; *Diplocephalus cristatus*, H00: fig. 6f).
1: present (Fig. 20H; H00: fig. 24b, *Savignia frontata*).

The distal tooth looks like the prolateral tooth but instead faces proximally (distal with respect to the radical tailpiece). This apophysis might rather be a slightly pointed tip of the radical tailpiece than a real apophysis. It can best be seen in ventral view. *Savignia* has three different apophyses on the radical tailpiece, the retrolateral knob-like process, the distal tooth and the prolateral tooth (H00: fig. 24b, *Savignia frontata*). This character is an ambiguous synapomorphy of nodes 37 and 46.

(171). Radical tailpiece, distal appendix

0: absent (Fig. 6A, *Dismodicus bifrons*; H00: fig. 7d, *Dismodicus decemoculatus*).
1: present (Fig. 7F, *Entelecara erythropus*; H00: fig. 9d, *Entelecara acuminata*).

This apophysis is an elongated rather than triangular appendix at the distal end of the radical tailpiece. It emerges ectally and faces distally with respect to the whole palp. This is a synapomorphy of *Entelecara* (node 9).

(172). Embolic division, general conformation

0: unmodified (Fig. 24A; H00: pl. 19b, *Diplocephalus cristatus*).
1: radical tailpiece, radix and embolus form a spiral (Fig. 6A, *Dismodicus bifrons*; H00: fig. 7d, *Dismodicus decemoculatus*).

This is a synapomorphy of node 10, *Walckenaeria* plus the *Pelecopsis*-group members.

Female genital morphology

Epigyne

173. Epigyne, dorsal plate (DP) scape

0: absent (MH04: fig. 19f, *Sphecozone crassa* (Millidge, 1991)).
1: present (H00: pl. 8d, *Linyphia triangularis*).

MH04-79, H00-32, A09-65. All taxa but *Linyphia triangularis* lack a dorsal plate scape and therefore this character is phylogenetically uninformative.

174. Epigyne, dorsal plate anterior lobe

0: absent (Miller 2007: fig. 21f, *Neocautinella neoterica*).
1: present (MH04: fig. 19f, *Sphecozone crassa*).

MH04-80. This character is a synapomorphy of *Dismodicus* (node 15).

175. Epigyne, ventral plate (VP) scape

0: absent (MH04: fig. 19f, *Sphecozone crassa*).
1: present (MH04: fig. 20a, *Valdiviella trisetosa*).

MH04-81, H00-33, A09-66. The ventral plate scape is only present in node 2.

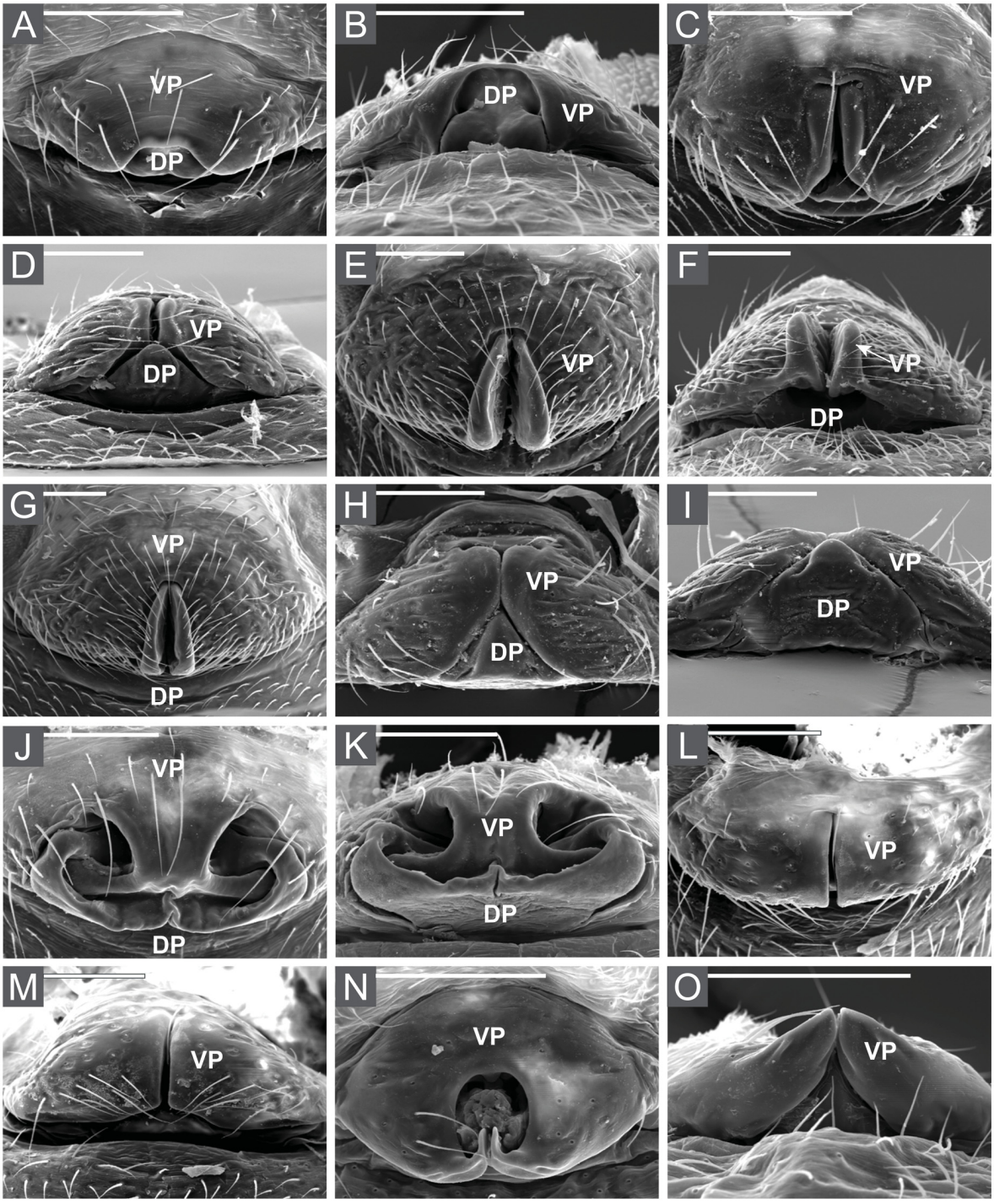

Fig. 10. Scanning Electron Microscope pictures of female epigyne types in ventral (A, C, E, G–H, J, L, N) and aboral (B, D, F, I, K, M, O) views. **A–B**. *Alioranus pastoralis* (O. Pickard-Cambridge, 1872) (3232; coll. E.G.). **C–D**. *Araeoncus humilis* (Blackwall, 1841) (Ar3186; NMBE). **E–F**. *Dicymbium nigrum* (Blackwall, 1834) (9996; ZMUC). **G**. *Dicymbium tibiale* (Blackwall, 1836) (11213; ZMUC). **H–I**. *Diplocephalus latifrons* (O. Pickard-Cambridge, 1863) (Ar161; NMBE). **J–K**. *Entelecara erythropus* (Westring, 1851) (Ar173; NMBE). **L–M**. *Erigonella hiemalis* (Blackwall, 1841) (ZMUC). **N–O**. *Glyphesis servulus* (Simon, 1882) (792f; NMB). Abbreviations: see Material and methods. Scale bars = 100 μm.

176. Epigyne, ventral plate socket

0: absent (MH04: fig. 19f, *Sphecozone crassa*).
1: present (H00: pl. 6a, *Tenuiphantes tenebricola*).

MH04-89, A09-70. The ventral plate socket is only present in node 2.

177. Epigyne, dorsal plate socket

0: absent (MH04: fig. 19f, *Sphecozone crassa*).
1: present (Wiehle 1956: fig. 509, *Linyphia triangularis*).

MH04-90, A09-71. This character is only present in *Linyphia triangularis*. However, this character is of importance to understand the relationships between the subfamilies of linyphiid spiders (MH04).

178. Epigyne, bisected

0: absent (MH04: fig. 19f, *Sphecozone crassa*).
1: present (Fig. 10H, *Diplocephalus latifrons*; H00: pl. 21d, *Diplocephalus cristatus*).

MH04-91, H00-35. The presence of an epigynal bisection is a synapomorphy of node 21 with one reversal at node 27 and therefore supports the *Savignia* genus group (node 21). It supports the idea that the bisected epigyne is typical (synapomorphic) for the *Savignia*-group (e.g., Millidge 1984; Bosmans 1996).

Not everything that looks like a bisected epigyne at first glance indeed is one: *Entelecara acuminata* was coded as having a bisected epigyne in MH04. However, a comparison with one of its closest conspecifics, *En. erythropus*, that certainly does not have a bisected epigyne revealed that what is seen in *En. acuminata* is similarly shaped as a bisected epigyne but formed in a different way (compare Fig. 10J–K, *En. erythropus* with H00: figs 6h–i and 9i of *D. cristatus* and *En. acuminata*, respectively).

A bisected epigyne is formed by two lateral lobes emerging from the ventral plate as seen in, e.g., *Diplocephalus latifrons* (Fig. 10H–I). Additionally, these two lateral lobes are flush on the dorsal plate that is formed like a tent seen in aboral view (Fig. 10I, *D. latifrons*). The form found in *Dicymbium* is most probably not a bisected epigyne in the strict sense because the dorsal plate and the two lobes of the ventral plate are not flush together (Fig. 10E, G, *Dicymbium nigrum*, *Di. tibiale*) and are only partly fused in *Di. libidinosum* (see Song *et al.* 1999: fig. 91e).

In the *Savignia*-group, the vulva of most females lack a "copulation duct" in the sense of a tube. In these taxa the sperm is injected through a fold formed by the ventral and the dorsal plate. Saaristo (1971) pointed out that in Linyphiidae "all vulval structures are deeper or shallower folds of the edges of the aperture or their derivates". Thus, the entrance ducts are not tubes, but open U-shaped invaginations, the spermathecae being bulges at the sides of these ducts. The fertilising ducts are also U-shaped. This finding can well be applied to erigonines, and was mentioned also for *Caracladus* (Frick & Muff 2009) and for *Savignia* (Lasut *et al.* 2009) and occurs widespread in linyphioids and other spider groups (Tu & Hormiga 2010). This crease, formed by the ventral and dorsal plates directs the embolus to the incoming of the receptaculum. The copulatory duct in the strict sense is present in most erigonines; however, in the *Savignia*-group the fold is more commonly found and might be a continuation of the typical, bisected ventral plate. The transparent outgrowth of the embolus (character 116) might be the male counterpart to enter the receptaculum through this fold, where the sclerotised part leads it through.

(179). Epigyne bisected, anterior end T-like modified

0: absent.
1: present (Fig. 10H, *Diplocephalus latifrons*; H00: pl. 57f, *Savignia frontata*).

Some bisected epigynes terminate T-like anteriorly.

(180). Epigyne bisected, T-like modification shape

0: terminated (Fig. 10H, *Diplocephalus latifrons*; H00: pl. 21d, *Diplocephalus cristatus*).
1: continuing below margin (H00: pl. 57f, *Savignia frontata*).

There are two T-like forms. One terminates on the surface, while the lateral lobes of the other continue below the anterior ends of the median bisection. The second state is a synapomorphy of node 41 with a reversal in *Diplocephalus montanus*.

(181). Epigyne bisected, posterior half flush or triangularly split

0: flush (Fig. 10L–M; Roberts 1987: fig. 36a, *Erigonella hiemalis*).
1: distinctly triangularly split (Fig. 10H–I; Roberts 1987: fig. 37a, *Diplocephalus latifrons*).

(182). Epigyne bisected, anterior end of ventral plate roundly broadened below surface

0: absent.
1: present (H00: pl. 57f, *Savignia frontata;* Eskov 1988: figs 72–73, *Savignia saitoi*).

This character describes the typical anterior ending seen in *Savignia* (synapomorphy of node 46), where the ventral plate seems to be broader below the surface than at the surface. The broadening is visible in cleared epigynes in ventral and in dorsal view.

(183). Epigyne, lip-like bisection margins

0: not rising ventrally (Fig. 10H, *Diplocephalus latifrons*; H00: pl. 57f, *Savignia frontata*).
1: protruding lip-like ventrally (Fig. 10E–G, *Dicymbium nigrum*, *Di. Tibiale*; Wiehle 1960: fig. 339, *Dicymbium tibiale*).

The median margins of the ventral plate protruding lip-like ventrally occur only in *Dicymbium* (node 29) but appears as a synapomorphy of node 27 (as an artifact of inapplicables considering fast character optimisation). The lip-like protuberance in *Diplocephalus montanus* has not been coded as present due to its different character: it is not clearly bordered towards the ectal side and only present in the posterior half of the epigynal median margin (Eskov 1988: figs 29-30, *D. montanus*). In *Dicymbium* these lips are bordered at the inside and the outside and along the whole epigyne (Fig. 10E–F, *Dicymbium nigrum*).

(184). Epigyne, oval-shaped

0: absent (Fig. 10H, *Diplocephalus latifrons*; H00: pl. 57f, *Savignia frontata*).
1: present (Fig. 10N; Roberts 1987: fig. 35e, *Glyphesis servulus*).

The oval-shaped epigyne is synapomorphic for *Glyphesis* excluding *G. cottonae* (node 23).

(185). Epigyne, glabrous ventrally protruding bisection margins

0: absent (Fig. 10H, *Diplocephalus latifrons*; H00: pl. 57f, *Savignia frontata*).
1: present (Fig. 22B; Eskov 1988: figs 22–23, *Diplocephalus mirabilis*).

In *Diplocephalus mirabilis* and *D. rostratus*, the median margins of the ventral plate protrude hook-like ventrally. This hook is glabrous and much more sclerotised than the remaining setose ventral plate. *Diplocephalus montanus* shows the presumably ancestral state towards this hook-like margins in the shape of paired sclerotised round ventral protuberances (Fig. 22D–E; Eskov 1988: fig. 30). The hook-like and round forms are coded as separate characters to account for the difference (character 186). This structure is present in *Diplocephalus rostratus*, *D. montanus* and *D. mirabilis*.

Also *D. marusiki* and *S. frontata* presumably have this structure but it faces posteriorly rather than ventrally. A closer examination of this character might suggest a transition series from *Hemistajus* to *Savignia* presumably showing that *Hemistajus* is a basal type of *Savignia*, i.e., paraphyletic with respect to *Savignia*.

(186). Epigyne, glabrous ventrally protruding bisection margins, form

0: round (Fig. 22D–E; Eskov 1988: fig. 30, *Diplocephalus montanus*).
1: hook-like (Fig. 22B; Eskov 1988: figs 22–23, *Diplocephalus mirabilis*).

This character is only applicable in three taxa with ventrally protruding bisection margins and therefore phylogenetically uninformative.

(187). Epigyne, ventral plate with paired inner longitudinal narrow lobes

0: absent (Fig. 10H, *Diplocephalus latifrons*; H00: pl. 57f, *Savignia frontata*).
1: present (Fig. 22F; Thaler 1972: figs 21–22, *Diplocephalus pavesii*).

The median margin of the lateral lobes of the ventral plate is rebordered with paired longitudinal narrow lobes, this a synapomorphy of node 54 (*Diplocephalus caucasicus*, *D. pavesii* and *D. arnoi*).

188. Epigyne, dorsal plate orientation

0: position of dorsal plate entirely dorsal to ventral plate (MH04: fig. 20a, *Valdiviella trisetosa*).
1: dorsal plate extends anteriorly, flush with ventral plate (Fig. 10J, *Entelecara erythropus*; H00: pl. 50f, *Oedothorax gibbosus*).

MH04-93. The dorsal plate extends ventrally flush with the ventral plate in two nodes: in *Saloca* (node 28) and in node 8 (including *Entelecara*, *Walckenaeria* and members of the *Pelecopsis*-group).

(189). Epigyne in aboral view, dorsal and ventral plate contact

0: dorsal plate flush with ventral plate (Fig. 10D, *Araeoncus humilis*).
1: dorsal plate separated to the ventral plate (Fig. 10F; Wiehle 1960: fig. 332, *Dicymbium nigrum*).

State 1 describes a discrete opening below the ventral plate while in state 0 the ventral and the dorsal plate are flush together, at least in aboral view. The separated conformation is found in *Dicymbium* (node 29) and independently also in *Glyphesis cottonae* and *Diplocephalus subrostratus*.

(190). Epigyne, ventral plate posterior tip turned anteriorly

0: absent (Fig. 22C; Eskov 1991b: fig. 3, *Paraglyphesis polaris*).
1: present (Fig. 10N; Roberts 1987: fig. 35e, *Glyphesis servulus*).

The posterior ends of the ventral plate protrude ventrally and then turn anteriorly in some species of *Glyphesis* (synapomorphy of node 24).

(191). Epigyne, ventral plate with paired anterior directed folds

0: absent.
1: present (Fig. 22A; Tanasevitch 1983: figs 9–10; 1989: fig. 127, *Dactylopisthes locketi*).

The posterior side of the ventral plate is folded anteriorly and inwards continuing to the very short (not even a duct) copulatory opening into the spermathecae. In *Glyphesis servulus* the copulatory duct is much longer (character 190; Wiehle 1960: fig. 1114). This is a synapomorphy of *Dactylopisthes* (node 20).

Vulva

192. Copulatory duct encapsulation

0: absent (H00: fig. 11f–h, *Gongylidiellum vivum*).
1: present (H00: fig. 18d–f, *Laminacauda plagiata*; Thaler, 1971: fig. 5: *Erigonella subelevata*).

MH04-95, H00-38, A09-75.

193. Spermathecae (S) shape

0: round to slightly oblong (MH04: fig. 17i, *Gravipalpus standifer* Miller, 2007).
1: strongly oblong (Miller 2007: fig. 114f, *Sphecozone rubescens* O. Pickard-Cambridge, 1871).

MH04-98, A09-78.

194. Fertilization duct orientation

0: posterior (MH04: fig. 17i, *Gravipalpus standifer*).
1: mesal (Miller 2007: fig. 25f, *Anodoration claviferum* Millidge, 1991).
2: anterior (Hormiga 1994b: figs 12–14, *Pimoa breuili* (Fage, 1931)).
3: dorsal (MH04: fig. 21a, *Rhabdogyna patagonica*).

MH04-99, H00-40, A09-79.

Somatic morphology

Male prosoma

(195). Sternum, texture

0: smooth (Fig. 11C–F; *Diplocephalus picinus*, *Erigonella hiemalis*, *E. ignobilis*).
1: rough (Fig. 11A–B, *Dicymbium tibiale*, *Diplocephalus latifrons*).

State 1 summarises different presumably non-homologous types that are difficult to separate with a stereomicroscope. It includes very short but regularly distributed papillae (exclusively in *Linyphia triangularis*), irregularly rough to regularly net-like sculpturations and ray-skin like surfaces. Rough surfaces are found in all basal taxa but are reduced in *Alioranus pastoralis* and in node 7 with four

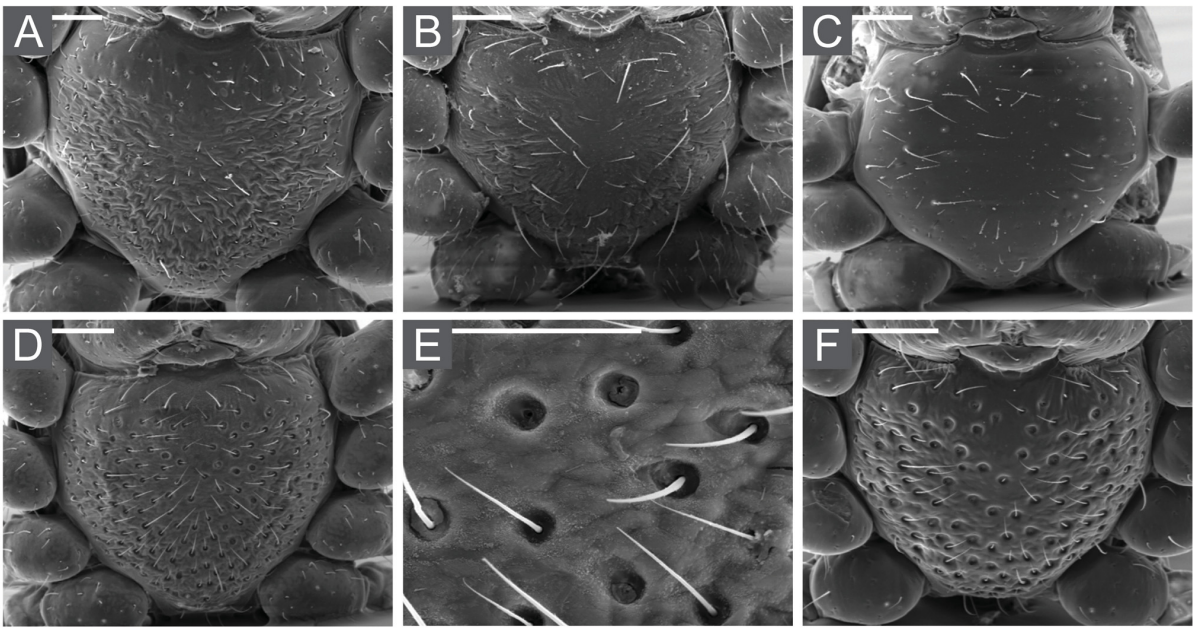

Fig. 11. Scanning Electron Microscope pictures of the male sternum in ventral view. **A**. *Dicymbium tibiale* (Blackwall, 1836) (11430; ZMUC). **B**. *Diplocephalus latifrons* (O. Pickard-Cambridge, 1863) (Ar1262; NMBE). **C**. *Diplocephalus picinus* (Blackwall, 1841) (Ar6645; NMBE). **D**. *Erigonella hiemalis* (Blackwall, 1841) (ZMUC). **E**. *Erigonella hiemalis*, detail (ZMUC). **F**. *Erigonella ignobilis* (O. Pickard-Cambridge, 1871) (Ar2880; NMBE). Abbreviations: see Material and methods. Scale bars: A–D, F = 100 μm; E = 50 μm.

secondary gains in *Saloca* (node 28), *Dicymbium* (without *D. libidinosum*, node 30), *Diplocephalus latifrons* and *Savignia zero*.

(196). Sternum, punctuation

0: absent (Fig. 11C, *Diplocephalus picinus*).
1: present (Fig. 11D–F; *Erigonella hiemalis*, *E. ignobilis*).

Dahl (1901) established the genus *Erigonella* based on the punctuated sternum. The punctuated sternum is present in *E. subelevata*, *E. hiemalis* and *E. ignobilis*.

197. Clypeus texture

0: nearly smooth (Fig. 12D, *Araeoncus humilis*; H00: pl. 20, *Diplocephalus cristatus*).
1: squamate (Fig. 12A–B, *Alioranus pastoralis*; H00: pl. 43, *Laminacauda plagiata*).

MH04-112, A09-86. Only a few scored species have a squamate clypeus, most are nearly smooth.

(198). Inter AME-PME setae, arrangement

0: random to uniform, not densely packed (Fig. 12D; H00: pl. 14b, *Araeoncus humilis*).
1: densely packed in longitudinal line (Fig. 13I; Locket & Millidge 1953: fig. 168d–e, *Saloca diceros*).

Saloca diceros and *Saloca kulczynskii* (node 28) have two parallel lines of slightly thickened setae between the anterior and posterior median eyes arranged longitudinally. State 1 is a synapomorphy of node 28.

(199). Diagonal flattened cephalic front

0: absent (Fig. 12G; Roberts 1987: fig. 39i, *Diplocephalus latifrons*).
1: present (Fig. 15B; Eskov 1988: fig. 12, *Diplocephalus marusiki*).

The frontal side of the male carapace is flat in frontal view and runs diagonally from the clypeal margin to the posterior median eyes in lateral view. This character is an ambiguous synapomorphy of node 40 with a reduction in node 46 and an independent occurrence in *Caucasopisthes procurvus*.

(200). Cephalic region, slightly raised

0: absent (Fig. 15A, *Paraglyphesis polaris*; H00: fig. 32a, *Tapinocyba praecox*).
1: present (Figs 13D, 15C; Roberts 1987: fig. 39e, *Erigonella ignobilis*).

This character accounts for taxa without a distinct lobe, i.e., with a slightly raised cephalic region as, e.g., in *Erigonella ignobilis* (Roberts 1987: fig. 39e), *Araeoncus humilis* (Fig. 12C) or *Dicymbium* (Fig. 12E–F).

201. Cephalic region, entirely raised dorsally

0: not raised (Fig. 15A, *Paraglyphesis polaris*; H00, fig. 32a, *Tapinocyba praecox*).
1: raised (Fig. 15D, *Pelecopsis elongata*; H00: fig. 32b, *Araeoncus crassiceps*).

MH04-101, H00-41, A09-80. This character accounts for lobes with all eyes above the thoracic furrow "Augenhügel", according to the definition of H00 and the original descriptions of different types of lobes in Schaible *et al.* (1986). It occurs in six species independently.

(202). Cephalic region, entirely raised forwardly

0: not raised (Fig. 15A, *Paraglyphesis polaris*; H00, fig. 32a, *Tapinocyba praecox*).
1: raised (Fig. 15E; Wiehle 1960: fig. 440, *Araeoncus anguineus*).

This lobe is directed frontally and bears all eyes frontal to the clypeus. This type of cephalic lobe is found in *Archaraeoncus proscipiens*, *Araeoncus anguineus* and node 66 (*A. caucasicus* and *A. victorianyanzae*).

(203). Cephalic region, AME position

0: more or less above the clypeus margin (Fig. 12H; Roberts 1987: fig. 39j, *Diplocephalus picinus*; Fig. 15G; Roberts 1987: fig. 39k, *Diplocephalus connatus*).
1: anterior to the clypeus margin (Figs 12G, 15F, *Diplocephalus latifrons*; Roberts 1987: fig. 39g, *Diplocephalus cristatus*).
2: posterior to the clypeus margin (Fig. 12I; Roberts 1987: fig. 16h, *Dismodicus bifrons*).

In some taxa the cephalic region is not only raised above the thoracic furrow, but also exceeds the clypeus. This character can be coded for all types of lobes. State 2 is found only in *Dismodicus* (node 15) and in node 40 with a reversal in node 46. State 1 is most common in node 31 and state 0 in most taxa basal to it.

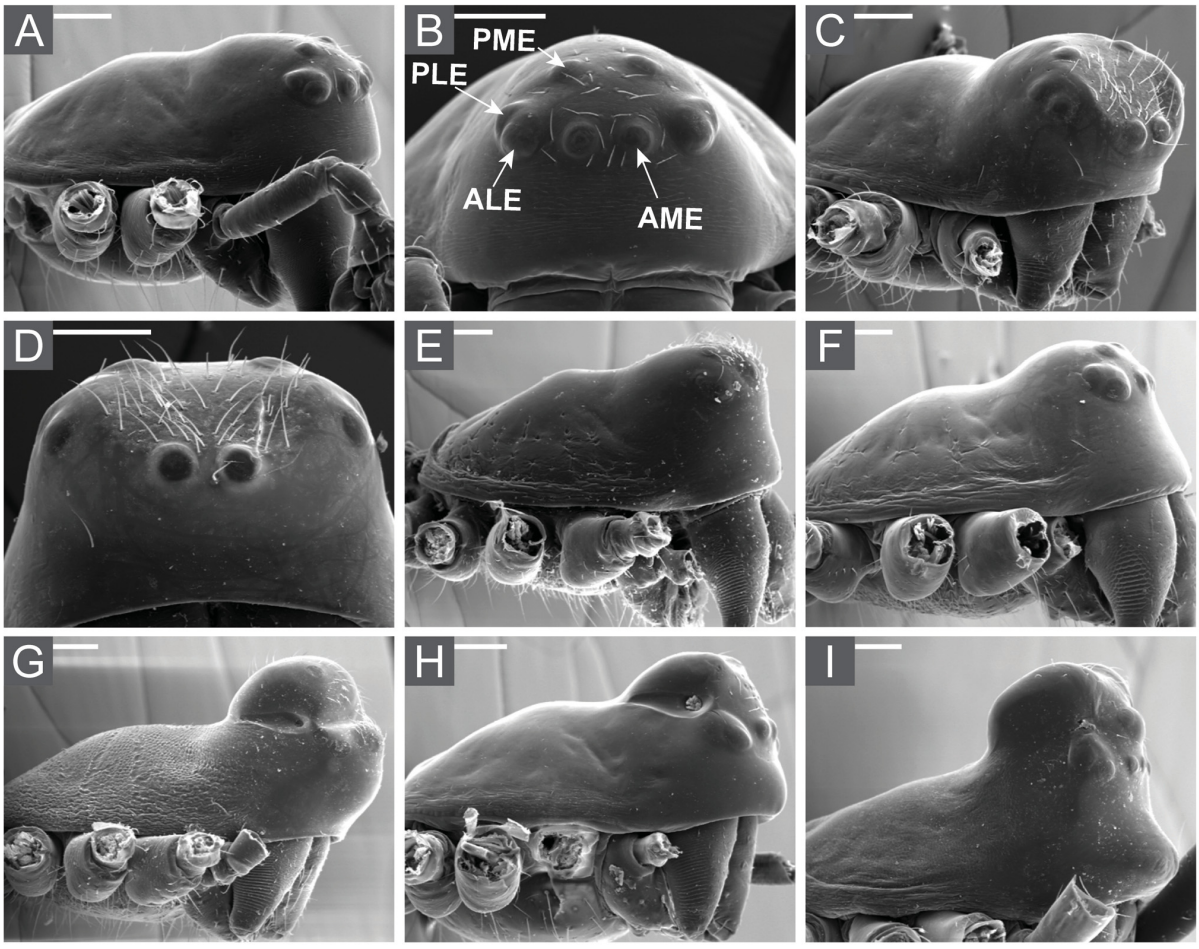

Fig. 12. Scanning Electron Microscope pictures of the male cephalic lobes in lateral (A, C, E–I) and frontal (B, D) views. **A–B**. *Alioranus pastoralis* (O. Pickard-Cambridge, 1872) (3695-3702; coll. E.G.). **C–D**. *Araeoncus humilis* (Blackwall, 1841) (Ar3186; NMBE). **E**. *Dicymbium nigrum* (Blackwall, 1834) (Ar637; NMBE). **F**. *Dicymbium tibiale* (Blackwall, 1836) (11430; ZMUC). **G**. *Diplocephalus latifrons* (O. Pickard-Cambridge, 1863) (Ar1262; NMBE). **H**. *Diplocephalus picinus* (Blackwall, 1841) (Ar6645; NMBE). **I**. *Dismodicus bifrons* (Blackwall, 1841) (Ar1192; NMBE). Abbreviations: see Material and methods. Scale bars = 100 µm.

204. Cephalic PME lobe

0: absent (Figs 13D, 15C; Roberts 1987: fig. 39e, *Erigonella ignobilis*).
1: present (Figs 12G, 15F; Roberts 1987: fig. 39i, *Diplocephalus latifrons*).

MH04-102, H00-42. PME lobes are the most common type of cephalic lobes within the *Savignia*-group (over 50% of the scored taxa). In *Diplocephalus connatus* the PME lobe is more precisely an inter PME lobe, since the PME are not elevated, but the thorax between the PME is. In node 31 all but five scored taxa and node 63 have a PME lobe.

(205). Cephalic PME lobe, form

0: broad (Fig. 12H; Roberts 1987: fig. 39j, *Diplocephalus picinus*).
1: narrow (Fig. 15G; Roberts 1987: fig. 39k, *Diplocephalus connatus*)

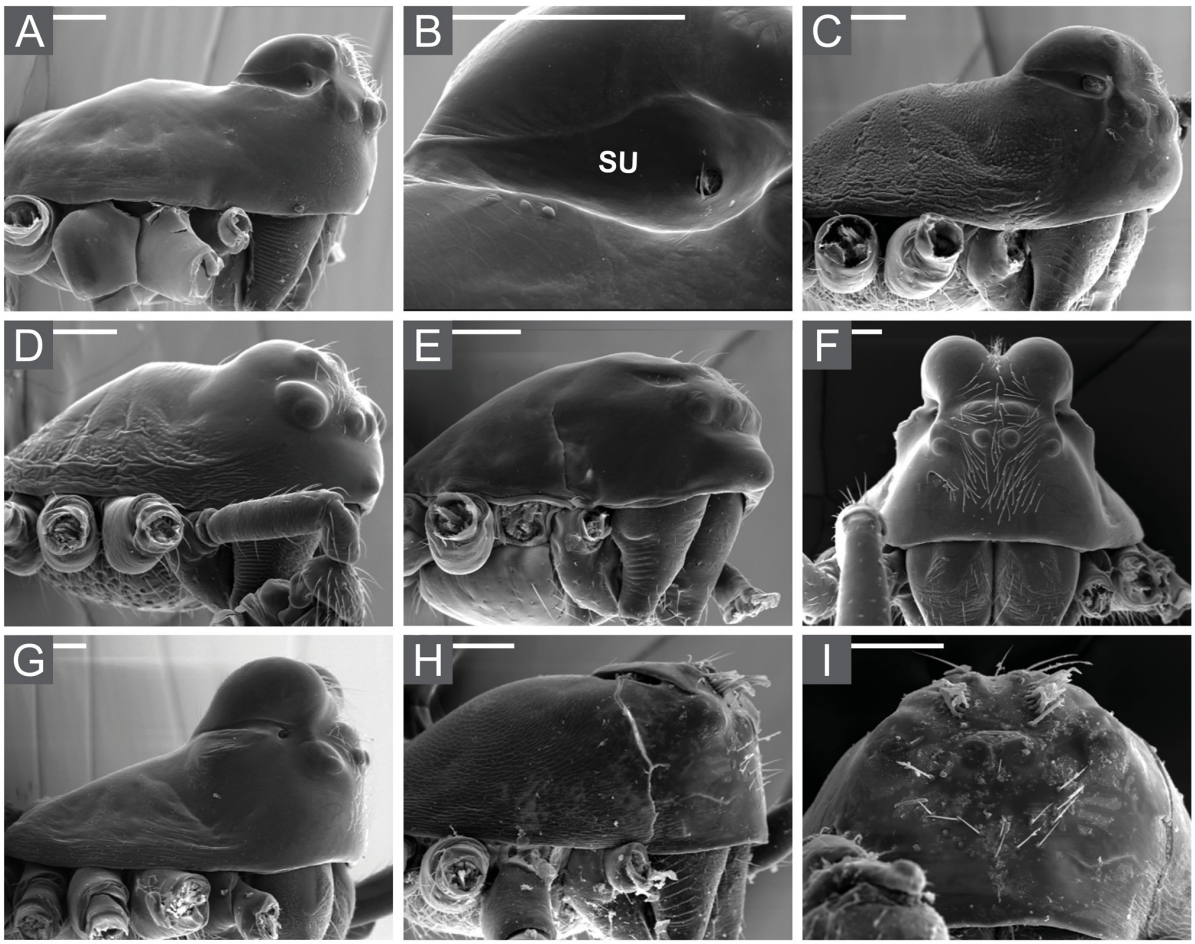

Fig. 13. Scanning Electron Microscope pictures of the male cephalic lobes in lateral (A–E, G–H) and frontal (F, I) views. **A–B**. *Entelecara erythropus* (Westring, 1851) (Ar172; NMBE). **C**. *Erigonella hiemalis* (Blackwall, 1841) (ZMUC). **D**. *Erigonella ignobilis* (O. Pickard-Cambridge, 1871) (Ar2880; NMBE). **E**. *Glyphesis servulus* (Simon, 1882) (792f; NMB). **F**. *Hypomma bituberculatum* (Wider, 1834) (Ar553; NMBE). **G**. *Hypomma bituberculatum* (Wider, 1834) (Ar553; NMBE). **H–I**. *Saloca diceros* (O. Pickard-Cambridge, 1871) (Ar2188; NMBE). Abbreviations: see Material and methods. Scale bars = 100 μm.

This character accounts for PME lobes that either bear the PME on top of a broad lobe or else on a narrow lobe, with the PME above the thoracic furrow but not at the tip of the lobe. The narrow PME lobe is only found in *Entelecara acuminata*, node 38 and also in node 56 with one reduction in *Diplocephalus alpinus*.

206. Cephalic post-PME lobe

0: absent (Figs 13D, 15C; Roberts 1987: fig. 39e, *Erigonella ignobilis*).
1: present (Roberts 1987: fig. 21e, *Oedothorax gibbosus*).

MH04-103, H00-43, A09-82. This is an autapomorphy of *Hilaira excisa*.

207. Cephalic inter AME-PME lobe

0: absent (Figs 13D, 15C; Roberts 1987: fig. 39e, *Erigonella ignobilis*).
1: present (Fig. 15L, *Janetschekia monodon*; H00: pl. 76a, *Walckenaeria directa* (O. Pickard-Cambridge, 1874)).

MH04-104, H00-44. *Janetschekia monodon* was coded as having such a lobe since the area between the AME and PME seems to have aroused from the cephalothorax forming a slightly backwards shifted lobe that does not bear the PMEs (see Thaler 1969: fig. 40). This is an autapomorphy of *Janetschekia monodon*.

208. Cephalic clypeal lobe

0: absent (Fig. 13C; Roberts 1987: fig. 39d, *Erigonella hiemalis*).
1: present (Figs 13E, 15I; Roberts 1987: fig. 39c, *Glyphesis servulus*).

MH04-105, H00-45. This lobe usually is very small (see, e.g., Thaler 1970: fig. 4: *Diplocephalus rostratus*). The clypeal lobe is present in *Dismodicus* (node 15), *Glyphesis* (node 22, reduced *Paraglyphesis polaris*) and independently in *Erigonella ignobilis*, *Diplocephalus rostratus* and *D. subrostratus*.

209. Cephalic AME lobe

0: absent (Fig. 12C; H00: pl. 14b, *Araeoncus humilis*).
1: present (Fig. 12G, *Diplocephalus latifrons*; Fig. 15J; Roberts 1987: fig. 39f, *Savignia frontata*).

MH04-106, H00-46. An AME lobe is present in nodes 35 (secondarily reduced in *Erigonella ignobilis*), 46, 56 and indepently in *Araeoncus galeriformis* and *Savignia harmsi*. We also coded males as having an AME lobe, if at least a slight elevation was present as in, e.g., *Diplocephalus cristatus* (Roberts 1987: fig. 39g) or *D. latifrons* (Fig. 12G). However, most AME lobes are very distinct as in *Savignia frontata* (Roberts 1987: fig. 39f).

(210). Cephalic semi post-PME lobe

0: absent (Figs 13D, 15C; Roberts 1987: fig. 39e, *Erigonella ignobilis*).
1: present (Fig. 15K; Roberts 1987: fig. 16h, *Dismodicus bifrons*).

Additionally, to the cephalic lobe types distinguished by H00 and MH04, Schaible *et al.* (1986) observed one more type, the "Scheitelfortsatz". This type is similar to the PME lobe but does not bear the PMEs. It lies behind the PMEs but is still not separated from them as seen in a post-PME lobe. *Dismodicus* and *Hypomma* were recoded from MH04 and Frick *et al.* (2010), respectively, as having this type of lobe rather than a PME lobe. This lobe is a synapomorphy of *Hypomma* and *Dismodicus* (node 14).

(211). Cephalic AME lobe in contact with PME lobe

0: separated (Figs 12G, 15F; Roberts 1987: fig. 39i, *Diplocephalus latifrons*).
1: in contact (Fig. 15G, *Diplocephalus connatus*; Eskov 1988: fig. 87, *Savignia zero*; Marusik 1988: fig. 5, *Savignia birostra*).

This character accounts for *Diplocephalus connatus* and node 48 (*Savignia birostra* plus *S. zero*) in which the AME lobe and the PME lobe are in contact. However, the lobes of these two taxa differ: while *D. connatus* has two narrow lobes, the AME and the PME lobe of *S. birostra* and *S. zero* are broad and are presumably not homologous with what is found in *D. connatus*.

212. Cephalic sulci (SU) on sides of prosoma

0: absent (Figs 13D, 15C; Roberts 1987: fig. 39e, *Erigonella ignobilis*).
1: present (Fig. 13A–B, *Entelecara erythropus*; Fig. 12H; Roberts 1987: fig. 39j, *Diplocephalus picinus*).

MH04-108, H00-48. Lateral cephalic sulci are very homoplastic and found in many taxa within the *Savignia*-group. The fast evolutionary mechanism of switching lateral sulci on and off is illustrated in *Diplocephalus connatus* and *D. connatus jacksoni*. These two subspecies are distinguishable exclusively by the presence (*D. conatus*) or absence of lateral sulci (*D. connatus jacksoni*).

213. Cephalic pits

0: absent (Figs 13D, 15C; Roberts 1987: fig. 39e, *Erigonella ignobilis*).
1: present (Fig. 13A–B, *Entelecara erythropus*; Fig. 13C; Roberts 1987: fig. 39d, *Erigonella hiemalis*).

MH04-109, H00-49. Pits can be present without sulci (e.g., Fig. 15K; Roberts 1987: fig. 16h, *Dismodicus bifrons*).

(214). Cephalic lateral dark spot or stripe

0: absent (Fig. 15J; Roberts 1987: fig. 39f, *Savignia frontata*).
1: spot or stripe (Fig. 15H; Eskov 1988: fig. 83, *Savignia zero*).

Besides lateral sulci that are incisions (e.g., Fig. 13F–G, *Hypomma bituberculatum*) according to the definition in H00, this character is seen in certain species of *Savignia*. They do not have incisions and pits but instead a longitudinal stripe darker than the areas around and glabrous instead of net-like or sculptured as the remaining carapace. In *Savignia saitoi* and *Diplocephalus cristatus* is a small darker spot visible (not "yet a stripe") bearing three or one small pores, respectively. *Savignia birostra* also bears a couple of pores in the frontal part of the stripe. The supposedly closely related *D. cristatus*, *D. alpinus* and *D. crassilobus* show a transition series from a dark stripe with a distinct pit (*D. crassilobus*) to a small dark spot with pores (*D. cristatus*) to lateral sulci with a pit (*D. alpinus*). This character is present in node 47 and in node 57 with a reduction in *D. alpinus*.

(215). Cephalic lateral dark spot or stripe, pores

0: absent (Fig. 15J; Roberts 1987: fig. 39f, *Savignia frontata*).
1: present (Fig. 15H; Eskov 1988: fig. 83, *Savignia zero*).

See discussion above. *Diplocephalus crassilobus* is the only species with a cephalic lateral dark spot or stripe that lacks pores.

216. Cephalic cuticular pores

0: rare.
1: common (H00: pl. 43, *Laminacauda plagiata*).

MH04-110, H00-50, A09-84. Cuticular pores could only be scored in the taxa for which SEM pictures were present. They were only considered as rare in *Hypomma bituberculatum*, *Dicymbium tibiale* and *Diplocephalus latifrons* (within node 4).

(217). Prosoma, texture

0: smooth, shiny (Fig. 13E, *Glyphesis servulus*).
1: sculptured, as snake or ray skin, very regular (Fig. 13H, *Saloca diceros*; H00: pl. 57a, *Savignia frontata*).
2: rough, irregular, smoother than state 1 (Fig. 13C, *Erigonella hiemalis*).

This character accounts for the texture behind the thoracic furrow and not the elevated head region if present.

Male chelicerae

218. Cheliceral stridulatory striae, shape

0: ridged (Fig, 14C–D, *Dicymbium nigrum*, *Di. tibiale*; H00: pl. 42e, *Laminacauda plagiata*).
1: scaly (H00: pl. 49e, *Oedothorax gibbosus*).
2: imbricated (Fig. 14E, *Diplocephalus latifrons*; H00: pl. 39e, *Islandiana cristata*).

MH04-117, H00-56, A09-91. Most species within node 7 have imbricated stridulatory striae (ridged in node 30, *Walckenaeria acuminata* and *Dactylopisthes mirabilis* and scaly in *Dicymbium libidinosum*) while most taxa basal to node 7 have ridged striae (scaly in *Linyphia triangularis*). State 2 is a synapomorphy of node 7.

219. Cheliceral stridulatory striae, rows

0: widely and evenly spaced (Fig. 14G, *Entelecara erythropus*; H00: pl. 19e, *Diplocephalus cristatus*).
1: compressed proximally (Fig. 14B; H00: pl. 13e, *Araeoncus humilis*).
2: compressed distally (H00: pl. 16a–b, *Ceratinops inflatus*).
3: compressed and evenly spaced (Fig. 14A, *Alioranus pastoralis*; H00: pl. 25b–c, *Erigone psychrophila*).
4: compressed proximally and distally, widely spaced centrally (H00: pl. 1e, *Bolyphantes luteolus*).

MH04-118, A09-92. Most erigonine taxa have widely and evenly spaced stridulatory ridges (state 0) while most taxa basal to node 7 have compressed and evenly spaced striae (state 3).

220. Cheliceral stridulatory striae, ridges

0: absent (H00: pl. 19e, *Diplocephalus cristatus*).
1: present (Fig. 14I, J, *Erigonella ignobilis*; H00: pl. 16b *Ceratinops inflatus*).

MH04-119. These ridges were only found in *Erigonella ignobilis*. However, SEM figures, which are needed to score this character, were available for only a fraction of the scored taxa.

221. Cheliceral setal bases on front-lateral face

0: nearly flush with chelicerae to small bumps (Fig. 14G, *Entelecara erythropus*; H00: pl. 61e, *Sisicus apertus*).
1: formed into distinct bumps (H00: pls 10e, 23e, *Novafroneta vulgaris* Blest, 1979, *Drepanotylus uncatus*).

MH04-120*, A09-93*. Distinct bumps are only found in *Linyphia triangularis*, *Hilaira excisa* and in *Alioranus chiardolae*. All other newly scored species have nearly flush setal bases.

222. Cheliceral fang furrow

0: narrow (H00: pl. 60c, *Sciastes truncatus* (Emerton, 1882)).
1: wide and flat to concave (H00: pl. 68a, *Tmeticus tolli* Kulczyński, 1908).

MH04-122, A09-95. The fang furrow is narrow in all taxa except for *Linyphia triangularis*.

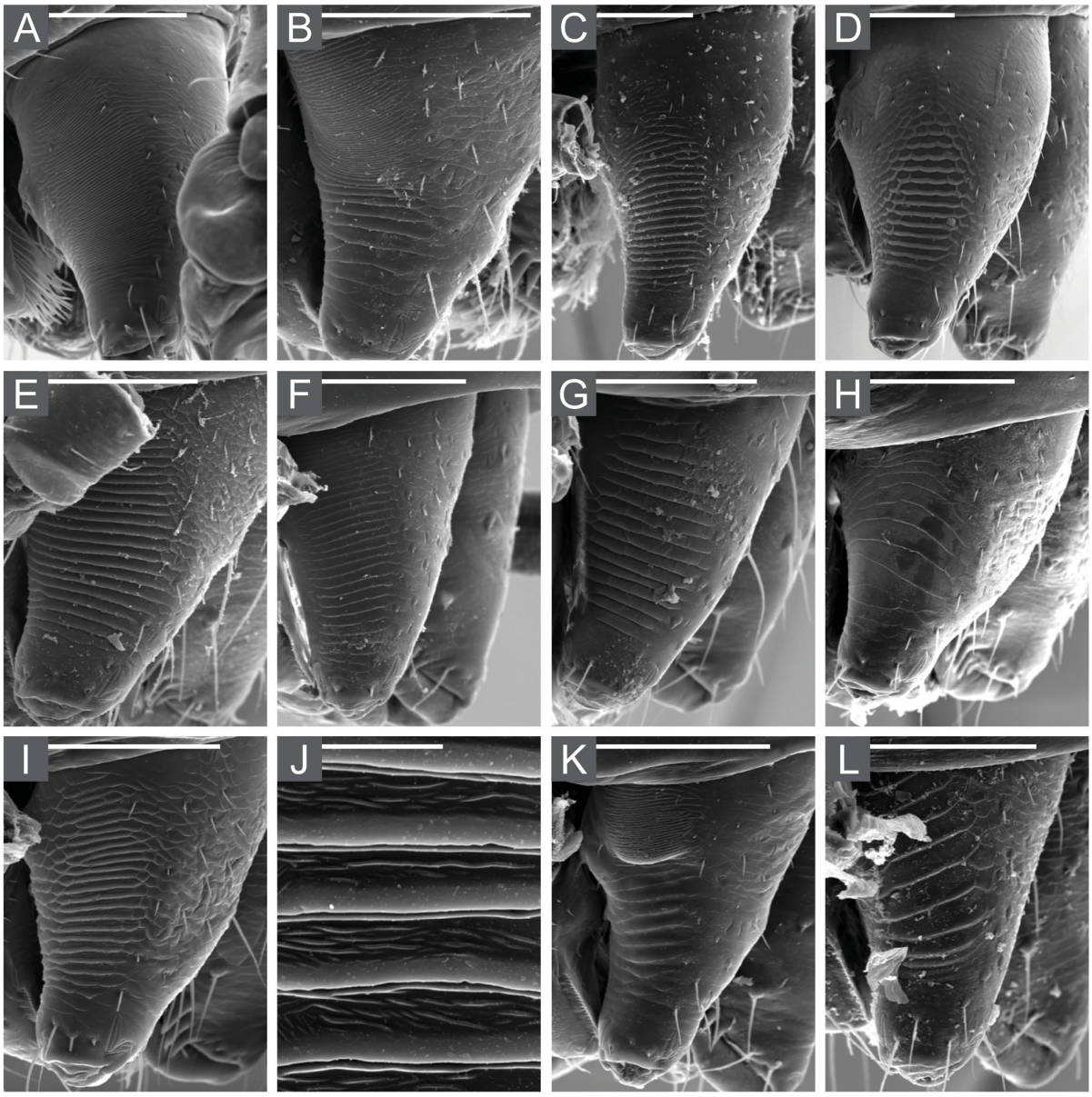

Fig. 14. Scanning Electron Microscope pictures of different male chelicera in lateral view. **A**. *Alioranus pastoralis* (O. Pickard-Cambridge, 1872) (3695-3702; coll. E.G.). **B**. *Araeoncus humilis* (Blackwall, 1841) (Ar3186; NMBE). **C**. *Dicymbium nigrum* (Blackwall, 1834) (Ar637; NMBE). **D**. *Dicymbium tibiale* (Blackwall, 1836) (11430; ZMUC). **E**. *Diplocephalus latifrons* (O. Pickard-Cambridge, 1863) (Ar1262; NMBE). **F**. *Diplocephalus picinus* (Blackwall, 1841) (Ar6645; NMBE). **G**. *Entelecara erythropus* (Westring, 1851) (Ar172; NMBE). **H**. *Erigonella hiemalis* (Blackwall, 1841) (ZMUC). **I**. *Erigonella ignobilis* (O. Pickard-Cambridge, 1871), ♂ (Ar2880; NMBE). **J**. *Erigonella ignobilis* (O. Pickard-Cambridge, 1871), detail (Ar2880; NMBE). **K**. *Glyphesis servulus* (Simon, 1882) (792f; NMB). **L**. *Saloca diceros* (O. Pickard-Cambridge, 1871) (Ar2188; NMBE). Scale bars: A–I, K–L = 100 μm; J = 10 μm.

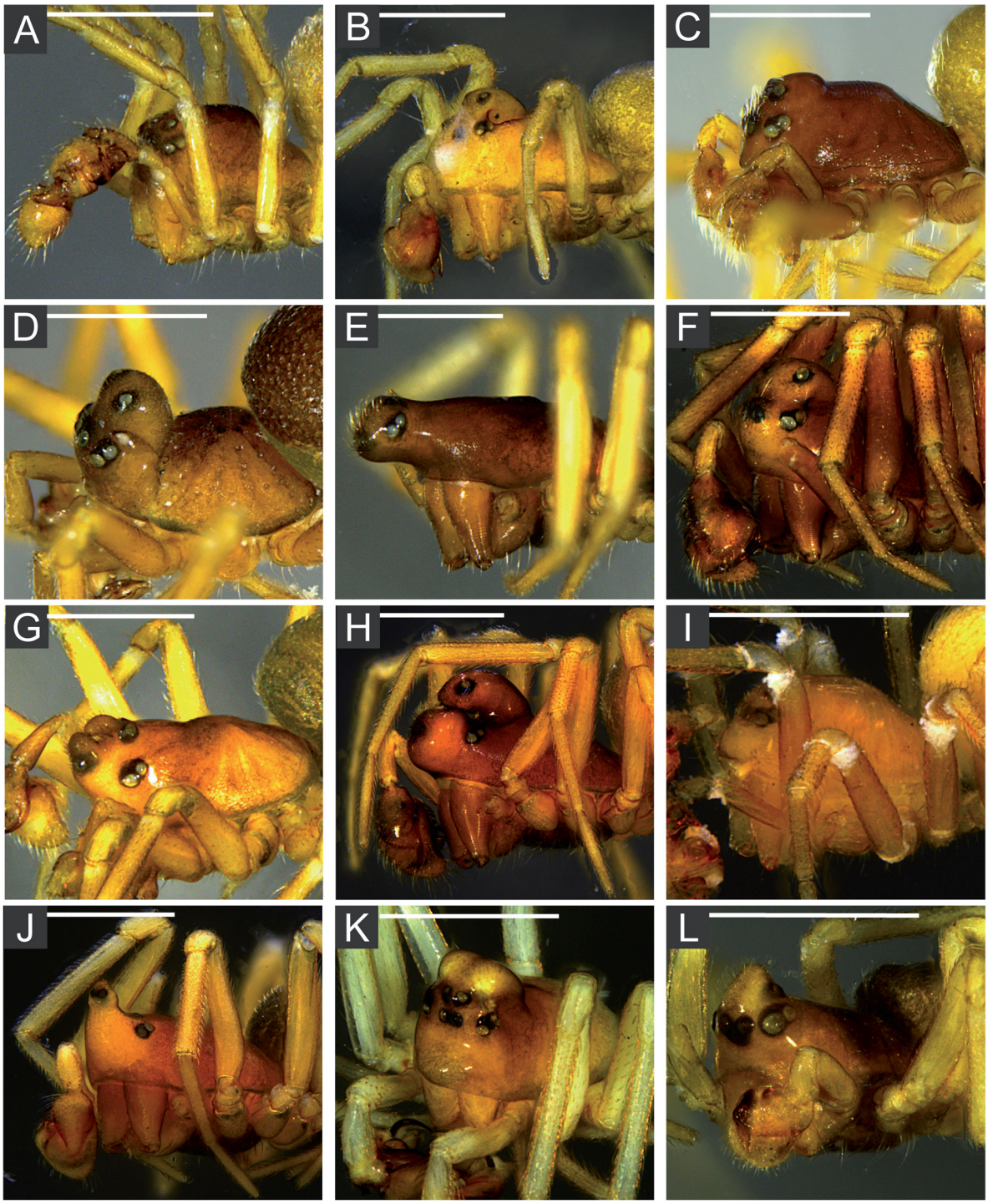

Fig. 15. Male cephalic lobes in lateral view. **A**. *Paraglyphesis polaris* Eskov, 1991 (coll. A.T.). **B**. *Diplocephalus marusiki* Eskov, 1988 (36878; SMF). **C**. *Erigonella ignobilis* (O. Pickard-Cambridge, 1871) (Ar2881; NMBE). **D**. *Pelecopsis elongata* (Wider, 1834) (Ar4869; NMBE). **E**. *Araeoncus anguineus* (L. Koch, 1869) (Ar3203; NMBE). **F**. *Diplocephalus latifrons* (O. Pickard-Cambridge, 1863) (Ar3662; NMBE). **G**. *Diplocephalus connatus* Bertkau, 1889 (Ar2281; NMBE). **H**. *Savignia zero* Eskov, 1988 (39671; SMF). **I**. *Glyphesis servulus* (Simon, 1882) (792a; NMB). **J**. *Savignia frontata* Blackwall, 1833 (1611c; NMB). **K**. *Dismodicus bifrons* (Blackwall, 1841) (Ar1192; NMBE). **L**. *Janetschekia monodon* (O. Pickard-Cambridge, 1873) (7033; SMF). Scale bars = 500 µm.

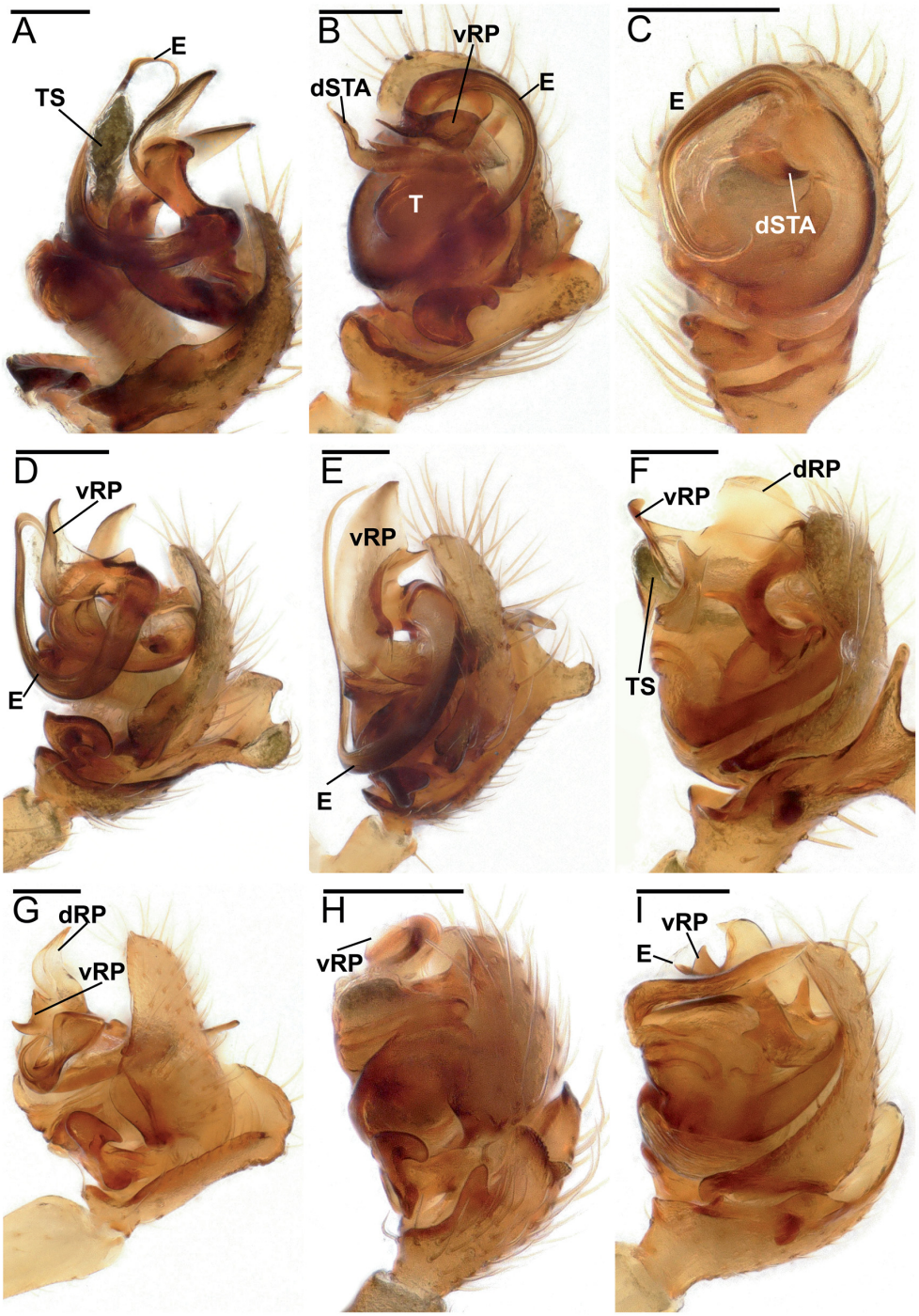

Fig. 16. Ventral radical process (vRP). Male palp in retrolateral (B, D–E, G–H), ventral (C) and prolateral (A, F, I) views. **A**. *Araeoncus anguineus* (L. Koch, 1869) (Ar3203; NMBE). **B**. *Diplocephalus protuberans* (O. Pickard-Cambridge, 1875) (coll. M.I.). **C**. *Diplocephalus dentatus* Tullgren, 1955 (2598a; NMB). **D**. *Araeoncus crassiceps* (Westring, 1861) (Ar1428; NMBE). **E**. *Araeoncus victorianyanzae* Berland, 1936 (00006708; ZMUC). **F**. *Araeoncus galeriformis* (Tanasevitch, 1987) (33822; SMF). **G**. *Diplocephalus caucasicus* Tanasevitch, 1987 (33790; SMF). **H**. *Paraglyphesis polaris* Eskov, 1991 (coll. A.T.). **I**. *Diplocephalus montanus* Eskov, 1988 (36879; SMF). Abbreviations: see Material and methods. Scale bars = 100 μm.

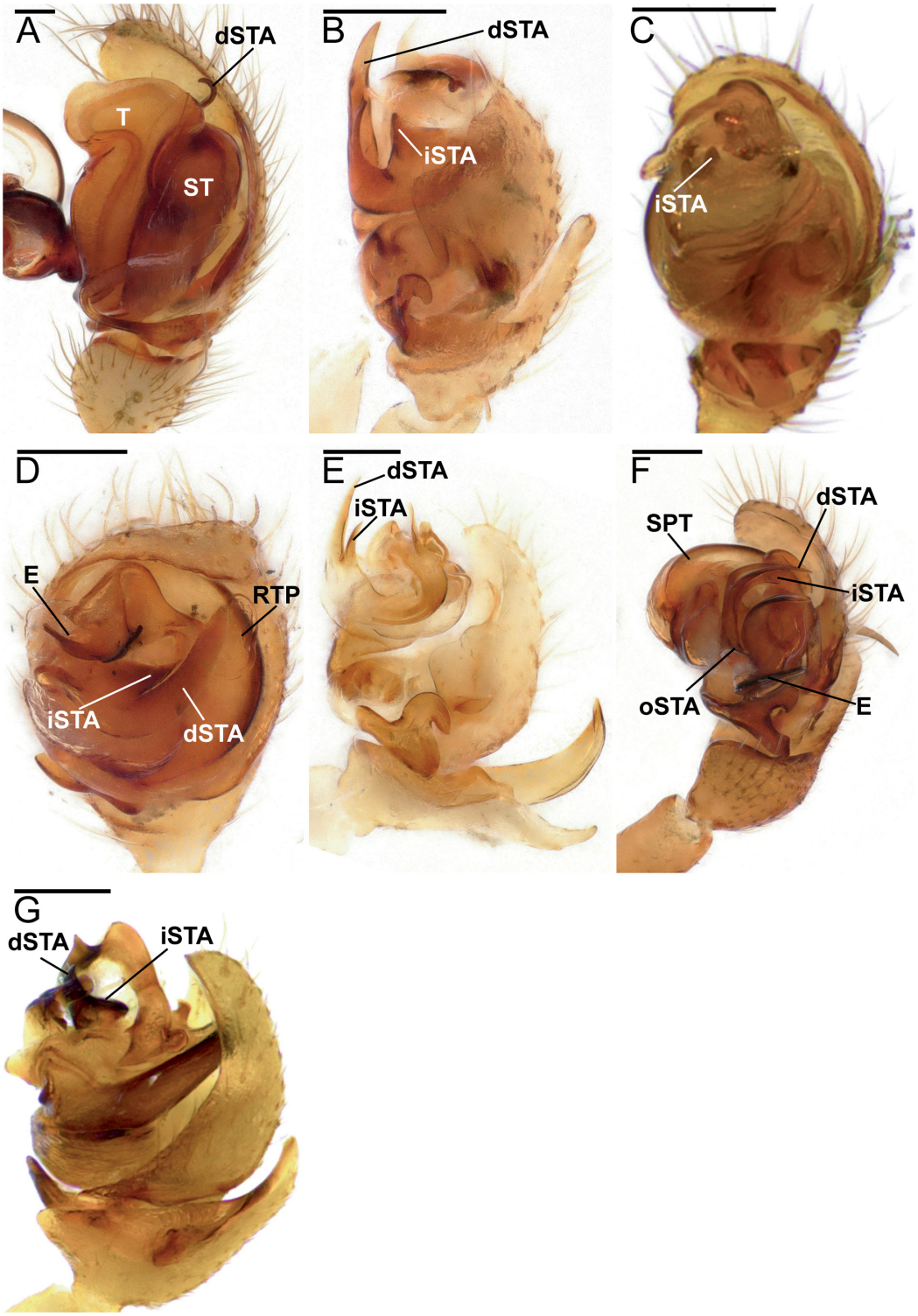

Fig. 17. Different types of inner suprategular apophyses (iSTA). Male palp in retrolateral (B, E–F), ventral (C), prolateral (A, P) and distal (D) views. **A**. *Linyphia triangularis* (Clerck, 1757) (Ar272; NMBE). **B**. *Dactylopisthes locketi* (Tanasevitch, 1983) (34850; SMF). **C**. *Glyphesis servulus* (Simon, 1882) (792a; NMB). **D**. *Diplocephalus rostratus* Schenkel, 1934 (1509a; NMB). **E**. *Savignia producta* Holm, 1977 (36885; SMF). **F**. *Dicymbium nigrum* (Blackwall, 1834) (Ar6602; NMBE). **G**. *Savignia frontata* Blackwall, 1833 (1611c; NMB). Abbreviations: see Material and methods. Scale bars = 100 µm.

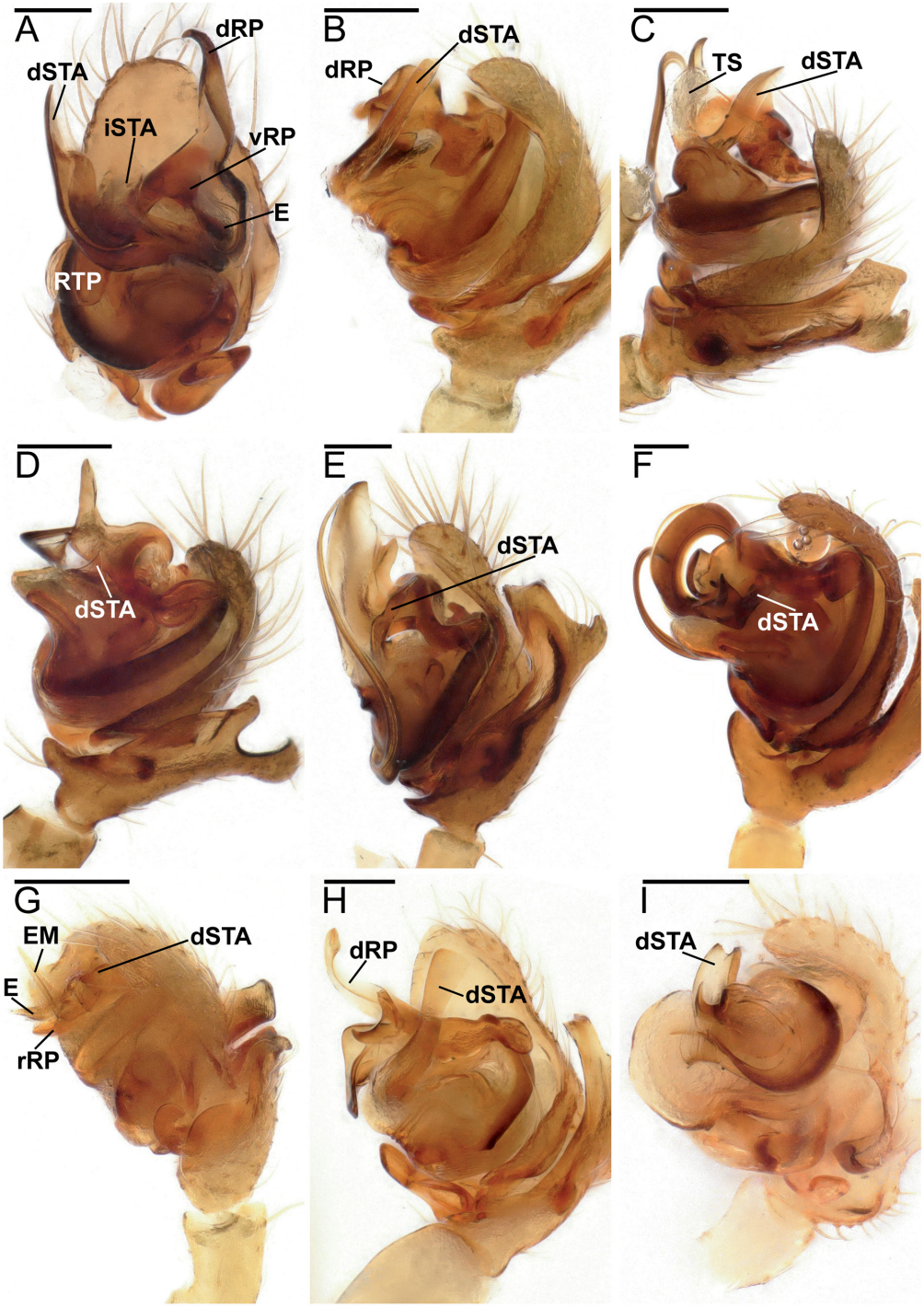

Fig. 18. Different types of distal suprategular apophyses (dSTA). Male palp in retrolateral (G), prolateral (B–F, H) and distal (A, I) views. **A**. *Diplocephalus pavesii* Pesarini, 1996 (coll. M.I.). **B**. *Diplocephalus marusiki* Eskov, 1988 (36878; SMF). **C**. *Araeoncus crassiceps* (Westring, 1861) (Ar1428; NMBE). **D**. *Araeoncus humilis* (Blackwall, 1841) (Ar3186; NMBE). **E**. *Araeoncus victorianyanzae* Berland, 1936 (00006708; ZMUC). **F**. *Dicymbium libidinosum* (Kulczyński, 1926) (39587; SMF). **G**. *Janetschekia monodon* (O. Pickard-Cambridge, 1873) (7033; SMF). **H**. *Diplocephalus caucasicus* Tanasevitch, 1987 (33790; SMF). **I**. *Saloca diceros* (O. Pickard-Cambridge, 1871) (Ar2188; NMBE). Abbreviations: see Material and methods. Scale bars = 100 μm.

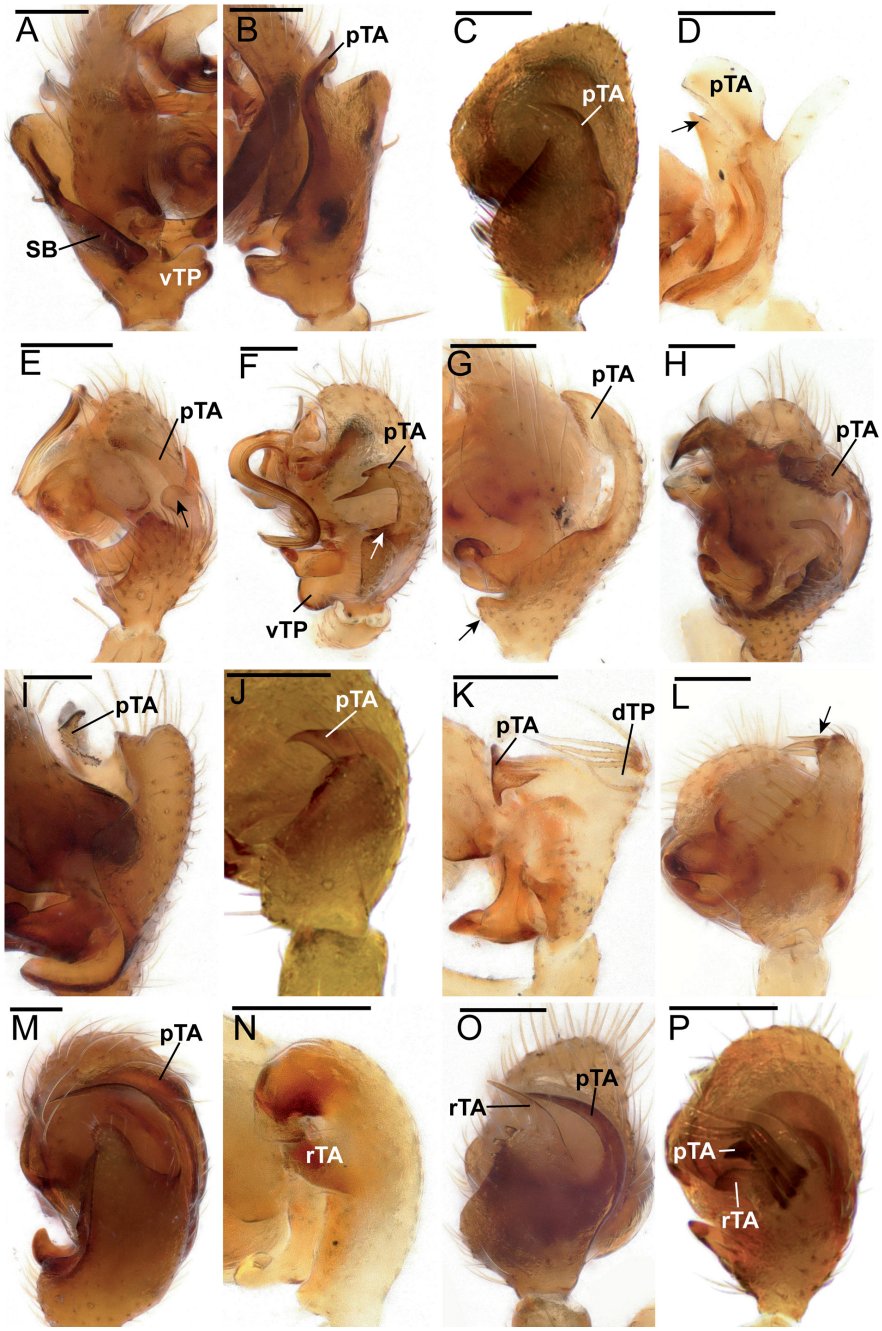

Fig. 19. Male palpal tibia in retrolateral (A, D–I, K, N), prolateral (B) and dorsal (C, J, L–M, O–P) views. **A–B**. *Diplocephalus cristatus* (Blackwall, 1833) (Ar1187; NMBE). **C**. *Savignia frontata* Blackwall, 1833) (1611c; NMB). **D**. *Savignia harmsi* Wunderlich, 1980 (29187; SMF). **E**. *Diplocephalus dentatus* Tullgren, 1955 (2598a; NMB). **F**. *Diplocephalus helleri* (L. Koch, 1869) (Ar3235; NMBE). **G**. *Diplocephalus rostratus* Schenkel, 1934 (1509a; NMB). **H**. *Erigonella subelevata* (L. Koch, 1869) (Ar5604; NMBE). **I**. *Diplocephalus arnoi* Isaia, 2005 (coll. M.I.). **J**. *Caucasopisthes procurvus* (Tanasevitch, 1987) (33788; SMF). **K**. *Glyphesis taoplesius* Wunderlich, 1969 (23978; SMF). **L**. *Diplocephalus permixtus* (O. Pickard-Cambridge, 1871) (33430; SMF). **M**. *Dicymbium libidinosum* (Kulczyński, 1926) (39587; SMF). **N**. *Glyphesis cottonae* (La Touche, 1946) (18756; SMF). **O**. *Diplocephalus connatus* Bertkau, 1889 (Ar2281; NMBE). **P**. *Glyphesis servulus* (Simon, 1882) (792a; NMB). Abbreviations: see Material and methods. Scale bars = 100 µm.

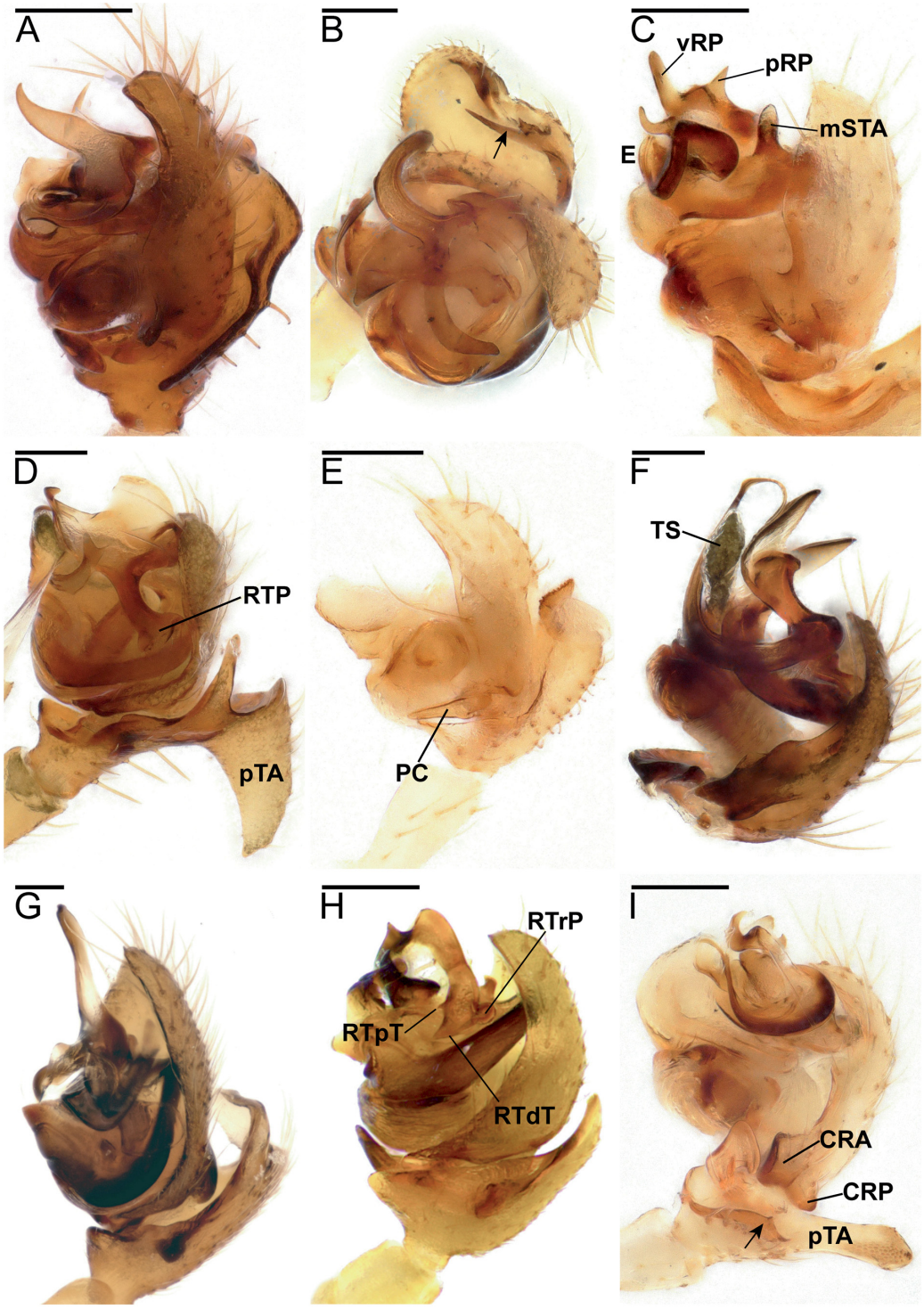

Fig. 20. Different structures. Male palp in retrolateral (A, C, E, I), prolateral (D, F–H) and distal (B) views. **A**. *Diplocephalus cristatus* (Blackwall, 1833) (Ar1187; NMBE). **B**. *Diplocephalus helleri* (L. Koch, 1869) (Ar3235; NMBE). **C**. *Savignia harmsi* Wunderlich, 1980 (29187; SMF). **D**. *Araeoncus galeriformis* (Tanasevitch, 1987) (33822; SMF). **E**. *Diastanillus pecuarius* (Simon, 1884). **F**. *Araeoncus anguineus* (L. Koch, 1869) (Ar3203; NMBE). **G**. *Diplocephalus arnoi* Isaia, 2005 (coll. M.I.). **H**. *Savignia frontata* Blackwall, 1833 (1611c; NMB). **I**. *Saloca diceros* (O. Pickard-Cambridge, 1871) (Ar2188; NMBE). Abbreviations: see Material and methods. Scale bars = 100 μm.

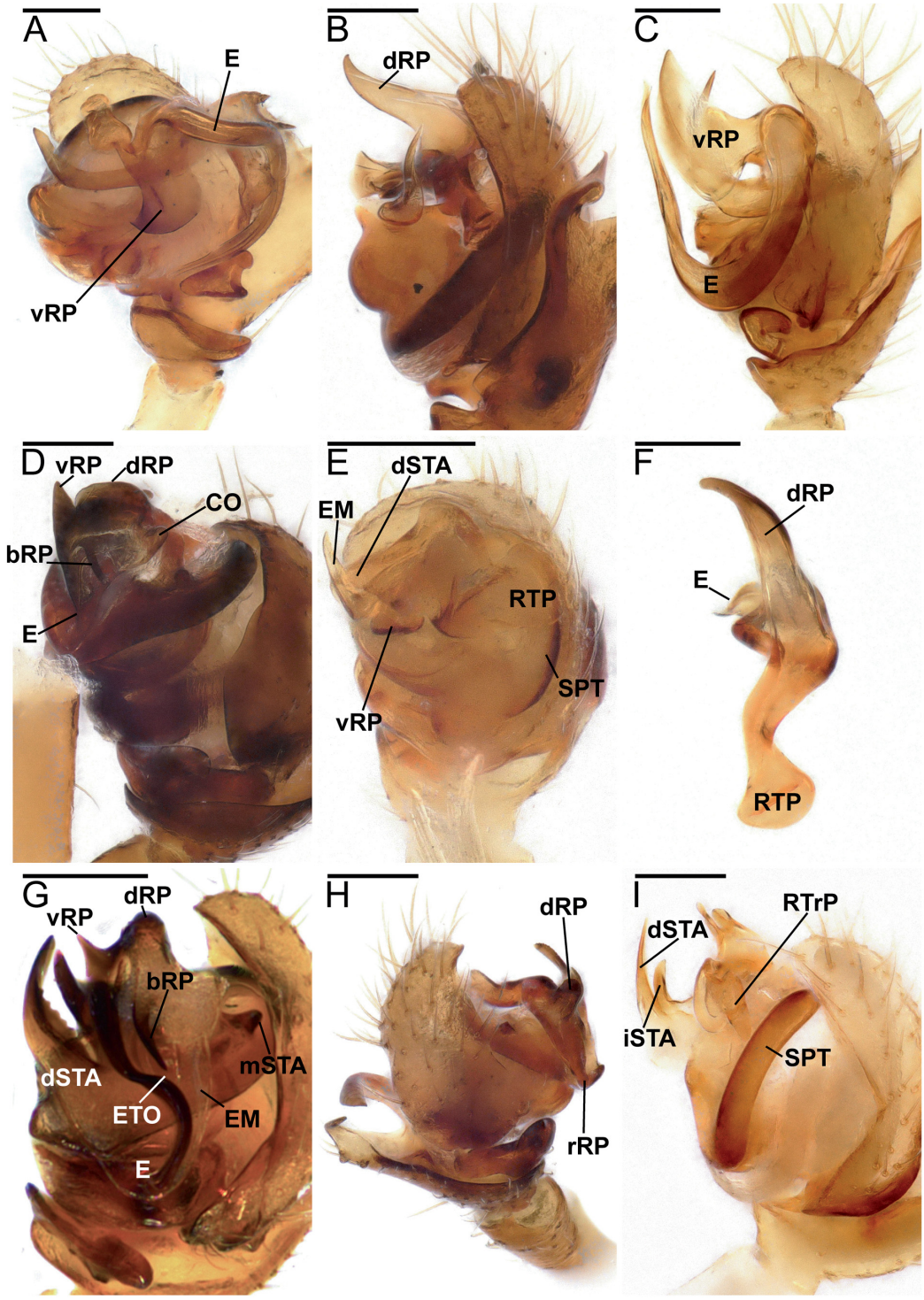

Fig. 21. Radical process types. Male palp in retrolateral (A, C–D, G–H) and prolateral (B, E–F, I) views. **A**. *Diplocephalus helleri* (L. Koch, 1869) (Ar3235; NMBE). **B**. *Diplocephalus cristatus* (Blackwall, 1833) (Ar1187; NMBE). **C**. *Araeoncus caucasicus* Tanasevitch, 1987 (33781; SMF). **D**. *Savignia birostra* (Chamberlin & Ivie, 1947) (Ar6744; NMBE). **E**. *Janetschekia monodon* (O. Pickard-Cambridge, 1873) (7033; SMF). **F**. *Diplocephalus crassilobus* (Simon, 1884) (Ar6668; NMBE). **G**. *Savignia frontata* Blackwall, 1833 (1611c; NMB). **H**. *Diplocephalus connatus* Bertkau, 1889 (Ar2281; NMBE). **I**. *Savignia producta* Holm, 1977 (36885; SMF). Abbreviations: see Material and methods. Scale bars = 100 µm.

223. Cheliceral lateral bulge

0: absent (Fig. 14I, *Erigonella ignobilis*).
1: present (Fig. 14K, *Glyphesis servulus*).

This bulge is situated laterally at the basal third of the chelicerae. In *Glyphesis servulus* it defines a border between a proximal area of compressed and a distal area of widely spaced striae. This bulge is a synapomorphy of node 23 with one reduction in *Glyphesis taoplesius*.

224. Endites

0: smooth (H00: pl. 64a, *Tapinocyba praecox*).
1: tuberculate (MH04: fig. 20d, *Triplogyna major* Millidge, 1991).

MH04-125, A09-99. This character is phylogenetically uninformative since tuberculate endites are only found in *Alioranus chiardolae*.

Male opisthosoma

225. Booklung covers

0: rugose (MH04: fig. 22A, *Erigone psychrophila*).
1: grooved (MH04: fig. 22B, *Gigapassus octarine* Miller, 2007).
2: squamate (MH04: fig. 22C, *Smermisia vicosana* (Bishop & Crosby, 1938)).
3: nearly smooth (MH04: fig. 22D, *Tutaibo phoeniceus* (O. Pickard-Cambridge, 1894)).

MH04-154, H00-54. We coded most erigonine taxa with stereo microscopes only. However, it seems possible to recognize at least squamate booklung covers with the appropriate illumination. Grooved booklung covers were present in *Hilaira excisa*, smooth ones in *Alioranus* (node 6) and in *Walckenaeria acuminata* and rugose ones in *Araeoncus victorianyanzae*. All other erigonines were scored as squamate if scored at all.

226. Abdomen of male with dorsal scutum

0: absent.
1: present.

MH04-155, H00-53. The scutum is present in *Alioranus pauper* and in *Pelecopsis elongata*.

227. Abdomen with ventral sclerite anterior to spinnerets

0: absent.
1: present.

MH04-156. This character is an autapomorphy of *Pelecopsis elongata*.

(228). Tibia I and II in males with hooked bristles

0: absent.
1: present (Bosmans 1996: figs 3, 20: *Araeoncus humilis*, *A. martinae* Bosmans, 1996).

This character summarises two types of special hooked setae found dorsally on tibia I and ventrally on tibia II of *Araeoncus humilis* and *A. martinae*. They are short and moderate on tibia I but very thick and distinct on tibia II (Wiehle 1960: fig. 428: *Araeoncus humilis*). This character is an autapomorphy of *Araeoncus humilis* but also present in *Araeoncus martinae*, which was not scored in the current analysis.

Female prosoma

(229). Eye pattern

0: PME–PME = d, PME–PLE > d, ALE–AME > d, AME–AME < d.
1: PME–PME = d, PME–PLE = d, ALE–AME = d, AME–AME < d.
2: PME–PME < d, PME–PLE < d, ALE–AME < d, AME–AME < d.
3: PME–PME > d, PME–PLE > d, ALE–AME > d, AME–AME > d.

The eye arrangement is very variable. These four states only account for some combinations found in females. "–" stands for the distance and "d" for the diameter of the PME.

(230). Eye pattern, posterior row

0: straight.
1: procurved.
2: recurved.

This character was scored in dorsal view. We usually scored only one female for this character so that intraspecific variation was not considered. In most species these character delimitations were clear while in a few taxa the eye row was only slightly curved (e.g., in *Diplocephalus rostratus*).

(231). Eye size, anterior row

0: diameter of the anterior median eyes equals diameter of anterior lateral eyes.
1: diameter of the anterior median eyes smaller than diameter of anterior lateral eyes.

(232). Eye size, posterior row

0: diameter of the posterior median eyes equals diameter of posterior lateral eyes.
1: diameter of the posterior median eyes smaller than diameter of posterior lateral eyes.

State 1 is very rarely found and only present in four taxa in the current analysis: *Paraglyphesis polaris*, *Glyphesis nemoralis*, *Diplocephalus montanus* and *Savignia frontata*.

233. Clypeal setae

0: hirsute (H00: pl. 2a *Bolyphantes luteolus*).
1: only one seta below the AMEs (H00: pl. 21a, *Diplocephalus cristatus*).

MH04-113*, A09-87*. The only seta below the AME's has a different constitution than the remaining setae on the clypeus. Therefore, the supplementary setae were scored as a separate character. The single seta below the AME's is a synapomorphy of the erigonines (node 3) in the current analysis.

(234). Supplementary clypeal setae

0: absent (H00: pl. 21a, *Diplocephalus cristatus*).
1: present (*Diplocephalus rostratus*).

MH04-113*, A09-87*. This character supplements MH04-113. A couple of setae (equal in size to other body setae) are present in some derived species in the current analysis, i.e., in node 43 (*Diplocephalus marusiki* and *D. montanus*, *D. rostratus*) and in node 13 with a reversal in *Dismodicus*. These species also have the typical distinct erigonine (and mynoglenine) single seta below the AME, but among other setae. These setae are considered non-homologous with the distinct setae found in several outgroup taxa (Linyphiinae, Pimoidae and others in MH04).

235. Cheliceral teeth, retrolateral margin of fang furrow

0: three.
1: four or more.

MH04-123*, H00-58*, A09-97*. In the current analysis only four taxa have less than four retrolateral teeth: *Bolyphantes luteolus*, *Tenuiphantes tenuis*, *Pelecopsis elongata* and *Dismodicus elevatus*, all with three teeth.

236. Palpal tarsus claw

0: absent.
1: present.

MH04-126, H00-59, A09-100. The lack of the palpal claw supports the Erigoninae (node 3). This is a synapomorphy of node 1 with a reversal in *Bolyphantes luteolus*.

Chaetotaxy

Female palpal macrosetae

237. Palpal tarsus proximal dorsomesal macrosetae

0: absent.
1: present.

MH04-127, A09-101. These macrosetae are lacking in only three nodes (12, 15 and 20, i.e., "*Saloca*", *Dismodicus*, *Dactylopisthes*, respectively) and *Diplocephalus dentatus*.

238. Palpal tarsus distal dorsomesal macrosetae

0: absent.
1: present.

MH04-128, A09-102. The lack of these macrosetae are a synapomorphy that supports the Erigoninae (node 3).

239. Palpal tarsus proximal dorsoectal macrosetae

0: absent.
1: present.

MH04-129, A09-103. The lack of these macrosetae are a synapomorphy that supports the Erigoninae (node 3).

240. Palpal tarsus distal dorsoectal macrosetae

0: absent.
1: present.

MH04-130, A09-104. The lack of these macrosetae are a synapomorphy that supports the Erigoninae (node 3).

241. Palpal tarsus ventromesal macrosetae

0: zero.
1: two.
2: three (MH04: fig. 21d, *Triplogyna major*).
3: four (MH04: fig. 21f, *Neocautinella neoterica*).
4: five or six.

MH04-131*, A09-105*. In the current analysis all taxa within node 3 have three macrosetae except for *Dactylopisthes* (node 20) and *Diplocephalus rostratus* that have two macrosetae.

242. Palpal tarsus ventroectal macrosetae

0: zero.
1: one.
2: two (MH04: fig. 21E, *Triplogyna major*).
3: three (MH04: fig. 21G, *Neocautinella neoterica*).

MH04-132*, A09-106*, where this character is discussed at length. In the current analysis all taxa have two macrosetae with the exceptions of *Linyphia triangularis* with three and *Dismodicus* (node 15) with one. State 1 is a synapomorphy of node 15.

(243). Palpal tibia distal dorsal macrosetae

0: absent.
1: present (MH04: fig. 21D, *Triplogyna major*).

This macroseta is always in line with the dorsomesal and the mesal macrosetae (characters 244 and 245). The only exceptions are *Linyphia triangularis* in which the dorsal and mesal macrosetae are shifted

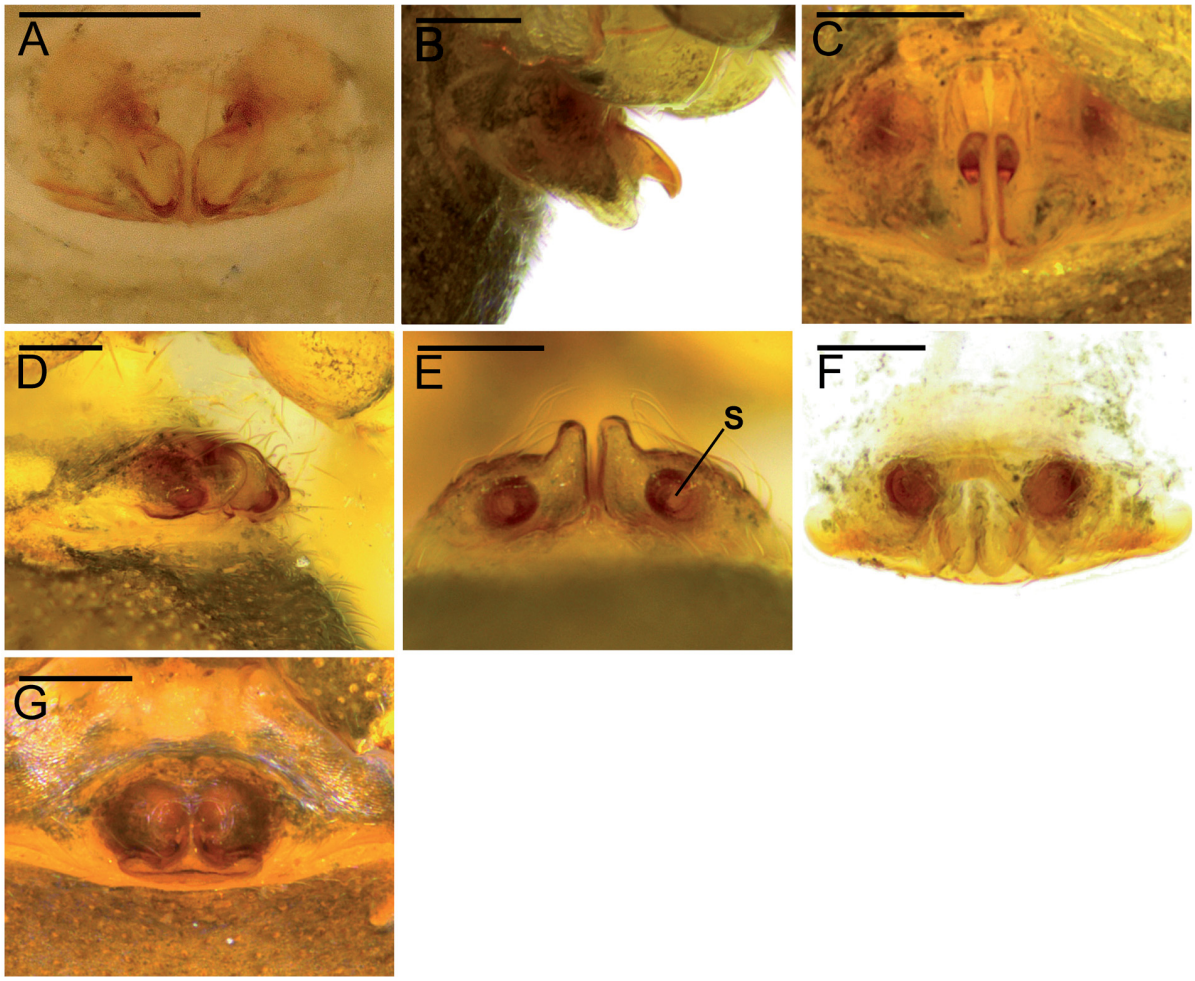

Fig. 22. Female epigynes in ventral (A, C, F–G), lateral (B, D) and posterior (E) views. **A**. *Dactylopisthes locketi* (Tanasevitch, 1983) (36881; SMF). **B–C**. *Diplocephalus mirabilis* (Tanasevitch, 1985) (36881; SMF). **D–E**. *Diplocephalus montanus* Eskov, 1988 (36879; SMF). **F**. *Diplocephalus pavesii* Pesarini, 1996 (2577b; NMB). **G**. *Paraglyphesis polaris* Eskov, 1991 (coll. A.T.). Abbreviations: see Material and methods. Scale bars = 100 µm.

proximally and *Hilaira excisa* in which the mesal macroseta shifted proximally. This macroseta is present in most taxa considered for the *Savignia*-group phylogeny but absent in two nodes (12 and 24) and another four species independently.

(244). Palpal tibia distal dorsomesal macrosetae

0: absent.
1: present (MH04: fig. 21D, *Triplogyna major*).

This macroseta can easily be confused with a seta that is often found at the corresponding position. But the macrosetae are stronger and it emerges nearly in right angle from the tibia, like the dorsal or mesal macrosetae, whereas the setae are in a smaller angle, pointing forward. This macrosetae is an ambiguous synapomorphy of nodes 13 and 64 but also present in five other species of Erigoninae and all Linyphiinae.

(245). Palpal tibia distal mesal macrosetae

0: absent.
1: present (MH04: fig. 21D, *Triplogyna major*).

The lack of this macroseta is an autapomorphy of *Dactylopisthes locketi*.

(246). Palpal tibia proximal dorsal trichobothria

0: zero.
1: one.
2: two.
3: three or more (MH04: fig. 21e, *Triplogyna major*).

At least one trichobothrium is present in all Linyphiidae considered in this analysis. Most species of the *Savignia*-group (node 16) have two dorsal trichobothria while three trichobothria are more common in the outgroup taxa (basal to node 16).

Leg macrosetae (scored on females if available)

247. Femur I prolateral macroseta(ae)

0: absent.
1: present.

MH04-135, A09-111. The loss of the prolateral femoral macrosetae is a synapomorphy that supports the monophyly of Erigoninae (node 3).

248. Tibia I proximal dorsal macroseta

0: absent.
1: present.

MH04-136. The data on tibial macrosetae were collected from female specimens. Sometimes, males reduce these macrosetae to a size that can hardly be distinguished from other leg setae. However, they arise at a nearly right angle from the tibia and can be recognised as vestigial macrosetae at the corresponding positions. The number of macrosetae on the tibia (leg formula of 2211; characters 248–255) supports the *Savignia*-group. It is also 2211 in other linyphiid species (see Roberts 1987: tables a–b). The macrosetae on tibia I and II are sometimes reduced in *Diplocephalus latifrons*.

Contrary to most species of the *Savignia*-group, *Glyphesis nemoralis* lacks proximal macrosetae on all legs but has distal macrosetae instead (spine formula 1111). This is very exceptional, as, e.g., MH04 never found distal macrosetae in the absence of proximal macrosetae. *Savignia birostra* has reduced all distal leg spines. This character is phylogenetically uninformative since it is only absent in *Savignia birostra*.

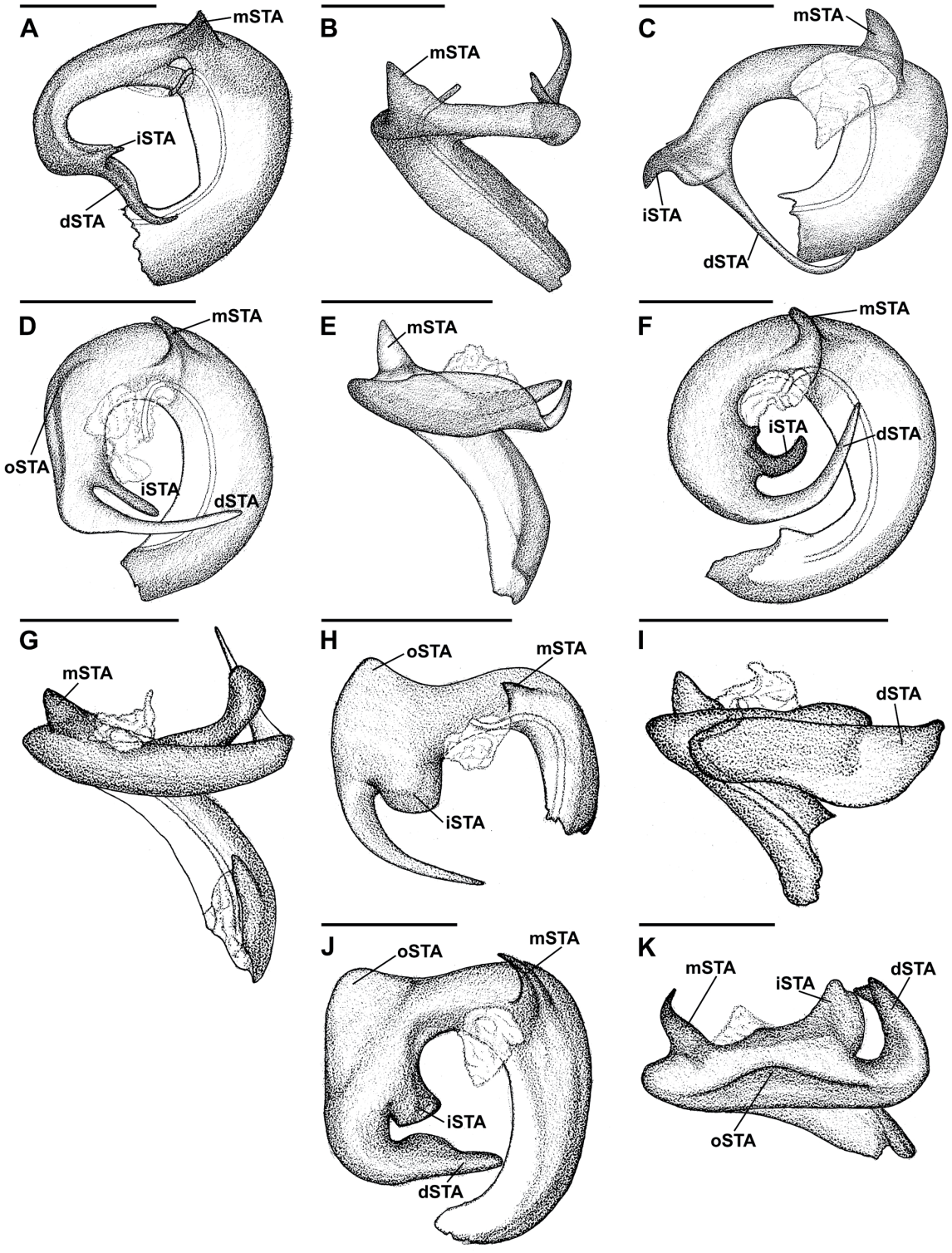

Fig. 23. Different types of suprategular apophyses of male palps in retrolateral (B, E, G, I, K) and distal (A, C–D, F, H, J) views. **A–B**. *Diplocephalus cristatus* (Blackwall, 1833), (Ar138; NMBE). **C**. *Diplocephalus crassilobus* (Simon, 1884) (Ar6668; NMBE). **D–E**. *Erigonella hiemalis* (Blackwall, 1841) (Ar1164; NMBE). **F–G**. *Erigonella subelevata* (L. Koch, 1869) (NMBE). **H–I**. *Erigonella ignobilis* (O. Pickard-Cambridge, 1871) (Ar2881; NMBE). **J–K**. *Diplocephalus latifrons* (O. Pickard-Cambridge, 1863) (Ar6699; NMBE). Abbreviations: see Material and methods. Scale bars = 100 µm.

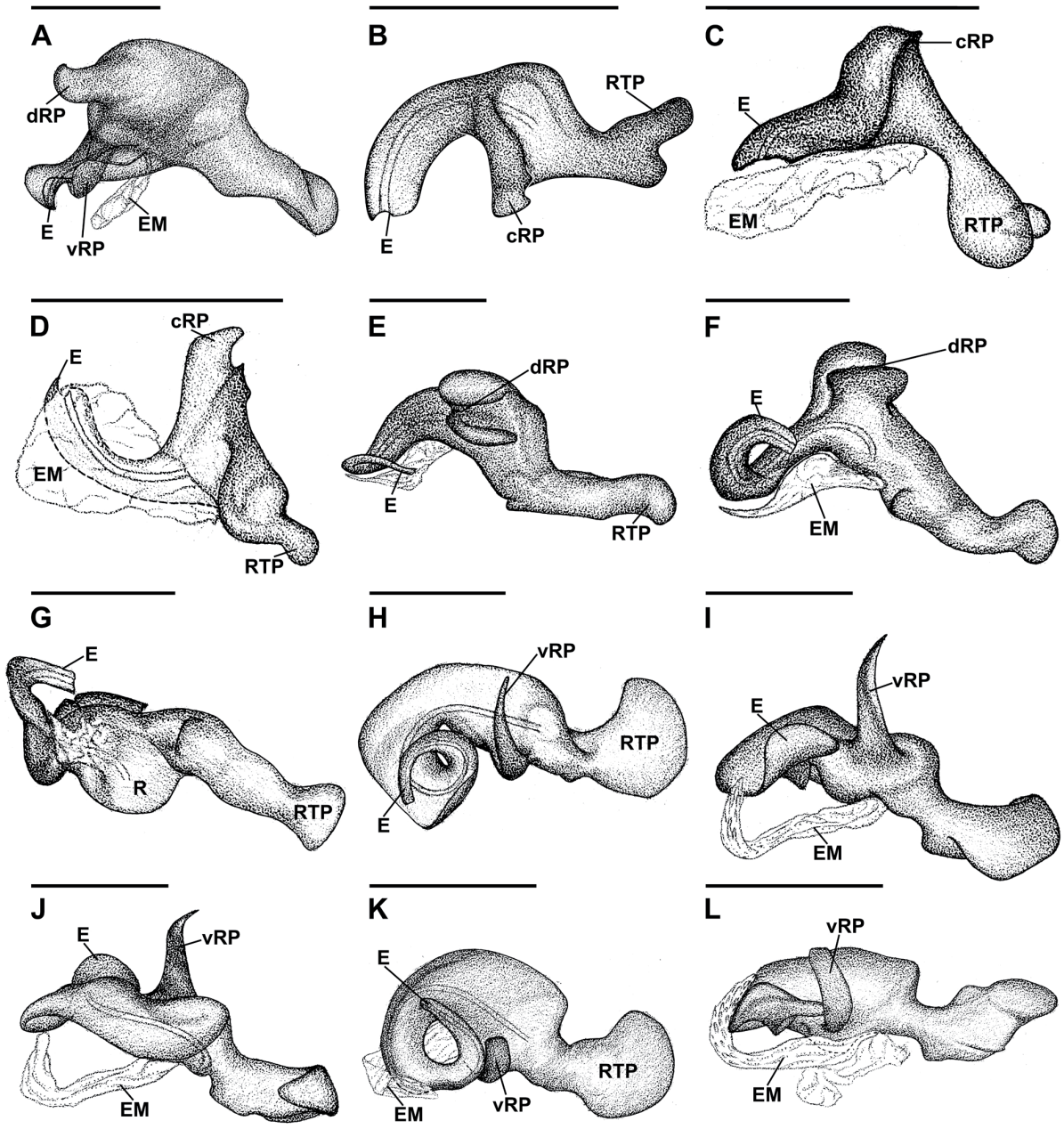

Fig. 24. Different types of embolic divisions of male palps in distal (A–B, E, H, K), ventral (C, F, I, L) and proximal (D, G, J) views. **A**. *Diplocephalus cristatus* (Blackwall, 1833) (Ar138; NMBE). **B–D**. *Erigonella ignobilis* (O. Pickard-Cambridge, 1871) (Ar2881; NMBE). **E–G**. *Diplocephalus latifrons* (O. Pickard-Cambridge, 1863) (Ar6699; NMBE). **H–J**. *Erigonella subelevata* (L. Koch, 1869) (NMBE). **K–L**. *Erigonella hiemalis* (Blackwall, 1841) (Ar1164; NMBE). Abbreviations: see Material and methods. Scale bars = 100 μm.

249. Tibia I distal dorsal macroseta

0: absent.
1: present.

MH04-137, A09-112.

250. Tibia II proximal dorsal macroseta

0: absent.
1: present.

MH04-138. This character is only absent in *Savignia birostra*.

251. Tibia II distal dorsal macroseta

0: absent.
1: present.

MH04-139, A09-113.

252. Tibia III proximal dorsal macroseta

0: absent.
1: present.

MH04-140, A09-114. This character is only absent in *Savignia birostra*.

253. Tibia III distal dorsal macroseta

0: absent.
1: present.

MH04-141, A09-115. This character is a synapomorphy of node 4.

254. Tibia IV proximal dorsal macroseta

0: absent.
1: present.

MH04-142. This character is only absent in *Savignia birostra*.

255. Tibia IV distal dorsal macroseta

0: absent.
1: present.

MH04-143, H00-61-64*, A09-116. This character is a synapomorphy of node 4.

256. Tibia I prolateral macroseta(ae)

0: absent.
1: present.

MH04-144, A09-117. This character is a synapomorphy of node 4.

257. Tibia I retrolateral macroseta(ae)

0: absent.
1: present.

MH04-145, A09-118. This character is a synapomorphy of node 3.

258. Tibia I ventral macroseta(ae)

0: absent.
1: present.

MH04-146, A09-119.

259. Metatarsus I dorsal macroseta(ae)

0: absent.
1: present.

MH04-147, A09-120. This character is a synapomorphy of node 3.

260. Metatarsus I prolateral macroseta(ae)

0: absent.
1: present.

MH04-148, A09-121.

261. Metatarsus I retrolateral macroseta(ae)

0: absent.
1: present.

MH04-149, A09-122.

262. Metatarsus I ventral macroseta(ae)

0: absent.
1: present.

MH04-150, A09-123.

263. Metatarsus IV trichobothrium

0: absent.
1: present.

MH04-152, H00-65, A09-124. The absence of a trichobothrium on metatarsus IV is a describing character of the *Savignia*-group (Millidge 1977) and only secondarily present in node 30 including *Dicymbium nigrum* and *Di. tibiale*.

(264). Metatarsus I trichobothrium position

0: proximal third (*Linyphia triangularis*).
1: central third (*Hilaira excisa*).
2: distal third (*Walckenaeria acuminata*).

In the *Savignia*-group phylogeny, the metatarsus I trichobothrium was in the proximal third in all Linyphiinae and in the central third in most Erigoninae, apart from *Walckenaeria acuminata* and node 14.

Tracheae morphology

265. Median tracheal trunks

0: unbranched (Blest 1976: fig. 1a).
1: branched (Hormiga 1994a: fig. 18a *Gonatium rubens*).

MH04-157, A09-127. The branched median trunks is a synapomorphy that supports the Erigoninae (node 3) in MH04.

266. Median tracheal trunks width

0: about as wide as laterals (Miller 2007: fig. 4c, *Triplogyna major*).
1: much wider than laterals (Hormiga 1994a: fig. 18a, *Gonatium rubens*).

MH04-159, A09-129. The wide median trunks are a synapomorphy that supports Erigoninae (node 3) in MH04.

267. Median tracheal trunk length

0: restricted to abdomen (Blest 1976: fig. 1a).
1: pass through pedicel into prosoma (Blest 1976: fig. 1c).

MH04-160, A09-130. State 1 provides is a synapomorphy that supports the Erigoninae (node 3) in MH04.

Spinneret morphology

268. Aggregate-flagelliform triplet in male PLS

0: absent.
1: present, at least in part (H00: pl. 42d, *Laminacauda plagiata*).

MH04-166, A09-137. The presence of the male triplet is a synapomorphy of erigonines (node 3) in the current analysis.

269. Epiandrous gland spigots

0: absent (MH04: fig. 22f, *Leptorhoptrum robustum*).
1: present (MH04: fig. 22e, *Stemonyphantes blauveltae* Gertsch, 1951).

MH04-169, A09-139. The loss of the epiandrous gland spigots is a synapomorphy that supports the monophyly of Erigoninae (node 3).

Results

Phylogeny

Equal weighting

Independent from the collapsing rule (rules 1 and 3) TNT found the same 192 most parsimonious trees (L = 1025 steps; CI = 0.33; RI = 0.67) (Table 1). All different combinations of number of replications and holds per replication resulted in the same 192 trees but with a varying number of hits (19–60%), except for the r10 h100000 analysis that resulted in 174 most parsimonious trees (Table 1). Zero length branches (Coddington & Scharff 1994) were not observed in any of the 192 topologies with both ACCTRAN and DELTRAN optimisations and they were all fully resolved. 240 characters were phylogenetically informative and 29 were not, from which two are invariant (characters 89 and 128, discussed in the Characters descriptions section) and the rest are autapomorphic. All characters are indicated directly in the Material and methods section in Characters descriptions. After excluding the uninformative characters, the most parsimonious trees were 992 steps long (CI = 0.30; RI = 0.66). The strict consensus tree is 1140 steps long (CI = 0.30; RI = 0.61; excluding uninformative characters: L = 1108; CI = 0.27; RI = 0.60) (Supp. file 2).

Table 1. Summarised results of the equal weighting analysis with different combination of replicates (r) and holds (h) and of the implied weighting analysis using different *k*-values. CI is ensemble consistency index. RI is ensemble retention index.

Analysis	Nº of Trees	Tree Length	CI	RI
Equal weighting (r1000 h1000)	192	1025	0.33	0.67
Equal weighting (r10 h100000)	174	1025	0.33	0.67
Equal weighting consensus	1	1140	0.30	0.61
Implied weighting (*k* = 1)	1	1043	0.33	0.66
Implied weighting (*k* = 2)	1	1047	0.33	0.66
Implied weighting (*k* = 3)	1	1041	0.33	0.66
Implied weighting (*k* = 4)	1	1039	0.33	0.66
Implied weighting (*k* = 5)	1	1038	0.33	0.66
Implied weighting (*k* = 6–7)	1	1035	0.33	0.66
Implied weighting (*k* = 8–10)	1	1034	0.33	0.66
Implied weighting (*k* = 11–14)	1	1032	0.33	0.66
Implied weighting (*k* = 15–22)	1	1029	0.33	0.66
Implied weighting (*k* = 23–26)	1	1026	0.33	0.67
Implied weighting (*k* = 27–50, 100, 250, 500, 1000)	1	1025	0.33	0.67
Implied weighting consensus	1	1266	0.27	0.55

Implied weighting

Implied weighting analysis resulted in one tree for every *k* value, but the tree topology with different *k*-values differed. *k*-values below 10 resulted in trees less congruent with the equal weighted topologies than did the trees with *k*-values over 27, which were the same to the equal weighted trees, as expected since high *k* values approximate equal weight. The analysis with the heaviest down weighting of homoplastic characters, i.e., with a *k*-value of one, shared the least number of nodes with the preferred implied weighted analysis based on a *k*-value of 23 (40 nodes out of 69). Tree statistics with the different *k* values and the strict consensus tree (Supp. file 3) are shown in Table 1.

Differences between weighting schemes

The preferred implied tree (*k* = 23) (Figs 25–26) and the strict consensus equal weighted tree shared 42 out of 69 nodes. Common to all analyses are a low support for the backbone nodes of the tree, i.e., the interrelationships of the larger groups of species are ambiguous. However, there are several well supported groups common to all analyses (Jackknife and Bremer support) (Fig. 26): *Diplocephalus* (node 53)(69-4), *Hemistajus* (node 43)(85-4), *Dicymbium* (node 29)(99-8) and *Glyphesis* (node 22)(98-6).

Maximum likelihood

The maximum likelihood tree (ML) (Fig. 27) showed high support values (SH-aLRT and bootstrap) of *Savignia* (node 45)(97.8-100), *Araeoncus* (node 59)(95.1-73), *Diplocephalus* (node 53)(90.8-95), *Hemistajus* (node 43)(91.6-99), *Erigonella* (node 33)(96.5-97), *Dicymbium* (node 29)(99.9-100) and *Glyphesis* (node 22)(99.1-100) (node numbers correspond to clades on Fig. 25). This result is in congruence with the trees from the MP analyses (both the equal and implied weights trees), showing

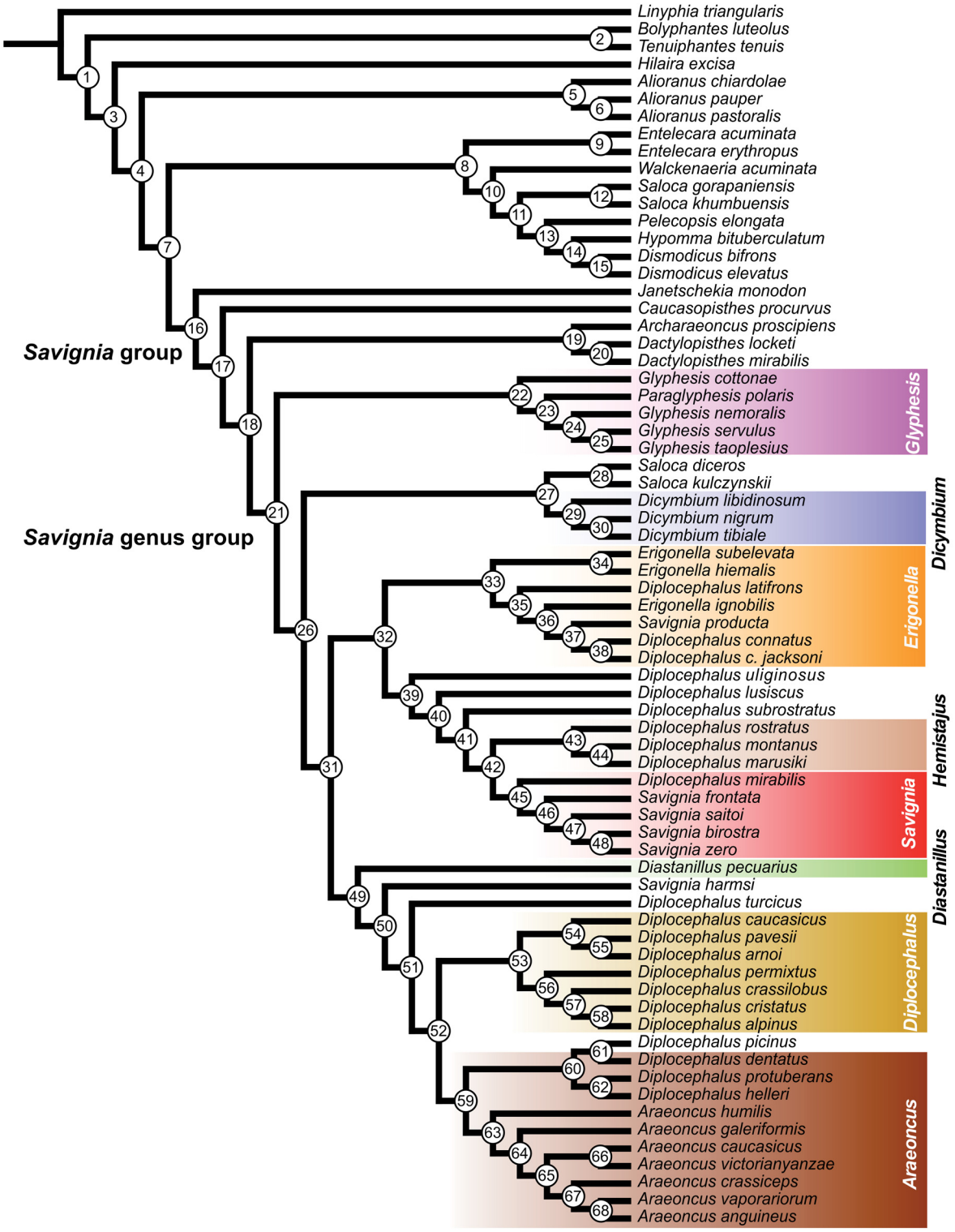

Fig. 25. Preferred tree, based on the implied weights analysis using a *k*-value of 23. It shows node numbers. Nomenclature corresponds to the genus assignments used until now. The different colours mark the new genus delimitations.

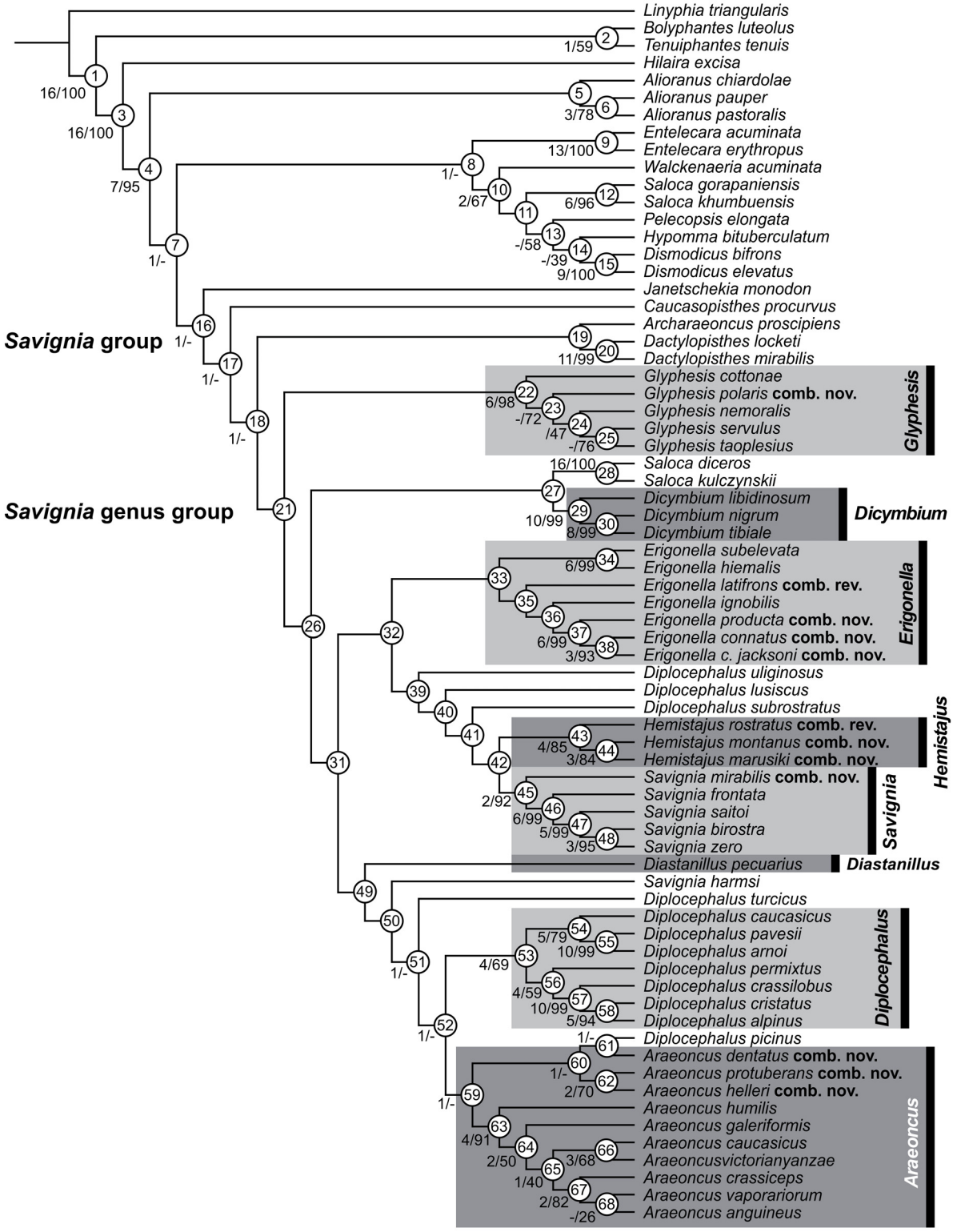

Fig. 26. Preferred tree as seen in Figure 25, showing nomenclatural changes resulting from the systematic revision (Table 9). Genera that are considered to belong to the *Savignia* genus group according to the current analysis are marked in grey and with bars. The marked groups define the new genus delimitations following the nomenclature established in the current analysis. It shows node numbers, Bremer and Jackknife support values respectively on the nodes.

Diplocephalus as a paraphyletic group mixed with species of *Erigonella* and *Savignia*. While *Araeoncus* and *Dicymbium* appear as monophyletic and well supported (bootstrap > 90).

Wild card taxa

The comparison of the different analyses revealed a few wild card taxa, i.e., taxa with ambiguous group assignments. These taxa mainly emerged from deep nodes of well-supported groups and tended to move in and out of these groups. Within the *Savignia* genus group such a taxon is *Diplocephalus picinus*, a species that emerged in node 61 as sister to *Araeoncus* in all analyses except with implied weighting and $k = 1–22$ where it appeared as sister species to *Dicymbium*. *Diplocephalus picinus* has a relatively simple male copulatory organ. This species is probably not the true sister of *Araeoncus* since mainly homoplastic characters support the relationships of *Diplocephalus picinus* with other species of *Araeoncus* (white squares in Figs 28–31).

The position and relations of the *Savignia*-group genera belonging to other subgroups could not be unambiguously solved. *Janetschekia*, *Caucasopisthes*, *Archaraeoncus* and *Dactylopisthes* emerge as

Fig. 27. Maximum likelihood tree with SH-aLRT and ultrafast bootstrap values respectively on the nodes. Genera assigned to the *Savignia*-group by Millidge (1977) are marked with colours and bars. The black bars indicate taxa from genera assigned to the *Savignia* genus group and those with grey bars to the other subgroups of the *Savignia*-group. The nomenclature corresponds to the genus assignments used until now. The different colours mark the new genus delimitations.

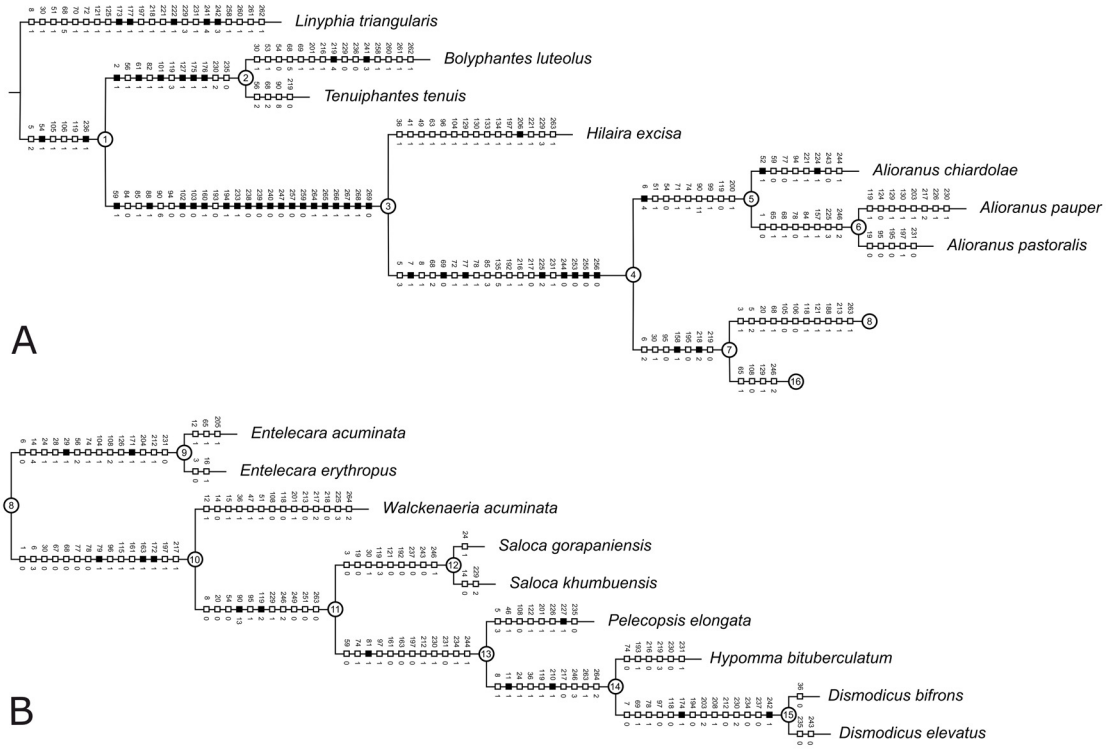

Fig. 28. Excerpt of the preferred tree, showing AccTran optimisation for nodes 1–7 (**A**) and 8–15 (**B**). Black squares account for unambiguous character changes (synapomorphies) and white squares for homoplastic character changes. Above the squares are the character numbers and below the state numbers. Node numbers are given in circles. The nomenclature corresponds to the genus assignments used until now.

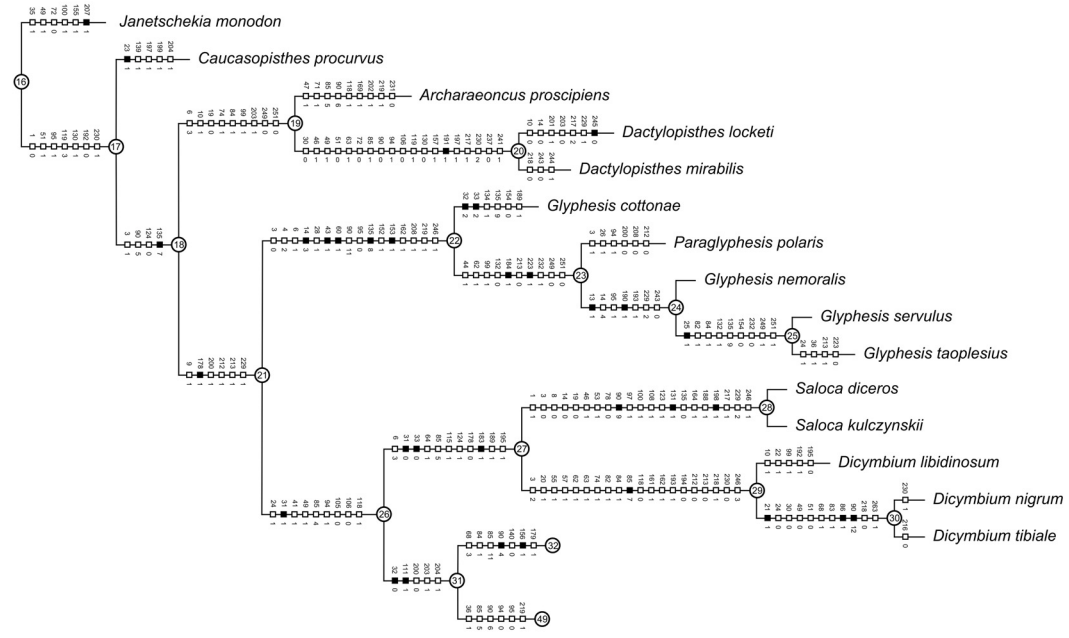

Fig. 29. Continuation of Figure 28 showing nodes 16 to 31. Showing *Dicymbium* Menge, 1868 (node 29) and the redefined genus *Glyphesis* Simon, 1926 (node 22).

close relatives in all analyses but with different relationships. They appear as sister to the *Savignia* genus group (Fig. 25) and closely related with some other taxa with relatively simple male copulatory organs like *Saloca*, *Alioranus* and *Glyphesis*.

Preferred tree

The preferred tree was selected based on the three analyses and is the output from the implied weight analysis with a *k* value of 23 (Figs 25–26). This tree was in congruence with the maximum likelihood tree (Fig. 27) and the strict consensus equal weighted tree (Supp. file 2) as it shared the same well supported

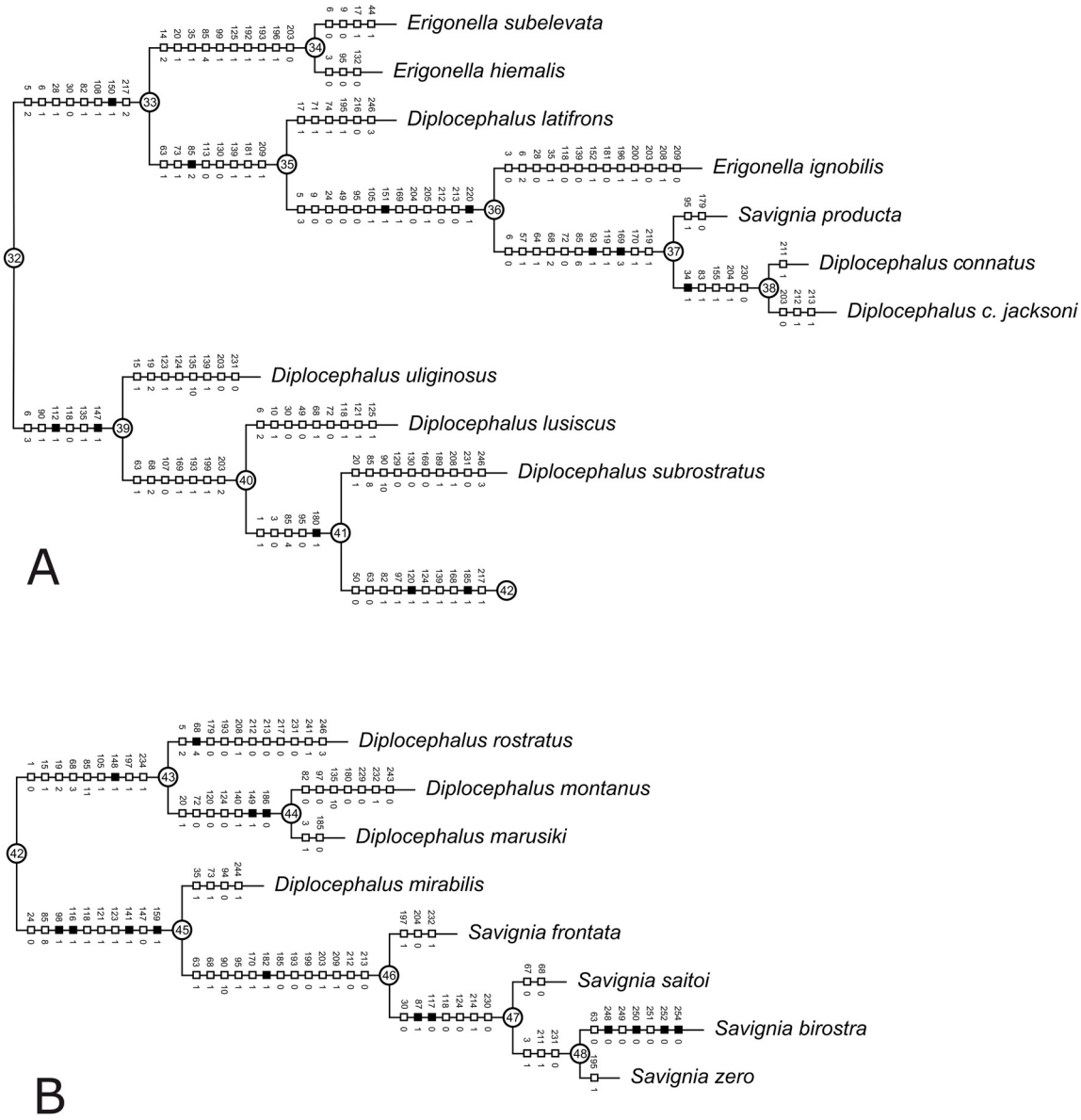

Fig. 30. Continuation of Figure 29 showing nodes 32 to 48. Showing the redefined genus *Erigonella* Dahl, 1901 (30A, node 33), *Hemistajus* Schenkel, 1934 **resurrected rank** (30B, node 43) and *Savignia* Blackwall, 1833 (30B, node 45).

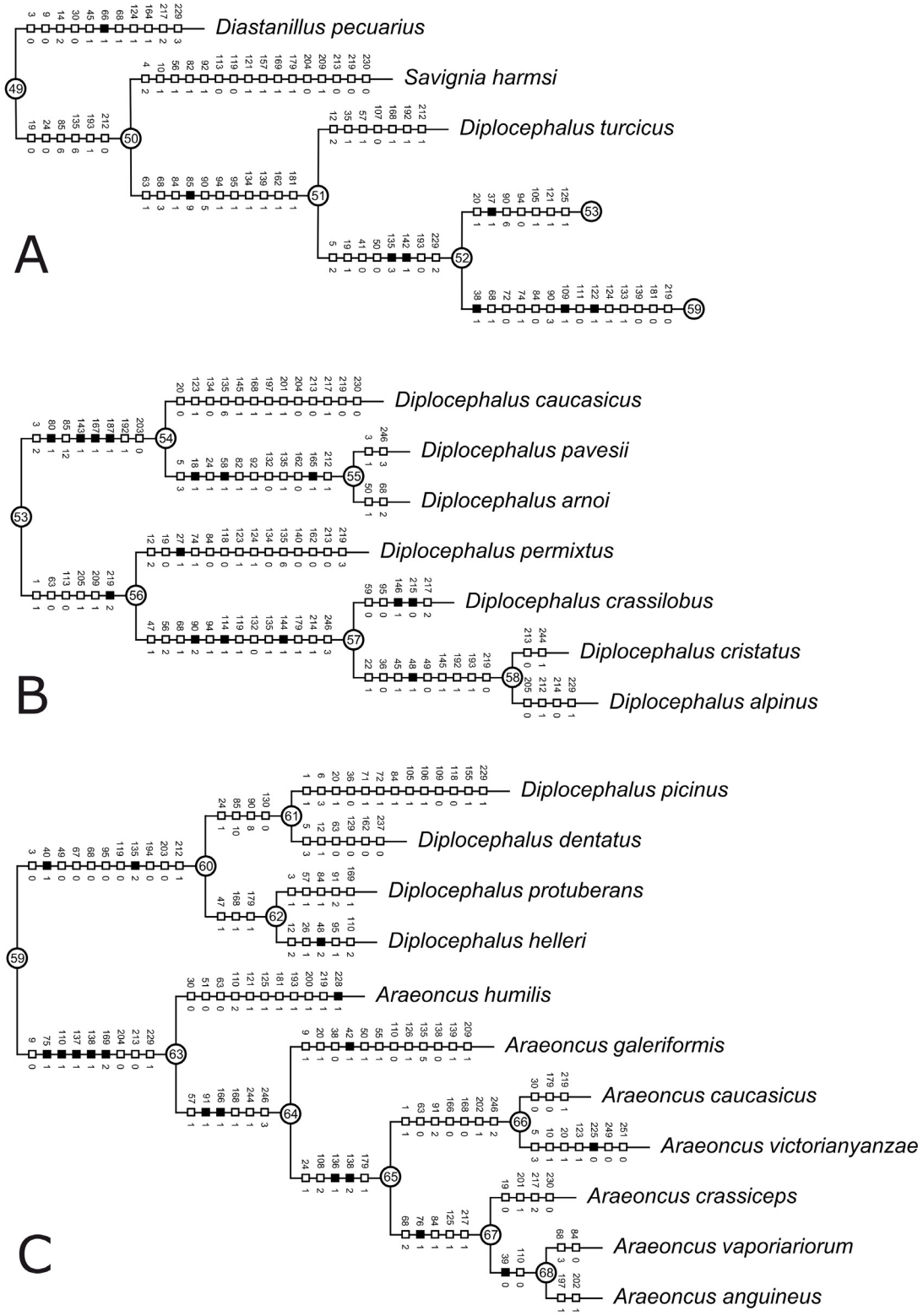

Fig. 31. Continuation of Figure 30 showing nodes 49 to 68. Showing the position of *Diastanillus* Simon, 1926 (31A, node 49) and the redefined genus *Diplocephalus* Bertkau, 1883 (31B, node 53) and *Araeoncus* Simon, 1884 (31C, node 59, omitting *D. picinus*).

groups found in the three analyses (nodes 43, 45, 53, 59) and it kept the relationships among *Araeoncus* and *Diplocephalus*, from the equal weights tree and *Erigonella* and *Savignia* from the ML tree.

Character transformations are mapped on the preferred tree (Figs 28–31). The characters supporting the different genera in the *Savignia* genus group are discussed in the Systematics section. In the preferred tree only *Araeoncus* and *Dicymbium* appeared as monophyletic while all other genera within the *Savignia* genus group were paraphyletic. Species of *Diplocephalus* appear at different points throughout clades within node 31.

Bremer support values are plotted on the preferred tree (Fig. 26). The average Bremer support of this analysis is 6.42. The average is likely to be influenced by some outliers of very well supported clades, like clades within nodes1 and 3 with a Bremer support of 16. The median is not influenced by these outliers and equals 5. The lower support values are found along the backbone of the *Savignia*-group (node 16) and account for the relations inside this group (Fig. 26). Jackknife support values are congruent with Bremer support with higher values (>90) at nodes: 22 (*Glyphesis*), 29 (*Dicymbium*), 45 (*Savignia*) and 63 (*Araeoncus*).

Generally, the relationships within groups with high Bremer supports are also supported by at least one non-homoplastic character (e.g., see node 53, Fig. 31B, *Diplocephalus*). However, the nodes uniting these groups with higher support, are only supported by homoplastic characters (see nodes 16, 17, 49, 50; Figs 28–31) with only two exceptions (nodes 21, 26 and 59; Figs 28–31).

Systematics

In this section we redefine the genera of the *Savignia* genus group based on synapomorphies and monophyletic groups from the phylogenetic analysis. We restrict the scope of this section to the largest subgroup of the *Savignia*-group including most genera that were considered as having more derived characters by Millidge (1977). Three of these genera, i.e., *Araeoncus*, *Diplocephalus* and *Savignia*, include over 75% of all *Savignia* genus group species and are responsible for the major systematic problems in this lineage. We primarily focus on taxa that we have examined and included in our phylogenetic analyses. Based on literature (Tables 2–8) we also discuss the generic assignments of the taxa belonging to the *Savignia*-group that were not included in the current analysis. If it was possible to unambiguously identify putative synapomorphies for some of these species based on the information in the literature, we also suggest nomenclatural changes as necessary. All node numbers mentioned in the Systematics section correspond to Figure 25.

Class Arachnida Cuvier, 1812
Order Araneae Clerck, 1757
Family Linyphiidae Blackwall, 1859
Subfamily Erigoninae Emerton, 1882

Genus ***Araeoncus*** Simon, 1884
Figs 1B, 2A, 4B, 5B, 7A, 9B, 10C–D, 12C–D, 14B, 15E, 16A–F, 18C–E, 19E–F, 20B, D, F, 21A, C; Table 2

Type species

Araeoncus humilis (Blackwall, 1841).

Diagnosis

In males, the presence of a spoon-like retrolateral distal lobe on the palpal tibia (character 38, Fig. 1B) in several species within node 63 (*A. anguineus*, *A. caucasicus*, *A. crassiceps*, *A. humilis*) and an

autapomorphic cone-like lobe lobe in *A. galeriformis* (character 42; Fig. 20D) as well as the long, robust and widely curved embolus (character 109) are two reliable characters to identify species of *Araeoncus*. Additionally, the massive kinked ventral radical process (character 135; Fig. 16D) with a feather-like shape and the cephalic region raised forwardly in many cases covered with setae in the front allow to separate *Araeoncus* from similar genera. Females can be distinguished from similar taxa such as *Diplocephalus* by the more elongated spermathecae with longer copulatory ducts. In *Diplocephalus* spermathecae have a more rounded shape and shorter copulatory ducts.

Synapomorphies

Four former species of *Diplocephalus*, i.e., *Araeoncus dentatus* (Tullgren, 1995) comb. nov., *Araeoncus helleri* (L. Koch, 1869) comb. nov., *Araeoncus marijae* (Bosmans, 2010) comb. nov. and *Araeoncus protuberans* (O. Pickard-Cambridge, 1875) comb. nov. show simple conformation of the male palp that characterise *Araeoncus* (with the long and curved embolus). They belong to *Araeoncus* (node 59; Bremer support of 1 (MP analysis; Fig. 26) and bootstrap of 73 (ML analysis; Fig. 27)) which is hereby defined based on the following putative synapomorphies (Fig. 31): the presence of a retrolateral distal lobe on the palpal tibia (character 38, state 1; Fig. 1B), which is broader than long in *A. dentatus*, *A. helleri* and *A. protuberans* (node 60; character 40, state 1; Fig. 19F) and longer than broad in the remaining species (*Araeoncus*, node 63; character 40, state 0; Fig. 1B). The presence of a long, robust, and widely curved embolus (character 109, state 1; Fig. 16C, *A. dentatus*) and the restricted embolus velum (character 122, state 1; Fig. 2A), although this is an autapomorphy of *A. humilis.*

Additionally, some homoplastic characters support *Araeoncus* (Fig. 31): among those are the lack of a protegulum (character 72) which is replaced by a tegular sac (character 75; Fig. 5B, *A. humilis* in clade 63; Fig. 31C) and the ventral radical process that is much larger than the radix (character 133; Fig. 16D, *A. crassiceps*), also present in *Hilaira excisa* (see discussion of character 133 for more details).

Remarks

Simon (1884) based his description of *Araeoncus* mainly on characters concerning the eye pattern and the legs. However, he also pointed out that all considered species have a specific forward-facing cephalic lobe of variable length, lacking lateral incisions. Additionally, the tibia is split into two apophyses of which the median one (the retrolateral distal lobe, character 38) is enlarged. Most authors after Simon have added taxa to this genus based on the specific forward-facing cephalic lobe, covered with setae frontally and the two tibial apophyses (the prolateral tibial apophysis and the retrolateral distal lobe). This is the only genus out of the three most species rich genera within the *Savignia*-group that was recovered as monophyletic in all analyses independent of taxon sampling or characters used (e.g., Figs 25, 27, Supp. file 2, Supp. file 3). Three species formerly belonging to *Diplocephalus* are recovered as a clade sister to *Araeoncus* (Figs 25, 27). Since these species share many characters with *Araeoncus*, we hereby transfer them to *Araeoncus* and redefine the genus (see Table 2).

***Araeoncus* species groups**

***victorianyanzae*-group**

A well-supported group of mainly African taxa with a massively enlarged, kinked ventral radical process (character 135, state 3) that exceeds the tip of the cymbium (e.g., Holm 1962: fig. 25a–b; Tanasevitch 1987: figs 63–64). Their prolateral tibial apophysis and retrolateral distal lobe (characters 7, 38) are indistinct and equally sized and arise from a longitudinally elongated male tibia (e.g., Tanasevitch 1987: figs 61, 63). They all have relatively simple cephalic lobes bearing all eyes on a forward to upwards facing lobe (e.g., Tanasevitch 1987: fig. 59) except for *A. subniger* Holm, 1962 with an AME and a PME lobe (Jocqué 1985: fig. 1).

Table 2 (continued on next page). This list contains all species that belonged to *Araeoncus* Simon, 1884, including those that are newly assigned to *Araeoncus* marked as comb. nov. Species that were scored for the cladistic analyses are marked with an asterisk (and the citation refers to figures illustrating the diagnostic characters). The remaining species are assigned to *Araeoncus* based on the figures cited showing the long, robust and widely curved embolus, the retrolateral distal lobe and the typical cephalic lobe. The different species groups are indicated in brackets, *victorianyanzae*-group (V), *dentatus*-group (D), *galeriformis*-group (G), *humilis*-group (H) and *anguineus*-group (A) with two subgroups a and b. "" = ambiguous species group assignments; ??? = of uncertain assignment and probably misplaced within *Araeoncus*.

Status	Species name	Scored according to
Araeoncus (Aa)	*A. altissimus* Simon, 1884	Bosmans 1996: figs 75–78
Araeoncus (Aa)*	*A. anguineus* (L. Koch, 1869)	Wiehle 1960: figs 440, 444–445
Araeoncus (V)	*A. banias* Tanasevitch, 2013	Tanasevitch 2013: figs 1–7
Araeoncus (V)*	*A. caucasicus* Tanasevitch, 1987	Tanasevitch 1987: figs 59, 61, 63
Araeoncus (Aa)	*A. clavatus* Tanasevitch, 1987	Tanasevitch 1987: figs 65, 67, 68
Araeoncus (Ab)	*A. clivifrons* Deltshev, 1987	Deltshev 1987: figs 2–4
Araeoncus (H)	*A. convexus* Tullgren, 1955	Tullgren 1955: fig. 25a–b
Araeoncus (Ab)*	*A. crassiceps* (Westring, 1861)	Hormiga 2000: figs 1a–d, 32b
Araeoncus ("A")	*A. curvatus* Tullgren, 1955	Tullgren 1955: fig. 23a–b
"*Araeoncus*"	*A. cypriacus* Tanasevitch, 2011	Tanasevitch 2011: figs 1–5
Araeoncus (D)*	*A. dentatus* (Tullgren, 1955) comb. nov.	Millidge 1977: fig. 129
Araeoncus (Ab)	*A. discedens* (Simon, 1881)	Bosmans 1996: figs 83–86
Araeoncus ("A")	*A. dispar* Tullgren, 1955	Tullgren 1955: fig. 26a–b
Araeoncus (V)	*A. etinde* Bosmans & Jocqué, 1983	Bosmans & Jocqué 1983: fig. 1a, c
Araeoncus (V)	*A. femineus* (Roewer, 1942)	Bosmans & Jocqué 1983: 584, 586
Araeoncus (G)*	*A. galeriformis* (Tanasevitch, 1987)	Tanasevitch 1987: figs 123, 126
Araeoncus (H)	*A. hanno* Simon, 1884	Bosmans 1996: figs 11–14
Araeoncus (D)*	*A. helleri* (L. Koch, 1869) comb. nov.	Millidge 1977: fig. 131
Araeoncus (H)*	*A. humilis* (Blackwall, 1841)	Bosmans 1996: figs 2, 5–6
Araeoncus ("D")	*A. hyalinus* Song & Li, 2010	Song & Li 2010: figs 1a–e, 2a–g, 3a–e
Araeoncus (V)	*A. impolitus* Holm, 1962	Holm 1962: figs 26c, 27c
Araeoncus ("D")	*A. longispineus* Song & Li, 2010	Song & Li 2010: figs 4a–d, 5a–h
Araeoncus ("H")	*A. longiusculus* (O. Pickard–Cambridge, 1875)	Simon 1884: figs 458–459; Simon 1926: fig. 647; Pantini & Sassu 2009: figs 1–4
Araeoncus (V)	*A. malawiensis* Jocqué, 1981	Jocqué 1981: figs 21–23
Araeoncus ("D")	*A. marijae* (Bosmans, 2010) comb. nov.	Bosmans *et al.* 2010: figs 23–29
Araeoncus (H)	*A. martinae* Bosmans, 1996	Bosmans 1996: figs 19, 21–23
Araeoncus (G)	*A. mitriformis* Tanasevitch, 2008	Tanasevitch 2008: figs 1–4; Tanasevitch 2009: 384, figs 7–11
Araeoncus (V)	*A. obtusus* Bosmans & Jocqué, 1983	Bosmans & Jocqué, 1983: fig. 2a–b
Araeoncus (V)	*A. picturatus* Holm, 1962	Holm 1962: figs 26b, 27b
Araeoncus (D)*	*A. protuberans* (O. Pickard-Cambridge, 1875) comb. nov.	Thaler 1978: figs 12–14
"*Araeoncus*"	*A. rhodes* Tanasevitch, 2011	Tanasevitch 2011: figs 6–12, 20
Araeoncus (V)	*A. subniger* Holm, 1962	Holm 1962: figs 26d, 27d

Table 2 (continued).

Status	Species name	Scored according to
Araeoncus (A)	*A. tauricus* Gnelitsa, 2004	Gnelitsa 2004: figs 1–4, 8
Araeoncus (Aa)	*A. toubkal* Bosmans, 1996	Bosmans 1996: figs 28–31
Araeoncus (Ab)*	*A. vaporariorum* (O. Pickard–Cambridge, 1875)	Pesarini 1996: figs 5–6
Araeoncus (V)*	*A. victorianyanzae* Berland, 1936	Holm 1962: fig. 25a–c
Araeoncus (V)	*A. viphyensis* Jocqué, 1981	Jocqué 1981: figs 24–26
Araeoncus ("V")	*A. vorkutensis* Tanasevitch, 1984	Tanasevitch 1984: figs 4.1, 4.3–6
Misplaced *Araeoncus* species		
Not *Araeoncus*	*A. gertschi* Caporiacco, 1949	Holm 1962; Scharff 1990
Not *Araeoncus*	*A. macrophthalmus* Miller, 1970	Miller 1970: figs 1–6
???	*A. sicanus* Brignoli, 1979	Brignoli 1979: fig. 9
???	*A. tuberculatus* Tullgren, 1955	Tullgren 1955: fig. 27a–b

The ventral plates of the females have two nearly parallel inner margins that form a right angle at the posterior edge. Their spermathecae are round to oval and are very close to each other right below the median margin of the ventral plates. The copulatory ducts enter the spermathecae at the lateral (ectal) side and are often also directed towards the lateral side of the vulva (e.g., Holm 1962: fig. 27a).

This group includes two species from Asia (*A. caucasicus* and *A. banias* Tanasevitch, 2013) and eight from Africa (*A. etinde* Bosmans & Jocqué, 1983, *A. obtusus* Bosmans & Jocqué, 1983, *A. subniger* and *A. victorianyanzae*) of which four are only known from females (*A. impolitus* Holm, 1962, *A. malawiensis* Jocqué, 1981, *A. picturatus* Holm, 1962 and *A. viphyensis* Jocqué, 1981). *Araeoncus femineus* (Roewer, 1942) from Equatorial Guinea is also known by females only and resembles females of *A. victorianyanzae* with respect to their body and eye size according to Bosmans & Jocqué (1983). The close relation of the African species was already noted by Holm (1962), who presumed a recent common ancestor for *A. victorianyanzae*, *A. picturatus*, *A. impolitus* and *A. subniger* due to their similarity.

Holm (1962) also mentioned the close relation of *A. victorianyanzae* (as *A. praeceps* Holm, 1962) to *A. crassiceps* and *A. anguineus* based on the palpal conformation and the cephalic lobe, respectively. In our analysis the representatives of this group (*A. caucasicus* and *A. victorianyanzae*) are sister taxa of node 67, which also includes *A. crassiceps* and *A. anguineus*.

Potentially *A. vorkutensis* Tanasevitch, 1984 belongs to this clade but see discussion of species of *Areaoncus* with uncertain assignment.

***dentatus*-group**

So far this clade includes four species formerly assigned to *Diplocephalus*, i.e., *A. dentatus* comb. nov., *A. helleri* comb. nov., *A. marijae* comb. nov. and *A. protuberans* comb. nov. Together they form node 60, including *D. picinus* which also has a simple palp and appeared in different positions on the different analyses (see Wild card taxa).

This group includes taxa that presumably have ancestral character states to species of *Araeoncus* within node 63. They have relatively simple male genital characters, i.e., their retrolateral distal lobe on the male palpal tibia is broader than long (character 40, synapomorphy of node 60, the *dentatus*-group). It seems to be not much more than a broadened margin but in ventral view the spoon-like form is well visible (Fig. 19E). The radical appendices are also relatively simple: they either lack a ventral radical process (character 130; Fig. 16C, *A. dentatus* comb. nov.) or have a ventral radical process shaped like

a ridged sail (character 135, state 2; Fig. 16B, *A. protuberans* comb. nov.; synapomorphy of node 60). This sail is presumably an ancestral version of the massive, kinked ventral radical process (character 135, state 3) found in the *Araeoncus* clade corresponding to node 63, the sister-clade of the *dentatus*-group. Additionally, they have a PME lobe (character 204) which is absent in the *Araeoncus* clade of node 63.

Araeoncus marijae comb. nov. is similar to *A. dentatus* comb. nov. based on the elongated curved embolus and the darker areas at the corners of the ventral plates of the epigyne. In addition, based on the shape of the palpal tibia with a retrolateral lobe and the elongated spermatechae it seems to belong to *Araeoncus*, and therein to the *dentatus*-group.

Potentially, also *A. hyalinus* Song & Li, 2010 and *A. longispineus* Song & Li, 2010 described from China belong into this group. Besides the long, robust embolus diagnostic for *Araeoncus*, they show a similarity in the shape of the ventral radical process with *A. protuberans* comb. nov. Also, they have a PME lobe typical for this group.

***galeriformis*-group**

This group includes two species, one exclusively known from the type locality in Iran, *A. mitriformis* (Tanasevitch 2008) and one from the Caucasian mountains, *A. galeriformis*. They are very distinct from members of the other groups: they lack a retrolateral distal lobe (character 38) but instead have a dorsal cone-like lobe (character 42; Fig. 20D); they lack the specific massive, kinked ventral radical process (character 135) but instead have a laterally flattened ventral radical process with a dorsal facing sclerotised tip (character 135, state 5; Fig. 16F) and additionally a laterally flattened sail-like dorsal radical process (Fig. 16F); their cephalic lobe is also extraordinary with respect to the other species of *Araeoncus* of node 63: it is more pointed and either bears no eyes on top of it in *A. mitriformis* (Tanasevitch 2008: figs 1–2), or only the AME, in *A. galeriformis* (Tanasevitch 1987: fig. 123). Tanasevitch (1987) mentioned similarities in the form of the epigyne of *A. galeriformis* with *A. altissimus* Simon, 1884, *A. crassiceps* and *A. vorkurtensis*.

***humilis*-group**

Currently, *Araeoncus humilis*, *A. convexus* Tullgren, 1955, *A. longiusculus* (O. Pickard-Cambridge, 1875) and two species from northern Africa (*A. hanno* and *A. martinae*) are assigned to this group. Bosmans (1996) already mentioned the close resemblance of three of these species (*A. humilis*, *A. hanno* and *A. martinae*). This group is defined based on the form of the embolus, which is narrowly curved at its tip (character 125; Fig. 9B, but present in many other taxa) but additionally bears a velum restricted to the narrowly curved section of the embolus (character 122; Figs 2A, 9B, *Araeoncus humilis*). The retrolateral side of the tibia, right below the retrolateral distal lobe (character 38) bears several edges in *A. humilis* (Bosmans 1996: fig. 5) and even a distinct sclerotised appendix in *A. hanno* and *A. martinae* (e.g., Bosmans 1996: figs 21–22). *Araeoncus humilis* and *A. martinae* present special hooked setae found dorsally on tibia I and ventrally on tibia II (character 228). *Araeoncus longiusculus* is presumably similar to *A. humilis* (see Simon 1884: fig. 458) based on the setose cephalic lobe, the shape of the spiral embolus and the setose lobe-like tibial apophysis (see Simon 1884: fig. 459; Pantini & Sassu 2009: figs 1–2) that might be a retrolateral distal lobe (character 38).

The females of this group have largely elongated spermathecae forming an outward-facing curve starting at the posterior side of the vulva and a kind of spiral at the anterior end (Wiehle 1960: fig. 424). These elongated spermathecae are also found in *A. convexus* (Tullgren 1955: fig. 25b), a species that is most probably conspecific with *A. humilis*. The latter is known to have spermathecae variable in size (e.g., Deltshev 1987: figs 12–13) and a variable epigyne shape (e.g., Roberts 1987). However, according to Tullgren (1955) *A. convexus* differs in many aspects from *A. humilis*. A comparison of type material is wished for to synonymise *A. convexus* with *A. humilis*.

***anguineus*-group**

This group includes nine species with an elongated tegular sac (character 76; Fig. 20F). This character is a synapomorphy of node 67, including all three species that were scored from the *anguineus*-group. Additionally, they have a specific narrowly curved embolic tip (Fig. 16A). The spermathecae are rounded at the posterior end and curved outwards at the anterior ends (one exception is *A. altissimus*; Bosmans 1996: fig. 81). Two subgroups can be recognised: the first one (a) includes *A. altissimus*, *A. anguineus*, *A. clavatus* Tanasevitch, 1987 and *A. toubkal* Bosmans, 1996. The males have a distinctly forward facing cephalic lobe (Wiehle 1960: fig. 440) and the posterior margin of the epigyne exceeds the epigastric furrow (Wiehle 1960: fig. 442). The second group (b) includes *A. clivifrons* Deltshev, 1987, *A. crassiceps*, *A. discedens* (Simon, 1881) and *A. vaporariorum*. These species have less distinct male cephalic lobes, usually arising diagonally and the posterior margin of the epigyne does not protrude over the epigastric furrow (Wiehle 1960: figs 435–436, respectively). Deltshev (1987) mentioned that the cephalothorax of *A. clivifrons* is close to *A. discedens* and the palpal tibia and embolus to *A. altissimus* and *A. anguineus*.

Araeoncus tauricus Gnelitsa, 2004 is somewhat intermediate, having a distinct forward facing cephalic lobe and an epigyne with a posterior margin not protruding over the epigastric furrow (Gnelitsa 2004: figs 5–8, respectively).

The current phylogenetic analysis supports the *anguineus*-group while the relationships within this group are not clear.

***Araeoncus* with uncertain species group assignments**

Based on the available figures it is not possible to place *A. vorkutensis* with confidence, but it seems close to *A. anguineus* or *A. victorianyanzae*. The form of the tibial appendices (Tanasevitch 1984: fig. 5) and the female genitalia argue for the *victorianyanzae*-group (Tanasevitch 1984: figs 7–8).

Tullgren (1955) described four species, from Sweden and/or Estonia according to females only (*A. convexus*, *A. curvatus* Tullgren, 1955, *A. dispar* Tullgren, 1955 and *A. tuberculatus* Tullgren, 1955). Kronestedt (2001) mentions in the list of Swedish spiders that Tullgren (1955) described a couple of species that have later been considered junior synonyms and does not list these four species of *Araeoncus* as present in Sweden. Checking this material is out of the scope of this work. Out of these four species *A. curvatus* and *A. dispar* most probably belong to the *anguineus*-group (node 67) based on the globular posterior part and the curved anterior part of the spermathecae. *Araeoncus convexus* is closely related to *A. humilis* and *A. tuberculatus* is uncertain concerning its assignment (see next section).

Tanasevitch (2011) described two species from the Mediterranean, *A. cypriacus* Tanasevitch, 2011 and *A. rhodes* Tanasevitch, 2011, characterised by the shape of two anterior radical processes and the embolic division. *Araeoncus rhodes* males present a peculiar shorter and thicker embolus and in the females, oblong spermathecae are well visible. Based on the cephalic shape they seem close to *A. crassiceps*.

Misplaced species of *Araeoncus*

Araeoncus tuberculatus could not be assigned to any of the newly defined groups and may not be an *Araeoncus* at all due to the very simple globular spermathecae that are not found in other species of *Araeoncus* apart from *A. vorkutensis* (Tanasevitch 1984: figs 7–8).

Araeoncus sicanus Brignoli, 1979 is close to *Araeoncus humilis* and to *Erigonella ignobilis* concerning the vulva (Brignoli 1979). Brignoli (1979) assigned it to *Araeoncus* based on the determination keys in Locket & Millidge (1953) and Wiehle (1960). Since this simple type of globular spermathecae are found also outside *Araeoncus*, it might belong to another genus within the *Savignia*-group as well.

Araeoncus macrophthalmus Miller, 1970 does not belong to *Araeoncus* due to the lack of a retrolateral distal tibial lobe and the lack of a massive, kinked ventral radical process (Miller 1970: figs 1–6). *Araeoncus gertschi* Caporiacco, 1949 is known from females only and is misplaced in this genus (Holm 1962; Scharff 1990) since its epigyne has no median fissure (Holm 1962).

Genus ***Dicymbium*** Menge, 1868
Figs 1C–D, 2B–C, 4C, 5C–D, 7B, 9C–D, 10E–G, 11A, 12E–F, 14C–D, 17F, 18F, 19M; Table 3

Type species

Dicymbium nigrum (Blackwall, 1834).

Diagnosis

Diagnostic characters for males are: the spiral embolus in a sagittal plane, very typical in all species of *Dicymbium* (character 108; Fig. 5D); the highly elongated palpal patella (character 3); the hook-like distal part of the prolateral tibial apophysis (Fig. 1C) and the distinct lobe-like retrolateral process on the paracymbium (character 62; Fig. 4C). The females are recognisable by the lip-like bisection margins (character 183; Fig. 10E–G); the fertilization ducts with a spiral ending; the long oblong spermathecae separated by a slit around the middle and the typical separated conformation of the ventral and dorsal plate of the epigyne seen in aboral view (character 189; Fig. 10F).

Synapomorphies

Dicymbium is well supported (node 29), with a Bremer support of 10, a jackknife support of 99 (MP analysis; Fig. 26) and a bootstrap of 100 (ML analysis; Fig. 27). It is supported by the following synapomorphies (Fig. 29): the massive, thin to leaf-like inner suprategular apophysis with a longitudinal backing (character 85, state 7) and the lip-like bisection margins of the epigyne (character 183). Due to fast optimisation (ACCTRAN), the latter state is shown already one step before, at node 27, including *Saloca*, for which this character is inapplicable. Additionally, this genus is supported by several homoplastic characters among which are: the male palpal patella that is more than 3.5 times as long as broad (character 3, state 2); the macrosetae on the cymbial retrobasal thin apophysis (character 55); the distinct retrolateral process on the paracymbium (character 62) that is found a second time in node 23; the distinct lobe-like ventral process on the paracymbium (character 64, state 1) that is also found in node 37; the spiraled radical tailpiece (character 161, state 1); the separation between the dorsal and the ventral plate of the epigyne (character 189, state 1) and the scaly or ridged cheliceral stridulatory striae (character 218, states 0 and 1). Characters 64 and 189 also appear one step before, at node 27, including *Saloca* for which these characters are inapplicable.

Remarks

Menge (1868) described this genus based on the elongated palpal tibia, the spiral embolus, the ventral radical tailpiece, the posteriorly separated ventral plate of the epigyne and a few other less conspicuous characters. A more detailed description of *Dicymbium* is given in Song *et al.* (2006). We included three out of the ten species in our analysis (see Table 3). *Dicymbium* emerged as monophyletic in all analyses.

***Dicymbium* species groups**

The genus *Dicymbium* is morphologically very homogeneous and the definition of the two species groups is based on the morphology of the male palpal tibia. However, *Di. libidinosum* is quite exceptional in its male genital characters. Therefore, the characters that support node 30 (i.e., the *nigrum*-group) are present also in many members of the *facetum*-group.

Node 30 is unambiguously supported by the ventral internal tooth on the prolateral tibial apophysis (character 21) which is also found in, e.g., *Di. yaginumai* Eskov & Marusik, 1994 (Eskov & Marusik

Table 3. This list contains all species that are currently assigned to *Dicymbium* Menge, 1868. Species that were scored for the cladistic analyses are marked with an asterisk (and the citation refers to figures illustrating the diagnostic characters). The remaining species are assigned to *Dicymbium* based on the figures cited showing the spiral embolus and the typical form of the spermathecae and epigyne for genus assignments and a second palpal tibial apophysis for group assignments. The different species groups are indicated in brackets, *nigrum*-group (N) and *facetum*-group (F). "" = ambiguous species-group assignments.

Status	Species name	Scored according to
Dicymbium (N)	*Di. brevisetosum* Locket, 1962	Roberts 1987: fig. 10e
"*Dicymbium*"	*Di. elongatum* (Emerton, 1882)	Paquin & Dupérré 2003: figs 894–897
Dicymbium (F)	*Di. facetum* (L. Koch,1879)	Song *et al.* 2006: figs 1–13
"*Dicymbium*"*	*Di. libidinosum* (Kulczyński, 1926)	Song *et al.* 1999: fig. 91e–f, k–l
Dicymbium (N)*	*Di. nigrum* (Blackwall, 1834)	Wiehle 1960: figs 329–337
Dicymbium (F)	*Di. pingqianense* Irfan, Wang & Zhang, 2023	Irfan *et al.* 2023: figs 7–9
Dicymbium (F)	*Di. salaputium* Saito, 1986	Ono *et al.* 2009: figs 196–200
Dicymbium (F)	*Di. sinofacetum* Tanasevitch, 2006	Song & Li 2008: figs 1–13
Dicymbium (N)*	*Di. tibiale* (Blackwall, 1836)	Wiehle 1960: figs 338–343
Dicymbium (F)	*Di. yaginumai* Eskov & Marusik, 1994	Eskov & Marusik 1994: figs 1–5

1994: fig. 1), the mesal second pointy tip on the inner suprategular apophysis (character 86) and the whip-like distal suprategular apophysis (character 90). It is also ambiguously supported by the pointed outer suprategular apophysis that is also present in *D. connatus* and *D. connatus jacksoni* (character 83), the ridged cheliceral stridulatory striae (character 218) and the presence of a trichobothrium on metatarsus four (character 263) that are lacking in all other members of the *Savignia*-group (including *Di. libidinosum*).

***nigrum*-group**

This group includes the European species, namely *Di. nigrum*, *Di. brevisetosum* Locket, 1962 and *Di. tibiale*, corresponding to node 30. Since *Di. nigrum* and *Di. brevisetosum* were identical in the scoring, *Di. brevisetosum* was omitted from the trees.

This group is established based on the simple male palpal tibia that only bears a prolateral apophysis and a ventral inside tooth.

***facetum*-group**

Most members of this group are distributed in Asia and have at least one extra apophysis besides the prolateral apophysis on the male palpal tibia. Usually, the prolateral apophysis is accompanied by a pointy apophysis (e.g., Song & Li 2008: fig. 7) or a more pronounced blunt apophysis in, e.g., *Di. yaginumai* (Eskov & Marusik 1994: fig. 2). This group contains *Di. facetum* (L. Koch, 1879), *Di. pingqianense* Irfan, Wang & Zhang, 2023, *Di. sinofacetum* Tanasevitch, 2006, *Di. salaputinum* Saito, 1986 and *Di. yaginumai*.

Species of *Dicymbium* with uncertain group assignments

Dicymbium libidinosum cannot be placed into the above mentioned groups but expresses most of the diagnostic characters of *Dicymbium*. This species is rather exceptional in the presence of two distinct male palpal apophyses and the presence of a blunt instead of a pointed ventral radical process like all other species of *Dicymbium*. *Dicymbium libidinosum* is also the only species in this genus that has a

dorsal trichobothrium on metatarsus four. The shape of the genitalia "seems extremely closely related" to *Di. yaginumai* according to Eskov & Marusik (1994). Together with the geographic distribution the presence of a second tibial apophysis points to a closer relation to *Di. facetum*.

Dicymbium elongatum (Emerton, 1882) seems to have some derived characters compared to the other species of *Dicymbium*, concerning the elongated tip of the prolateral tibial apophysis and the expanded spiral (rather than spiral in one plane) embolus. Additionally, the cephalic region is extended forward (only slight to no cephalic elevations in the other species of the genus) and the ventral radical process is much thinner than in all other species (see Paquin & Dupérré 2003: figs 894–896).

Genus ***Diplocephalus*** Bertkau, 1883
Figs 1F, 2E, 4E, 5F, 7D, 9F, 11C, 12H, 14F, 16G, 18A, H, 19A–B, I, L, 20A, G, 21B, F, 22F, 23A–C, 24A; Table 4.

Type species

Diplocephalus cristatus (Blackwall, 1833).

Diagnosis

Diplocephalus is not easy to recognise based on the below mentioned synapomorphies apart from one very typical character in the males: the large dorsal radical process (character 142) which is considered most reliable to assign species to *Diplocephalus*. This is a large, elongated dorsal radical process with a curved tip (Figs 18A, 21B, F). Additionally, males usually have a cephalic PME lobe (e.g., Fig. 12H); a retrolaterally directed prolateral tibial apophysis that runs parallel to the distal margin of the tibial apophysis and a tibial apophysis with a squarish (e.g., Fig. 19B; Roberts 1987: fig. 36d) rather than triangular shape (e.g., Fig. 19C) as usually seen in *Savignia* but also in *Diplocephalus permixtus* that has distal spines on a retrolateral thickening of the palpal tibial (character 27; Fig. 19L). Another character that distinguishes *Diplocephalus* from closely related genera is the short embolus with a blunt tip (characters 105 and 124; Figs 21F, 24A). No unambiguous diagnostic characters could be found for females. However, the lateral lobes of the ventral plate of their epigyne is often T-shaped and create a triangle posteriorly. Also, their spermathecae are usually rounded to curved.

Synapomorphies

Diplocephalus is restricted to the taxa in node 53 which is supported by all analyses independent of the weighting scheme and by a Bremer support of 4, jackknife support of 69 (MP analysis; Fig. 26) and a bootstrap of 95 (ML analysis; Fig. 27). The only unambiguous synapomorphy of this clade is the retrolateral distal thickening on the palpal tibia (character 37; Fig. 19I) that is present in most taxa of node 53 (Fig. 31). The only exceptions are *Diplocephalus cristatus* (see, e.g., Roberts 1987: fig. 36d) and *D. alpinus*, which have a setose outgrowth, that might be a vestigial version of this distal thickening which was considered as inapplicable in these species since a lobe or sac was coded as absent (character 36). However, *Diplocephalus* is also supported by a few ambiguous synapomorphies among which are the twisted prolateral tibial apophysis (character 20), that is plane in *D. caucasicus*, the short embolus (character 105) and the narrowly curved embolic tip (character 125).

Remarks

We included 23 out of the 52 described species (World Spider Catalog 2025) in the present analysis. Our analysis revealed that eleven of these taxa belong to other genera in the *Savignia*-group (see Table 9). This does not come as a surprise as *Diplocephalus* was used as a container for many species that could not be placed easily in any of the *Savignia*-group genera. We hereby try to define the genus based on the phylogenetic analysis and discuss the placements of species formerly assigned to *Diplocephalus* with reference to the new definition and its potential placement (see Table 4).

Diplocephalus species groups

cristatus-group

This group corresponds to node 57. With a Bremer support of 10, jackknife support of 99 (MP analysis; Fig. 26) and a bootstrap of 100 (ML analysis; Fig. 27) this node is one of the best-supported nodes in the current analysis. Synapomorphies are the delicate sigmoid type of distal suprategular apophysis (character 90, state 2), the typical embolus that is a secondarily shortened "elongated" lamella with a tip fused to the radix (character 114) and the flat, simple dorsal radical process with a simple pointed tip (character 144; Fig. 31). Moreover, several homoplastic characters support this group. Among those are the ventral tibial process (character 47), the narrow cymbial retrobasal thin apophysis (character 56; state 2) and the lateral dark spot or stripe (character 214, lacking in *D. alpinus*). Additionally, all these species have both a cephalic PME lobe and an AME lobe. Two subgroups can be recognised. The first subgroup (a; node 58) is defined by the presence of the retrolateral blunt sclerotised structure on the male palpal tibia (character 45) and the lack of a distinct tooth emerging from the retrolateral side of the dorsal radical process (character 146). The following species belong to this subgroup: *D. alpinus* and *D. cristatus*. The second subgroup (b), represented by only one species in the current analysis, *D. crassilobus*, lacks the retrolateral blunt sclerotised structure on the male palpal tibia (character 45, state 0) but instead has a distinct tooth emerging from the retrolateral side of the dorsal radical process (character 146). This tooth is an autapomorphy of *D. crassilobus*. However, it is also present in the following species that also belong to this subgroup and that were not included in the current analyses: *D. hungaricus* Kulczyński, 1915 and *D. pseudocrassilobus*. Gnelitsa (2006) already pointed out the close relationship of these three species and mentions that Millidge (1979) even thought that *D. crassilobus* and *D. hungaricus* are synonyms. Comparison of type material is therefore needed to solve this taxonomic problem which is out of the scope of the current analysis.

Diplocephalus komposchi Milasowszky, Bauder & Hepner, 2017 might belong to the *cristatus*-group based on the shape of the palpal tibia with a narrow ventral tibial process, the short lamella-like embolus and the distinct radical process. The epigyne resembles to the one of *D. pseudocrassilobus*. However, *D. komposchi* has a wider dorsal radical process and it lacks the lateral teeth characteristic for the species of the *cristatus*-group (b).

pavesii-group

This group includes a few species with very derived characters and corresponds to node 54. It is supported by a Bremer support of 5, a jackknife support of 79 (MP analysis; Fig. 26) and a bootstrap of 100 (ML analysis; Fig. 27) and the following synapomorphies (Fig. 31): the distinctly forward curved marginal suprategular apophysis (character 80), the large flat and ventrally folded dorsal radical process (character 143), the basal tooth on the radical tailpiece (character 167) and the paired inner longitudinal narrow lobes of the epigyne (character 187). Two subgroups can be differentiated; first, the Caucasian one (a) that is represented only by *D. caucasicus* in the phylogenetic analysis but also includes *D. transcaucasicus* Tanasevitch, 1990. They have a bifurcate ventral radical process with a thin sclerotised distal tip (character 135, state 6) that is distinct in both species and connected to the prolateral margin of the dorsal radical apophysis (Fig. 16G). The tip of the dorsal radical process faces dorsally in these species. The second subgroup (b) includes node 55. It is supported by a Bremer support of 10, a jackknife support of 99 (MP analysis; Fig. 26) and a bootstrap of 100 (ML analysis; Fig. 27) and the following unambiguous characters: the double folded prolateral tibial apophysis (character 18), the cymbial retrobasal striated glabrous bump (character 58) and the massively broadened radical tailpiece tip with an inner thickening (character 165). Additionally, their dorsal radical process is highly enlarged and points ventrally and bears retrolateral striations. The males of all these species have a PME lobe (except for *D. guidoi* Frick & Isaia, 2012 which has a small post PME lobe instead). Based on the dorsal radical process and the double folded prolateral tibial apophysis we assigned the following species to

Table 4 (continued on next page). This list contains all species that are currently assigned to *Diplocephalus* Bertkau, 1883. Species that were scored for the cladistic analyses are marked with an asterisk (and the citation refers to figures illustrating the diagnostic characters). The remaining species are assigned to *Diplocephalus* based on the figures cited. The different species groups are indicated in brackets, *cristatus*-group (C) and *pavesii*-group (P), both with two subgroups a and b. One group was formed that may not belong to *Diplocephalus* but share a couple of characters, the Mediterranean *graecus*-group (G). "" = ambiguous assignments; ??? = of uncertain assignment and probably misplaced within *Diplocephalus*.

Status	Species name	Scored according to
"*Diplocephalus*" (G)	*D. algericus* Bosmans, 1996	Bosmans 1996: figs 62–65
Diplocephalus (Ca)*	*D. alpinus* (O. Pickard-Cambridge, 1872)	Pesarini 1996: figs 13–14
"*Diplocephalus*" (G)	*D. altimontanus* Deltshev, 1984	Deltshev 1984: figs 1–9
Diplocephalus (Pb)*	*D. arnoi* Isaia, 2005	Isaia 2005: figs 2–8
"*Diplocephalus*"	*D. bifurcatus* Tanasevitch, 1989	Tanasevitch 1989: figs 131–137
"*Diplocephalus*"	*D. bosmansi* Lecigne, 2025	Lecigne *et al.* 2025: fig. 44a–h
"*Diplocephalus*"	*D. caecus* Denis, 1952	Denis 1952: figs 42–47
Diplocephalus (Pa)*	*D. caucasicus* Tanasevitch, 1987	Tanasevitch 1987: figs 95–105
"*Diplocephalus*"	*D. circularis* Irfan, Zhang & Peng, 2025	Irfan *et al.* 2025: figs 53–57
Diplocephalus (Cb)*	*D. crassilobus* (Simon, 1884)	Millidge 1979: figs 50–59
Diplocephalus (Ca)*	*D. cristatus* (Blackwall, 1833)	Hormiga 2000: fig. 6a–i, pl 19a–d, 20a
"*Diplocephalus*" (G)	*D. graecus* (O. Pickard-Cambridge, 1872)	Bosmans 1996: figs 44–50
Diplocephalus (Pb)	*D. guidoi* Frick & Isaia, 2012	Frick & Isaia 2012: figs 1–10
"*Diplocephalus*"	*D. hispidulus* Saito & Ono, 2001	Saito & Ono 2001: figs 87–91
Diplocephalus (Cb)	*D. hungaricus* Kulczyński, 1915	Kulczyński 1915: figs 37–42
"*Diplocephalus*"	*D. inanis* Tanasevitch, 2014	Tanasevitch, 2014: figs 1–8
Diplocephalus (C)	*D. komposchi* Milasowszky, Bauder & Hepner, 2017	Milasowszky *et al.* 2017: figs 1–12
"*Diplocephalus*" (G)	*D. lancearius* (Simon, 1884)	Bosmans 2002: figs 67–72
Diplocephalus (Pb)	*D. longicarpus* (Simon, 1884)	Thaler 1972: figs 25–29, 33
"*Diplocephalus*"*	*D. lusiscus* (Simon, 1872)	Wiehle 1963: figs 24–33
"*Diplocephalus*"	*D. machadoi* Bosmans & Cardoso, 2010	Bosmans *et al.* 2010: figs 14–22
"*Diplocephalus*"	*D. montaneus* Tanasevitch, 1992	Tanasevitch 1989: figs 136–141
"*Diplocephalus*" (G)	*D. mystacinus* (Simon, 1884)	Bosmans 1996: figs 52–58
"*Diplocephalus*"	*D. parentalis* Song & Li, 2010	Song & Li 2010: figs 9–11
Diplocephalus (Pb)*	*D. pavesii* Pesarini, 1996	Thaler 1972: figs 12–24, 30–32 as *D.* aff. *procerus*
*Diplocephalus**	*D. permixtus* (O. Pickard-Cambridge, 1871)	Wiehle 1960: figs 935–941; Millidge 1977: fig. 133
"*Diplocephalus*"*	*D. picinus* (Blackwall, 1841)	Wiehle 1960: figs 951–960; Merrett 1963: fig. 67a–c
Diplocephalus (Pb)	*D. procer* (Simon, 1884)	Brignoli 1971: figs 106–108, 110, 112–113
"*Diplocephalus*"	*D. protuberiscus* Wunderlich, 2022	Wunderlich 2022: figs 118–121
Diplocephalus (Cb)	*D. pseudocrassilobus* Gnelitsa, 2006	Gnelitsa 2006: figs 1a–f, 2a
"*Diplocephalus*"	*D. sphagnicola* Eskov, 1988	Eskov 1988: figs 32–37

Table 4 (continued).

Status	Species name	Scored according to
"*Diplocephalus*"*	*D. subrostratus* (O. Pickard-Cambridge, 1873)	Eskov 1988: figs 40–45; Paquin & Dupérré 2003: figs 914–917
"*Diplocephalus*"	*D. tongrenensis* Irfan, Zhang & Peng, 2025	Irfan *et al.* 2025: figs 58-59
"*Diplocephalus*" (G)	*D. toscanaensis* Wunderlich, 2011	Wunderlich, 2011: figs 126–130
Diplocephalus (Pa)	*D. transcaucasicus* Tanasevitch, 1990	Tanasevitch 1990: figs 17.1–4, 18.1–2
"*Diplocephalus*" ("G")*	*D. turcicus* Brignoli, 1972	Brignoli 1972: figs 9–15, 17
"*Diplocephalus*"*	*D. uliginosus* (Eskov, 1988)	Eskov 1988: figs 47–52
Misplaced *Diplocephalus* species		
Not *Savignia* genus group	*D. bicurvatus* Bösenberg & Strand, 1906	Ono *et al*. 2009: figs 230–234; Bösenberg & Strand 1906: pl. 12 fig. 272e
Not *Savignia* genus group	*D. culminicola* Simon, 1884	Simon 1884: figs 807–808; Denis 1953: 5–7
Not *Savignia* genus group	*D. gravidus* Strand, 1906	Ono *et al*. 2009: figs 235–238
???	*D. tiberinus* (Caporiacco, 1936)	Caporiacco 1936: fig. 3

this species group: *D. arnoi*, *D. guidoi*, *D. longicarpus* (Simon, 1884), *D. pavesii* and *D. procer* (Simon, 1884).

Species and groups of *Diplocephalus* with uncertain assignment

Many species currently placed in *Diplocephalus* do not belong to *Diplocephalus* in the strict sense following the synapomorphies and diagnostic characters described above. As revising the whole genus *Diplocephalus* on species level is out of the scope of this paper, we discuss potential groups, single wild card taxa of the current analysis and additional taxa with respect to their potential placement within the *Savignia* genus group. Out of the 52 species that were assigned to this genus (World Spider Catalog 2025) 21 are not possible to place based on the current analysis and/or literature data. Most of these taxa are discussed in this section but are provisionally kept in *Diplocephalus*.

***graecus*-group**

This group includes six Mediterranean species that were not scored for the current phylogenetic analysis and lack the above described large dorsal radical process: *D. graecus* (O. Pickard-Cambridge, 1872), *D. lancearius* (Simon, 1884), *D. mystacinus* (Simon, 1884), *D. algericus* Bosmans, 1996, *D. altimontanus* Deltshev, 1984 and *D. toscanaensis* Wunderlich, 2011. Four species form a group based on the simple and broad prolateral tibial apophysis (e.g., Bosmans 1996: figs 46, 54): *D. graecus*, *D. lancearius*, *D. mystacinus* and *D. toscanaensis*. The cephalic lobe of *D. graecus* is very similar to *D. picinus* and *D. algericus* but different from what is found in *D. lancearius* and *D. mystacinus* (Bosmans 1996: fig. 52; 2002: fig. 67). Three of the taxa with the broad prolateral tibial apophysis (*D. graecus*, *D. lancearius* and *D. mystacinus*) have distinct ventral radical processes, like *D. altimontanus* and *D. algericus* and presumably also *D. turcicus* (as far as it can be judged from illustrations; see Table 4). Additionally, all these species have a flattened and curved to spiral embolus. The females have a relatively simple vulva with spermathecae situated at the posterior to central part of the epigyne.

Species of *Diplocephalus* with uncertain assignment

Diplocephalus permixtus is also a "*Diplocephalus*" in the strict sense following our diagnostic characters, i.e., having the specific enlarged dorsal radical process (character 142). However, it emerged between the *cristatus*- and the *pavesii*-group, sharing the narrow cephalic PME lobe with the *cristatus*-group.

Diplocephalus turcicus, which emerged at node 51, might also be associated with the *graecus*-group by having a less distinct ventral radical process and curved spermathecae, located at the anterior side of the epigyne. Additionally, *D. turcicus* has a relatively special prolateral tibial apophysis with a tooth emerging from it at its retrolateral side (Brignoli 1972: fig. 15) and superficially similar to *Savignia kawachiensis* (Oi 1960: fig. 157). Bosmans *et al.* (2009: figs 7–12) illustration of *D. turcicus* seems to correspond to *A. rhodes* based on the male palp and the epigyne conformation, and the location record also from an island in Greece.

Diplocephalus picinus (node 61) appears within the *Araeoncus* clade (node 59) (Figs 25–26). However, this species is problematic as it changes position through different analyses (Supp. file 2, Supp. file 3), most likely because of its singular palp morphology. As its position is unstable, we leave it provisionally in *Diplocephalus*.

Within node 39 are two well-supported nodes corresponding to *Savignia* (node 45) and *Hemistajus* (node 43). The three remaining taxa in this clade are problematic: *D. uliginosus*, *D. lusiscus* and *D. subrostratus*. *Diplocephalus lusiscus* appears within node 39 (Fig. 25) which might be correct at least based on the embolic division that shares some similarities with other members in node 39, especially the flattened embolus. However, *D. lusiscus* is a cave dweller (Wiehle 1963) with morphological adaptations to that habitat that have led to some derived characters that are difficult to homologise. The same is true for the cave dwelling *Savignia rostellatra* Song & Li, 2009 with very derived characters of the embolic division (see *Savignia* section) but no obvious morphological adaptations to cave dwelling (Song & Li 2009).

Diplocephalus uliginosus seems to be a simpler type of *Hemistajus* concerning the form of the cephalic lobe that resembles many members of *Erigonella* (e.g., Fig. 15C, F) while the other species in *Hemistajus* have diagonally flattened cephalic fronts (Fig. 15B). Also, the simpler prolateral tibial apophysis and the unmodified triangular dorsal radical process underline the basal position of *D. uliginosus* with respect to the other species of *Hemistajus*.

Diplocephalus subrostratus probably belongs to *Hemistajus*, and was thought to be very similar to *D. picinus* (e.g., Eskov 1988) but differs in its embolic division. In our phylogeny, both species emerge well separated from each other (Fig. 25). *Diplocephalus subrostratus* is also very similar to *D. uliguinosus* but even simpler; it lacks any radical processes on the embolic division, has smaller suprategular apophyses and lacks a protruding inner margin of the epigyne (Eskov 1988: figs 42, 44). However, the curved, slightly elongated spermathecae, the diagonally flattened cephalic front and the inwards turned prolateral tibial apophysis (Eskov 1988: figs 40, 43) resemble very much to what is found in, e.g., *D. montanus* (Eskov 1988: figs 25, 28).

According to Denis (1952), *D. caecus* Denis, 1952, a cave dweller from Romania, is very close to *D. lusiscus*. The form of the cephalic lobes, the arrangement of the eyes in the males of both species, and the male prolateral tibial apophysis are very similar.

There are also two eyeless species from caves from Morocco, *D. inanis* Tanasevitch, 2014 and *D. bosmansi* Lecigne, 2025. *Diplocephalus bosmansi* resembles *D. picinus* but with a broader epigynal fissure. *Diplocephalus inanis* males can be distinguished by the broad prolateral tibia and a curved

embolus and females by the thick seminal ducts and wide epigynal fissure in the proximal part of the ventral plate, similar to *D. picinus*.

Diplocephalus protuberiscus Wunderlich, 2022 is known from the male and is named based on the similarities to *A. protuberans* comb. nov. and *D. lusiscus*. It has a cephalic part raised with a setose clypeus like in *Hemistajus* and *Savignia*, a palpal tibia with a retrolateral branch, and a thick and curved embolus.

The associations of *D. montaneus* Tanasevitch, 1992, *D. bifurcatus* Tanasevitch, 1989, *D. hispidulus* Saito & Ono, 2001 and *D. sphagnicola* Eskov, 1988, that are likely not closely related to each other, remain obscure. Tanasevitch (1989) mentions the close resemblance of *D. montaneus* with *D. cristatus*. However, the lack of an enlarged dorsal radical process argues against a close relationship. *Diplocephalus sphagnicola* has a very distinct ventral radical process and a particularly long embolus (Eskov 1988: fig. 33) with a corresponding long copulatory duct in the female (Eskov 1988: fig. 37). Both characters are not found in any other group of taxa apart from maybe *Araeoncus* to which *D. sphagnicola* is presumably not closely related due to the lack of synapomorphic characters.

Diplocephalus circularis Irfan, Zhang & Peng, 2025 and *D. tongrenensis* Irfan, Zhang & Peng, 2025 are two species recently described from China. Based on the median fissure, the wide copulatory opening of the epigyne and the long and spiral embolus in *D. circularis*, they probably belong to another genus of the *Savignia* genus group.

Diplocephalus parentalis Song & Li, 2010 is closely related to *D. hispidulus* based on the palpal tibial apophysis shape, which is also covered by papillae (similar to several species of *Erigonella*) and the complicated dorsal plate of the epigyne (Song & Li 2010: figs 9–11). It was placed in *Diplocephalus* based on the long copulatory ducts and it has a particular embolic division with a large radix with a sclerotised margin with no apophyses. The lack of a radical process on the radix and the different shape of the ventral plate with a "column-shaped complex" anteriorly, indicates that it does not belong to *Diplocephalus* and probably corresponds to another genus of the *Savignia* genus group.

Diplocephalus machadoi Bosmans & Cardoso, 2010 males occur in two forms. In one, the cephalic PME lobe is very similar to *D. picinus* and the other has a pointed AME lobe that resembles to the one of *A. galeriformis.* It shares characters with species from different genera of the *Savignia* genus group and cannot be assigned to any based on the available figures.

Species of *Diplocephalus* misplaced in the *Savignia* genus group

Diplocephalus gravidus Strand, 1906 does not belong to the *Savignia* genus group due to the lack of a bisected epigyne (Ono *et al.* 2009: fig. 238) that is synapomorphic for this node (21). Therefore, it does not belong to *Diplocephalus* and presumably not to any other genus in the *Savignia*-group. Only the female is known from this species and compared to the other taxa included in the current analysis, it has a slightly elevated cephalothorax (Ono *et al.* 2009: fig. 236).

Diplocephalus bicurvatus Bösenberg & Strand, 1906 also lacks the bisected epigyne (Bösenberg & Strand 1906: pl. 12 fig. 272e) and the prolateral tibial apophysis is more pronounced than in other *Savignia*-group members and is initially facing dorsally. The embolic division is also very different from what is found in any *Savignia*-group species (Ono *et al.* 2009: figs 230–234).

The epigyne of *D. culminicola* Simon, 1884 seems to lack a median fissure (Denis 1953: figs 6–7) and therefore is most probably not a *Savignia*-group member. The current information on *D. tiberinus* (Caporiacco, 1936) is restricted to one figure showing the male palp in Caporiacco (1936: fig. 3) and a description in Latin, which are not sufficient for any discussion of generic assignment.

Genus ***Erigonella*** Dahl, 1901
Figs 1E, I–J, 2D, 3B–C, 4D, H, 5E, 6C, G, 7C, 9E, H–I, 10H–I, L–M, 11B, D–F, 12G, 13C–D, 14E, H–J, 15C, F–G, 17E, 19H, O, 21H–I, 23D–K, 24B–L; Table 5

Type species

Erigonella hiemalis (Blackwall, 1841).

Diagnosis

The diagnosis does not include *E. ignobilis*, which is discussed in section "uncertain assignments". Diagnostic characters for males are the presence of a prolateral and a retrolateral tibial apophysis where the prolateral apophysis is sometimes papillate (character 14, state 2); the short coiled embolus with a blunt tip, the presence of ventral, central or dorsal radical processes, the pointed (in *E. hiemalis* and *E. subelevata*) or blunt (in *E. latifrons* comb. rev. and *E. ignobilis*) inner suprategular apophysis and the simple straight to slightly curved distal suprategular apophysis (character 90; state 4) with a blunt to slightly to sharply pointed tip (character 93). Additionally, they present a punctuated sternum (character 196), which is only found in *E. hiemalis*, *E. subelevata* (node 34) and *E. ignobilis* within the members of the *Savignia*-group. Females usually present a triangularly split on the posterior side of the epigyne (character 181) (also present in *Diplocephalus*) and spermathecae with an L-shape (e.g., *E. hiemalis* and *E. subelevata*) in contrast to the rounded spermathecae of similar *Diplocephalus* females (e.g., *D. cristatus*).

Synapomorphies

This genus corresponds to node 33 that is supported by a Bremer support of 1 (MP analysis; Fig. 26) and a bootstrap of 97 (ML analysis; Fig. 27) and includes two species-groups: the *hiemalis*-group (node 34) and the *connatus*-group (node 35 excluding *E. ignobilis*).

Species of *Erigonella* shared only one unambiguous synapomorphy (Fig. 30): the cramp-like dorsal radical process (character 150) that was inapplicable in the *hiemalis*-group and *E. ignobilis*. Additional supportive homoplastic characters include the retrolateral tibial apophysis (character 28) that is lacking in *E. ignobilis* and only also present in *Glyphesis* and *Entelecara*; the outer suprategular apophysis (character 82); the transverse spiraled embolus (character 108; state 1) and the rough irregular cephalothorax surface (character 217). They also have in common the simple straight to slightly curved distal suprategular apophysis (character 90, state 4), but this character appears as a synapomorphy one step before, at node 32, despite it is only present in all *Erigonella* taxa (node 33). The retrolateral tibial apophysis is glabrous and initially distal facing only in *Erigonella* (characters 31, 32).

Remarks

The genus *Erigonella* was described by Dahl (1901) based on the punctuated sternum that differs from *Lophomma punctatum* (Blackwall, 1841) by additional rugose areas in between (Fig. 11D–F) and the lack of punctuations on the cephalothorax. The generic definition and assignment of taxa did not change much since. Dahl (1901) included *E. hiemalis*, *E. subelevata*, *E. ignobilis* and one species that was later transferred to *Diplocephalus* but belongs to *Erigonella* according to our phylogenetic analysis and is therefore a revived combination: *E. latifrons* comb. rev. Since then, *E. groenlandica* Strand, 1905, *E. stubbei* Heimer, 1987 and *E. subelevata pyrenaea* Denis, 1965 were added. The current analysis suggests that at least three more taxa belong to this genus (*E. connatus* comb. nov., *E. latifrons* comb. rev. and *E. producta* comb. nov.) and the genus definition should include more characters than only the punctuated sternum. Wunderlich (1970) suggested a synonymy with *Diplocephalus*, which was not followed by later authors. The similarity of species from *Erigonella* with representatives of *Diplocephalus* is very high, especially concerning the shape of the cephalic lobes. However, instead of lumping all these genera into one (*Savignia* by priority) we prefer to keep most of the genera defined within the *Savignia*-group and instead revise the genus *Diplocephalus* by transferring some of its species to other genera.

Table 5. This list contains all species that are currently assigned to *Erigonella* Dahl, 1901, including those that are newly or again assigned to *Erigonella* marked as comb. nov. and comb. rev., respectively. Species that were scored for the cladistic analyses are marked with an asterisk (and the citation refers to figures illustrating the diagnostic characters). The remaining two species are currently not possible to assign to any group within or outside *Erigonella* and therefore remain in *Erigonella*. The different species groups are indicated in brackets, *hiemalis*-group (H) and *connatus*-group (C). "" = ambiguous assignments; ??? = of uncertain assignment and probably misplaced within *Erigonella*.

Status	Species name	Scored according to
Erigonella (C)*	*E. connatus* (Bertkau, 1889) comb. nov.	Wiehle 1960: figs 916–925; Roberts 1987: figs 37b, 39k
Erigonella (H)*	*E. hiemalis* (Blackwall, 1841)	Wiehle 1960: figs 1023–1030; Merrett 1963: fig. 64a–c
"*Erigonella*"*	*E. ignobilis* (O. Pickard-Cambridge, 1871)	Wiehle 1960: figs 1031–1038
Erigonella (C)*	*E. latifrons* (O. Pickard-Cambridge, 1863) comb. rev.	Wiehle 1960: figs 942–950; Roberts 1987: figs 37a, 39i
Erigonella (C)*	*E. producta* (Holm, 1977) comb. nov.	Holm 1977: figs 1–7 Eskov 1988: figs 38–39
Erigonella (H)*	*E. subelevata* (L. Koch, 1869)	Thaler 1971: figs 1–7
Erigonella (H)	*E. subelevata pyrenaea* Denis, 1965	Denis 1965: figs 1–3
Misplaced *Erigonella* species		
???	*E. groenlandica* Strand, 1905 nom. dub.	Strand 1905: 26–27.
???	*E. stubbei* Heimer, 1987	Heimer 1987: figs 28–29

In our analysis, we included three of the six species previously described as *Erigonella*. *Erigonella* turned out to be a relatively well-supported clade when two species from *Diplocephalus* and one from *Savignia* are included (see Table 5).

Erigonella species groups

hiemalis-group

This group corresponds to node 34 plus *E. subelevata pyrenaea*. It is ambiguously supported by several characters among which are: the papillate prolateral tibial apophysis (character 14, state 2), a thin, long inner suprategular apophysis with a blunt tip (character 85, state 4) and the punctuated sternum (character 196). *Erigonella subelevata* and *E. subelevata pyrenaea* are very similar but differ in the size of the AME lobe and the PME lobe (Denis 1965: fig. 2; Thaler 1971: fig. 6) and the shape of the retrolateral tibial apophysis (Denis 1965: fig. 3; Thaler 1971: fig. 3).

connatus-group

This group is defined based on the cramp-like dorsal radical process (character 150) that is only present in *E. latifrons* comb. rev., *E. producta* comb. nov. and *E. connatus* comb. nov., which together form this group. The triangularly split posterior side of the epigyne (character 181) is also typical in this group and the presence of a more or less distinct AME lobe (character 209). *Erigonella latifrons* comb. rev. is basal to the remaining species.

Erigonella producta comb. nov., *E. connatus* comb. nov., and *E. connatus jacksoni* comb. nov. form node 37 which is supported by a Bremer support of 6 a jackknife support of 99 (MP analysis; Fig. 26) and a bootstrap of 100 (ML analysis; Fig. 27) and the following synapomorphies (Fig. 30): the sharply pointed simple to slightly curved type of distal suprategular apophysis (character 93, state 1) and the proximally

directed and pointed dorsal to retrolateral radical tailpiece (character 169, state 3) and as ambiguous synapomorphy, the pointed inner suprategular apophysis that is flush with the distal suprategular apophysis (character 85, state 6). Additionally, the flat cramp-like dorsal radical process (character 151) that is only found in these three species but is inapplicable in the other members of *Erigonella*, appears as a synapomorphy of node 36. They also have a distinct lobe-like ventral process on the paracymbium (character 64) that is otherwise only present in *Dicymbium*.

Holm (1977) assigned *E. producta* comb. nov. to *Savignia* due to its great similarity of the cephalic lobe even though he pointed out that secondary sexual characters such as the cephalic lobes are not reliable for genus delimitations. In the current analysis this species is the sister taxon of *E. connatus* comb. nov. plus *E. connatus jacksoni* comb. nov. Meanwhile, the latter subspecies has been synonymised with *E. connatus* comb. nov.

Species of *Erigonella* with uncertain assignment

Strand (1905) described *E. groenlandica* from one subadult female based to the punctuated sternum that is not found in any other member of the *Savignia*-group. However, this character is also found in other linyphiid taxa, e.g., *Lophomma punctatum* (Hormiga 2000: pl. 47a–b). Meanwhile, this species has been considered a nomen dubium. The assignment of *E. stubbei* that is known from females only is also uncertain and considered as preliminary by Heimer (1987). He mentions the similarity of the vulva with *Tapinocyba* Simon, 1884 but assigned this species to *Erigonella* based on the habitus, the leg spination and the position of the metatarsal trichobothria. The globular spermathecae are similar to *E. ignobilis* and according to the figures, the epigyne is bisected. However, a punctuated sternum was not mentioned, so, until males are available clear generic assignment for this species is not possible.

Erigonella ignobilis is very difficult to place within *Erigonella* and even may not belong to this genus. It emerged within *Erigonella* in all analyses but it emerged between *Glyphesis* and *Dicymbium* in Frick *et al.* (2010) rather than between *E. latifrons* comb. rev. and *E. producta* comb. nov. Problematic is the lack of derived characters in this species. *Erigonella ignobilis* lacks a cephalic lobe and has a central radical process that is otherwise only present in *Glyphesis* and a very simple conformation of the male palpal tibia. However, it shares the retrolateral glabrous edge on the male palpal tibia (character 35) and the punctuated sternum (character 196). *Erigonella ignobilis* might change its position within the *Savignia*-group (to which it certainly belongs) in future phylogenetic studies.

Genus ***Glyphesis*** Simon, 1926

Figs 3D, 4I, 6D, 8A, 9J, 10N, O, 13E, 14K, 15A, I, 16H, 17C, 19K, N, P, 22G; Table 6

Type species

Glyphesis servulus (Simon, 1882).

Diagnosis

The males of *Glyphesis* can best be recognised by the cymbial prolateral basal glabrous apophysis (character 60; Fig. 6D) and the central radical process (character 152; Fig. 6D) in combination with the clypeal lobe (lacking in the former *Paraglyphesis*) (character 208; Fig. 13E), the usually ridged or scaled pro- (character 14; Fig. 19N) and retrolateral tibial apophysis (character 31; Fig. 3D) (the retrolateral tibial apophysis directs towards the inside in the *cottonae*-group) and the presence of a prolateral sickle on the prolateral tibial apophysis (character 13; Fig. 19P). Some species of *Glyphesis* (like *G. servulus* and *G. taoplesius*) can also be recognised by the long strong inter pro- to retrolateral tibial apophysis macrosetae (character 25; Fig. 19P). The females can be recognised by the oval-shaped epigyne (character 184; Fig. 10N) and the anteriorly turned posterior tip on the ventral plate of the epigyne (character 190) (lacking in the basal *cottonae*-group).

Table 6. This list contains all species that are currently assigned to *Glyphesis* Simon, 1926, including those that are newly assigned to *Glyphesis* marked as comb. nov. Species that were scored for the cladistic analyses are marked with an asterisk (and the citation refers to figures illustrating the diagnostic characters). The remaining species are assigned to *Glyphesis* based on figures cited showing the dorsal or retrolateral facing retrolateral tibial apophysis or the robust setae between the prolateral and the retrolateral tibial apophysis. The different species groups are indicated in brackets, *cottonae*-group (C), *polaris*-group (P) and *servulus*-group (S) with two subgroups a and b. "" = ambiguous species-group assignments.

Status	Species name	Scored according to
Glyphesis (C)	*G. asiaticus* Eskov, 1989	Eskov 1989: figs 1–4
Glyphesis (C)*	*G. cottonae* (La Touche, 1946)	Locket & Millidge 1953: fig. 173a–e; Merrett 1963: fig. 61a–c
Glyphesis (Sb)	*G. idahoanus* (Chamberlin, 1949)	Paquin & Dupérré 2003: figs 1050–1052
Glyphesis (P)	*G. lasiargoides* (Eskov, 1991) comb. nov.	Eskov 1991b: figs 10–13
Glyphesis (P)	*G. monticola* (Eskov, 1991) comb. nov.	Eskov 1991b: figs 5–9
"*Glyphesis*"*	*G. nemoralis* Esyunin & Efimik, 1994	Esyunin & Efimik 1994: figs 1–8
Glyphesis (P)*	*G. polaris* (Eskov, 1991) comb. nov.	Eskov 1991b: figs 1–4
Glyphesis (Sb)	*G. scopulifer* (Emerton, 1882)	Paquin & Dupérré 2003: figs 1053–1055
Glyphesis (Sa)*	*G. servulus* (Simon, 1881)	Roberts 1987: figs 35e, 39c
Glyphesis (Sa)*	*G. taoplesius* Wunderlich, 1969	Wunderlich 1969: figs 23–25, 27–28, 30–31, 34

Synapomorphies

We follow the suggestion of Eskov (1991b) in his description of *Paraglyphesis*, where he pointed out the close similarity to *Glyphesis*. We agree with Eskov (1991b) in this respect and hereby synonymise *Paraglyphesis* with *Glyphesis*. Simon (1926) described *Glyphesis* based on the cephalic clypeal lobe (character 208), the tibial apophyses with thickened retrolaterally curved setae and the semicircular epigyne. These characters are still valuable to describe *Glyphesis*.

This genus corresponds to node 22 and is monophyletic in the current analysis, supported by a Bremer support of 6, a jackknife support of 98 (MP analysis; Fig. 26) and a bootstrap of 100 (ML analysis; Fig. 27). Species of *Glyphesis* share the following synapomorphies (Fig. 29): the ridged or scaled texture of the prolateral tibial apophysis (character 14, states 3 and 4; are also found in *Entelecara*), the inter pTA-rTA dorsal protuberance (character 43), the cymbial prolateral basal glabrous apophysis (character 60), the blunt, small, thin and short ventral radical process (character 135, state 8) and the retro- to prolateral bulb-like central radical process (character 153). Additionally, a few more ambiguous characters support this genus. Among these are the lack of a prolateral trichobothrium on the male palpal tibia (character 4); the general conformation of the palpal tibia showing two short fingers on a broad base (character 6; state 1); the presence of a retrolateral tibial apophysis (character 28); the small distal suprategular apophysis with a blunt or pointed tip (character 90, state 11); the cephalic clypeal lobe (character 208, reduced in former *Paraglyphesis*) and the single proximal dorsal trichobothrium on the female palpal tibia (character 246).

The scored taxa also had a ventral radical process that was either blunt, small, thin and short (character 135, state 8) or a pointed small tooth (character 135, state 9). Additional characters but present also in other taxa are the scaled texture of the retrolateral tibial apophysis (character 31). The females of *Glyphesis* excluding the *cottonae*-group have an oval-shaped epigyne (character 184).

Remarks

We included four out of the seven known species of *Glyphesis* (see Table 6). Our results revealed that *Paraglyphesis* should be synonymized with *Glyphesis*, adding another three taxa (see Table 9).

***Glyphesis* species groups**

***cottonae*-group**

This group contains the early branching species of *Glyphesis*. It is represented by *G. cottonae* in our analysis. *Glyphesis cottonae* and *G. asiaticus* Eskov, 1989, that also belongs to this species group, share a few characters that are not found in any other species group within *Glyphesis*. The males have a highly sclerotised dorsal facing retrolateral tibial apophysis (character 32) and the comparatively broad and highly sclerotised retrolateral facing prolateral tibial apophysis (e.g., Eskov 1989: fig. 2). The females have a bisected epigyne with flush lateral lobes of the ventral plate until the posterior end of the epigyne (e.g., Eskov 1989: fig. 3) like most other *Savignia* genus group members. This is another argument for the common origin of the bisected epigyne in the *Savignia* genus group (node 21).

***servulus*-group**

This group is equivalent with the former *Glyphesis.* It can be recognised by the long strong inter pro- to retrolateral tibial apophysis macrosetae (character 25). There are two distinct subgroups within this group: first (a), *G. servulus* and *G. taoplesius* with a pronounced retrolateral sickle (character 13; *G. nemoralis* with a smaller one), a well-developed cephalic clypeal lobe (character 208; e.g., Wunderlich 1969: fig. 23) and a well visible retrolaterally directed retrolateral tibial apophysis. The second subgroup (b) includes the North American taxa of this genus *G. idahoanus* (Chamberlin, 1949) and *G. scopulifer* (Emerton, 1882). They reduced both the pro- and retrolateral tibial apophysis in size compared to the European taxa of the *servulus*-group, lack a distinct cephalic clypeal lobe and have a more pronounced (towards the posterior end of the epigyne) posterior tip of the epigyne. The central radical process is much more pronounced distally than in the other species of this subgroup.

***polaris*-group**

This group corresponds to the former genus *Paraglyhesis* and includes the very homogenous species *G. lasiargoides* (Eskov, 1991) comb. nov., *G. monticola* (Eskov, 1991) comb. nov. and *G. polaris* (Eskov, 1991) comb. nov. Eskov (1991b) diagnosed *Paraglyphesis* by the "unmodified male carapace with neither postocular pits nor any clypeal projections" a character that was shown to be highly variable in other well-defined genera (e.g., see discussion of *E. connatus* comb. nov. and *E. connatus jacksoni* comb. nov.). He also noticed the well-separated posterior tips of the lateral lobes of the ventral plate that are touching each other in the *servulus*-group. Members of this group lack the long strong inter pro- to retrolateral tibial apophysis macrosetae and have globular spermathecae.

Species of *Glyphesis* with uncertain species group assignments

Glyphesis nemoralis is intermediate between the *servulus*- and the *polaris*-group. It has a less developed retrolateral sickle than seen in the *servulus*-group but it is not lacking as in the *polaris*-group. It lacks an inter pro- to retrolateral tibial apophysis macrosetae found in the *servulus*-group but shares the elongated spermathecae with it, while the *polaris*-group has nearly globular spermathecae. This intermediate position is also reflected by our analyses where it emerges between these two groups in the implied weighting analyses.

Genus ***Hemistajus*** Schenkel, 1934 resurrected rank
Figs 15B, 16I, 17D, 18B, 19G, 22D–E; Table 7.

Type species

Hemistajus rostratus (Schenkel, 1934) comb. rev.

Table 7. This list contains all species that are currently assigned to *Hemistajus* Schenkel, 1934 resurrected rank and marked as comb. nov. and as comb. rev., if it is a revived combination. Species that were scored for the cladistic analyses are marked with an asterisk (and the citation refers to figures illustrating the diagnostic characters). *Hemistajus barbiger* comb. nov. was assigned to *Hemistajus* based on the figures cited showing the broad tip of the prolateral apophysis and the retrolateral facing protuberance on the dorsal triangular radical process.

Status	Species name	Scored according to
Hemistajus	*H. barbiger* (Roewer, 1955) comb. nov.	Holm 1967: figs 32–36; Eskov 1988: figs 7–11
*Hemistajus**	*H. marusiki* (Eskov, 1988) comb. nov.	Eskov 1988: figs 12–17
*Hemistajus**	*H. montanus* (Eskov, 1988) comb. nov.	Eskov 1988: figs 25–31
*Hemistajus**	*H. rostratus* (Schenkel, 1934) comb. rev.	Thaler 1970: figs 1–9

Diagnosis

Hemistajus males can be distinguished from similar genera by the broad prolateral tibial apophysis ending in a broad cut off and papillate tip (character 15; Fig. 19G). The males of this group have a diagonally flattened cephalic front (character 199; Fig. 15B) that is densely covered with setae and even setose in females. The females can be recongised by the rebordered, sclerotised median margins of the epigyne (character 185; Fig. 22E), but also present in *D. mirabilis* and *S. frontata*.

Within *Hemistajus*, *H. montanus* comb. nov., *H. barbiger* comb. nov. and *H. marusiki* comb. nov. present the most derived characters concerning the retrolateral protuberance (character 149) arising from the triangular dorsal radical process (character 147) and the elongated dagger- to dirk-like distal suprategular apophyses (character 90, state 1).

Hemistajus rostratus comb. rev. is closely related to *H. barbiger* comb. nov. based on genital morphology (Schenkel 1934; Thaler 1970). Thaler (1970) underlines the isolated position of these species within the "*Diplocephalus*-group" (which corresponds to the *Savignia*-group later defined by Millidge 1977) and that the subgenus *Hemistajus* should be kept in mind in a future revision. We agree with Thaler (1970) in this respect and the description of a few more taxa with similar characters by Eskov (1988) seems to justify the new generic rank of *Hemistajus*.

Synapomorphies

This definition corresponds to node 43 in the preferred tree (Fig. 25). The ventral ridge on the triangular dorsal radical process (character 148) is the only unambiguous character that supports this clade.

However, it is also supported by a Bremer support of 4, jackknife support of 85 (MP analysis; Fig. 26) and a bootstrap of 99 (ML analysis; Fig. 27) and several homoplastic characters among which are the following (Fig. 30): the ventral facing distal part of the prolateral tibial apophysis (character 19); the very large and flat inner suprategular apophysis formed like an equilateral triangle (character 85, state 11) and the supplementary clypeal setae in females (character 234). Additionally, the prolateral tibial apophysis is broadened and broadly cut off at its tip (e.g., Eskov 1988: figs 9, 15, 28).

Remarks

Hemistajus was described by Schenkel (1934) as a subgenus of *Diplocephalus* with the type species *H. rostratus* (Schenkel, 1934) comb. rev. Schenkel (1934) established this genus to account for the quite different morphology of *Diplocephalus rostratus* and *D. barbiger* (Roewer, 1955). *Hemistajus* was later elevated to genus in Janetschek (1956) and then synonymised to *Diplocephalus* by Thaler (1970) by the transfer of its type species.

We included three out of four species of *Hemistajus* in the phylogenetic analysis (see Table 7). All four species were transferred here from *Diplocephalus*: *H. barbiger* (Roewer, 1955) comb. nov., *H. marusiki* (Eskov, 1988) comb. nov., *H. montanus* (Eskov, 1988) comb. nov. and revive the combination *H. rostratus* (Schenkel, 1934) comb. rev. (see Table 9).

Genus ***Savignia*** Blackwall, 1833
Figs 15H, J, 17G, 19C, 20H, 21D, G, 22B–C; Table 8

Type species

Savignia frontata Blackwall, 1833.

Diagnosis

Males of *Savignia* are well recognisable by the specific embolic division, where the embolus forms a so called "transparent outgrowth" (character 116; Fig. 21G) and also by the radical processes including an unique tooth-like basal radical process (character 159; Fig. 21G) and the dorsal radical process having a fold (character 141; Fig. 21D).

Homoplastic but also present in all species of node 45 is the elongated tip of the embolus bearing a slim projection (character 123; Lasut *et al*. 2009: figs 4, 8, 12) and the massive inner suprategular apophysis (character 85; Fig. 17G). Additionally, males often have a triangular palpal tibia with a hook-like prolateral tibial apophysis ending in a pointed tip (Fig. 19C). Females are best recognised by the roundly broadened anterior end of the ventral plate (character 182), the straight parallel interior margins of the ventral plate, the triangular shape of the ventral plate and oval-shaped spermathecae, oblique to parallel to each other. However, this is modified in certain species like *S. rostellatra* (Song & Li 2009: figs 33, 35) with very derived characters.

Synapomorphies

Savignia (node 45; Bremer support of 2, jackknife support of 92 (MP analysis; Fig. 26) and a bootstrap of 100 (ML analysis; Fig. 27)) is supported by the following synapomorphies (Fig. 30): the column apophysis (character 98; Fig. 21D); the transparent outgrowth at the embolus (character 116; Fig. 21D); the dorsal radical fold (character 141; Fig. 21D) and the tooth-like basal radical process (character 159; Fig. 21D). Additionally, some homoplastic characters support *Savignia*. Among these are the massive, highly sclerotised inner suprategular apophysis (character 85) and the twisted embolus (character 118). Node 46 corresponds mainly to what Eskov (1988) considered as *Savignia* excluding *S. mirabilis* comb. nov. It is worth mentioning this clade since it is supported by many characters that account for most distal species of *Savignia* and are therefore diagnostic for most species of *Savignia* (i.e., in the current analysis for all but *S. mirabilis* comb. nov. with simpler palpal conformations). Node 46 is unambiguously supported by the roundly broadened anterior end of the ventral plate (character 182). Several homoplastic characters also support this clade. Among them are the highly sclerotised, massive, blunt distal suprategular apophysis (character 90, state 10; Fig. 17G); the distal tooth on the radical tailpiece (character 170; Fig. 20H) and the AME lobe (character 209; Fig. 15J). Another character that is found in all *Savignia* but was not scored in the current analysis is the retrolaterally curved, usually twisted prolateral tibial apophysis of the male palp (e.g., Eskov 1988: fig. 85).

Remarks

This genus was described based on male specimens of *S. frontata* from England according to the six eyes (overlooking the AME on the AME lobe) and other eye characters, which are not diagnostic anymore.

The spelling of *Savignia* was a cause for debate (e.g., Bonnet 1958; Bosselaers & Hendrickx 2002; summary of spellings used since the original description in World Spider Catalog 2025). Even though

Table 8. This list contains all species that are currently assigned to *Savignia* Blackwall, 1833. Species that were scored for the cladistic analyses are marked with an asterisk (and the citation refers to figures illustrating the diagnostic characters). The remaining species are assigned to *Savignia* based on the figures cited showing the tooth-like basal radical process. The different species groups are indicated in brackets, *mirabilis*-group (M) and *zero*-group (Z). "" = ambiguous species group assignments; ??? = of uncertain assignment and probably misplaced within *Savignia*.

Status	Species name	Scored according to
Savignia (Z)	*S. amurensis* Eskov, 1991	Eskov 1991a: figs 1.1–6
Savignia (M)	*S. badzhalensis* Eskov, 1991	Eskov 1991a: figs 2.1–6
Savignia (Z)	*S. basarukini* Eskov, 1988	Eskov 1988: figs 53–59
Savignia (Z)*	*S. birostra* (Chamberlin & Ivie, 1947)	Marusik 1988: figs 5–7; Lasut *et al*. 2009: figs 1, 4
Savignia (Z)	*S. borea* Eskov, 1988	Eskov 1988: figs 60–66
Savignia (Z)	*S. bureensis* Tanasevitch & Trilikauskas, 2006	Tanasevitch & Trilikauskas 2006: figs 1–8
Savignia (M)	*S. centrasiatica* Eskov, 1991	Eskov 1991a: figs 3.1–4
Savignia ("M")	*S. ericola* Tanasevitch, 2023	Tanasevitch 2023a: figs 11–12
Savignia (Z)	*S. eskovi* Marusik, Koponen & Danilov, 2001	Marusik *et al*. 2001: figs 49–52
Savignia (M)*	*S. frontata* Blackwall, 1833	Merrett 1963: fig. 68a–d; Roberts 1987: figs 36c, 39f
Savignia (M)*	*S. mirabilis* (Eskov, 1988) comb. nov.	Eskov 1988: figs 18–24
Savignia ("M")	*S. rostellatra* Song & Li, 2009	Song & Li 2009: figs 19–35
Savignia (Z)*	*S. saitoi* Eskov, 1988	Eskov 1988: figs 67–72
Savignia (M)	*S. ussurica* Eskov, 1988	Eskov 1988: figs 76–81
Savignia (Z)	*S. yasudai* (Saito, 1986)	Saito 1986: figs 23–24, 26
Savignia (Z)*	*S. zero* Eskov, 1988	Eskov 1988: figs 83–85; Lasut *et al*. 2009: figs 9, 12
Misplaced *Savignia* species		
Not *Savignia*	*S. erythrocephalus* (Simon, 1908)	Simon 1908
Not *Savignia*	*S. fronticornis* (Simon, 1884)	Bosmans 1996: figs 36–40
Not *Savignia**	*S. harmsi* Wunderlich, 1980	Wunderlich 1980a: figs 46–51
???	*S. kartalensis* Jocqué, 1985	Jocqué 1985: figs 1–7
???	*S. kawachiensis* Oi, 1960	Oi 1960: figs 154–157
Not *Savignia*	*S. naniplopi* Bosselaers & Henderickx, 2002	Bosselaers & Henderickx 2002: figs 1–11
Not *Savignia*	*S. pseudofrontata* Paik, 1978	Paik 1978: figs 40–51
Not *Savignia*	*S. superstes* Thaler, 1984	Thaler 1984: figs 6–14

Blackwall (1833) dedicated this genus name to Jules-César Savigny he spelled it as *Savignia* throughout the original description (two times). Bonnet (1958: 3937, note 39) referring to the rules of nomenclature (art. 8, par. H, note b) neglected the spelling of *Savignia* (Blackwall 1833) and *Savignyia* (Simon 1926) and proposed *Savignya* as the correct spelling. However, according to the International Code of Zoological Nomenclature (1999), *Savignia* is an original spelling (art. 32.1.); therefore, the correct spelling of this genus is *Savignia* as spelled in the original work of Blackwall (1833).

Eskov (1988) redescribed *Savignia* according to the slightly curved and backwards directed embolus; the curved distal suprategular apophysis and the leaf-like broadened inner suprategular apophysis; the

broadly rounded, terminally unciform prolateral tibial apophysis; the distinctly emarginated anterior part of the epigyne and the pronounced dorsal plate covering half of the oval spermathecae. The current analysis agrees with most of his diagnostic characters but found some more that are discussed hereafter.

The genus *Savignia* is not monophyletic in the current analysis due to two taxa, *S. producta* and *S. harmsi* that are both proposed to be transferred to other genera. However, many more taxa that we did not include in our analysis likely do not belong to *Savignia* as defined by Eskov (1988). We agree with Eskov (1988) that *Savignia* has a few very derived characters that are not found in any other genus within the *Savignia*-group. According to our analysis this is true for node 46 that includes all Far East *Savignia* species plus *S. frontata* and is well supported by a Bremer support of 6, a jackknife support of 99 (MP analysis; Fig. 26) and a bootstrap of 100 (ML analysis; Fig. 27). We hereby include one more species, *S. mirabilis* comb. nov., that is a simpler type of *Savignia* (node 45) but shows most of the derived characters also. This is why Eskov (1988) described the species as a *Diplocephalus* rather than a *Savignia.*

In the current analysis we included six out of 24 known species of the genus *Savignia* (see Table 8). Out of all *Savignia* taxa, eleven occur in Russia (one also in Alaska), four in the Far East (Japan, China or Korea), four are known from Europe only and two are occurring all over the Palaearctic. Another one from Australia (*S. erythrocephalus* (Simon, 1908)) can be excluded from the *Savignia*-group. One from the Comoro Islands (*S. kartalensis* Jocqué, 1985) and one from Ethiopia (*S. ericola* Tanasevitch, 2023) both have uncertain assignments. We included the two Palaearctic species, one that is only found in Europe and three from the most Eastern regions of Russia (around Magadan). The Russian species are underrepresented in our matrix and the three species from Japan, China and Korea are not represented. Since the Russian species are very closely related to each other it seems that we cover most of the known variety within the Russian species. Since the three species scored from Russia occur in the most Eastern regions (around Magadan), the species from Japan, China and Korea would not have added generally new morphological features (e.g., figures in Eskov 1988, 1991a).

Savignia species groups

mirabilis-group

This group includes taxa with a massive inner suprategular apophysis that has a highly sclerotised distal facing tip (character 85, state 8; Fig. 17G) but lacking the massive highly sclerotised proximal facing tip (character 87). They have relatively simple cephalic lobes compared with the *zero*-group, i.e., a PME lobe (e.g., Eskov 1988: figs 18, 76, *S. mirabilis* comb. nov. and *S. ussurica* Eskov, 1988) but sometimes with an additional small extension of some sort (e.g., Eskov 1991a: pl. 2 fig. 1, pl.3 fig. 1, *S. badzhalensis* Eskov, 1991 and *S. centrasiatica* Eskov, 1991). It includes two species that were considered in the phylogenetic analysis, *S. mirabilis* comb. nov. and *S. frontata*, the type species of *Savignia*. However, *S. frontata* is somewhat intermediate of the *mirabilis*- and the *zero*-group, as it has an inner suprategular apophysis with only a distal branch (*mirabilis*-group) but also a very long AME lobe (*zero*-group). Three more taxa can be assigned to this group based on literature data: *S. badzhalensis*, *S. centrasiatica* and *S. ussurica*.

zero-group

This group includes species restricted to the Far East. These taxa have both a massive highly sclerotised distal and proximal facing tip on the inner suprategular apophysis (characters 85, 87). Additionally, they have very derived cephalic lobes, i.e., have an AME lobe and a PME lobe (e.g., Eskov 1988: figs 67, 83, *S. saitoi* and *S. zero*) or at least a very long AME lobe (Eskov 1988: fig. 53, *S. basarukini* Eskov, 1988). It includes: *S. amurensis* Eskov, 1991, *S. basarukini*, *S. birostra*, *S. borea* Eskov, 1988, *S. bureensis* Tanasevitch & Trilikauskas, 2006, *S. saitoi* and *S. zero*.

Savignia eskovi Marusik, Koponen & Danilov, 2001 should also belong to the *zero*-group according to the form of the cephalic lobe, which Marusik *et al.* (2001: fig. 51) discussed as being closest to *S. borea*.

The same reasoning concerns *S. yasudai* (Saito, 1986) that was assigned to *Savignia* from *Diplocephalus* by Eskov (1988) due to the cephalic lobe that is most similar to that of *S. borea*. The male palpal tibial apophysis, the embolus, the tooth-like basal radical process, the dorsal radical fold and the cephalic lobes of both species are typical for *Savignia*.

Savignia with uncertain species group assignments

The cave dwelling *S. rostellatra* cannot be assigned to any species group based on morphology alone due to its very derived male copulatory organs. It clearly belongs to *Savignia* having the unique tooth-like basal radical process (character 159; Fig. 21G) but its inner suprategular apophysis is fused to the suprategulum (distal part), covered with papillae and bearing a tooth (Song & Li 2009: fig. 28). Its cephalic lobe, however, is a simple PME lobe that would argue for the *mirabilis*-group.

Savignia ericola as mentioned by the author (Tanasevitch 2023a) is conditionally placed in *Savignia* until a female is found, based on the different shape of the distal suprategular apophysis, lacking the broad inner suprategular apophysis and the distinct shape of the male palpal tibia bearing three long strong setae. We agree with the genus assignment, as *S. ericola* has the radical conformations, including the unique tooth-like basal radical process (character 159; Fig. 21G). However, the species group assignments are more difficult. Interpretating the large sclerotised part of the suprategulum as inner suprategular apophysis rather than a distal one, would argue for the *mirabilis*-group. This would also be supported by the presence of an AME lobe like in *S. frontata* and lacking any other cephalic lobes.

Misplaced species of _Savignia_

Paik (1978) assigned *S. pseudofrontata* Paik, 1978 to *Savignia* based on its close resemblance to *S. frontata*. We do not agree with that: the vulva is spiral and much more complex than the globular spermathecae found in *S. frontata* and the radix lacks the typical processes. The radical processes and the form of the embolus (Paik 1978: figs 48, 49, 51) are somewhat similar to *S. harmsi* (Wunderlich 1980a: figs 48–49) and *D. lusiscus* (Wiehle 1963: fig. 30). The cephalic lobe looks like one found in *Araeoncus* (e.g., Tanasevitch 1987: fig. 59) and the prolateral tibial apophysis resembles what is found in some species of *Diplocephalus* (e.g., Isaia 2005: fig. 4). Based only on these observations and without phylogenetic analyses, it is not possible to assign *S. pseudofrontata* to any other genus, but it clearly belongs to the *Savignia*-group.

The position of *S. harmsi* is ambiguous in the phylogenetic analysis but always outside *Diplocephalus*. It does not have the diagnostic characters of males or females of *Savignia*. We agree with Wunderlich (1980a), who mentioned the close resemblance of the male cephalic lobe and the male secondary genital organs to *S. fronticornis*. Both seem to be intermediate between *Araeoncus* and *Diplocephalus* while *S. harmsi* seems to be closer to *Diplocephalus* and *S. fronticornis* closer to *Araeoncus*. Based on figures (e.g., in Bosmans 1996: fig. 38), *S. fronticornis* seems to have a lobe emerging from the retrolateral side of the male palpal tibia similar to *Araeoncus*. Since it is not possible to solve the appropriate generic assignment without a phylogeny that includes both taxa plus some more potential relatives, we prefer not to draw systematic conclusions for these two species here. One of these potential close relatives is *S. naniplopi* as discussed in Bosselaers & Henderickx (2002). This species is probably very close to *S. harmsi* and *S. fronticornis* based on the radix and its appendices. The cephalic lobe however bears the PME rather than the AME. Also, the epigyne and vulva of *S. naniplopi* (Bosselaers & Henderickx 2002: fig. 8) are similar to *S. fronticornis* (Bosmans 1996: fig. 40). Simon (1908) described *S. erythrocephalus* from Western Australia as similar to the Mediterranean *S. fronticornis* and *Coreorgonal monoceros* (Keyserling, 1884) from North America (Millidge 1981: fig. 147), based on the eyes and the palp but differing from them by the simpler clypeus that is neither elongated nor a small bump. No native erigonines are known from Australia and this species does not belong to the *Savignia*-group nor to *Savignia*.

Thaler (1984) underlined the problematic position of *S. superstes* Thaler, 1984 within the erigonines but placed it in the *Savignia*-group based on the form of the suprategulum and the chaetotaxy despite the lack of a bisected epigyne. The cephalic lobe resembles some species of *Diplocephalus* (e.g., *E. latifrons* comb. rev.; Fig. 15F) but differs in the position of the AME (Thaler 1984) and the epigyne is close to *Saloca*. Due to the problematic relationships within the *Savignia*-group he preferred to place in its "typical" genus rather than in another monotypic genus. The current phylogenetic analysis showed that the bisected epigyne (character 178) is synapomorphic for the *Savignia* genus group (node 21). *Savignia* is deeply nested in this group so that *S. superstes* does not belong to *Savignia*. However, a pointed radical tailpiece (character 163; Fig. 8B) is found in *S. superstes* (Thaler 1984: fig. 12) that was only observed in three taxa in the outgroup (*Walckenaeria* and "*Saloca*" in node 10) pointing to its exclusion from the *Savignia*-group also.

Oi (1960) placed *S. kawachiensis* Oi, 1960 in *Savignia* due to the close resemblance of the palp with *S. frontata* but also mentions the similarity of the cephalic lobe with certain species of *Araeoncus*. Unfortunately, the figures and text do not allow discussing this assignment. The genus assignment of *S. kartalensis* is also difficult. It does not belong to *Savignia.* Based on the literature data only, it is not possible to discuss its assignment, however, we agree with Jocqué (1985) that it belongs to the *Savignia*-group.

Miscellaneous genera within the Savignia-group

Genus *Diastanillus* Simon, 1926 (Fig. 20E)

Type species: *Diastanillus pecuarius* (Simon, 1884).

This genus was established mainly based on the form of the male cephalic lobe, leg and eye characters and its association with ants (Simon 1926) and includes only the type species *Dia. pecuarius*. It emerged as sister of node 50 that includes *Diplocephalus*, *Araeoncus* and related taxa. Its genital and somatic morphology shows characters found in one or the other of these genera, but it is clearly different to all of them. Despite the problems of monotypic genera (e.g., Platnick 1976; Prószyński 1986) this species clearly does not belong to other genera considered in this study and should keep its status. The phylogenetic position of this species is difficult to reconstruct with morphology alone due to its very derived characters that developed as adaptation to life in ant-nests.

Genus *Janetschekia* Schenkel, 1939 (Figs 15L, 18G, 21E)

Type species: *Janetschekia monodon* (O. Pickard-Cambridge, 1873).

This genus includes two species, *J. monodon* and *J. necessaria* Tanasevitch, 1985. They have a very special male cephalic lobe that is an autapomorphy of *J. monodon* in our phylogenetic analysis and only found in this genus in the current study: the inter AME–PME lobe (character 207; Fig. 15L). This genus is the earliest branching representative of the *Savignia*-group in our preferred tree (Fig. 25). It has a very simple form of circular suprategular apophysis lacking any secondary appendices like the inner or outer suprategular apophysis (but still has a marginal suprategular apophysis) and has an unmodified distal suprategular apophysis with a rounded tip. Species of this genus have a sclerotised embolic membrane (like *Saloca*) and have a massively broadened (at least the type species, unknown to the authors if this is also true for *J. necessaria*) radical tailpiece (Millidge 1977: fig. 143).

Genera *Caucasopisthes*, *Archaraeoncus*, *Dactylopisthes* and *Saloca*

The nodes between these genera are either unresolved or have a Bremer support of 1. Bootstrap values are also low (< 50) with the exception of node 19, including *Archaraeoncus* and *Dactylopisthes* with a bootstrap value of 84. The interrelationships of these taxa and the position of the subclades of this group

remain ambiguous. They share several characters like the presence of a prolateral tibial apophysis with or without appendices; the ventral or prolateral radical process of some kind (usually thin and pointed); the large, distal suprategular apophysis, directing distally; the lack of a retrolateral tibial apophysis and the lack of a bisected epigyne.

Genus *Caucasopisthes* Tanasevitch, 1990 (Fig. 19J)

Type species: *Caucasopisthes procurvus* (Tanasevitch, 1987).

This is a monotypic genus including the species *Caucasopisthes procurvus*. Tanasevitch (1987) described this species tentatively as *Dactylopisthes* and assigned it to the *Savignia*-group based on the well-developed suprategular apophysis. Its position was unclear since it showed associations to *Alioranus pauper* concerning the embolic division, to *Diplocephalus* and *Erigonella ignobilis* concerning the palpal tibia and had a unique female copulatory organ (Tanasevitch 1987). The embolic division and the suprategular apophyses are similar to *Dactylopisthes* at least based on literature data (compare Tanasevitch 1987: figs 91–92 with, e.g., Tanasevitch 1985b: figs 3–4). Based on our phylogenetic analysis and comparing the simpler cephalic lobe, the simpler tibial apophysis, the lack of an inner suprategular apophysis and the simpler epigyne *Caucasopisthes* might be a close relative of *Dactylopisthes*.

Genus *Dactylopisthes* Simon, 1884 (Figs 17B, 22A)

Type species: *Dactylopisthes digiticeps* (Simon, 1882).

This genus includes 11 species of which *Da. locketi* and *Da. mirabilis* (Tanasevitch, 1985) are particularly similar based on several ambiguous characters from the phylogenetic analysis and the unambiguous synapomorphy (Fig. 29): the anteriorly folded ventral plate (character 191; Fig. 22A). Among the supporting homoplastic characters are the short, robust, blunt and twisted triangular inner suprategular apophysis (character 85, state 1); the distal suprategular apophysis that protrudes and covers the tegulum and exceeds the cymbium (character 90, state 0) and the prolateral radical apophysis (character 157).

Another nine species, of which five have recently been described, are currently assigned to *Dactylopisthes.* Based on the figures available, *Da. ramit* Tanasevitch, 2023 seems to fit well to the above mentioned species (Tanasevitch 2023b: figs 1–12, 14–15). According to Zhao & Li (2014: figs 30–31) this is also true for *Da. separatus* Zhao & Li, 2014 only known from females.

Dactylopisthes video (Chamberlin & Ivie, 1947) (Tanasevitch 1984: pl. 5, figs 3–10) and *Da. digiticeps* (Bosmans *et al.* 2009: figs 1–6) can also be assigned to this group of species based on figures of the prolateral radical process, the form of the distal suprategular apophysis, the thin but long tibial apophysis and the anteriorly curved posterior ends of the dorsal plate in females. *Dactylopisthes khatipara* Tanasevitch, 2017 also shares most characters with *Da. video* according to Tanasevitch (2017: figs 1–8).

The assignments of *Da. mirificus* (Georgescu, 1976) and *Da. diphyus* (Heimer, 1987) are more difficult for the females since the anteriorly folded posterior tips of the ventral plate are not detectable on the figures. However, the males of *Da. mirificus* (Georgescu 1976: figs 1–13) and *Da. diphyus* (Heimer 1987: figs 4–8; Song *et al*. 1999: fig. 91a–d) seem to have a prolateral radical process and the same type of tibial apophysis with a retrolateral appendix upon it. The cephalic PME lobes, even though smaller in *Da. mirificus*, are also similar to *Da. video* and *Da. digiticeps*.

Dactylopisthes dongnai Tanasevitch, 2018 and *Da. marginalis* Tanasevitch, 2018 form a separate species group as already noted by Tanasevitch (2018a, 2018b). They are morphologically quite outstanding from the other species of *Dactylopisthes*, lacking most of the typical characters (Tanasevitch 2018a: figs 1–7, 2018b: figs 1–10).

Table 9. Systematic consequences (see genus sections for synapomorphies).

Junior synonym	**Valid genus**
Paraglyphesis Eskov, 1991	*Glyphesis* Simon, 1926
Previous rank	**New rank**
Diplocephalus Bertkau, 1883 subgenus *Hemistajus* Schenkel, 1934	*Hemistajus* Schenkel, 1934 resurrected rank Type species: *Hemistajus rostratus* (Schenkel, 1934) comb. rev.
Previous combination	**New and revived combinations (comb. nov. / comb. rev.)**
Savignia producta Holm, 1977	*Erigonella producta* (Holm, 1977) comb. nov.
Diplocephalus latifrons (O. Pickard-Cambridge, 1863)	*Erigonella latifrons* (O. Pickard-Cambridge, 1863) comb. rev.
Diplocephalus connatus Bertkau, 1889	*Erigonella connatus* (Bertkau, 1889) comb. nov.
Diplocephalus marusiki Eskov, 1988	*Hemistajus marusiki* (Eskov, 1988) comb. nov.
Diplocephalus montanus Eskov, 1988	*Hemistajus montanus* (Eskov, 1988) comb. nov.
Diplocephalus rostratus Schenkel, 1934	*Hemistajus rostratus* (Schenkel, 1934) comb. rev.
Diplocephalus barbiger (Roewer, 1955)	*Hemistajus barbiger* (Roewer, 1955) comb. nov.
Diplocephalus mirabilis Eskov, 1988	*Savignia mirabilis* (Eskov, 1988) comb. nov.
Paraglyphesis polaris Eskov, 1991	*Glyphesis polaris* (Eskov, 1991) comb. nov.
Paraglyphesis monticola Eskov, 1991	*Glyphesis monticola* (Eskov, 1991) comb. nov.
Paraglyphesis lasiargoides Eskov, 1991	*Glyphesis lasiargoides* (Eskov, 1991) comb. nov.
Diplocephalus protuberans (O. Pickard-Cambridge, 1875)	*Araeoncus protuberans* (O. Pickard-Cambridge, 1875) comb. nov.
Diplocephalus dentatus Tullgren, 1955	*Araeoncus dentatus* (Tullgren, 1955) comb. nov.
Diplocephalus helleri (L. Koch, 1869)	*Araeoncus helleri* (L. Koch, 1869) comb. nov.
Diplocephalus marijae Bosmans, 2010	*Araeoncus marijae* (Bosmans, 2010) comb. nov.
Saloca ryvkini Eskov & Marusik, 1994	*Walckenaeria ryvkini* (Eskov & Marusik, 1994) comb. nov.

Genus *Archaraeoncus* Tanasevitch, 1987

Type species: *Archaraeoncus prospiciens* (Thorell, 1875).

This genus currently includes four species of which *Ar. alticola* Tanasevitch, 2008 and *Ar. proscipiens* are presumably closely related based on the very similar tibial apophysis and inner suprategular apophysis (character 85, state 5). The preferred tree proposes *Dactylopisthes* as the closest relative of *Archaraeoncus* (node 19). This is also supported by the cephalic PME lobe of *Ar. alticola* that is very similar to *Da. video* and *Da. mirificus*. The radical process in *Ar. proscipiens* was coded as a ventral radical process; however, it might be a prolateral one, which would argue again for a closer relation to *Dactylopisthes*. *Archaraeoncus sibiricus* Eskov, 1988 shows many conformations intermediate to *Archaraeoncus*, *Dactylopisthes* and *Dactylopisthoides*. The male cephalic lobe is closest to *Ar. proscipiens* and the radical process to *Dactylopisthoides*, at least according to literature data (compare Eskov 1988: fig. 3 with Eskov 1990: fig. 2). A closer comparison of the epigyne and the vulva of these genera might enlighten their relationships. According to Eskov (1988), *Archaraeoncus* is closer to the *Leptorhoptrum*/*Lophomma* group of Millidge (1977) and does not belong to the *Savignia*-group. This cannot be answered without considering any member of that group, but Millidge (1977) already mentions

the close relations of this group with *Hilaria*, *Tapinocyba* and *Savignia*. In the current phylogenetic analysis *Archaraeoncus* emerged closer to *Hilaira* than to *Savignia.*

Genus *Saloca* Simon, 1926 (Figs 1L, 3F, 8C, 9L, 13H–I, 14L, 18I, 20I)

Type species: *Saloca diceros* (O. Pickard-Cambridge, 1871).

The genus *Saloca* currently includes six species. However, only two very similar species, *Sa. diceros* and *Sa. kulczynskii*, belong to this genus in the current analysis. They emerge as sister species (node 28) in the phylogenetic analyses and are well supported by a Bremer support of 16, a jackknife support of 100 (MP analysis; Fig. 26) and a bootstrap of 100 (ML analysis; Fig. 27) with the following synapomorphies (Fig. 29): the simple broad distal suprategular apophysis with an incised tip (character 90, state 9); the twisted ventral radical process (character 131) and the longitudinally and densely packed inter AME–PME setae (character 198). Additionally, some ambiguous characters support this clade. Among these characters are the cymbial retrobasal process (character 53) that is also present in *Bolyphantes* L. Koch, 1837, the sclerotised embolic membrane (character 100); the ventral radical hook (character 135, state 0); the massively broadened tip of the radical tailpiece (character 164) that is only basally constricted in this clade; the anteriorly extending dorsal plate of the epigyne (character 188, supporting node 8 also) and the single proximal dorsal trichobothrium on the female palpal tibia (see character 246). *Saloca* is also the only taxon within the *Savignia*-group that lacks a marginal suprategular apophysis (character 78).

Currently four more species are assigned to *Saloca*, which are not closely related to *Saloca* or any other *Savignia*-group member. Of these, *Sa. ryvkini* was considered as "extremely close to *Sa. nigra*" "by the shape of the male carapace and genitalia" (Eskov & Marusik 1994). *Saloca nigra* was synonymised with *Walckenaeria stylifrons* (O. Pickard-Cambridge, 1875) by Wunderlich (1972). This close resemblance can be seen in the drawings of, e.g., Eskov & Marusik (1994: figs 54, 57) and Roberts (1987: figs 3d, 8e). We agree that *Sa. ryvkini* is morphologically more similar to *W. stylifrons* than to any other species currently assigned to *Saloca*. The form of the embolus and the two bunches of merged setae on the male cephalic lobe and the form of the tibial apophysis for example. Consequently, *Sa. ryvkini* is hereby transferred to *Walckenaeria* (see Table 9). According to Wunderlich (2011), *Saloca elevata* Wunderlich, 2011, described from Turkey, is probably closely related to the European species of *Saloca* as it also bears tiny denticles on the retrolateral side of the prolateral tibial apophysis.

Saloca gorapaniensis and *Sa. khumbuensis* (node 12) were also questioned to belong to *Saloca* (Eskov & Marusik 1994). In the current analyses, they show affiliations with *Walckenaeria* (node 10) supported by the general conformation of the embolic division (the radical tailpiece, radix and embolus form a spiral; unambiguous synapomorphy of node 10; character 172) and with members of the *Pelecopsis*-group (node 13) rather than with the *Savignia*-group (Fig. 28). This confirms the isolated morphological position of these two species. Based on the characters scored for the current analysis, these two species belong to the *Pelecopsis*-group. Homoplastic characters like the membranous distal suprategular apophysis (character 90, state 13; convergently also present in *Diplocephalus turcicus*) and the spine formula 1111 (2211 in the *Savignia*-group) account for this. These two species should be considered in a similar project as the current one on the *Pelecopsis*-group to synonymise them with an already existing genus or to establish a new genus for them. According to Wunderlich (1983), they are close to *Horcotes strandi* (Sytshevskaja, 1935) and *Alioranus chiardolae* while Eskov & Marusik (1994) argue that they neither belong to *Saloca* nor *Horcotes* Crosby & Bishop, 1933.

Outside the Savignia genus group

Genus *Alioranus* Simon, 1926 (Figs 1A, 4A, 5A, 6F, 9A, 10A, B, 12A, B, 14A)

Type species: *Alioranus pauper* (Simon, 1882).

We included three out of four species from this genus in the *Savignia* genus group phylogeny. *Alioranus chiardolae* always emerged outside the *Savignia*-group close to *Hilaria*, while *Al. pauper* the type species and *Al. pastoralis* either emerged in a clade with *Al. chiardolae* (equal weights; ML; implied weights *k* value 23 or higher) or else as sister clade to *Dactylopisthes* (implied weights with a *k* value lower than 11).

Alioranus should be restricted to *Al. pauper* and *Al. pastoralis*, i.e., node 6, which is supported by a Bremer support of 3, a jackknife support of 78 (MP analysis; Fig. 26) and a bootstrap of 99 (ML analysis; Fig. 27) and by several homoplastic characters, among which are the following (Fig. 28): the prolateral radical process (character 157) and the nearly smooth booklung covers (character 225). The prolateral radical process is absent in most taxa; however, node 6, uniting *Al. pauper* and *Al. pastoralis*, has a unique thread-like prolateral radical process that does not occur in any other species in the current analysis and might be a diagnostic of *Alioranus* (character 158, state 0).

Alioranus chiardolae has a very simple palpal conformation compared to the former species and is probably not very closely related with *Alioranus*. Wunderlich (1995) mentions that *Al. chiardolae* is most probably a new monotypic genus due to its long palpal tibial apophysis and the form of the epigyne. *Alioranus diclivitalis* Tanasevitch, 1990 lacks a thread-like prolateral radical process and therefore probably does not belong to *Alioranus*. However, its epigyne is quite similar to *Al. pastoralis* (Wunderlich 1980b: fig. 14). It is also clearly different from *Al. chiardolae* (e.g., the tibial apophysis; Tanasevitch 1990: fig. 3) but cannot be assigned to any other taxon considered in this analysis.

Discussion

Relationships in the *Savignia* genus group

We find that most genera in the *Savignia* genus group (node 21) are not monophyletic and *Alioranus* does not belong to the *Savignia* genus group (Fig. 25). *Saloca* emerges within the early branching taxa of the *Savignia* genus group (Fig. 25). It is also polyphyletic according to our analyses as two of the species that we included seem to be more closely related to taxa in the *Pelecopsis*-group. This position of *Saloca* is in accordance with Frick *et al.* (2010). The only two genera that emerge as monophyletic in the equal weights analysis are *Araeoncus* and *Dicymbium* (Supp. file 2), however, many of their species were not included here. *Archaraeoncus* and *Dactylopisthes* form a clade (node 19) which is the sister group to the *Savignia* genus group. Within the *Savignia* genus group the main problem is the genus *Diplocephalus*, where many species with uncertain assignments have been dumped traditionally, often based on characters such as the form of the cephalic lobes. However, this character has been known as inappropriate for generic delimitations (Holm 1977). In our results, species assigned to *Diplocephalus* appear all over the tree of the *Savignia* genus group indicating the need for a revision of this genus. Here, as several species are not included in the analyses, our taxonomic decisions are restricted to a minimum (see Table 9) and we redefine *Diplocephalus* as the clade that includes *Diplocephalus cristatus* which is the type species of the genus. Further taxonomic discussion is provided in the Systematics section.

The addition of new characters in the present work resulted in a higher number of most parsimonious trees compared to Frick *et al*. (2010). The strict consensus tree in the equal weighting analyses (Supp. file 2) has only four polytomies (nodes 11, 17, 23 and 67) and the implied weighting analysis always resulted in fully resolved topologies. However, deeper nodes of the tree remain poorly supported (Figs 26–27). The weak support for the backbone of the *Savignia* genus group can be traced back to the fact that only a few synapomorphies were found at that level (Fig. 29). Finding informative characters above genus level is often more difficult due to difficulties assessing homologies and difficulties with scoring morphological variation into discrete character states. Current practice usually avoids defining characters that summarize several other subordinate characters. In the current analysis we found a few

characters for which this was possible like character 36 that includes several presumably homologous non-sclerotised extensions of the male palpal tibia. Alternatively, many authors refined characters by splitting them into a set of characters each with a small number of states. The latter option unfortunately often leads to the appearance of inapplicables. However, the practice of defining multistate characters might have a negative effect on support values of backbone nodes. Poor backbone support is a common problem in morphological analyses (see, e.g., Ruta *et al.* 2003: fig. 4; Miller & Hormiga 2004: fig. 3).

In the current analysis, shallower nodes were generally well supported and have many synapomorphies (e.g., nodes 22, 28, 29, 34, 37, 43, 46, 53, 57, 63). However, some taxa remain problematic, especially those with only a few derived characters. Character systems like the various apophyses of the male palpal tibia offered nearly 40 characters altogether. However, the absence of one of these structures (e.g., the retrolateral tibial apophysis) leads to many inapplicables. The absence of these structures can either be an ancestral state or can be due to a secondary loss. In the current analysis some of the taxa with "simple" genital morphology clustered together which may be an artifact because of inapplicables (e.g., node 19). Some problems concerning morphological characters mentioned in Rieppel (2007) were also found in the current analysis. These problems arise from "scope expansions" leading to incomplete characters, subdivision of characters and ambiguity of anatomical terms.

It is also worth noting that not all newly defined characters are entirely novel. In a few cases we refined previous characters to account for different states discernible within the current set of taxa.

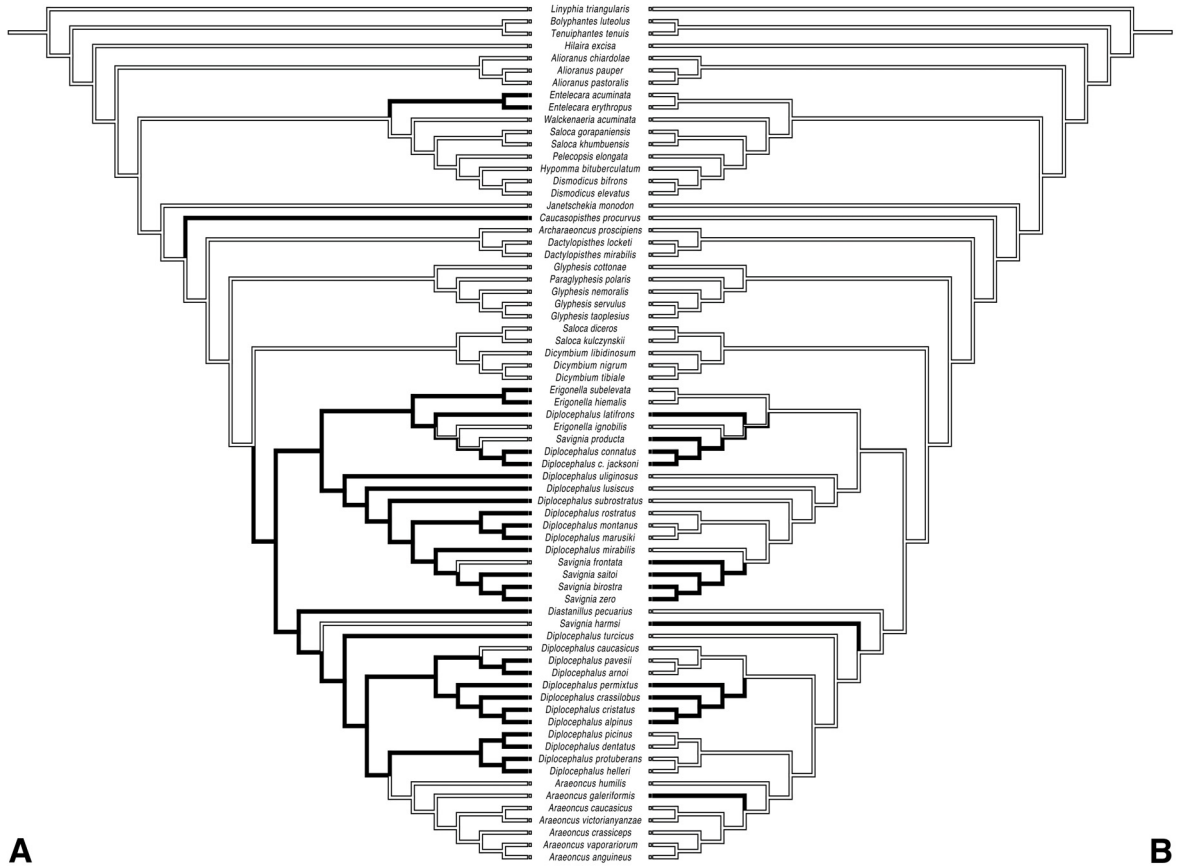

Fig. 32. Preferred tree showing the evolution of (32A) the PME lobe (character 204) (black) and (32B) the AME lobe (character 209) (black).

Some instances of ambiguity of anatomical terms arose, for example, the cymbial retrobasal process (character 53) in Miller & Hormiga (2004) as character 4. Most of the newly scored taxa have a structure at the same position but referring to the character description in Miller & Hormiga (2004) its conformation was different in the newly scored taxa (see discussion of character 53). Consequently, a new character was defined to account for that variation. Even after the analysis it remains unclear whether these two characters are the same.

The current manuscript also highlights the value of morphology-based phylogenies in a time when molecular analyses are becoming dominant in systematics research. Highly diverse taxa with species-specific and often narrow ecological niches like erigonines make it difficult to obtain abundant material for all species. Thus, some species are often known only from their type specimens which hinders molecular work (given their small size and long time since specimens were collected) but these are still available to score for morphological characters.

Morphology and evolution of cephalic lobes in the *Savignia* genus group

Erigonine spiders exhibit a wide variety of cephalic modifications (e.g., lobes, sulci, pits and pores) in males which seem to be involved in courtship (Hormiga 2000; Lin *et al*. 2021). During courtship females insert the cheliceral fang in the cephalic modifications such as the sulci of the male and ingest the glandular secretions produced by the male cephalic secretory gustatory glands (Hormiga 2000; Kunz *et al*. 2012). These traits involved during courtship have been suggested to be under the

Fig. 33. Preferred tree showing the evolution of (33A) the clypeal lobe (character 208) (black) and (33B) the cephalic sulci (character 212) (black).

influence of sexual selection because of its role during mating behaviour (Lin *et al*. 2022). Previous studies (Hormiga 2000; Lin *et al.* 2021) have mentioned that cephalic modifications have most probably evolved independently multiple times. Our results support this idea (Figs 32–33). The three main types of cephalic lobes, i.e., the AME lobe, the PME lobe and the clypeal lobe as well as the cephalic sulci appear multiple times across species of the *Savignia* genus group. Some of these modifications have a single origin within a given clade, for example the cephalic clypeal lobe (character 208) can be used as a diagnostic character in *Glyphesis* (Fig. 33A), but in general, genera commonly include species with and without these cephalic lobes (Figs 32–33).

The cephalic PME lobe appears at node 31 which includes *Erigonella*, *Hemistajus*, *Savignia*, *Diastanillus*, *Diplocephalus* and *Araeoncus* (excluding the taxa originally assigned to *Araeoncus* (node 63)) (Fig. 32A). The cephalic AME lobe appears arbitrarily within *Erigonella*, *Savignia*, *Diplocephalus* and *Araeoncus* clades (Fig. 32B). We scored several other cephalic modifications like sulci, pits and cuticular pores that appear independently throughout the *Savignia* genus group taxa (e.g., Fig. 33B). Although, we should take into consideration that making hypothesis about the evolution of the male cephalic modifications is risky as this is a very complex character system (Hormiga 2000), our results support that cephalic modifications are highly homoplastic as similar cephalic modifications occur multiple times in closely related groups. The convergent occurrence of these traits and the fact that they are involved in courtship (Michalik & Uhl 2011; Kunz *et al*. 2012; Lin *et al*. 2021) suggest that they are likely under sexual selection, leading to high phenotypic plasticity and very dynamic evolutionary patterns of these characters.

Acknowledgements

We would like to thank the following individuals and institutions for the loan of material: Peter Jäger (Senckenberg Museum Frankfurt, DE; SMF), Ambros Hänggi (Natural History Museum Basel, CH; NMB), Peter Schwendinger (Natural History Museum of Geneva, CH; MHNG), Yvonne Kranz-Baltensperger (Natural History Museum of Bern, CH; NMBE), Yuri Marusik (Institute for Biological Problems of the North, Magadan, RU), Andrei Tanasevitch (Russian Academy of Sciences, Moscow, RU), Robert Bosmans (Ghent University, BE), Rudy Jocqué (Musée royal de l'Afrique centrale, Tervuren, BE; MRAC), Nikolaj Scharff (Natural History Museum of Denmark, Copenhagen, DK; ZMUC), Efrat Gavish-Regev (Hebrew University of Jerusalem, IL), Christo Deltshev (Bulgarian Academy of Sciences, Sofia, BG), Barbara Knoflach-Thaler (University of Innsbruck, AT) and Marco Isaia (University of Turin, IT). This project was financed by a scholarship from the Liechtensteinische Stipendienkommission, the University of Bern and the Natural History Museum of Bern. SEM photography in Copenhagen was supported by a grant from the European Commission's (FP 6) Integrated Infrastructure Initiative programme SYNTHESYS (DK-TAF 3480). For translations we would like to thank Youna Zahn and Gian-Luca Bernasconi. For the support providing funding we would like to thank Wolfgang Nentwig (University of Bern, CH). For the help with the revision of the manuscript and with the analysis of the data we would like to thank Dimitar Dimitrov (University Museum of Bergen, Norway). Annui Sanz is also thankful for the Meltzerfondets tildeling 2023 support to visit museum collections (Prosjektstipend 104147101). For the comprehensive review of the manuscript we would like to thank Gustavo Hormiga and one anonymous reviewer as well as Pepe Fernández for editing the manuscript.

References

Arnedo M.A., Hormiga G. & Scharff N. 2009. Higher-level phylogenetics of linyphiid spiders (Araneae, Linyphiidae) based on morphological and molecular evidence. *Cladistics* 25: 231–262. https://doi.org/10.1111/j.1096-0031.2009.00249.x

Blackwall J. 1833. XXI. Characters of some undescribed genera and species of Araneidae. *The London, Edinburgh, and Dublin Philosophical Magazine and Journal of Science* 3 (14): 104–112. https://doi.org/10.1080/14786443308648135

Blackwall J. 1834. IX. Characters of some undescribed species of Araneidae. *The London, Edinburgh, and Dublin Philosophical Magazine and Journal of Science* 5 (25): 50–53. https://doi.org/10.1080/14786443408648400

Blackwall J. 1836. LXXXIII. Characters of some undescribed species of Araneidae. *The London and Edinburgh Philosophical Magazine and Journal of Science* 8 (49): 481–491. https://doi.org/10.1080/14786443608648925

Blackwall J. 1841. XLII. The difference in the number of eyes with which spiders are provided proposed as the basis of their distribution into tribes; with descriptions of newly discovered species and the characters of a new family and three new genera of spiders. *Transactions of the Linnean Society of London* 18 (4): 601–670. https://doi.org/10.1111/j.1095-8339.1838.tb00210.x

Blackwall J. 1852. A catalogue of British spiders including remarks on their structure, function, economy and systematic arrangement. *Annals and Magazine of Natural History* 9 (49, 52, 44): 15–22, 268–275, 464–471; 10 (57, 58): 182–189, 248–253. https://doi.org/10.1080/03745485609495691

Blest A.*D.* 1976. The tracheal arrangement and the classification of linyphiid spiders. *Journal of Zoology* 180 (2): 185–194. https://doi.org/10.1111/j.1469-7998.1976.tb04672.x

Blick T. & Szinetar C. 1996. *Glyphesis conicus* ist ein jüngeres Synonym von *Glyphesis taoplesius* (Araneae: Linyphiidae). *Arachnologische Mitteilungen* 11: 39–42. https://doi.org/10.5431/aramit1105

Bonnet P. 1958. *Bibliographia araneorum: analyse méthodique de toute la littérature aranéologique jusqu'en 1939, Vol. 2 (4)*: 3027–4230.

Bösenberg W. & Strand E. 1906. Japanische Spinnen. *Abhandlungen der Senckenbergischen Naturforschenden Gesellschaft* 30: 93–422.

Bosmans R. 1996. The genera *Araeoncus* Simon, *Delorripis* Simon and *Diplocephalus* Bertkau in northern Africa (Araneae: Linyphiidae: Erigoninae) Studies on north African Linyphiidae VII. *Belgian Journal of Zoology* 126 (2): 123–151.

Bosmans R. 2002. Les genres *Acartauchenius* Simon et *Thaumatoncus* Simon en Afrique du Nord. Études sur les Linyphiidae nord-africaines no. IX (Araneae: Linyphiidae: Erigoninae). *Revue arachnologique* 14 (1): 1–24.

Bosmans R. & Jocqué R. 1983. Scientific report of the Belgian Mount Cameroon Expedition 1981. No. 9. Family Linyphiidae (Araneae). *Revue de Zoologie africaine* 97 (3): 581–617.

Bosmans R., Baert L., Bosselaers J., De Koninck H., Maelfait J.-P. & Van Keer J. 2009. Spiders of Lesbos (Greece). *Nieuwsbrief van de Belgische Arachnologische Vereniging* 24: 1–70.

Bosmans R., Cardoso P. & Crespo L.C. 2010. A review of the linyphiid spiders of Portugal, with the description of six new species (Araneae: Linyphiidae). *Zootaxa* 2473 (1): 1–67. https://doi.org/10.11646/zootaxa.2473.1.1

Bosselaers J. & Hendericks H. 2002. A new *Savignia* from Cretan caves (Araneae: Linyphiidae). *Zootaxa* 109 (1): 1–8. https://doi.org/10.11646/zootaxa.109.1.1

Breitling R. 2021. A completely resolved phylogenetic tree of British spiders (Arachnida: Araneae). *Ecologica Montenegrina* 46: 1–51. https://doi.org/10.37828/em.2021.46.1

Bremer K. 1994. Branch support and tree stability. *Cladistics* 10: 295–304. https://doi.org/10.1111/j.1096-0031.1994.tb00179.x

Brignoli P.M. 1971. Note su ragni cavernicoli italiani (Araneae). *Fragmenta Entomologica* 7 (1): 121–229.

Brignoli P.M. 1972. Terzo contributo alla conoscenza dei ragni cavernicoli di Turchia (Araneae). *Fragmenta Entomologica* 8: 161–190.

Brignoli P.M. 1979. Ragni d'Italia XXXII. Specie cavernicole di Sicilia (Araneae). *Animalia* 5 (1–3): 273–286.

Burger M. & Nentwig W. 2002. *Opopaea fosuma*, n. sp. from Sumatra, Indonesia (Araneae, Oonopidae). *Bulletin of the British Arachnological Society* 12: 244–248.

Chamberlin R.V. & Ivie W. 1947. The spiders of Alaska. *Bulletin of the University of Utah* 37 (10): 1–103.

Clerck C. 1757. *Aranei Svecici. Svenska spindlar, uti sina hufvud-slågter indelte samt under några och sextio särskildte arter beskrefne och med illuminerade figurer uplyste.* Laurentius Salvius, Stockholm. https://doi.org/10.5962/bhl.title.119890

Coddington J. & Scharff N. 1994. Problems with zero-length branches. *Cladistics* 10: 415–423. https://doi.org/10.1111/j.1096-0031.1994.tb00187.x

Comstock J.H. 1910. The palpi of male spiders. *Annals of the Entomological Society of America* 3 (3): 161–185. https://doi.org/10.1093/aesa/3.3.161

Crosby C.R. & Bishop S.C. 1933. American spiders: Erigoneae, males with cephalic pits. *Annals of the Entomological Society of America* 26 (1):105–182. https://doi.org/10.1093/aesa/26.1.105

Dahl F. 1886. Monographie der *Erigone*-Arten im Thorell'schen Sinne, nebst anderen Beiträgen zur Spinnenfauna Schleswig-Holsteins. *Schriften des Naturwissenschaftlichen Vereins für Schleswig-Holstein* 6: 65–102. Available from https://www.biodiversitylibrary.org/page/12082668 [accessed 7 Apr. 2025].

Dahl F. 1901. Über die Seltenheit gewisser Spinnenarten. *Sitzungsberichte der Gesellschaft Naturforschender Freunde zu Berlin* 10: 257–266.
Available from https://www.biodiversitylibrary.org/page/8798665 [accessed 7 Apr. 2025].

Deltshev C.D. 1984. A new *Diplocephalus* species from the Bulgarian Mountains (Arachnida, Araneae, Erigonidae). *Reichenbachia* 22: 91–93.

Deltshev C. 1987. A critical review of genus *Araeoncus* Simon in Bulgaria, with description of a new species (*Araeoncus clivifrons* sp. n.) (Arachnida, Araneae, Erigonidae). *Reichenbachia* 25 (19): 97–102.

Denis J. 1952. Araignées récoltées en Roumanie par Robert Leruth, avec un appendice sur quelques araignées cavernicoles de Belgique. *Bulletin de l'Institut royal des Sciences naturelles de Belgique* 28: 1–50.

Denis J. 1953. Araignées des environs du Marcadau et du Vignemale (Hautes-Pyrénées). *Bulletin de la Société d'Histoire naturelle de Toulouse* 88 (1–2): 83–112.

Denis J. 1965. Notes sur les érigonides. XXIX. Une forme pyrénéenne d'*Erigonella subelevata* (L. Koch). *Bulletin de la Société zoologique de France* 89: 673–675.

di Caporiacco L. 1935. Aracnidi dell'Himalaia e del Karakoram, raccolti dalla Missione italiana al Karakoram (1929–VII) (Continuazione). *Memorie della Società Entomologica Italiana* 13: 161–263. Available from https://www.biodiversitylibrary.org/page/64054057 [accessed 7 Apr. 2025].

di Caporiacco L. 1936. Saggio sulla fauna aracnologica del Casentino, Val d'Arno Superiore e Alta Val Tiberina. *Festschrift für Prof. Dr. E. Strand* 1: 326–369.

di Caporiacco L. 1949. Aracnidi della colonia del Kenya raccolti da Toschi e Meneghetti negli anni 1944-1946. *Commentationes Pontificia Academia Scientiarum* 13: 309–492.

Eskov K.Y. 1988. The spider genera *Savignya* Blackwall, *Diplocephalus* Bertkau and *Archaraeoncus* Tanasevitch (Aranei, Linyphiidae) in the fauna of Siberia and the Soviet Far East. *Folia Entomologica Hungarica* 49: 13–39.

Eskov K.Y. 1989. New Siberian species of erigonine spiders (Arachnida, Aranei, Linyphiidae). *Spixiana* 11 (2): 97–109.

Eskov K.Y. 1990. On the erigonine spider genera *Dactylopisthes* Simon, 1884 and *Dactylopisthoides* gen. nov. (Arachnida, Araneae: Linyphiidae). *Reichenbachia* 28 (1): 1–5.

Eskov K.Y. 1991a. A spider genus *Savignya* (s. str.) (Aranei, Linyphiidae) in the fauna of the Far East and central Asia. *Zoologichesky Zhurnal* 70 (5): 140–144.

Eskov K.Y. 1991b. New linyphiid spiders from Siberia and the Far East 2. The genus *Paraglyphesis* gen. nov. (Arachnida, Araneae: Linyphiidae). *Reichenbachia* 28: 103–107.

Eskov K.Y & Marusik YM. 1994. New data on the taxonomy and faunistics of North Asian linyphiid spiders (Aranei Linyphiidae). *Arthropoda Selecta* 2 (4): 41–79.

Esyunin S.L & Efimik V.E. 1994. *Glyphesis nemoralis* sp. n. (Aranei, Linyphiidae) from nemoral forests of the east European plain and the Urals. *Zoologichesky Zhurnal* 73 (1): 157–159.

Farris J.S., Albert V.A., Källersjö M., Lipscomb D. & Kluge A.G. 1996. Parsimony jackknifing outperforms neighbor-joining. *Cladistics* 12: 99–124. https://doi.org/10.1111/j.1096-0031.1996.tb00196.x

Frick H. & Isaia M. 2012. Comparative description of the Mediterranean erigonine spider *Diplocephalus guidoi* n. sp. (Araneae, Linyphiidae). *Zootaxa* 3475: 65–68. https://doi.org/10.11646/zootaxa.3475.1.6

Frick H. & Muff P. 2009. Revision of the genus *Caracladus* Simon, 1884 with the description of *Caracladus zamoniensis* spec. nov. (Araneae, Linyphiidae, Erigoninae). *Zootaxa* 1982 (1): 1–37. https://doi.org/10.11646/zootaxa.1982.1.1

Frick H. & Scharff N. 2014. Phantoms of Gondwana? – phylogeny of the spider subfamily Mynogleninae (Araneae: Linyphiidae). *Cladistics* 30 (1): 67–106. https://doi.org/10.1111/cla.12025

Frick H., Nentwig W. & Kropf K. 2010. Progress in erigonine spider phylogeny – the *Savignia*-group is not monophyletic (Araneae: Linyphiidae). *Organisms, Diversity & Evolution* 10: 297–310. https://doi.org/10.1007/s13127-010-0023-1

Georgescu M. 1976. *Scytiella mirifica* n.g. n.sp. (Araneae-Micryphantidae) de Roumanie. *Travaux de l'Institut de Spéologie "Émile Racovitza"* 15: 9–16.

Gnelitsa V.A. 2004. *Araeoncus tauricus* sp.n.: a new spider species (Araneae: Linyphiidae) from the Crimea, Ukraine. *In*: Logunov D.V. & Penney D. (eds) *European Arachnology 2003. Proceedings of the 21st European Colloquium of Arachnology* St Petersburg. *Arthropoda Selecta* Special Issue 1: 79–82.

Gnelitsa V.A. 2006. A new species of the genus *Diplocephalus* Bertkau, 1883 (Aranei: Linyphiidae) from the Crimea. *Arthropoda Selecta* 14 (4): 373–376.

Goloboff P.A. 1993. Estimating character weights during tree search. *Cladistics* 9 (1): 83–91. https://doi.org/10.1111/j.1096-0031.1993.tb00209.x

Goloboff P.A., Farris J.S. & Nixon K.C. 2008a. TNT, a free program for phylogenetic analysis. *Cladistics* 24 (5): 774–786. https://doi.org/10.1111/j.1096-0031.2008.00217.x

Goloboff P.A., Carpenter J.M., Arias J.S. & Miranda-Esquivel D.R. 2008b. Weighting against homoplasy improves phylogenetic analysis of morphological data sets. *Cladistics* 24 (5): 1–16. https://doi.org/10.1111/j.1096-0031.2008.00209.x

Heimer S. 1987. Neue Spinnenarten aus der Mongolei (MRV) (Arachnida, Araneae, Theridiidae et Linyphiidae). *Reichenbachia* 24 (20): 139–151.

Hoang D.T., Chernomor O., Von Haeseler A., Minh B.Q. & Vinh L.S. 2018. UFBoot2: Improving the ultrafast bootstrap approximation. *Molecular Biology and Evolution* 35 (2): 518–522. https://doi.org/10.1093/molbev/msx281

Holm Å. 1962. The spider fauna of the East African Mountains. *Zoologiska Bidrag fran Uppsala* 35: 19–210.

Holm Å. 1967. Spiders (Araneae) from west Greenland. *Meddelelser om Grønland* 184 (1): 1–99.

Holm Å. 1977. Two new species of the erigonine genera *Savignia* and *Silometopus* (Araneae: Linyphiidae) from Swedish Lapland. *Entomologica Scandinavica* 8 (3): 161–166. https://doi.org/10.1163/187631277X00224

Hormiga G. 1994a. Cladistics and the comparative morphology of linyphiid spiders and their relatives (Araneae, Araneoidea, Linyphiidae). *Zoological Journal of the Linnean Society* 111 (1): 1–71. https://doi.org/10.1111/j.1096-3642.1994.tb01491.x

Hormiga G. 1994b. A revision and cladistic analysis of the spider family Pimoidae (Araneoidea: Araneae). *Smithsonian Contributions to Zoology* 549: 1–104. https://doi.org/10.5479/si.00810282.549

Hormiga G. 2000. Higher level phylogenetics of erigonine spiders (Araneae, Linyphiidae, Erigoninae). *Smithsonian Contributions to Zoology* 609: 1–160. https://doi.org/10.5479/si.00810282.609

International Commission on Zoological Nomenclature 1999. *International Code of Zoological Nomenclature. Fourth edition*. The International Trust for Zoological Nomenclature, London. Available from https://www.iczn.org/the-code/the-code-online/ [accessed 7 Apr. 2025].

Irfan M., Wang L.Y. & Zhang Z.S. 2023. Survey of Linyphiidae spiders (Arachnida: Araneae) from Wulipo National Nature Reserve, Chongqing, China. *European Journal of Taxonomy* 871: 1–85. https://doi.org/10.5852/ejt.2023.871.2129

Irfan M., Zhou G.C. & Peng X.J. & Zhang Z. 2025. Survey of Linyphiidae spiders (Arachnida: Araneae) from some oriental regions of China. *Megataxa* 15 (1): 1–248. https://doi.org/10.11646/megataxa.15.1.1

Isaia M. 2005. *Diplocephalus arnoi* n. sp. un nuovo Linyphiidae d'Abruzzo (Araneae). *Fragmenta Entomologica* 37: 1–7.

Janetschek H. 1956. Das Problem der inneralpinen Eiszeitüberdauerung durch Tiere (Ein Beitrag zur Geschichte der Nivalfauna). *Österreichische Zoologische Zeitschrift* 6 (3/5): 421–506.

Jocqué R. 1981. Erigonid spiders from Malawi (Araneida, Linyphiidae). *Revue de Zoologie africaine* 95: 470–492.

Jocqué R. 1985. Linyphiidae (Araneae) from the Comoro Islands. *Revue de Zoologie africaine* 99 (2): 197–230.

Koch C. L. 1837. *Übersicht des Arachnidensystems. Heft 1*. C.H. Zeh'sche Buchhandlung, Nürnberg. https://doi.org/10.5962/bhl.title.39561

Koch C.L. 1838. *Die Arachniden: Getreu nach der Natur abgebildet und beschrieben Vols 4–5*. C.H. Zeh'sche Buchhandlung, Nürnberg. https://doi.org/10.5962/bhl.title.43744

Koch L. 1869. Beitrag zur Kenntniss der Arachnidenfauna Tirols. *Zeitschrift des Ferdinandeums für Tirol und Vorarlberg* 14: 149–206.

Kronestedt T. Checklist of spiders (Araneae) in Sweden. Ver. 15 Feb. 2001.

Kulczyński W. 1915. Fragmenta arachnologica, XVIII. Araneorum species nonnullae novae aut minus cognitae. Descriptiones et adnotationes. *Bulletin international de l'Académie des sciences de Cracovie* 1: 897–942.

Kulczyński W. 1926. Arachnoidea Camtschadalica. *Yezhegodnik Zoologicheskogo Muzeya Akademii Nauk SSSR Leningrad* 27: 29–72.

Kunz K., Garbe S. & Uhl G. 2012. The function of the secretory cephalic hump in males of the dwarf spider *Oedothorax retusus* (Linyphiidae: Erigoninae). *Animal Behaviour* 83 (2): 511–517. https://doi.org/10.1016/j.anbehav.2011.11.028

La Touche A.A.D. 1946. Hampshire spiders, including the description of a new species, *Diplocephalus cottoni*. *Proceedings of the Zoological Society of London* 115 (3–4): 281–295. https://doi.org/10.1111/j.1096-3642.1946.tb00091.x

Lasut L., Marusik Y.M. & Frick H. 2009. First description of the female of the spider *Savignia zero* Eskov, 1988 (Araneae: Linyphiidae). *Zootaxa* 2267 (1): 65–68. https://doi.org/10.11646/zootaxa.2267.1.5

Lecigne S., Moutaouakil S. & Lips J. 2025. Contribution to the knowledge of the spider fauna of Morocco (Arachnida: Araneae) – second note. On new species and new records from caves and miscellaneous terrestrial ecosystems. *Journal of the Belgian Arachnological Society* 40 (1): 1–184.

Lin S.W., Lopardo L. & Uhl G. 2021. Diversification through gustatory courtship: an X-ray micro-computed tomography study on dwarf spiders. *Frontiers in Zoology* 18 (51): 1–33. https://doi.org/10.1186/s12983-021-00435-8

Lin S.W., Lopardo L. & Uhl G. 2022. Evolution of nuptial-gift-related male prosomal structures: taxonomic revision and cladistic analysis of the genus *Oedothorax* (Araneae: Linyphiidae: Erigoninae). *Zoological Journal of the Linnean Society* 195 (2): 417–584. https://doi.org/10.1093/zoolinnean/zlab033

Locket G.H. & Millidge A.F. 1953. *British Spiders, Vol. II.* Ray Society, London.

Locket G.H., Millidge A.F. & Merrett P. 1974. *British Spiders, Vol. III.* Ray Society, London.

Loksa I. 1981. Die Bodenspinnen zweier Torfmoore im Oberen Theiss-Gebiet Ungarns. *Opuscula Zoologica, Budapest* 17 (18): 91–106.

Maddison W.P. & Maddison D.R. 2010. Mesquite: a modular system for evolutionary analysis, Version 2.73. Available from http://mesquiteproject.org [accessed 7 Apr. 2025].

Marusik Y.M. 1988. Three new spider species of the family Linyphiidae (Aranei) from the north-east of the USSR. *Zoologichesky Zhurnal* 67 (12): 1914–1918.

Marusik Y.M., Koponen S. & Danilov S.N. 2001. Taxonomic and faunistic notes on linyphiids of Transbalkalia and South Siberia (Araneae, Linyphiidae). *Bulletin of the British Arachnological Society* 12 (2): 83–92.

Menge A. 1868. Preussische Spinnen. II. Abtheilung. *Schriften der Naturforschenden Gesellschaft in Danzig* 2: 153–218. Available from https://www.biodiversitylibrary.org/page/35932111 [accessed 7 Apr. 2025].

Merrett P. 1963. The palpus of male spiders of the family Linyphiidae. *Proceedings of the Zoological Society of London* 140 (3): 347–467. https://doi.org/10.1111/j.1469-7998.1963.tb01867.x

Michalik P. & Uhl G. 2011. Cephalic modifications in dimorphic dwarf spiders of the genus *Oedothorax* (Erigoninae, Linyphiidae, Araneae) and their evolutionary implications. *Journal of Morphology* 272 (7): 814–832. https://doi.org/10.1002/jmor.10950

Milasowszky N., Bauder J. & Hepner M. 2017. *Diplocephalus komposchi* n. sp., a new species of erigonine spider (Araneae, Linyphiidae) from Austria. *Zootaxa* 4268 (2): 296–300. https://doi.org/10.11646/zootaxa.4268.2.10

Miller F. 1970. Spinnenarten der Unterfamilie Micryphantinae und der Familie Theridiidae aus Angola. *Publicações Culturais da Companhia de Diamantes de Angola* 82: 75–166.

Miller F. & Kratochvíl J. 1939. Einige neue Spinnen aus Mitteleuropa. *Sborník Entomologického Oddělení Národního Musea v Praze* 17: 32–38.

Miller J.A. 2007. Review of erigonine spider genera in the Neotropics (Araneae: Linyphiidae, Erigoninae). *Zoological Journal of the Linnean Society* 149: 1–272. https://doi.org/10.1111/j.1096-3642.2007.00233.x

Miller J.A & Hormiga G. 2004. Clade stability and the addition of data: A case study from erigonine spiders (Araneae: Linyphiidae, Erigoninae). *Cladistics* 20 (5): 385–442. https://doi.org/10.1111/j.1096-0031.2004.00033.x

Millidge A.F. 1977. The conformation of the male palpal organs of Linyphiid spiders, and its application to the taxonomic and phylogenetic analysis of the family (Araneae: Linyphiidae). *Bulletin of the British Arachnological Society* 4 (1): 1–60.

Millidge A.F. 1979. Some erigonine spiders from southern Europe. *Bulletin of the British Arachnological Society* 4: 316–328.

Millidge A.F. 1981. The erigonine spiders of North America. Part 3. The genus *Scotinotylus* Simon (Araneae: Liyphiidae). *The Journal of Arachnology* 9: 167–213.

Millidge A.F. 1984. The taxonomy of the Linyphiidae, based chiefly on the epigynal and tracheal characters (Araneae: Linyphiidae). *Bulletin of the British Arachnological Society* 6 (6): 229–267.

Nixon K.C. 2002. Winclada (BETA) version 1.00. 08. Published by the author, Ithaca, New York.

Oi R. 1960. Linyphiid spiders of Japan. *Journal of the institute of Polytechnics, Osaka City University* 11: 137–244.

Ono H., Matsuda M. & Saito H. 2009. Linyphiidae, Pimoidae. *In:* Ono H. (ed.) *The Spiders of Japan with Keys to the Families and Genera and Illustrations of the Species*: 253–344. Tokai University Press, Kanagawa.

Paik K.Y. 1978. Seven new species of Korean spiders. *Research Review of Kyungpook National University* 25 (26): 45–61.

Pantini P. & Sassu A. 2009. I ragni dell'isola dell'Asinara (Sardegna NW) (Arachnida, Araneae). *Annali del Museo Civico di Storia Naturale di Genova* 100: 619–647.
Available from https://www.biodiversitylibrary.org/part/396952 [accessed 7 Apr. 2025].

Paquin P. & Dupérré N. 2003. Guide d'identification des araignées de Québec. *Fabreries, Supplement* 11: 1–251.

Pesarini C. 1996. Note su alcuni Erigonidae italiani, con descrizione di una nuova specie (Araneae). *Atti della Società Italiana di Scienze Naturali e del Museo Civico di Storia Naturale di Milano* 135 (2): 413–429.

Pickard-Cambridge O. 1871. XVI. Descriptions of some British spiders new to science, with a notice of others, of which some are now for the first time recorded as British species. *Transactions of the Linnean Society of London* 27 (3): 393–464. https://doi.org/10.1111/j.1096-3642.1871.tb00218.x

Pickard-Cambridge O. 1872. General list of the spiders of Palestine and Syria, with descriptions of numerous new species, and characters of two new genera. *Proceedings of the Zoological Society of London* 40: 212–354. Available from https://www.biodiversitylibrary.org/page/28611578 [accessed 7 Apr. 2025].

Pickard-Cambridge O. 1873. Descriptions of twenty-four new species of *Erigone*. *Proceedings of the Zoological Society of London* 40: 747–769.
Available from https://www.biodiversitylibrary.org/page/28612221 [accessed 7 Apr. 2025].

Pickard-Cambridge O. 1875. On some new species of *Erigone*. *Proceedings of the Zoological Society of London* 43: 190–224, 323–335.

Pickard-Cambridge O. 1904. On new and rare British spiders. *Proceedings of the Dorset Natural History and Antiquarian Field Club* 24: 149–171.

Platnick N.I. 1976. Are monotypic genera possible? *Systematic Zoology* 25 (2): 198–199. https://doi.org/10.2307/2412749

Prószyński J. 1986. What, if anything, is a genus in Salticidae (Araneae)? *Actas X Congreso Internacional de Aracnología, Jaca/España* 1: 367–372.

Prószyński J. & Staręga W. 1971. Pajaki-Aranei. *Katalog Fauny Polski* 33: 1–382.

Rieppel O. 2007. The performance of morphological characters in broad-scale phylogenetic analyses. *Biological Journal of the Linnean Society* 92 (2): 297–308. https://doi.org/10.1111/j.1095-8312.2007.00847.x

Roberts M.J. 1987. *The Spiders of Great Britain and Ireland, Vol. 2: Linyphiidae and Check List.* Harley Books, Colchester, England.

Ruta M., Coates M.I. & Quicke D.L.J. 2003. Early tetrapod relationships revisited. *Biological Reviews of the Cambridge Philosophical Society* 78 (2): 251–345. https://doi.org/10.1017/s1464793102006103

Saaristo M.I. 1971. Revision of the genus *Maro* O.P.-Cambridge (Araneae, Linyphiidae). *Annales Zoologici Fennici* 8: 463–482.

Saito H. 1986. New erigonine spiders found in Hokkaido, Japan. *Bulletin of the National Museum of Nature and Science Tokyo* 12: 9–24.

Saito H. & Ono H. 2001. New genera and species of the spider family Linyphiidae (Arachnida, Araneae) from Japan. *Bulletin of the National Museum of Nature and Science Tokyo* 27 (1): 1–59.

Schaible U., Gack C. & Paulus H.F. 1986. Zur Morphologie, Histologie und biologischen Bedeutung der Kopfstrukturen männlicher Zwergspinnen (Linyphiidae: Erigoninae). *Zoologische Jahrbücher. Abteilung für Systematik, Ökologie und Geographie der Tiere* 113 (3): 389–408.

Scharff N. 1990. A catalogue of African Linyphiidae (Araneae). *Steenstrupia* 16: 117–152.

Schenkel E. 1934**.** Kleine Beiträge zur Spinnenkunde. *Revue suisse de Zoologie* 41:85–104. https://doi.org/10.5962/bhl.part.145993

Schenkel E. 1939. Beitrag zur Spinnenkunde. I. Spinnen des Lotschentals. II. Beschreibungen neuer europäischer Spinnen. *Revue suisse de Zoologie* 46: 95–114. https://doi.org/10.5962/bhl.part.155012

Sherwood D. 2024. Studies on spider nomenclature – I: miscellaneous notes on unrecognisable species, new synonyms, and untenable subspecies (Araneae: Araneomorphae). *The Indochina Entomologist* 1 (23): 189–235. https://doi.org/10.70590/ice.2024.01.23

Simon E. 1882. Description d'espèces nouvelles du genre *Erigone*. *Bulletin de la Société zoologique de France* 6: 233–257. Available from https://www.biodiversitylibrary.org/page/11089309 [accessed 7 Apr. 2025].

Simon E. 1884. *Les Arachnides de France*. *Tome cinquième, deuxième et troisième partie*. Roret, Paris, 180-885.

Simon E. 1908. Araneae, 1re partie. *In*: Michaelsen W. & Hartmeyer R. (eds) *Die Fauna Südwest-Australiens. Ergebnisse der Hamburger südwest-australischen Forschungsreise 1905. Band 2, Lieferung 12*: 359–446. Gustav Fischer, Jena. https://doi.org/10.5962/bhl.title.7416

Simon E. 1926. *Les arachnides de France. Synopsis générale et catalogue des espèces françaises de l'ordre des Araneae. Tome VI. 2e partie*. Roret, Paris, 309-532.

Song D.X., Zhu M.S. & Chen J. 1999. *The Spiders of China.* Hebei Science and Technolology Publishing House, Shijiazhuang.

Song Y.J. & Li S.Q. 2008. A taxonomic study of five erigonine spiders (Araneae: Linyphiidae) from China. *Arthropoda Selecta* 17: 87–100.

Song Y.J. & Li S.Q. 2009. Two new erigonine species (Araneae: Linyphiidae) from caves in China. *The Pan-Pacific Entomologist* 85 (2): 58–69. https://doi.org/10.3956/2007-55.1

Song Y.J. & Li S.Q. 2010. The spider genera *Araeoncus* Simon, 1884 and *Diplocephalus* Bertkau, 1883 (Arachnida, Araneae, Linyphiidae) of China. *Zoosystema* 32 (1): 117–137. https://doi.org/10.5252/z2010n1a6

Song Y.J., Li S.Q. & Marusik Y. 2006. Redescription on *Dicymbium facetum* (L. Koch) (Araneae, Linyphiidae) with first report on its male. *Acta Zootaxonomica Sinica* 31: 330–334.

Strand E. 1905. Coleoptera, Hymenoptera, Lepìdoptera und Araneae. *In*: *Report of the Second Norwegian Arctic Expedition in the 'Fram' 1898–1902, Vol. 1 (3)*: 22–30. A.W. Brogger, Kristiania. Available from https://www.biodiversitylibrary.org/bibliography/55607 [accessed 7 Apr. 2025].

Sytshevskaja V. J. 1935. Étude sur les araignées de la Kamtchatka. *Folia Zoologica et Hydrobiologica, Rigā* 8 (1): 80–103.

Tanasevitch A.V. 1983. New species of spiders of the family Linyphiidae (Aranei) from Uzbekistan. *Zoologichesky Zhurnal* 62 (12): 1786–1795.

Tanasevitch A.V. 1984. New and little-known spiders of the family Linyphiidae (Aranei) from Bolshezemelskaya Tundra. *Zoologichesky Zhurnal* 63 (3): 382–391.

Tanasevitch A.V. 1985a. A study of spiders (Aranei) of the Polar Urals. *Trudy Zoologicheskogo Instituta Akademii Nauk SSSR, Leningrad* 139: 52–62.

Tanasevitch A.V. 1985b. New species of spiders of the fam. Linyphiidae (Aranei) from Kirghizia. *Entomologicheskoe Obozrenie* 64 (4): 845–854.

Tanasevitch A.V. 1987. The linyphiid spiders of the Caucasus, USSR (Arachnida: Araneae: Linyphiidae). *Senckenbergiana Biologica* 67 (4–6): 297–383.

Tanasevitch A.V. 1989. The linyphiid spiders of Middle Asia (Arachnida: Araneae: Linyphiidae). *Senckenbergiana Biologica* 69 (1–3): 83–176.

Tanasevitch A.V. 1990. The spider family Linyphiidae in the fauna of Caucasus (Arachnida, Aranei). *In:* Striganova B.R. (ed.) *Fauna nazemnykh bespozvonochnykh Kavkaza*: 5–114. Akademia Nauka, Moscow.

Tanasevitch A.V. 2006. On some Linyphiidae of China, mainly from Taibai Shan, Qinling Mountains, Shaanxi Province (Arachnida: Araneae). *Zootaxa* 1325 (1): 277–311. https://doi.org/10.11646/zootaxa.1325.1.18

Tanasevitch A.V. 2008. On linyphiid spiders (Araneae) collected by A. Senglet in Iran in 1973–1975. *Revue suisse de Zoologie* 115 (3): 471–490. https://doi.org/10.5962/bhl.part.80437

Tanasevitch A.V. 2009. The linyphiid spiders of Iran (Arachnida, Araneae, Linyphiidae). *Revue suisse de Zoologie* 116 (3–4): 379–420. https://doi.org/10.5962/bhl.part.81325

Tanasevitch A.V. 2011. On linyphiid spiders from the eastern and central Mediterranean kept at the Muséum d'histoire naturelle, Geneva. *Revue suisse de Zoologie* 118 (1): 49–91. https://doi.org/10.5962/bhl.part.117799

Tanasevitch A.V. 2013. On linyphiid spiders (Araneae) from Israel. *Revue suisse de Zoologie* 120 (1): 101–124. Available from https://www.biodiversitylibrary.org/page/50402172 [accessed 7 Apr. 2025].

Tanasevitch A.V. 2014. Linyphiid spiders (Araneae, Linyphiidae) from caves of Morocco. *Revue suisse de Zoologie* 121 (2): 277–290. Available from https://www.biodiversitylibrary.org/page/52964639 [accessed 7 Apr. 2025].

Tanasevitch A.V. 2017. A new *Dactylopisthes* Simon, 1884 from the Caucasus (Aranei: Linyphiidae). *Arthropoda Selecta* 26 (1): 63–65. https://doi.org/10.15298/arthsel.26.1.08

Tanasevitch A.V. 2018a. A new species of *Dactylopisthes* Simon, 1884 from Thailand (Araneae, Linyphiidae). *Revue suisse de Zoologie* 125 (2): 217–219. https://doi.org/10.5281/zenodo.1414201

Tanasevitch A.V. 2018b. The second, new species of *Dactylopisthes* Simon, 1884 from southeastern Asia (Aranei: Linyphiidae). *Arthropoda Selecta* 27 (4): 363–365. https://doi.org/10.15298/arthsel.27.4.13

Tanasevitch A.V. 2023a. Survey of the Ethiopian linyphiid spider fauna. I. Subfamily Erigoninae (Arachnida, Araneae, Linyphiidae). *Zootaxa* 5346 (4): 420–442. https://doi.org/10.11646/zootaxa.5346.4.4

Tanasevitch A.V. 2023b. A new species of *Dactylopisthes* Simon, 1884 from Tajikistan (Aranei: Linyphiidae). *Arthropoda Selecta* 32 (2): 220–224. https://doi.org/10.15298/arthsel.32.2.07

Tanasevitch A.V. & Marusik Y. 2023. On the synonymy of *Dactylopisthoides* Eskov, 1990 and *Uusitaloia* Marusik, Koponen & Danilov, 2001 (Araneae, Linyphiidae). *ZooKeys* 1184: 291–299. https://doi.org/10.3897/zookeys.1184.113255

Thaler K. 1969. Über einige wenig bekannte Zwergspinnen aus Tirol (Arachnida: Araneae, Erigonidae). *Berichte des naturwissenschaftlich-medizinischen Vereins Innsbruck* 57: 195–219.

Thaler K. 1970. Über einige wenig bekannte Zwergspinnen aus den Alpen (Arachnida: Araneae, Erigonidae). *Berichte des naturwissenschaftlich-medizinischen Vereins Innsbruck* 58: 255–276.

Thaler K. 1971. Über drei wenig bekannte hochalpine Zwergspinnen (Arachnida: Aranei, Erigonidae). *Mitteilungen der Schweizerischen Entomologischen Gesellschaft* 44: 309–322. https://doi.org/10.5169/seals-401662

Thaler K. 1972. Über einige wenig bekannte Zwergspinnen aus den Alpen II. (Arachnida: Aranei, Erigonidae). *Berichte des naturwissenschaftlich-medizinischen Vereins Innsbruck* 59: 29–50.

Thaler K. 1978. Über wenig bekannte Zwergspinnen aus den Alpen – V (Arachnida: Aranei, Erigonidae). *Beiträge zur Entomologie Berlin* 28 (1): 183–200.

Thaler K. 1984. Sechs neue mediterrane Zwergspinnen (Aranei, Linyphiidae: Erigoninae). *Archives des Sciences Genève* 37 (2): 193–210.

Thorell T. 1875. Verzeichniss südrussischer Spinnen. *Horae Societatis Entomologicae Rossicae* 11: 39–122. Available from https://www.biodiversitylibrary.org/page/12777773 [accessed 7 Apr. 2025].

Trifinopoulos J., Nguyen L.T., von Haeseler A. & Minh B.Q. 2016. W-IQ-TREE: a fast online phylogenetic tool for maximum likelihood analysis. *Nucleic Acids Research* 44 (W1): W232–W235. https://doi.org/10.1093/nar/gkw256

Tu L.H. & Hormiga G. 2010. The female genitalic morphology of "micronetine" spiders (Araneae, Linyphiidae). *Genetica* 138: 59–73. https://doi.org/10.1007/s10709-009-9368-9

Tullgren A. 1955. Zur Kenntnis schwedischer Erigoniden. *Arkiv för Zoologi (N.S.)* 7: 295–389.

Wang F., Ballesteros J.A., Hormiga G., Chesters D., Zhan Y., Sun N., Zhu C., Chen W. & Tu L. 2015. Resolving the phylogeny of a speciose spider group, the family Linyphiidae (Araneae). *Molecular Phylogenetics and Evolution* 91: 135–149. https://doi.org/10.1016/j.ympev.2015.05.005

Westring N. 1851. Förteckning öfver de till närvarande tid Kände, i Sverige förekommande Spindlarter, utgörande ett antal af 253, deraf 132 äro nya för svenska Faunan. *Göteborgs Kungliga Vetenskaps och Vitterhets Samhälles Handlingar* 2: 25–62.

Westring N. 1861. Araneae svecicae. *Göteborgs Kungliga Vetenskaps och Vitterhets Samhälles Handlingar* 7: 1–615.

Wider F. 1834. *Arachniden*. *In*: Reuss A. (ed.) Zoologische Miscellen. *Museum Senckenbergianum, Abhandlungen aus dem Gebiete der beschreibenden Naturgeschichte* 1: 197–282.
Available from https://www.biodiversitylibrary.org/page/45889372 [accessed 7 Apr. 2025].

Wiehle H. 1956. Spinnentiere oder Arachnoidea (Araneae). 28. Familie: Linyphiidae-Baldachinspinnen. *Tierwelt Deutschlands und der angrenzenden Meeresteile* 44: 1–178.

Wiehle H. 1960. Spinnentiere oder Arachnoidea (Araneae). 11: Micryphantidae- Zwergspinnen. *Tierwelt Deutschlands und der angrenzenden Meeresteile* 47: 1–620.

Wiehle H. 1963. Beiträge zur Kenntnis der deutschen Spinnenfauna, III. *Zoologische Jahrbücher, Abteilung für Systematik, Geographie und Biologie der Tiere* 90: 227–298.

Wiehle H. 1967. Beiträge zur Kenntnis der deutschen Spinnenfauna, V. (Arachnida: Araneae). *Senckenbergiana Biologica* 48: 1–36.

World Spider Catalog 2025. World Spider Catalog. Version 26.0. Natural History Museum Bern. Available from http://wsc.nmbe.ch [accessed 7 Apr. 2025]. https://doi.org/10.24436/2

Wunderlich J. 1969. Zur Spinnenfauna Deutschlands, IX. Beschreibung seltener oder bisher unbekannter Arten (Arachnida: Araneae). *Senckenbergiana Biologica* 50 (5/6): 381–393.

Wunderlich J. 1970. Zur Synonymie einiger Spinnen-Gattungen und -Arten aus Europa und Nordamerika (Arachnida: Araneae). *Senckenbergiana Biologica* 51: 403–408.

Wunderlich J. 1972. Zur Kenntnis der Gattung *Walckenaeria* Blackwall 1833 unter besonderer Berücksichtigung der europäischen Subgenera und Arten (Arachnida: Araneae: Linyphiidae). *Zoologische Beiträge* 18: 371–427.

Wunderlich J. 1980a. Linyphiidae aus Süd-Europa und Nord-Afrika (Arach.: Araneae). *Verhandlungen des Naturwissenschaftlichen Vereins in Hamburg* 23: 319–337.

Wunderlich J. 1980b. Drei neue Linyphiidae-Genera aus Europa (Arachnida: Araneae). *Senckenbergiana Biologica* 61: 119–125.

Wunderlich J. 1983. Linyphiidae aus Nepal, IV. Bisher unbekannte und für Nepal neue Arten (Arachnida: Araneae). *Senckenbergiana Biologica* 63: 219–248.

Wunderlich J. 1992. Die Spinnen-Fauna der Makaronesischen Inseln: Taxonomie, Ökologie, Biogeographie und Evolution. *Beiträge zur Araneologie* 1: 1–619.

Wunderlich J. 1995. Zur Taxonomie europäischer Gattungen der Zwergspinnen (Arachnida: Araneae: Linyphiidae: Erigoninae). *Beiträge zur Araneologie* 4: 643–654.

Wunderlich J. 2011. Extant and fossil spiders (Araneae). *Beiträge zur Araneologie* 6: 1–640.

Wunderlich J. 2022. Some spiders (Araneae) of the Western Palearctic. *Beiträge zur Araneologie* 15: 4–78, 199.

Zhao Q.Y. & Li S.Q. 2014. A survey of linyphiid spiders from Xishuangbanna, Yunnan Province, China (Araneae, Linyphiidae). *ZooKeys* 460: 1–181. https://doi.org/10.3897/zookeys.460.7799

Printed versions of all papers are deposited in the libraries of two of the institutes that are members of the *EJT* consortium: Muséum national d'Histoire naturelle, Paris, France and Royal Museum for Central Africa, Tervuren, Belgium. The other members of the consortium are: Royal Belgian Institute of Natural Sciences, Brussels, Belgium; Meise Botanic Garden, Meise, Belgium; Natural History Museum of Denmark, Copenhagen, Denmark; Naturalis Biodiversity Center, Leiden, the Netherlands; Museo Nacional de Ciencias Naturales-CSIC, Madrid, Spain; Leibniz Institute for the Analysis of Biodiversity Change, Bonn – Hamburg, Germany; National Museum of the Czech Republic, Prague, Czech Republic; The Steinhardt Museum of Natural History, Tel Aviv, Israël.

Supplementary files

Supp. file 1. Data matrix (nexus file) including the 269 morphological characters, their states, and the scorings for all taxa. https://doi.org/10.5852/ejt.2026.1071.3296.14519

Supp. file 2. Figure SF1. Strict consensus tree of the 192 most parsimonious trees from the equal weighting analysis. https://doi.org/10.5852/ejt.2026.1071.3296.14520

Supp. file 3. Figure SF2. Strict consensus tree of the 54 trees from the implied weighting analysis with *k* values between 1 and 1000 (Table 1). https://doi.org/10.5852/ejt.2026.1071.3296.14521